Author:
Cordero Llana, Oscar

Title:
Tales of Neurotrophism

Neurotrophic Factors in Neural Stem Cells and the 6-OHDA Model of Parkinson's Disease

Tales of Neurotrophism

Neurotrophic Factors in Neural Stem Cells and the 6-OHDA model of Parkinson's Disease

Óscar Cordero Llana

A dissertation submitted to the University of Bristol in accordance with the requirements of the degree of Doctor of Philosophy in the Faculty of Medicine and Dentistry, December 2012.

Word Count: 47,120

A mis abuelos

This thesis is dedicated
to my grandparents
Manuel, Inés and Fredesvinda
who died while writing it
and Gregorio who I never knew.

Junín

Soy, pero también soy el otro, el muerto,
el otro de mi sangre y de mi nombre,
soy un vago señor y soy el hombre
que detuvo las lanzas del desierto.
Vuelvo a Junín, donde no estuve nunca,
A tu Junín, abuelo Borges. ¿Me oyes,
sombra o ceniza última, o desoyes
en tu sueño de bronce esta voz trunca?
Acaso busques por mis vanos ojos
el épico Junín de tus soldados,
el árbol que plantaste, los cercados
y en el confín la tribu y los despojos.
Te imagino severo, un poco triste;
Quién me dirá cómo eras y quién fuiste.

Jorge Luís Borges

Author's Declaration

I declare that the work in this dissertation was carried out in accordance with the Regulations and Code of Practice for Research Degree Programs of the University of Bristol. The work is original except where indicated by special reference in the text and no part of this dissertation has been submitted for any other degree. Work done in collaboration with, or with the assistance of others, is indicated as such. Any views expressed in this dissertation are those of the author and in no way represent those of the University of Bristol.

Signed: Date:

Abstract

This thesis is divided in three independent result chapters or *tales of neurotrophism*. On each of these chapters I sought to characterize or validate novel neurotrophic factors and their ability to promote neuronal differentiation or survival. In the first chapter, I will establish the role of clusterin as an astrocyte-secreted protein that acts as a novel neurotrophic factor for human neural stem cells in vitro and I will discuss its implications for neurodegeneration in Alzheimer's disease. The second chapter is focused on galanin – a pleiotropic neuropeptide with neuroprotective and neuroregenerative properties in the nervous system. I will study the effects of galanin on neural differentiation of fetal and adult mouse neural stem cells in vitro and the consequences of galanin disruption on adult neurogenesis in vivo. I will consider my findings in relation to the complex behavioural phenotypes described for galanin knockout mice. In the final chapter, I will test the efficacy of lentiviral delivery of CDNF (Conserved Dopamine Neurotrophic Factor) and MANF (Mesencephalic Astrocyte-derived Neurotrophic Factor) – members of a newly-described family of neurotrophic factors for dopaminergic neurons – in the 6-hydroxy-dopamine rat model of Parkinson's disease and I will discuss our findings in the context of gene therapy approaches for this disease.

Acknowledgements

These acknowledgments must start with a big thank you to my supervisor Dr Maeve Caldwell. She has been a great mentor during all these years and she has an incredible ability to let her students work independently and at the same time give them the right level of supervision. I am sure this is not easy, especially with Spanish students, so thank you again Maeve! Special thanks must go too to Lucy Crompton. Lucy! I am thinking of all the time we have spent together, all the talks, all the teas and all the cakes we have shared and all the science, of course! All of a sudden I have a big knot in my throat and I cannot imagine being in a lab if you are not there.

I am really going to miss the Caldwell group. The past and present members, Hannah, Fiona, Bang Fu, Pete, Simon… Special thanks to Kirsty because whenever I spoke with her I felt immediately happier and because nobody understands the beauty of the small things in life like her. A quick see you soon to Jennie, I will be eagerly waiting for you in Oxford (specially if you get a puppy). Honestly, I could not have been in a better or friendlier group (maybe in Ravenclaw).

I would also like to thank James Uney and his group, especially to Jo and Helen. I must have asked you a thousand questions in all these years and you have always given me a helpful answer and a warm smile ☺. I could not forget little Matt, Liz, Tony, Jess… you made those early PhD years really fun and I will always remember you. Thank you also to Stephen Kelly, for forcing me to improve my English, to Craig for his lectures and his thoughts and to Liang for her vectors, her unusual laugh and her advice (although this might change after my viva).

And no, I have not forgotten you Federica! I love your happiness, your smile and your mum's food and I honestly do not think I would have finished this thesis without your support and friendship. Fede, do not think you are getting rid of me; I hope to have you always near me and I intend to visit Italy soon.

In the Asturian front I want to thank María for visiting me and for believing in me. And of course Noelia for bringing her wrath to Bristol more times than I can remember. My family, because I would not be here without them. Especially to my sister, for acknowledging me in her dissertation and because Laura, you too make my life better. And to Ben for sharing these last three years with me.

To my grandparents, for everything…

Foreword

In this thesis we have followed the gene nomenclature guidelines from the National Centre for Biotechnology Information (NCBI), the Human Genome Organisation (HUGO) nomenclature committee and Mouse Genome Informatics (MGI) database. Human genes will appear italicised with all letters in uppercase (e.g. *CLU*), whereas mouse genes will appear italicised but with only the first letter in uppercase (e.g. *Clu*). Gene products will appear with all letters in uppercase both for mouse and human proteins (e.g. CLU).

Abbreviations

6-OHDA: 6-hydroxy dopamine

A

ACh: Acetyl-choline
ACM: Astrocyte conditioned medium
AD: Alzheimer's disease
AKT: Protein kinase B
ANOVA: Analysis of variance
ApoE: Apolipoprotein E
APP: Amyloid precursor protein
APS: Ammonium persulfate
AraC: Arabinofuranosyl cytidine
AVE: Anterior visceral endoderm
Aβ: Amyloid beta

B

BBB: Brain blood barrier
BCA: Bicinchoninic acid assay
BDNF: Brain-derived neurotrophic factor
bHLH: Basic helix-loop-helix
BMP: Bone morphogenetic protein
BP: Basal progenitor
BrdU: Bromodeoxyuridine
BSA: Bovine serum albumin

C

CDNF: Conserved dopamine neurotrophic factor
ChAT: Choline acetyltransferase
Clu-KO: Clusterin knockout
cmv: Cytomegalovirus
CNS: Central nervous system
CNTF: Ciliary neurotrophic factor
CREB: Cyclic AMP response element biding protein
CSF: Cerebro-spinal fluid
CT-1: Cardiotrophin-1

Ctrl: Control

CTX: Cortex

D

DAB: 3-3'-Diaminobenzidine

DCX: Double courtin

DG: Dentate gyrus

DMEM: Dulbecco's modified Eagle medium

DMSO: Dimethyl sulfoxide

DNA: Deoxyribonucleic acid

dNTP: Deoxynucleotide triphosphate

DRG: Dorsal root ganglia

DTT: Dithiothreitol

E

EGF: Epidermal growth factor

ER: Endoplasmic reticulum

ERK: Extracellular regulated kinase

EtBr: Ethidium bromide

F

FACS: Fluorescence activated cell sorting

FCS: Fetal calf serum

FGF-b: Basic Fibroblast growth factor

G

GA: Golgi apparatus

GABA: Gamma-aminobutyric acid

***Gal*-KO**: Galanin knockout mice

***Gal*-OE**: Galanin overexpressing

***GalRi*-KO**: Galanin receptor *i* knockout

Gas1: Growth arrest specific protein-1

Gbx2: Gastrulation brain homeobox-2

GDNF: Glial cell-derived neurotrophic factor

GFAP: Glial fibrillary acidic protein

GH: Growth hormone

GWAS: Genome wide association study

H

HEK: Human embryonic kidney

Hep: Heparin

hfNSCs: Human fetal neural stem cells

HIV: Human immunodeficiency virus

HPC: Hippocampus

HRP: Horseradish peroxidase

I

ICM: Inner cell mass

IMZ: Involuting cell mass

IP: Intraperitoneal

IsO: Isthmic organiser

J

JAK: Janus kinase

JNK: c-Jun N-terminal kinase

K

KO: Knock out

L

LB: Luria-Bertani medium

LH: Luteinizing hormone

LIF: Leukaemia inhibitory factor

LOAD: Late-onset Alzheimer's disease

M

MANF: Mesencephalic astrocyte-derived neurotrophic factor

MB: Midbrain

MPP^+: Methyl-4-phenylpyridinium ion

mRNA: Messenger RNA

MS: Multiple sclerosis

MTT: Methyl-thiazolyl-diphenyl-tetrazolium

N

nCLU: Nuclear clusterin

Nf-1: Nuclear factor-1

NGF: Nerve growth factor

NGS: Normal goat serum

NSCs: Neural stem cells

NTF: Neurotrophic factor

O

OB: Olfactory bulb

Oct-4: Octamer-binding transcription factor-4

Otx2: Orthodenticle homologue-2

P

PAGE: Polyacrylamide gel electrophoresis

PBS: Phosphate-buffered saline

PCR: Polymerase chain reaction

PD: Parkinson's disease

PDL: Poly-*D*-lysine

Pdm: POU domain protein

PFA: Para-formaldehyde

PI3K: Phosphatidylinositol 3-kinase

PNS: Peripheral nervous system

PPT: Perforant path transection

PRL: Prolactin

PS: Penicillin-Streptomycin

PSA-NCAM: Poly-Sialated Neural Cell Adhesion Molecule

Ptch1: Protein patched homolog-1

PVDF: Poly-vinylidene difluoride

PVN: Para-ventricular nucleus

Q

qPCR: Quantitative polymerase chain reaction

R

RA: Retinoic acid

RCF: Relative centrifugal force

RG: Radial glia

RMS: Rostral-migratory stream

RNA: Ribonucleic acid

RT: Reverse transcription

S

sCLU: Secreted clusterin

SDS: Sodium dodecyl sulphate

SEM: Standard error of the mean

sffv: Spleen focus-forming virus

SGZ: Subgranular zone

SHH: Sonic hedgehog

SN: Substantia nigra

SNPs: Single nucleotide polymorphisms

Sod-1: Superoxide dismutase-1

Sox: Sry-related HMG box

SPARC: Secreted protein rich in cysteine

STAT: Signal transducer and activation of transcription

STFP: Social transmission of food preference

Str: Cortex striatum

SVZ: Sub-ventricular zone

T

T[H^3]: Tritiated thymidine

TAE: Tris-acetate buffer

TBS: Tris-buffered saline

TGF-β: Transforming growth factor beta

TH: Tyrosine hydroxylase

TNS: Tris non-saline buffer

TrK: Tyrosine receptor kinase

TUC-4: TOAD-64/Ulip/CRMP

Tuj1: Neuron-specific class III β-tubulin

Tx^{100}: Triton-X 100

U

UPDRS: Unified PD rating scale

V

VEGF: Vascular endothelial growth factor

VSVG: Vesicular stomatitis virus G

VZ: Ventricular zone

W

WT: Wild-type (mice)

Wnt: Wingless homologue to Int1

Contents

List of figures

List of tables

Equations

Chapter 1

Chapter 1

Introduction

> "You can know the name of a bird in all the languages of the world, but when you're finished, you'll know absolutely nothing whatsoever about the bird... So let's look at the bird and see what it's doing - that's what counts. I learned very early the difference between knowing the name of something and knowing something."
>
> ***Richard Feynman***

1.1 Neural stem cells

Neural stem cells (NSCs) are a heterogeneous population of cells present both in the developing and the adult central nervous system (CNS). They are defined according to their functional properties: ***multipotency***, which reflects their ability to differentiate into neurons, astrocytes and oligodendrocytes and ***self-renewal*** by which a NSC divides asymmetrically producing a daughter progenitor cell with a more restricted differentiation potential and a multipotent NSC. NSCs are mitotically active and proliferate by undergoing symmetric divisions giving rise to two identical daughter NSCs.

NSCs can be isolated from the adult and the developing brain and cultured in vitro. Classically, NSCs are cultured as free-floating neurospheres which are heterogeneous cell aggregates that contain NSCs and more committed progenitors, as well as differentiated glia and neurons - depending on the time in culture and the size of the neurosphere (Figure 1—1) To promote the proliferation of undifferentiated NSCs and select against more committed or post-mitotic cells, NSCs are typically expanded in the presence of mitogens: epidermal growth factor (EGF) (Reynolds et al., 1992; Reynolds and Weiss, 1996) and/or fibroblast growth factor (FGF-b) (Gritti et al., 1996). However, it has been suggested that

EGF and FGF-responsive cells represent two different developmental NSC populations with FGF-responsive NSC appearing as early as E8.5 in the mouse development (Tropepe et al., 1999) and FGF-b inducing the appearance of later EGF-responsive NSCs by up-regulation of Egf-Receptor expression (Ciccolini and Svendsen, 1998; Olalla and Covarrubias, 1999; Lillien and Raphael, 2000). To induce differentiation, mitogens are withdrawn from the culture medium and NSCs are plated on a permissive substrate. This gives rise to a heterogeneous population with different neuronal and glial cell composition depending on the regional origin and developmental stage of the initial NSC.

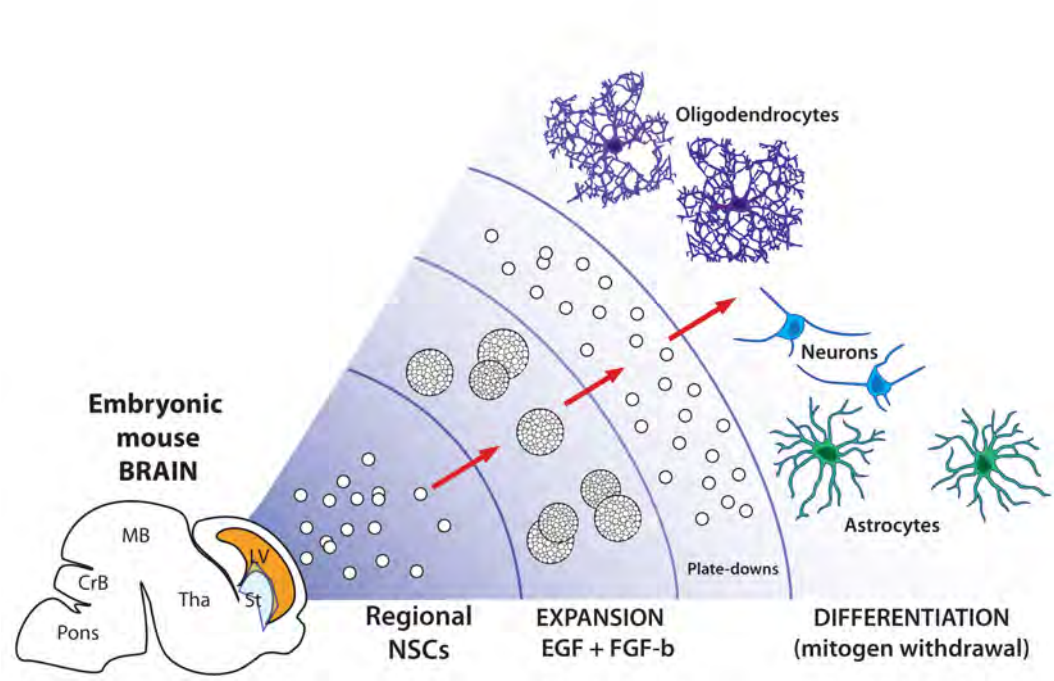

Figure 1—1 Classical fetal neural stem cell culture
NSCs isolated from the developing brain can be expanded as neurospheres in the presence of EGF and/or FGF and differentiated upon mitogen withdrawal.

NSC expanded in vitro survive upon transplantation, differentiate into neurons and astrocytes in vivo (Gage et al., 1995) and maintain their positional identity after exposure to mitogens in vitro. Indeed, Zappone et al. have showed that

cortical E14.5 NSCs, but not spinal-cord derived NSCs, express telencephalic transcription factors even after two months in culture in the presence of EGF and FGF (Zappone et al., 2000). Similarly, Hitoshi et al. demonstrated that hindbrain, midbrain and forebrain embryonic NSCs maintain regional specific expression of regulatory genes in culture (Hitoshi et al., 2002). Accordingly, Chen et al. have shown that hippocampal but not subventricular zone-derived NSCs generate dentate gyrus neurons - neuronal nuclear antigen (*NeuN*) and Prospero homeobox protein-1 (*Prox-1*) expressing cells - upon transplantation into the adult dentate gyrus (Chen et al., 2011). However, Santa-Olalla et al. have reported that the expression of several regional-specific gene markers is altered or lost in vitro and that neurospheres derived from one single NSC co-express several regional-specific markers (Santa-Olalla et al., 2003). This suggests that NSC fate is the result of a combination of extrinsic signals and intrinsic programming and that under certain culture conditions, regionally specified NSCs can revert to a less committed state.

1.1.1 Embryogenesis of NSCs

Following fertilisation, the egg undergoes a series of rapid cell divisions that give rise to a blastocyst. This is a relatively simple structure formed of an outer layer of cells, an inner cell mass (ICM) and a cavity or blastocoel. The outer cells form the trophoectoderm that will give rise to the placenta, while the ICM gives rise to the extraembryonic ectoderm and the epiblast. This segregation is partially controlled by the expression of octamer-binding transcription factor-4 (*Oct-4*), as *Oct-4* down-regulation occurs in the trophoectoderm (Palmieri et al., 1994) and blastocysts lacking *Oct-4* fail to generate a pluripotent ICM (Nichols et al., 1998).

After implantation into the uterine wall, the blastocyst becomes a three-layered structure by a process of complex tissue rearrangements called gastrulation (for review see Lu et al., 2001). At this stage, cells on the involuting marginal zone (IMZ) of the embryo migrate from the surface of the blastocyst into the centre through a small invagination called the blastopore. These cells are the origin of all mesodermal tissues in the embryo and also form a transient rod-shaped structure (the notochord) that is essential for neural induction. In mammals, neurogenesis begins with the formation of the neuroectoderm, which gives rise to the neural plate (at E7.5 in mice) and subsequently folds into the neural tube (at E8.5 in mice). The sry-related HMG box genes (*Sox*) genes - *Sox1*, *Sox2* and *Sox3* among others - are some of the earliest transcription factors expressed in the neural primordial tissues and seem to have a conserved role in neural determination and neural plate formation in metazoans (Sasai, 2001; Uchikawa et al., 2011). NSCs in the neural tube give rise to all neurons and glia in the CNS of vertebrates.

Neural crest cells arise at the interphase between the future neural tube and the non-neural ectoderm. These are transient embryonic NSCs that are exclusive to vertebrates. Neural crest cells undergo profound cytoskeletal and morphological changes, delaminate from the neuroepithelium and will eventually migrate to all areas of the embryo to terminally differentiate into neurons and glia from the sympathetic and parasympathetic PNS but also melanocytes and cartilage derivatives (for review see Sauka-Spengler and Bronner-Fraser, 2008).

The neural tube is initially composed of a single pseudostratified neuroepithelium. Neuroepithelial cells have strong apical-basal polarity and tight cellular junctions in the apical or luminal region. Prior to the onset of neurogenesis (around E9 in

mice), the neuroepithelial cells lose some of their epithelial characteristics, such as apical tight junctions, (Aaku-Saraste et al., 1996) and acquire astroglial features becoming radial glial (RG) cells. These astrocytic features include the expression of glial fibrillary acidic protein (GFAP) in primates (Levitt and Rakic, 1980; Choi, 1981), astrocyte-specific glutamate transporter (GLAST) and brain lipid binding protein (BLP) in rodents (Hartfuss et al., 2001) RG cells present a bipolar morphology that spans the entire radial axis of the neural tube and act as a cellular scaffold that provides cues for radially migrating neuroblasts (Rakic, 1972).

Both neuroepithelial and RG cells are mitotically active and display interkinetic nuclear migration during mitosis. In this process, the nucleus of these cells is located in the apical or luminal side, migrates towards the basal side during G1, undergoes the S phase at the basal side and finally returns to the apical side during G2. Nuclear migration spans the whole apical-basal axis in neuroepithelial cells but is restricted to the apical side in radial glial cells (Takahashi et al., 1993). This process is thought to be important in modulating the exposure of the nucleus to instructive signals originating from the apical membrane. Interestingly, RG cells maintain the expression of neural precursor cell markers such as the intermediate filament proteins vimentin and nestin (Chanas-Sacre et al., 2000) and not only guide neuronal migration but also function as NSCs (Noctor et al., 2001).

In the luminal or ventricular zone (VZ) neuroepithelial and RG cells undergo symmetric or proliferative divisions and asymmetric or neurogenic divisions giving rise to basal progenitors (BP). These cells form the new proliferating subventricular zone (SVZ or intermediate zone) that appears at E13.5 and expands dramatically during late development. BP are more fate-restricted NSCs that lose

apical contact and divide symmetrically in the SVZ to generate two immature neurons. This additional level of cell division at the SVZ increases the number of neurons derived from one single NSC and is associated with the evolutionary expansion of the neocortex (Miyata et al., 2004; Noctor et al., 2004). It is not completely clear how this fine balance between migration, symmetric and asymmetric divisions in SVZ and VZ NSCs is achieved, but cytoskeletal proteins – such as doublecortin (DCX) or centrosomal protein 152 (CEP152) - are likely to play an important role as mutations in these proteins affect cortical development and can cause lissencephaly (smooth cortical surface), microcencephaly (abnormally small brain) or abnormal cortical thickness (for review see Manzini and Walsh, 2011).

After the formation of the neural tube, a series of vesicles develop along the anterior-posterior axis: the prosencephalon (forebrain), the mesencephalon (midbrain) and the rhombencephalon (hindbrain). Simultaneously, the neural tube is also patterned dorso-ventrally to form the floor plate and the roof plate (for review see Lumsden and Krumlauf, 1996). Integration and decoding of positional and temporal information enables the generation of an extraordinary diverse range of neuronal and glial cell types with differential morphological, electrophysiological and molecular features from a limited number of NSCs.

1.1.1.1 Dorso-ventral patterning

Dorso-ventral patterning in the neural tube is determined by gradients of diffusible ventralising factors of the hedgehog family and by dorsalising factors of the bone morphogenetic protein family (*Bmps*).

BMPs are member of the transforming growth factor-β (*Tgf-β*) family that bind to two types of serine-threonine kinase receptor (BMPR-I or BMPR-II). Receptor activation leads to phosphorylation of SMAD proteins, complexing with the cofactor co-SMAD. These complexes are then translocated into the nucleus where they control gene expression. BMP signalling can be modulated at several levels: extracellular BMP antagonists (such as noggin or chordin), decoy receptors like BAMBI, intracellular inhibitory iSMAD proteins or SMURF proteins that induce Smad degradation (for review see Liu and Niswander, 2005). BMP signalling is required for ectodermal differentiation during early embryogenesis but must be inhibited to allow neural induction and the formation of the neuroectoderm (Lamb et al., 1993; Wilson and Hemmati-Brivanlou, 1995). Interestingly, after closure of the neural tube, BMP signalling is necessary for the specification of neural crest cells (Nguyen et al., 2000) and the roof plate of the neural tube becomes a new organizing centre that generates a dorso-ventral BMP gradient. BMP signalling arising from the roof plate is essential for the dorsal specification of the spinal cord (Lee et al., 2000), telencephalon (Hébert et al., 2002) and cerebellar granule neurons (Rios et al., 2004).

Sonic hedgehog (SHH) is a ventralising signal initially released by the notochord and at later stages by the midline of the neural tube (Marti et al., 1995). SHH acts as a long-range morphogen that induces differential gene expression in a concentration and time dependent manner. In target cells, SHH signalling results in the activation of the glioma-associated oncogene family members (*Gli1*, *Gli2* and *Gli3*) for review see (Hui el al., 2011). GLI proteins are transcriptional activators and repressors that control the expression of homeodomain and basic helix-loop-helix (bHLH) transcription factors and modulate the cellular

responsiveness to SHH itself. Downstream genes include SHH inhibitors such as protein patched homolog-1 (*Ptch1*) (Incardona et al., 2002) or transmembrane Shh enhancers such us growth arrest specific protein-1 (*Gas1*) and the membrane protein *Cdo* (Allen et al., 2007). Furthermore, SHH-regulated genes have different responsiveness to SHH levels depending on the number of GLI binding sites present on their promoter. Therefore morphogen concentration and signal duration are modulated by target NSCs in the neural tube which means that SHH patterning along the DV axis is not simply the result of localised SHH-production by the floor plate (for review see Dessaud et al., 2008). This originates a dynamic regulatory network that integrates positional and temporal information to specify NSC identity.

1.1.1.2 Anterior-posterior patterning

In mammals, forebrain patterning during early embryogenesis is mediated by the anterior visceral endoderm (AVE) – an extraembryonic tissue that underlies the prospective neural plate - as removal of the AVE causes a reduction in forebrain markers (Thomas and Beddington, 1996). At E7, the AVE expresses molecules such as cerberus and dickkopf that can block WNT signalling as well as acting as nodal and BMP antagonists. By E7.5, the neural tube is divided by the expression of the two transcription factors: orthodenticle homologue-2 (*Otx2*) that is expressed in the anterior neural tube (Simeone et al., 1992) and gastrulation brain homeobox-2 (*Gbx2*) that is expressed in the posterior neural tube (Wassarman et al., 1997). The boundary between *Otx2* and *Gbx2* expressing areas marks the position of the isthmic organiser (IsO) and consequently the separation between mesencephalon and rhombencephalon. The IsO acts as an organizing centre that is

necessary and sufficient for the development of the midbrain and hindbrain domains (for review see Wurst and Bally-Cuif, 2001). *Otx2*-KO mice do not develop the midbrain but have instead a giant cerebellum (Acampora et al., 1997) whereas *Gbx2*-KO mice have a extended midbrain and lack rhombomeres 1-3 and a cerebellum (Wassarman et al., 1997) By E8.5 the transcription factor paired box-2 (*Pax2*) becomes expressed in the mid-hindbrain boundary (Rowitch and McMahon, 1995) and leads to the expression of *Wnt1* mostly in the anterior-*Otx2* region and *Fgf8* in the posterior *Gbx2* expressing area (Crossley and Martin, 1995). Both WNT1 and FGF8 are required for mid-hindbrain patterning as midbrain and cerebellum fail to form in *Wnt1*-KO (McMahon et al., 1992) or *Fgf8*-KO mice (Meyers et al., 1998). Interestingly, FGF8 alone can induce ectopic midbrain formation in the forebrain regions (Crossley et al., 1996) and repress *Hox* genes allowing the specification of the first rhombomere (Irving and Mason, 2000). Once established, the midbrain-forebrain boundary is reinforced by complex genetic interactions. *Gbx2*, *Fgf8* and *Pax* genes in the hindbrain and Otx2, Wnt1 and engrailed genes 1 & 2 (En1 & En2) in the midbrain form a positive feedback regulatory loop that maintains the mid-hindbrain identity (Wurst and Bally-Cuif, 2001). The di-mesencephalic boundary is defined by *Pax6* which represses mesencephalic fate by repressing the expression of *En1*, *En2*, *Pax2*, *Pax5* (Matsunaga and Nakamura, 2000).

Hindbrain is formed by regionalisation of the caudal neural tube into seven lineage-restricted cellular compartments or rhombomeres (r1-7). Segmentation is initially driven by a gradient of retinoic acid (RA) that is produced by somites flanking the caudal hindbrain (Gavalas, 2002). RA activates the expression of the homeobox protein genes (*Hoxa1* and *Hoxb1*) caudally to the prospective r2.

Hoxb1 expression induces the production of KROX20 within r3. This event initiates a process of compartmentalisation driven by complex auto and cross-regulatory loops between *Hox* genes that culminates with the segmentation of the hindbrain (for review see Alexander et al., 2009). Ephrin receptors are expressed in r3 and r5 while their membrane bound ligands - the ephrins - are expressed in r2, r4 and r6. This creates differences in cell adhesion and repulsion that help to maintain the cellular boundaries between adjacent rhombomeres (Cooke and Moens, 2002). The specific expression pattern of *Hox* genes acts as a transcription factor code that provides positional identity to hindbrain NSCs.

1.1.1.3 Temporal patterning

It is important to emphasise that positional information alone cannot determine the fate of a NSC. Instead the developmental program integrates a fourth coordinate given by the temporal dimension. Indeed, CNS and PNS neurons arise before glial cells and specific cell types have specific birthdates. It is also well known that different types of neurons arise in a stereotypical order during development. In the retina, all neurons and glia arise from a common NSC (Turner and Cepko, 1987) following progressive restriction in cell competence that is modulated by both intrinsic and extrinsic factors. Amacrine interneurons appear around E10 in the mouse embryo followed by cone cells and bipolar cells. Müller glial cells are born mainly postnatally whereas rods are produced both pre and postnatally (Cepko et al., 1996). Another classical example is the development of the cerebral cortex, where different neuronal temporal identities are organized into six morphologically distinct layers. Layer specific neuronal subtypes within the cortical plate are generated from RG-NSCs in the VZ and

BP-NSCs in the SVZ with later-born neurons migrating to more superficial layers than earlier-born neurons (for review see Molyneaux et al., 2007). Early cortical NSCs can produce late-born neurons upon transplantation into the late SVZ, however late NSCs transplanted into a younger environment can not respond to early environmental cues and are restricted to late neuronal fates (Desai and McConnell, 2000). Furthermore, using time-lapse imaging, Shen et al. demonstrated that a single cortical NSC can generate both Cajal-Retzius neurons (one of the earliest born neurons in the neocortex) and cortical-layer neurons in vitro and that these neurons are born following the same developmental time line and fate restriction observed in vivo. (Shen et al., 2006). This suggests the existence of an intrinsic developmental program in cortical progenitors that drives the specific temporal generation of different neuronal subtypes. Such intrinsic program is well known in *Drosophila melanogaster,* where temporal transcription factors are expressed in a stereotypical developmental sequence within individual neuroblasts (Grosskortenhaus et al., 2005). Neuroblasts from *D. melanogaster* express hunchback first, followed by kruppel, which specify early temporal neuronal identity. These are followed by expression of POU domain protein 1-2 (Pdm1-2) and castor which regulate late motor neuron identity (Grosskortenhaus et al., 2006). Regulatory loops between these transcription factors ensure that orderly expression of Hunchback ➔ Kruppel ➔ Pdm1/2 ➔ Castor is followed. However, a similar developmental sequence in mammalian NSCs has not been established.

Another interesting example of temporal pattering is the neuro-glial switch in vertebrates. Both neurons and glia originate from a multipotent NSC. However, neurons appear first in development (from E12 to E18), whereas astrogliogenesis

begins around E18 and oligodendrogenesis occurs postnatally (Miller and Gauthier, 2007). Accordingly, NSCs isolated from E10 mouse embryos give rise to neurons after 4-7 days in vitro whereas astrocytes and oligodendrocytes appear only after 10-14 days in vitro. Furthermore, the ability of NSCs to generate neurons decreases with embryonic age of the donor tissue (Qian et al., 2000), suggesting the existence of an intrinsic cellular program that governs this switch. Ciliary neurotrophic factor (CNTF), leukaemia inhibitory factor (LIF) and cardiotrophin-1 (CT-1) are known be potent stimulators of astrocytic fate by activation of the Janus kinase (JAK) – signal transducer and activation of transcription (STAT) pathway (for review see Miller and Gauthier, 2007). However, in early NSCs, the promoters of key astrocytic genes are methylated and therefore cannot be activated by STAT binding (Takizawa et al., 2001). Reciprocally, in late NSCs, the promoters of proneuronal genes such as neurogenin-1 and 2 (*Ngn1/2*) are rarely associated with RNApol II and present methylation and acetylation patterns that are consistent with a closed chromatin conformation (Hirabayashi et al., 2009). Taken together, these results suggest that NSCs lose their competence to generate neurons during development due, at least in part, to intrinsic epigenetic changes. Remarkably, Namihira et al. have shown that during mid-gestation, newly born $NGN1^{+}$ neurons express Notch ligands that induce the expression of the transcription nuclear factor-1 (*Nf-1*) in neighbouring NPCs. Upon NF-1 binding, the *Gfap* promoter is demethylated, becoming responsive to JAK-STAT activation by CT-1 which is also released by newly-born neurons (Namihira et al., 2009). This provides an elegant mechanism by which NSCs that are intrinsically programmed to generate exclusively neurons start producing astrocytes once a sufficient number of neurons have been formed.

1.1.2 Adult NSCs

The first evidence for the persistence of neurogenesis after birth was provided by Altman and Das in 1965. They injected tritiated thymidine (T[H^3]) into 10 days to 8 month-old rats and found prominent T[H^3] incorporation in the DG of the hippocampus. They also found that the number of dividing cells decreased sharply with age but remained active throughout adulthood. Unfortunately, Altman and Das failed to understand the true significance of their finding. They postulated a ventricular origin for the newly formed neurons in the DG and hypothesised that these neurons would act as gonadal hormones sensors (Altman and Das, 1965). Perhaps for this reason and the controversy over newly form neurons in the adult brain, their findings received little attention. Twelve years later, Kaplan and Hings recapitulated these results and demonstrated the existence of newly-generated neurons in the granular layers of the hippocampus and the olfactory bulb (OB) that survived for at least 30 days and postulated that adult neurogenesis could contribute to plasticity of the brain (Kaplan and Hinds, 1977). This theory was confirmed in studies with canaries, where continuous generation of new neurons was shown to be important for song acquisition (reviewed in Nottebohm, 2004). Moreover, adult neurogenesis seems to be a common feature in vertebrates including primates (Gould et al., 1999) and humans (Eriksson et al., 1998). In rodents, adult neurogenesis is restricted to the subventricular zone (SVZ) of the lateral ventricles, where around 30,000 neuroblasts are generated each day (Lois and Alvarez-Buylla, 1994) and the subgranular zone (SGZ) of the DG in the hippocampus where between 3,000 to 9,000 neuroblasts are generated every day (Cameron and McKay, 2001). Apoptotic neurons are present in neurogenic areas and it is estimated that at least 50% of the newly-generated neurons do not survive

after 30 days (Petreanu and Alvarez-Buylla, 2002), which is why adult neurogenesis does not result in increased hippocampal or OB volume.

Astrocyte-like cells, termed type B cells, are slowly proliferating NSCs that give rise to a rapidly amplifying and transient NSC population: In the DG, astrocytic type B cells give rise to intermediate progenitor cells (type D cells) that then differentiate into granule neurons (type G), see Figure 1—2, (Seri et al., 2001). In the SVZ, early studies suggested that ependymal cells (surrounding the ventricle) could represent the NSC population in this area and give rise to new neurons and astrocytes (Johansson et al., 1999). However, this was refuted in a seminal paper from Fiona Doetsch and colleagues in 1999, which demonstrated that the SVZ regenerates completely after antimitotic treatment with arabinofuranosyl cytidine (AraC). This eliminated rapidly proliferating progenitors (type C) and migratory neuroblasts (type A) but spared the slowly proliferating type B cells and ependymal cells. T[H^3] labelling appeared initially in the surviving Type B cells and was then transferred to type C nuclei and subsequently to type A nuclei, suggesting that these two cell types originate from the type B NSCs. Furthermore, when type B astrocytes were specifically infected with an alkaline phosphatase (AP)-expressing retrovirus, AP^+ cells could be detected along the rostral migratory stream (RMS) after 24 hours and gave rise to glomerular and granular OB interneurons after 14 days. Moreover, only type B cells but not ependymal cells gave rise to multipotent neurospheres in vitro (Doetsch et al., 1999). All together, these data firmly established that type B astrocytes in the SVZ are true NSCs that give rise to all other cell types in the SVZ (Figure 1—2). Once formed, neuroblasts (type A cells) originated in the SVZ travel up to 5mm along the RMS towards the OB through specialised glial tubes formed by astrocytes, a process

that is termed *chain migration* (Lois et al., 1996). Despite the initial controversy, ependymal cells are, key components of the SVZ niche. SVZ NSCs express BMPs and their receptors that are potent inhibitors of neuronal differentiation. Ependymal cells adjacent to the SVZ release noggin that antagonises BMP signalling creating a permissive neurogenic niche in the vicinity of the ventricles (Lim et al., 2000). Adult neurogenic niches, are also closely associated with the vascular niche as endothelial cells have been shown to release soluble factors that stimulate self-renewal and promote neurogenesis in the embryo and in the adult (Shen et al., 2004).

Adult neurogenesis is transiently increased with stroke in the SVZ (Zhang et al., 2004), with pregnancy in the DG of the hippocampus and SVZ (Shingo et al., 2003), with enriched environment (Kempermann et al., 1997), voluntary exercise (Van Praag et al., 1999) and dietary restriction (Lee et al., 2002). It is also stimulated after ischemia (Yagita et al., 2001) or seizures in the hippocampus (for review see Scharfman, 2004). The two main inhibitory factors are corticosteroids/stress (Cameron and McKay, 1999) and ageing (Kuhn et al., 1996). The functional implications of adult neurogenesis remain controversial, however, some studies have suggested a potential implication in maternal behaviour, odour discrimination, fear conditioning and memory and learning. It has also been suggested that incorporation of new neurons into a functional network could improve the adaptability or plasticity of the system (reviewed in Zhao et al., 2008).

In summary, brain development begins with the induction of the neural plate and the appearance of the first NSCs, the neuroepithelial cells. These cells develop

into RG-NSCs and then give rise to immature neurons and a more restricted type of NSC, the BP-NSCs. Along the process, the intrinsic NSC developmental program is driven by positional and temporal cues that lead to the generation of all neuronal and glial subpopulations in the nervous system. In general terms neurogenesis is completed prenatally whereas gliogenesis, synaptogenesis, myelination and neuronal pruning culminate during early postnatal life. However, in at least two areas of the adult mammalian brain, adult NSCs remain active throughout life and new neurons and glia are incorporated into functional neural networks. Thus, in a way, brain development – and NSC involvement - is a never ending story.

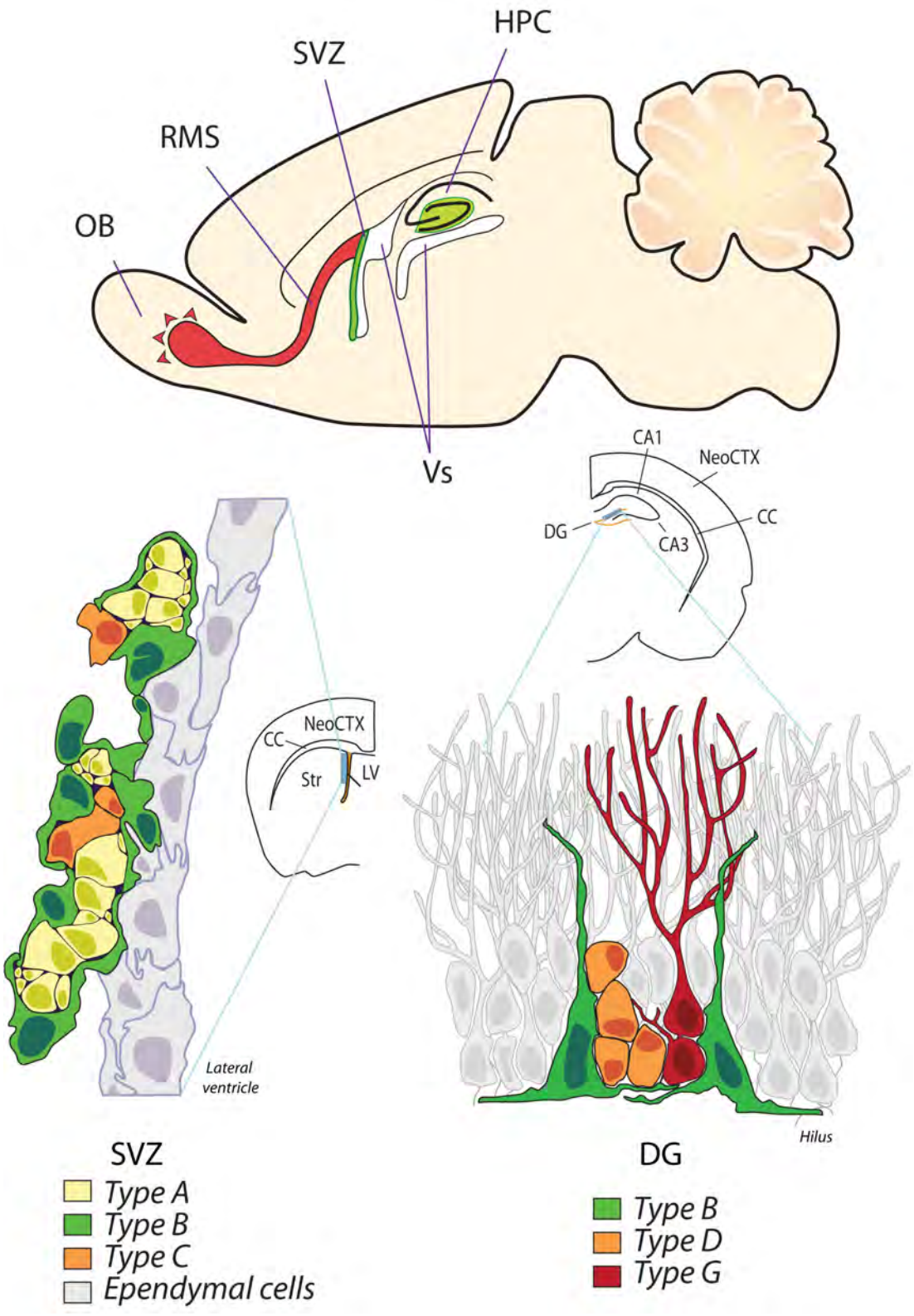

Figure 1—2 Adult neurogenic areas

Cellular composition of the two main neurogenic areas in the adult rodent brain. CC: corpus callosum; HPC: hippocampus; LV: lateral ventricle; CTX: cortex; OB: olfactory bulb; RMS: rostral migratory stream SVZ: subventricular zone Vs: ventricles.

1.2 Neurotrophic factors

In this thesis, the term neurotrophic factor (NTF) will be used in its broad sense to include any secreted protein that can promote differentiation, survival and maturation of developing neurons or support and protect mature neuronal populations.

It is generally believed that NTFs are essential for the survival and selection of postnatal and adult neuronal populations but not strictly required for the formation of the nervous system *per se*. This is sustained by the fact that most of NTF-KO mice display relatively normal brain development and die only postnatally and by the apparent absence of conserved neurotrophins in *Drosophila melanogaster*. However, some NTFs (such as *Bdnf*, Fukumitsu et al., 2006) have also been implicated in early embryonic patterning and specification of cortical neurons. Moreover, the specific trophic requirements and extrinsic signals required by specific NSC and neuronal populations within the brain have not been completely elucidated so a role for NTFs in brain development cannot be excluded.

A comprehensive review of all NTFs described in the current literature is beyond the scope of this thesis. However, for illustrative purposes we will briefly describe some of the most widely studied NTFs: the *Ngf* and the *Gdnf* family.

1.2.1 Neurotrophins

In the 1950's, Rita Levi-Montalcini discovered that protein extracts from mouse sarcomas had potent growth-promoting effects on chick embryonic sensory ganglions in vitro. These cells extended neurites within minutes of application of

very small amounts of the extract and formed a remarkable sun-like halo around the sensory ganglion within 24 hours (Levi-Montalcini and Hamburger, 1953). Levi-Montalcini and colleagues subsequently found similar biological activities in mice salivary gland extracts and also in snake's venom (Cohen and Levi-Montalcini, 1956). This led to the identification of nerve growth factor (NGF) as the active protein present in the sarcoma extracts. For this discovery, Rita Levi-Montalcini was awarded the Nobel Prize in Medicine and Physiology in 1986.

Since then, three other neurotrophins have been discovered in mammals with similar abilities to promote nerve growth: Brain derived neurotrophic factor (*Bdnf*), neurotrophin-3 (*Ntf-3*) and neurotrophin-4 (*Ntf-4*). NGF binds preferentially to tyrosine receptor kinase A (TRKA); BDNF and NT-4 to TRKB and NT-3 to TRKC (Chao, 2003). Ligand binding causes receptor dimerisation, autophosphorylation and activation of phosphatidylinositol 3-kinase (PI3K); AKT, known to be involved in cell survival or extracellular-signal regulated kinase (ERK), also known to be involved in cell survival, cell cycle regulation, synaptic plasticity and neurite outgrowth. All neurotrophins can also bind to the p75 receptor which leads to c-Jun N-terminal kinase (JNK) activation and apoptosis (for review see Chao, 2003). Additional functional complexity results from the formation of heterodimeric complexes between p75-NTR and TrkA, TrkB, or TrkC modulating the signalling properties of both members of the complex. This dual role makes neurotrophins master regulators of neuronal fate, capable of controlling both cell death and survival.

1.2.1.1 Ngf

Ngf is essential for the development and survival of specific neuronal populations in the PNS. In the classical paradigm, NGF is synthesised within innervated tissues and provides trophic support for the afferent neurons by activating intracellular pro-survival pathways via TRKA (Reichardt, 2006). However, Deppmann et al. have demonstrated that NGF signalling plays a more aggressive role during development, helping to achieve effective target-tissue innervation by promoting sympathetic neuronal competition. In this model, target-released NGF promotes the expression of its own receptor *TrkA* and enhances TRKA mediated signals, which result in a positive trophic feedback within the innervating neuron. This leads to the release of BDNF and NTF-4 that bind to p75 in neighbouring neurons causing cell apoptosis in those cells with low pro-survival NGF signalling or unsuccessful target contact (Deppmann et al., 2008).

Crowley et al. showed that *Ngf*-KO mice exhibited severe neuronal loss in sensory and sympathetic ganglia and do not respond to sensory stimuli. These mice died perinatally and no abnormalities were described in the CNS at this age - within 4 weeks (Crowley et al., 1994). Ruberti et al. generated mouse lines that expressed NGF-autoantibodies resulting in a 50% reduction in the levels of NGF in the adult brain. They reported marked reduction in the number of cholinergic neurons in the basal forebrain and hippocampus at two months, sympathetic and sensory neuronal loss and skeletal muscle dystrophy (Ruberti et al., 2000). Similarly, loss of the NGF receptor *TrkA* causes perinatal lethality, severe sympathetic and dorsal root ganglia (DRG) neuronal loss as well as reduced cholinergic innervation to the hippocampus and basal forebrain (Smeyne et al., 1994). Remarkably, NGF can

revert the age-associated atrophy of basal forebrain cholinergic neurons in rhesus monkeys (Smith et al., 1999) and has been shown to partially delay the cognitive decline in Alzheimer's disease (AD) (Tuszynski et al., 2005). The potential of NGF to halt or reverse neuronal cell loss in AD is currently being explored in several clinical trials.

1.2.1.2 Ntf-3

Ntf-3 is highly expressed in regions of on-going NSC proliferation, migration and differentiation (Maisonpierre et al., 1990). *Ntf-3* levels decline postnatally but are maintained in the hippocampus where they promote differentiation of newly generated neurons and spatial learning (Shimazu et al., 2006). *Ntf3*-KO mice have severe limb movement deficits, pronounced peripheral sensory and sympathetic neuronal loss and die shortly after birth (Ernfors et al., 1994; Fariñas et al., 1994). Furthermore, double KO mice for *Ntf3* and its receptor *TrkC* die within 48 hours of birth and show a great reduction in oligodendrocyte progenitor numbers, mature oligodendrocytes and astroglial markers (Kahn et al., 1999), indicating that NTF-3 and TRKC signalling are not only required for neuronal but also for glial survival.

1.2.1.3 Bdnf

Brain derived neurotrophic factor (BDNF) was initially purified from pig brain and similarly to NGF promoted survival and neurite outgrowth from chicken sensory neurons (Barde et al., 1982). BDNF is synthesised as a pre-pro-peptide, packed into secretory vesicles as a pro-peptide and released from neurons via constitutive secretion or activity-dependent secretion (Mowla et al., 1999). Once

secreted, pro-BDNF is cleaved by extracellular proteases giving rise to mature BDNF (Lee et al., 2001). As explained above, there are two main classes of BDNF receptors in the brain, the tropomyosin-related kinase receptor type B (TRKB) (Soppet et al., 1991) and p75 which belongs to the *Tnf* receptor family. Mature BDNF binds preferentially to TRKB whereas pro-BDNF has higher affinity for p75 (Lee et al., 2001). Interestingly, while mature GNDF binding to TrkB leads to AKT and ERK activation and enhancing cell survival, proGDNF binding to p75 leads to JNK and caspase-3 activation and eventually apoptosis (Koshimizu et al., 2010). Therefore, BDNF processing is a key regulatory step to control BDNF function. During embryogenesis, *Bdnf* is required for the specification of the cortical layers (Fukumitsu et al., 2006). In the adult brain, BDNF is anterogradely transported from cell somas in the entorhinal cortex and substantia nigra and released at nerve terminals in the hippocampus and striatum respectively (Altar et al., 1997) triggering dendrite (but not axonal) outgrowth and branching in neighbouring neurons (Horch and Katz, 2002). BDNF secretion is regulated by neuronal network activity and controls synaptic potentiation and the formation of dendritic structures at the level of single spines (Tanaka et al., 2008). This is important for long-term potentiation at glutamaergic synapses and memory consolidation. Indeed several studies have established a role for BDNF and TRKB activation in learning and memory (Yamada et al., 2002). Furthermore, administration of BDNF increases hippocampal neurogenesis (Scharfman et al., 2005) and BDNF is required for the rise in neurogenesis following environmental enrichment (Rossi et al., 2006). Accordingly, conditional loss of *TrkB* severely reduces neurogenesis in the adult DG (Li et al., 2008) and the incorporation and arborisation of newly-generated neurons into the hippocampal network (Bergami

et al., 2008). Remarkably a valine to methionine (V66M) substitution in the pro-region of human *BDNF* that compromises the activity-dependent release of BDNF but not its constitutive secretion, causes poorer episodic memory, altered hippocampal activation - assessed by functional magnetic resonance imaging (fMRI) - and lower hippocampal synaptic activity in human patients (Egan et al., 2003).

Interestingly, *BDNF* levels are reduced in the entorhinal cortex and hippocampus of AD patients and it has been suggested that this reduction of trophic support could contribute to the severe neurodegeneration observed in AD (Hock et al., 2000). Supporting this hypothesis, Nagahara et al. demonstrated that lentiviral mediated delivery of *Bdnf* into the entorhinal cortex in the $APP^{sw/ind}$ mouse model of AD results in improved water maze performance, synaptic recovery in the hippocampus and entorhinal cortex and improved gene deregulation caused by amyloid precursor protein (*App*) overexpression. Furthermore, BDNF reduced amyloid-β-induced neuronal death in vitro and hippocampal neurodegeneration caused by perforant path transection (PPT) in vivo. Similarly, BDNF treatment in aged rats and primates reversed cognitive decline, age-related gene disregulation and abnormal cell signalling (Nagahara et al., 2009). Interestingly, NSC transplantation into the hippocampus of triple transgenic mice carrying mutations in tau, presenilin and APP as a model of AD, results in increased hippocampal synaptic density accompanied with improved water maze and novel object recognition performance. Remarkably, these effects were mediated by *Bdnf* as knock down in the transplanted NSCs abolished any cognitive improvement (Blurton-Jones et al., 2009).

BDNF is a well known neurotrophic factor for dopaminergic neurons in the substantia nigra (SN) (Hyman et al., 1991) and is commonly used to induce dopamine neuron differentiation in vitro. Interestingly, conditional loss of *Bdnf* in the SN and cortical neurons leads to impaired striatal development, severe motor deficits and postnatal death in mice (Li et al., 2012). Furthermore, the levels of BDNF are reduced in the SN in Parkinson's disease (PD) (Mogi et al., 1999) again suggesting that loss of neurotrophic support can be one of the causes that underlie neurodegeneration.

1.2.2 Glial cell line-derived neurotrophic factor family

The glial cell line-derived neurotrophic factor (*Gdnf*) family is composed of four members: *Gdnf*, neurturin, persephin and artemin. All family members have seven conserved cysteine residues with similar spacing and are distant relatives of the *Tgf-β* superfamily. *Gdnf* family ligands bind to receptor complexes formed by a specific Gdnf family receptor α protein (GFRα1 for GDNF; GFRα2 for neurturin; GFRα3 for artemin and GFRα4 for persephin) and RET, a tyrosine kinase receptor. RET autophosphorylation leads to the activation of multiple intracellular cascades involved in cell survival, differentiation and proliferation (for review see Sariola and Saarma, 2003). All four members have been found to exert neurotrophic effects on midbrain dopaminergic neurons in vitro and vivo, but special attention has been given to GDNF and neurturin, which have been used in clinical trials to halt or reverse the dopaminergic cell loss in PD.

1.2.2.1 Glial cell line-derived neurotrophic factor

GDNF was initially discovered for its ability to promote the survival and differentiation of dopaminergic neurons in embryonic midbrain NSC cultures (Lin et al., 1993). *Gdnf*-KO mice display abnormal embryogenesis of enteric, sympathetic and sensory neurons and die postnatally but have normal midbrain and CNS development (Moore et al., 1996). Despite this lack of effect on midbrain development, GDNF is essential for the postnatal survival of midbrain dopaminergic neurons (Granholm et al., 2000) and can induce the expression of tyrosine hydroxylase (TH) – the main enzyme in the dopamine synthesis pathway (Theofilopoulos et al., 2001). Furthermore, GDNF can reduce apoptosis of cultured dopaminergic neurons (Sawada et al., 2003) and protect these neurons against methyl-4-phenylpyridinium ion (MPP^+) (Hou et al., 2002), 6-hydroxydopamine (6-OHDA) (Eggert et al., 1999) or lipopolysaccharide (LPS) (Xing et al., 2010) in vitro.

In vivo, intranigral (Hoffer et al., 1994; Bowenkamp et al., 1995) or intrastriatal (Shults et al., 1996) injections of GDNF have been shown to reduce motor deficits and protect dopaminergic neurons in the 6-OHDA model of PD, but also to promote axonal sprouting and re-innervation in the deafferated striatum (Rosenblad et al., 1997). Similarly, in rhesus monkeys treated with the precursor of MPP^+ (MPTP), single injections (Gash et al., 1996) or long-term overexpression of *Gdnf* (Kordower et al., 2000) resulted in behavioural improvement and preservation of the nigro-striatal dopaminergic system. This suggests that the actions of GDNF are not restricted to the 6-OHDA model, but can protect dopaminergic neurons against various insults. Furthermore, GDNF has

been shown to enhance the survival and integration of midbrain grafts in rat models of PD (Rosenblad et al., 1996) and to increase the numbers of endogenous dopaminergic neurons in aged and MPTP-treated rhesus monkeys (Palfi et al., 2002), indicating that *Gndf*, in addition to its neuroprotective properties can enhance the plasticity of the nigro-striatal system.

Despite the promising preclinical evidence, GDNF has been used in clinical trials for the treatment of PD with mixed results. In a randomized controlled trial in patients with relatively advanced PD, intraventricular delivery of GDNF failed to provide any clinical improvement (Nutt et al., 2003) although this negative result was attributed to the failure of GNDF to reach the nigro-striatal system from this delivery route. Two open-label studies with GDNF infusion into the putamen did find significant decreases in unified PD rating scale (UPDRS) scores, accompanied with reduced dyskinesias and improved dopamine function assessed by positron emission tomography of F^{18}-dopamine uptake (Gill et al., 2003; Slevin et al., 2007) although these effects were lost after discontinuing the treatment (Slevin et al., 2007). These two studies lead to a randomized controlled trial with intraputaminal chronic infusion of GDNF in patients with advanced bilateral PD. After six months, F^{18}-dopamine uptake was improved in the GDNF group, in agreement with Gill et al. However, no differences were observed in the UPDRS scores or dyskinesias between GDNF-treated and placebo groups (Lang et al., 2006).

In summary, *Gdnf* is the prototypical neurotrophic factor for midbrain dopaminergic neurons and remains, to date, one of the most effective

neuroprotective factors in toxin models of degeneration. However, its efficacy in the treatment of PD is uncertain.

1.2.2.2 Neurturin

Neurturin was initially discovered due its ability to promote the survival of postnatal sympathetic neurons deprived of NGF in vitro (Kotzbauer et al., 1996). Neurturin is expressed in the developing nigrostriatal system and enhances survival and function of midbrain dopaminergic neurons (Horger et al., 1998). Similarly to *Gdnf*, neurturin can protect dopaminergic neurons and restore motor function in the 6-OHDA rat model of PD (Horger et al., 1998; Gasmi et al., 2007) and the MPTP model in rhesus monkeys (Li et al., 2003; Kordower et al., 2006). Based on this experimental evidence, neurturin delivered by adeno-associated virus into the putamen was used in an open-label clinical trial in patients with advanced PD. Ceregene initially reported significant improvements in UPDRS scores and dyskinesias (Marks et al., 2008). However, this was also followed by an unsuccessful double-blind trial in which neurturin not only failed to improve motor function but severe side-effects were reported (Marks et al., 2010).

1.2.2.3 Artemin and persephin

Like *Gdnf* and neurturin, persephin promotes the survival of midbrain dopaminergic neurons in vitro and after 6-OHDA lesion in vivo (Milbrandt et al., 1998). Artemin appears to be a more potent neurotrophic factor for dorsal root sensory neurons than for dopaminergic neurons (Baloh et al., 1998) and systemic administration of artemin has been used for the treatment of neuropathic pain (Gardell et al., 2003).

1.2.3 Other neurotrophic factors

Among the many other secreted proteins that can promote neuronal survival and maturation we should briefly mention two other factors: vascular endothelial growth factor (*Vegf*) and *Cntf*. Although initially characterised as an angiogenic secreted factor, *Vegf* also promotes axonal growth and maturation from DRG neurons (Sondell et al., 2008) and protects hippocampal neurons against glutamate excitotoxicity (Matsuzaki et al., 2001) as well as ischemic insults (Jin et al., 2000). Remarkably, deletion of the hypoxia-response element in the *Vegf* promoter causes adult-onset progressive motor neurons degeneration in the spinal cord (Oosthuyse et al., 2001) and *Vegf* overexpression delays motor neuron loss and increases life-span in superoxide dismutase-1 (*Sod-1*) mutant mice (Wang et al., 2007) which could suggest a potential role for *Vegf* in the treatment of amyotrophic lateral sclerosis (ALS). *Cntf* is a member of the four alpha-helical cytokine family including interleukin 6 (*Il-6* and *Lif*). *Cntf* plays an important role during brain development (Stöckli et al., 1991) and *Cntf*-KO mice display progressive loss of motor neurons and muscular atrophy (Masu et al., 1993). CNTF also promotes survival of DRG, hippocampal (Ip et al., 1991) and striatal neurons in vitro and is also considered a gliotrophic factor for astrocytes (Dallner et al., 2002) and oligodendrocytes (Stankoff et al., 2002).

In summary, NTFs are important factors for neuronal maturation and survival. Although the first NTFs were discovered in the last century, it is likely the many more factors will be discovered in the coming years. Many of these will probably be relevant for very specific neuronal populations, which would have hindered their discovery in the past. However, the current induced pluripotent stem cell

technology, the development of methodologies that allow the study of gene and protein expression within individual cells and the ever-growing list of cellular markers and transgenic models will, undoubtedly, accelerate the research in the field.

In this thesis, we will utilise NSCs isolated from the developing human or mouse brain as an in vitro model of neurogenesis. We will use this system as a tool to uncover and characterise novel NTFs that can promote the proliferation, neuronal differentiation and survival of fetal NSCs. Finally, in the last chapter we will use two recently-described NTFs in an attempt to prevent the neuronal cell loss in a rat model of neurodegeneration for PD.

Chapter 2

Chapter 2

Material and Methods

"It happens every time, they all become blueberries"
Willy Wonka, Charlie and the Chocolate Factory

2.1 Molecular biology methods

2.1.1 Horizontal agarose gel electrophoresis of DNA

In order to purify the desired DNA fragments or to determine their nucleotide length, plasmid DNA or PCR (polymerase chain reaction) products were routinely run on horizontal electrophoresis gels. This was done as follows. Electrophoresis grade agarose (Melford) was dissolved in 1X Tris-acetate buffer (TAE, Fisher) by boiling in a microwave oven. The gel mixture (2% [w/v] agarose in TAE buffer) was kept in a dry oven at 60ºC for later use. When required, this was mixed with 1X TAE to reach the desired agarose percentage (typically 1% [w/v]), reboiled in the microwave and allowed to cool. $0.5 mg \cdot l^{-1}$ of ethidium bromide (EtBr, Sigma) was added to the gel before casting, using a gel former containing a suitably sized comb. Once solidified, the gel was submerged in a horizontal gel electrophoresis tank containing 1X TAE buffer. To allow visualization and loading, samples were mixed with 6X *loading dye* {60% [v/v] glycerol (Sigma); 0.09% [w/v] orange G (<100bp, Sigma) and 0.09% [w/v] of xylene cyanol (>8,000bp, Sigma) or bromophenol blue (≈500bp, Sigma) or cresol red (≈2,000bp, Sigma)} and transferred into the wells. 5µl of standard molecular weight markers were run alongside the samples (*2-log DNA ladder*, New England Biolabs, NEB). The gel was run under a constant voltage ($5\text{-}10 V \cdot cm^{-1}$) until separation of the DNA

fragments of interest was achieved, before examination under UV-light (302nm). Images were taken using a *Gel Document System* (UltraViolet Products). If required, the DNA fragments of interest were excised using a clean scalpel blade and transferred into a 1.5ml-polypropylene tube.

2.1.2 Restriction digests

To facilitate different cloning strategies or to confirm the identity of cloning constructs, DNA fragments excised at specific nucleotide sequences were generated by digestions with the appropriate restriction endonucleases. These enzymes were purchased from *NEB* and incubated with the digestion buffer recommended by the manufacturer. For DNA analysis 0.3-1μg of plasmid were digested with the appropriate enzyme (using one unit of enzyme per microgram of DNA). Reactions were always performed in a 50μl volume with 10% [v/v] digestion buffer at the recommended incubation temperature and never allowed to proceed for more than 4h. When digesting DNA for gel extraction, see (2.1.6), 5-10μg of DNA were used and the amount of restriction endonuclease was adjusted accordingly. Enzymes were inactivated at the end of the digestion according to NEB's recommendations (typically by incubation at 65ºC for 20min). Reactions were done on a thermal cycler (*MJ Mini Personal TC*, Biorad).

2.1.3 Purification of DNA after enzymatic digestion

After a restriction reaction, the resulting DNA fragments appear contaminated with other components of restriction reaction mixture - including proteins, salts and glycerol. To isolate the DNA fragments to be used in subsequent cloning

steps, restriction reaction mixtures were purified using the QIAquick PCR Purification Kit (Qiagen) following manufacturer's instructions. Briefly, five volumes of the binding buffer PB were added per volume of digestion reaction. This mixture was then applied to a *QIAquick spin column* and centrifuged for 1min at 17,000 RCF (*Heraeus Pico 17*, bench top centrifuge, Thermo-Fisher). The flow-through was discarded and 750µl of wash *buffer PE* were applied to the column, followed by centrifugation as in the previous step. The flow-through was discarded and the column was centrifuged as before to ensure the complete elimination of *PE buffer*. Finally, 20-30µl of ddH_2O were added to the centre of the column and incubated for 5min at room temperature. The eluted DNA was recovered from the column by centrifugation as in previous steps.

2.1.4 Dephosphorylation of digested DNA fragments

To enhance the formation of insert-vector constructs during ligation reactions, the vector DNA was dephosphorylated prior to ligation. 5' phosphate groups in the DNA are necessary for the enzymatic action of DNA ligases, thus dephosphorylation of the DNA vector will prevent its re-circularization. This was done by enzymatic removal of the 5' phosphate groups of the vector DNA by treatment with Antarctic phosphatase (NEB). The reaction was set as follows:

Backbone dephosphorylation

	VOLUME	INCUBATION
DNA (1-5 µg)	**30µl**	***30min at 37ºC***
10X Buffer	**5µl**	
Antarctic phosphatase (5,000 U·ml^{-1})	**4µl**	
ddH_2O	**11µl**	

Table 2-1 Backbone dephosphorylation with Antarctic phosphatase
One enzymatic unit is defined as the amount of enzyme that dephosphorylates 1µg of vector in 30min at 37ºC.

2.1.5 Repairing DNA overhangs or cohesive ends

If no compatible restriction sites were found for cloning, DNA overhangs resulting from an enzymatic digestion were removed and the fragments were joined using a blunt ligation approach. 5' overhangs were filled in using the Klenow fragment of DNApol I from E. coli (NEB). 3' overhangs were removed by incubation with DNApol from T4 bacteriophage (NEB). Reactions were set up as follows:

Klenow fragment of DNA polymerase I

	VOLUME	INCUBATION
DNA (1-5 μg)	**10-20μl**	***1h at 37ºC***
10X NEB Buffer 2	**5μl**	
Klenow fragment (5,000 U·ml^{-1})	**2μl**	***20min at 75ºC***
10mM dNTPs	**2μl**	
ddH_2O	**Up to 50μl**	

T4 DNA polymerase

	VOLUME	INCUBATION
DNA (1-5 μg)	**10-20μl**	***15min at 12ºC***
10X NEB Buffer 2	**5μl**	
T4 DNApol (3,000 U·ml^{-1})	**3μl**	
10mM dNTPs	**2μl**	***20min at 75ºC***
BSA (10g·l^{-1})	**0.25μl**	
ddH_2O	**Up to 50μl**	

Table 2-2 Removal of ssDNA overhangs
Klenow fragment of DNApol I is used to fill in 5' overhangs (due to its 5'-3' DNApol activity but no exonuclease activity). T4 DNApol is used to remove 3' overhangs due to its 3'-5' exonuclease activity). One unit is defined as the amount of enzyme that can incorporate 10nmol of dNTP in 30min at 37ºC.

2.1.6 Purification of DNA From agarose gels

Frequently, following the electrophoretic separation of DNA products, specific fragments needed to be harvested and purified in order to facilitate subsequent

cloning steps. For this, restriction reaction or PCR mixtures were run on a horizontal gel as detailed in 2.1.1. Once the DNA band of interest was excised, DNA was extracted from the agarose gel using the *QIAquick Gel Extraction Kit* (Qiagen) following manufacturer's instructions. Briefly 3µl of *QG buffer* were added to 1mg of gel and incubated at 55ºC until the agarose was fully dissolved. 1µl of isopropanol was then added per milligram of gel and the mixture was applied to a QIAquick spin column and centrifuged for 1min at 17,000 RCF (*Heraeus Pico 17*, bench-top centrifuge, Thermo-Fisher). The flow-through was discarded and 750µl of *PE buffer* were applied to wash the column and centrifuged as in the previous step. The flow-through was again discarded and the column centrifuged as before to ensure the complete elimination of *PE buffer*. Finally, 20-30µl of ddH_2O were added to the centre of the column and incubated for 5min at room temperature. The eluted DNA was recovered from the column by centrifugation as in previous steps and kept at -20ºC for later use.

2.1.7 Nucleic acid quantification

In order to allow equimolar mixtures of insert to vector in ligation reactions or to enable the loading of equal amounts of RNA into PCR reactions, the concentration of DNA or RNA in samples was measured either using a Pearl nanophotometer (Implen) or by agarose-gel electrophoresis. For the second method, 1 and 5µl of the sample and 5µl of standard molecular weight markers of known concentration (*2-log DNA ladder*, NEB) were run alongside on an agarose gel as described in 2.1.1. For a similar DNA length, the band intensity is proportional to the amount of DNA in the gel. Therefore, comparison of the

brightness of the band of interest and that of the molecular weight markers can be used to approximate the DNA concentration in the sample.

2.1.8 Ligation of DNA fragments into plasmid vectors

To introduce cloning inserts into previously linearized and dephosphorylated vectors, insert DNA and vector DNA were mixed at different molar ratios (1:1, 3:1 and 5:1; insert to backbone. The molecular weights of vector and insert were calculated using the following expression:

$$dsDNA\ MW = \frac{length}{100} \times \left(\underbrace{\%GC \times 617.4\ g/mol}_{G\text{-}C\ pair\ MW} + \underbrace{(100 - \%GC) \times 618.4\ g/mol}_{A\text{-}T\ pair\ MW} \right) + \underbrace{36\ g/mol}_{2H_2O\ MW}$$

Equation 1 Molecular weight of dsDNA as function of GC% and length dsDNA=double stranded DNA; length=base pairs; 617.4= MW of (dGMP + dCMP – $2H_2O$); 618.4= MW of (dAMP + dTMP – $2H_2O$). This equation assumes the presence of a phosphate group at 5' of both DNA strands

Vector and insert DNA were joined using the *DNA ligation Mighty Mix* (Takara) following manufacturer's recommendations. Backbone and insert were mixed together in a 0.2ml-polypropylene tube (Anachem Ltd) and the final volume was adjusted to 10µl. To these, 10µl of Takara Mighty mix were added. The ligation reactions were done on a thermal cycler (*MJ Mini Personal* TC, Biorad) as follows:

Takara ligation	
	AMOUNT
Backbone	**25fmol**
Insert	**25-250fmol**
ddH_2O	**Up to 10µl**
3min at 65ºC 5min at 4ºC	
Takara Mighty Mix	**10µl**
Overnight at 16ºC	

Table 2-3 Backbone and insert ligation using Takara Mighty Mix

2.1.9 Transformation of competent *Escherichia coli* with recombinant DNA

In bacterial transformation using ligated DNA, a maximum volume of 5µl of each ligation reaction was added to 50µl of competent *Escherichia coli NEB-5-α High efficiency* (NEB). For plasmid DNA, 0.1-100ng of DNA in a maximum volume of 5µl was used to transform 50µl of competent *NEB-5-α* cells. Transformation was performed following manufacturer's specifications. Briefly, vials of competent cells were kept at -80ºC and thawed on ice when needed. The DNA was added to the cells, mixed gently and incubated on ice for 30min. Competent cells were heat-shocked at 42ºC for 30s on a water bath and then placed back on ice for five additional minutes. 500µl of pre-warmed SOC medium {20g·l^{-1} bacto-tryptone (Difco), 5g·l^{-1} yeast extract (Difco), 0.5g·l^{-1} NaCl (Melford), 0.9g·l^{-1} KCl (Sigma), 0.95g·l^{-1} $MgCl_2$ (Sigma) and 3.6g·l^{-1} *D*-glucose (Melford), pH7.0)} were added to cells and incubated in an *Innova 4230 Incubator Shaker* (New Brunswick Scientific) at 37ºC, 225rpm for 1h.

Lentiviral backbones contain direct repeat regions that are prone to recombination. For this reason, when large-scale preparation of lentiviral vector was required, the plasmids were transformed into *One Shot Stbl-3 Chemically*

competent E. coli (a recombination deficient strain from Invitrogen). Transformation of *Stbl-3* was done according to manufacturer's instructions. This protocol is similar to that of *NEB-5-α* except that it requires a longer heat-shock (45s) and the cells are recovered in a reduced volume of *SOC medium* (250µl).

Following recovery of heat shock in *SOC medium* 10% and 90% of the total cell suspension volume were spread (using a flame-sterilised glass rod) onto 90-mm Petri-dishes (Nunc) containing 10ml of solid Luria-Bertani medium {*LB-medium*: $25g \cdot l^{-1}$ LB (Fisher), $15g \cdot l^{-1}$ granulated agar (Difco) and 1mM NaOH} with the appropriate antibiotic. The bacterial plates were incubated overnight at 37ºC in an inverted position to allow bacterial growth, sealed and kept at 4ºC for short-term storage (less than two months).

2.1.10 *Miniprep*: Small-scale purification of plasmid DNA

Individual colonies were picked from bacterial plates prepared as described in 2.1.9 and inoculated into 5ml LB broth with the appropriate antibiotic. Cultures were incubated in an *Innova 4230 Incubator Shaker* (New Brunswick Scientific) at 37ºC, 225rpm for 16h. Plasmid DNA was purified using the *QIAprep kit* (Qiagen) following manufacturer's instructions, briefly: 1.5ml of the confluent culture were transferred into a 1.5ml-polypropylene (Fisher) tube and centrifuged at 4000 RCF (*Heraeus Pico 17*, bench-top centrifuge, Thermo-Fisher). The cell pellet was resuspended in 250µl of *PI buffer* and mixed with 250µl of the lysis *P2 buffer*. The lysis reaction was stopped by mixing with 350µl of *N3 buffer* and centrifuged for 10min at 17,000 RCF. The supernatant was applied to a *QIAprep spin column* and spun for 1min at 17,000 RCF. Flow-through was discarded and

500µl of *PB buffer* were applied through the column and discarded as previously. This was followed by addition of 750µl of *PE buffer* to wash the column and centrifugation as in the previous steps. The flow-through was again discarded and the column centrifuged as before to ensure the complete elimination of *PE buffer*. Finally, 20-30µl of ddH_2O were added to the centre of the column and incubated for 5min at room temperature. The eluted DNA was recovered from the column by centrifugation and kept at -20ºC until later use.

2.1.11 Long-term storage of bacterial clones

500µl of a confluent *miniprep*-culture were mixed with 500µl of sterile glycerol (Sigma) and stored at -80ºC. Bacterial clones were regrown by spreading bacteria picked from the surface of the frozen glycerol-stock (using a flame-sterilised glass rod) onto 90-mm Petri-dishes (Nunc). These were grown on LB medium with the appropriate antibiotic as explained in 2.1.9 and 2.1.10.

2.1.12 *Maxiprep*: Large-scale purification of plasmid DNA

500µl of a confluent *miniprep* culture were inoculated to 500ml of *LB-broth* medium, containing the appropriate antibiotic and incubated at 37 ºC, 200rpm for 16h in an orbital incubator shaker (Calenkamp). The resulting bacterial culture was centrifuged at 4,000 RCF (*Sorval Legend RT centrifuge*, Kendro) at room temperature for 20min. The culture medium was then discarded and the bacterial pellet resuspended in 18ml of *Solution I* (50mM glucose, 25mM Tris HCl pH8.0, 10mM EDTA pH8.0). The cells were then lysed by the addition of 2ml of lysozyme solution {$10g \cdot l^{-1}$ lysozyme (Sigma) in 10mM Tris-HCl pH8.0} and 40ml of *Solution II* {200mM NaOH; 1% [w/v] sodium dodecyl sulphate (SDS,

Sigma)} followed by incubation at room temperature for 10min. The lysis reaction was stopped by the addition of 20ml of ice-cold *Solution III* {3M CH_3CO_2K (Melford) and 5M CH_3CO_2H (Fisher)} and incubated on ice for 10min, until a white precipitate formed. After centrifugation at 4,000 RCF, the lysate was filtered through Whatman No1 filter paper (Whatman) into 50ml-polypropylene tubes (Corning) and the cell debris was discarded. 0.6 volumes of isopropanol were added per volume of lysate, mixed thoroughly and incubated at room temperature for 20min to allow the precipitation of the plasmid DNA. After centrifugation at 4,000 RCF (Rotanta 46R) at room temperature for 20min, the supernatant was discarded. The pellet was then briefly dried and resuspended in 3ml of TE Buffer {10mM Tris-HCl, pH8; 0.1mM EDTA, pH8}.

The resulting DNA suspension was purified by double CsCl gradient ultra-centrifugation. In order to do this, 1g of CsCl (Melford) was added per millilitre of TE-DNA, followed by $10g \cdot l^{-1}$ of EtBr and centrifugation at 4,000 RCF (*Rotanta 46R*) for 10min at room temperature. The pellet was discarded, the supernatant transferred into 11.2ml-*Optiseal tube* (Beckman), topped up with TE:CsCl solution (1ml of TE: 1g of CsCl) and centrifuged at $4 \cdot 10^5$ RCF (*LE-80K Ultracentrifuge*, NVTi65.1 rotor, Beckman) at 25ºC under vacuum for 16h. After this step the lower DNA-EtBr band corresponding to circular, non-nicked plasmid DNA was transferred into a new Optiseal tube. The tube was topped up with TE:CsCl and re-spun at $4 \cdot 10^5$ RCF at 25ºC, under vacuum, for 6h. After this second ultracentrifugation the DNA-EtBr band was collected and mixed with an equal volume of ddH_2O-saturated 1-butanol. This resulted in two liquid phases: EtBr concentrated in the upper-organic phase, whereas DNA remained in the

lower-aqueous phase. The organic extraction was repeated until no traces of EtBr were visible in the aqueous phase; this was collected, topped up to 10ml with ddH_2O, then to 45ml with ethanol (EtOH) in a 50ml-polypropylene tube and incubated at 4ºC for at least 20min. The suspension was centrifuged at 4,000 RCF (Rotanta 46R) at 4ºC for 20min. The supernatant was discarded and the pellet washed with 5ml of 70% [v/v] EtOH following by centrifugation at 4,000 RCF at 4ºC for 5min. This washing-step was repeated until the DNA-pellet appeared salt-free. Finally, the DNA was resuspended in 500µl of ddH_2O, quantified as described in 2.1.7 and stored at -20ºC for later use.

2.1.13 RNA purification

Cell pellets or tissue to be used for RNA extractions were snap frozen on dry-ice and stored at -80ºC before processing. Each sample was transferred into a 1.5ml-polypropylene DNAse and RNAse free (Anachem) and 1m of *Trizol* (Invitrogen) added to each tube. The samples were homogenised using a 25G needle and incubated in *Trizol* at room temperature for 5min. 200µl of Chloroform (Sigma) were added to each tube and shaken vigorously for 15s. The tubes were left at room temperature for 5min and then centrifuged at 12,000 RCF for 10min at 4ºC (*Eppendorf Centrifuge 5430R*, Eppendorf). At this point two phases are visible, the phenol-chloroform layer (bottom) that contains DNA and an aqueous layer (top) that contains RNA, cellular proteins accumulate in the interphase and in the phenol-chloroform phase. The RNA-containing layer was transferred to a clean DNAse and RNAse free tube, 500µl of ice-cold isopropanol were added, mixed and incubated at room temperature for 10min. The samples were then centrifuged at 12,000 RCF at 4ºC for 10min. The supernatant was

discarded and the pellet washed in 1ml of 75% [v/v] EtOH by vortexing. This was centrifuged at 7,500 RCF at 4ºC for 5min, the supernatant removed and the pellet allowed to dry before resuspending in 30-50µl of DNAse-RNAse-free ddH_20 (Sigma).

In order to remove any contaminating DNA, the RNA was treated with DNAse I (Roche) in the presence of RNAse inhibitors (*RNAse out*, Invitrogen) and dithiothreitol (DTT, Invitrogen). The reaction was set up as follows:

DNAse I treatment

	VOLUME	SUPPLIER	INCUBATION
Sample	**15-25µl**		
DNAse I (10,000U·ml^{-1})	**2µl**	*Roche*	**30min at 37ºC**
10X Buffer	**5µl**	*Roche*	**5min at 65ºC**
RNAse out	**1µl**	*Invitrogen*	
0.1M DTT	**2µl**	*Invitrogen*	
ddH_2O	**Up to 50µl**	*Sigma*	

Table 2-4 Purification of RNA from contaminating DNA

At this point, the RNA samples were re-precipitated by mixing with 0.1 volumes of 3M CH_3CO_2Na pH5.2, followed by one volume of ice-cold isopropanol and kept overnight at -80ºC. The next morning, samples were centrifuged at 12,000 RCF for 30min at 4ºC, washed with 1ml of 75% [v/v] EtOH and re-centrifuged at 12,000 RCF for 30min at 4ºC. Finally, the supernatant was removed and the pellet allowed to dry before resuspending in 30µl of DNAse and RNAse-free ddH_20 (Sigma). The RNA concentration was quantified using a *Pearl nanophotometer* (Implen) and the samples were kept at -80ºC for later use.

2.1.14 Semi-quantitative RT-PCR

RNA samples were prepared and quantified as described in 2.1.13. Equal amounts of RNA were retro-transcribed (RT) into cDNA using *superscript III* (Invitrogen) according to manufacturer's instructions. Briefly, RNA, random primers, triphosphate deoxyribonucleotides (dNTPs) and ddH_2O were mixed in a 0.2ml-polypropylene tube and annealed at 65ºC for 5min before the addition of the remaining components of the RT-mix. The RT-reactions were set up on a thermal cycler (*MJ Mini Personal* TC, Biorad) as follows:

RT-reaction

	AMOUNT	SUPPLIER
RNA	**100-500ng**	
Random Primers	**300ng**	*Invitrogen*
10mM dNTPs	**2µl**	*Invitrogen*
ddH_2O	**Up to 25µl**	*Sigma*
5min at 65ºC **5min at 4ºC**		
5X First-Strand Buffer	**5µl**	*Invitrogen*
RNAse out	**1µl**	*Invitrogen*
0.1M DTT	**1µl**	*Invitrogen*
Superscript III	**1µl**	*Invitrogen*
5min at 25ºC **60min at 50ºC**		

Table 2-5 cDNA synthesis using Superscript III

To amplify the cDNA corresponding to the mRNA of the gene of interest, RT-products were then distributed into 0.2ml-PCR tubes. Amplification was achieved using specific primers and the *Thermus aquaticus* (Taq)

DNA-polymerase, PCR mixtures were prepared and run on a thermal cycler (MJ Mini Personal TC, Biorad) as described in Table 2-6. Once the reactions were completed, PCR products were directly loaded into a 1% [w/v] agarose-gel. No loading dye was required in this case, as the *5X Green Reaction Buffer* from Promega already has the appropriate density and colour. PCR products were run, visualised and photographed as explained in section 2.1.1

Semi-quantitative-PCR

	AMOUNT	SUPPLIER
cDNA	**3µl**	
Forward primer (10µM)	**0.5µl**	*Sigma*
Reverse primer (10µM)	**0.5µl**	*Sigma*
25mM $MgCl_2$	**1.2µl**	*Promega*
10mM dNTPs	**2µl**	*Invitrogen*
5X Green Reaction Buffer	**5**	*Promega*
GoTaq DNA polymerase	**0.25µl**	*Promega*
ddH_2O	**Up to 25µl**	*Sigma*
5min at 95ºC		
30s at 94ºC **30s at 42-65ºC*[1]** **45s at 72ºC**	**X 25-35 cycles*[2]**	
10min at 72ºC		

Table 2-6 Semi-quantitative Polymerase Chain Reaction
****[1] The annealing temperature is optimized for each new set of primers.***
****[2] The number of cycles is increased for low-expression genes.***

2.1.15 High fidelity PCR

High amplification accuracy was required when generating PCR-products that were subsequently used in any cloning strategy. For this reason, *cloning PCRs* were performed using an engineered DNA-polymerase from

Pyrococcus furiousus, *PfuUltra II* (Agilent Technologies) that has higher fidelity than normal Taq DNA-polymerase. Furthermore, cloning primers can be unusually long and only partially complementary to the DNA template, making predicting their optimal annealing temperature difficult. Consequently, *high fidelity PCRs (hfPCRs)* were always performed using a temperature gradient for the annealing cycle and 5% [v/v] dimethyl sulfoxide (DMSO, Roche) was added to the PCR-mixture if products were predicted to form strong secondary structures. PCR mixtures were prepared and run on a thermal cycler (*MJ Mini Personal* TC, Biorad) as described in Table 2-7.

High fidelity PCR

	AMOUNT	SUPPLIER
Template	**20-40ng**	
Forward primer (10μM)	**1μl**	*Sigma*
Reverse primer (10μM)	**1μl**	*Sigma*
10X Reaction Buffer	**5μl**	*Agilent Tech*
10mM dNTPs	**4μl**	*Invitrogen*
$(CH_3)_2SO$[1]*	**0-2.5μl**	*Roche*
PfuUltra II DNA-pol	**1μl**	*Agilent Tech*
ddH_2O	**Up to 50μl**	*Sigma*
2min at 95ºC		
30s at 95ºC		
30s at ∇55-65ºC*[2]	**X 35 cycles**	
50s at 72ºC		
10min at 72ºC		

Table 2-7 High fidelity PCR using PfuUltra II

****[1] 5% [v/v] Dimethyl sulfoxide (DMSO) was included if PCR products were predicted to form strong secondary structures. *[2] Cloning PCRs were always run on an annealing temperature gradient (typically between 55-65ºC).***

2.2 Cell Culture

All work described bellow was performed under sterile conditions in a laminar flow hood unless otherwise stated. All cells were grown in a humidified incubator with 5% CO_2 and 20% O_2 atmosphere at 37ºC unless otherwise stated

2.2.1 Culturing of cell lines

2.2.1.1 Expansion of cell lines

In general, cell lines were grown in "*DMEM**". This consisted in Dulbecco's Modified Eagle Medium with 4.5g·l^{-1} *D*-glucose (DMEM; Sigma), supplemented with 10% [v/v] fetal calf serum (FCS; Gibco), 100U·ml^{-1} penicillin, 0.1g·l^{-1} streptomycin (Sigma), 2mM *L*-alanyl-*L*-glutamine (*Glutamax*, Gibco), 1% [v/v] *MEM* (minimum essential medium) non-essential aminoacids (Gibco). Cells were grown in 25cm^2, 75cm^2 or 175cm^2 Nunc culture flasks (Thermo-Fisher).

2.2.1.2 Passaging cells

When cells had formed an 80-90% confluent monolayer, culture medium was removed and the cells were washed once with sterile phosphate buffered saline (PBS, Gibco). The cells were then treated with 1-4ml of a

trypsin-ethylene-diamine-tetra-acetic acid solution {500μg·ml^{-1} trypsin and 200μg·ml^{-1} EDTA in PBS, Sigma} for 3-5min at 37ºC. To facilitate the detachment of the cells, the flasks were gently rocked and tapped every 1-2min. Following enzymatic passaging, cells were mechanically triturated using a *p200 Gilson* pipette. Trypsin was inactivated by the addition of 5-8ml of *DMEM** and the suspension was transferred into a sterile 15ml-polypropylene tube (Corning) and centrifuged at 1,200 RCF at room temperature for 5min (*Megafuge-20R*, Heraeus Sepatech). The cell pellet was resuspended in 10ml of *DMEM** and 1ml of this cell suspension was transferred into a new culture flask containing fresh *DMEM**

2.2.1.3 Preparation of poly-D-lysine coated plates

13mm-diameter glass coverslips were pre-sterilised by flaming with EtOH and placed on 24-well plates (Nunc) before coating with poly-*D*-lysine (PDL). PDL solution (0.1g·l^{-1}; Sigma) was added to each well followed by incubation at 4ºC overnight. PDL was then recovered and coverslips washed three times with sterile ddH_20, for 10min. Once the final wash had been removed, the plates were dried in a laminar flow hood for at least 1h.

2.2.1.4 Viable-cell counts

On some occasions the precise number of viable cells needed to be determined prior to seeding. In order to do this, the cell suspension was diluted 1:25 in *DMEM* and mixed with equal volume of a 0.2% [w/v] trypan blue solution (Sigma). 10μl of this mixture were placed on an improved Neubauer haemocytometer. Cells were examined under a microscope and viable cells

(non-stained by Trypan blue) within 5 squares of a 1-mm^2 grid were counted. The counting chamber on an improved Neubauer haemocytometer is 0.1mm deep, thus the cells on a 1-mm^2 square correspond to the number of cells in 0.1mm^3 and the viable cell concentration can be calculated as follows.

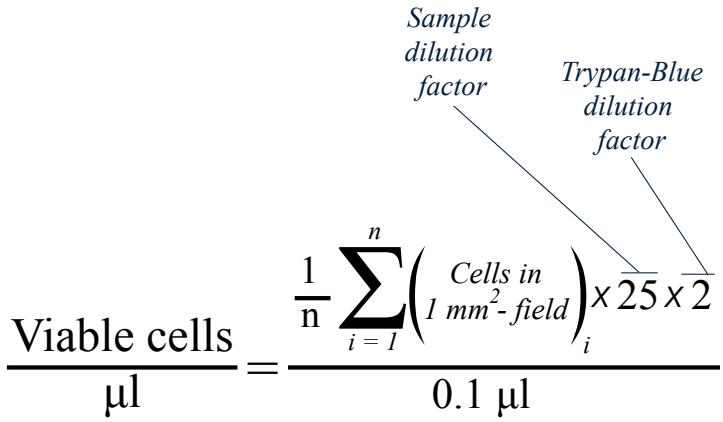

Equation 2 Estimating cell concentration

2.2.1.5 Cryopreservation of cells

A single-cell suspension was prepared as described in section 2.2.1.2 and the number of viable cells calculated as described in section 2.2.1.4. A suspension of $6 \cdot 10^6$cells·ml^{-1} in 60% [v/v] DMEM*, 30% [v/v] FCS and 10% [v/v] DMSO (Sigma) was prepared and transferred into cryovials (Nunc) in 1ml aliquots. The cryovials were then placed in an isopropanol-filled container ("Mr Frosty") and incubated at -80ºC for 24h. This allowed for a cooling rate of 1ºC·min^{-1}, minimising cellular damage. Once frozen, the vials were transferred to liquid nitrogen for long-term storage.

2.2.1.6 Recovery of frozen cell stocks

Cryovials kept in liquid nitrogen were promptly thawed in a 37ºC-water bath. The cell suspension was then transferred into a sterile 15ml-polypropylene tube, supplemented with 10ml of pre-warmed DMEM* and centrifuged at 1,200 RCF at room temperature for 5min (*Megafuge-20R*; Heraeus Sepatech). The pellet was resuspended in 10ml DMEM* and seeded onto a 25cm^2 cell culture flask (Nunc). Once the cell monolayer reached confluence the cells were passaged into bigger flasks as described in section 2.2.1.2.

2.2.2 Rat embryonic primary neuronal cultures

2.2.2.1 Dissection of cortices.

All surgical instruments were cleaned and sterilised in the laminar flow hood. Pregnant Wistar rats at E18 gestation day were obtained from the central animal facility (University of Bristol) and anesthetised by isoflurane inhalation and sacrificed by cervical dislocation. The animal was swabbed with 100% EtOH before an incision through the abdominal wall was performed to expose the uterus. The embryos were removed and sacrificed by decapitation. The heads placed into a 90mm-Petri dish containing 10ml of DMEM. Tissue dissection was performed under a *MZ6 microscope* (Leica) with a *K1500 electronic light source* (Schott). The skin and soft bone tissue were discarded using forceps and the brain transferred into another dish containing 10ml of fresh DMEM. The cerebellum was then removed and the two brain hemispheres separated. Each hemisphere was placed on its side to enable the removal of the thalamus, followed by the complete removal of the meninges. Finally the cortex was dissected out and

placed into fresh DMEM medium on ice. Hereafter, all work was performed under sterile conditions in a laminar flow hood.

2.2.2.2 Trituration and plating of cortical neurons

Once all cortices had been removed they were placed in 5ml of *Hanks Balanced Salt Solution* (HBSS, Gibco) containing 0.05% [v/v] trypsin-EDTA (Sigma) and incubated for 15min at 37°C. The cortices were then washed three times in HBSS and triturated with a flame-polished *Pasteur* pipette in 1ml of *Cortical neuron plating medium* {*Neurobasal medium* (Gibco); 2% [v/v] *B-27 supplement* (Gibco); 0.5mM *L*-glutamine (Sigma); 25μM *L*-glutamate (Sigma); $100U \cdot ml^{-1}$ penicillin and $0.1g \cdot l^{-1}$ streptomycin (Sigma)}. Following trituration, the viability of the cells was determined (as described in section 2.2.1.4) and the cell concentration adjusted to $1.5 \cdot 10^6 cells \cdot ml^{-1}$. 50μl of this cell suspension (containing $7.5 \cdot 10^4$ cells) were carefully placed into the centre of PDL-coated coverslips, previously prepared as described in 2.2.1.3. Plates were incubated for 1h in a 5% CO_2 and 20% O_2 humidified atmosphere at 37ºC to allow cells to settle, before an additional 500μl of *plating medium* was added to each well.

2.2.2.3 Culture maintenance

After 3 days, half of the volume of medium in each well was removed and replaced with fresh *feeding medium* {*Neurobasal medium* (Gibco); 2% [v/v] B-27 supplement; $100U \cdot ml^{-1}$ penicillin and $0.1g \cdot l^{-1}$ streptomycin (Sigma)}. Thereafter, cultures were fed every 3-4 days.

2.2.3 Rat postnatal primary astrocytic cultures

Mixed glial cultures from P0-3 rat pups were prepared as previously described.(McCarthy and De Vellis, 1980). Tissue was dissected as in 2.2.2.1., transferred into a 15ml-polypropylene tube and incubated with 1ml of *Trypsin solution* {200U·ml^{-1} Trypsin (Worthington Laboratories); 240U·ml^{-1} DNAse I (Sigma); 0.6% [w/v] *D*-glucose (Melford) in sterile PBS pH7.4} for 15-20min at 37ºC. The reaction was stopped by adding 1ml of *Trypsin inhibitor solution* {0.1% [w/v] trypsin inhibitor (Sigma) in HBSS (Gibco)} and 1ml of *DNAse I solution* {240KU·l^{-1} DNAse I (Sigma); 0.6% [w/v] *D*-glucose (Melford) in sterile PBS pH7.4} and centrifuged at 1,000 RCF for 5min (*Megafuge-20R*, Heraeus Sepatech). The resulting cell pellet was washed and re-centrifuged three times in *DNAse I solution.* Finally, the cells were centrifuged at 1,000 RCF at room temperature for 5min, carefully resuspended in DMEM* and triturated to obtain a single-cell suspension using a *Gilson p200* pipette. Cell number and viability were assessed by Trypan blue exclusion (Sigma) using Neubauer Haemocytometer as described in 2.2.1.4.

$6 \cdot 10^4$cells·cm^{-2} were plated onto a Nunc culture flask previously coated with PDL (as described in 2.2.1.3) and plates were incubated for 1h in a 5% CO_2 and 20% O_2 humidified atmosphere at 37ºC. Medium was changed after 24h and twice weekly thereafter until the cells reached confluence (8–10 days). Microglial cells were removed by vigorous shaking of the cultures at 240rpm on a horizontal rocker (Stuart Scientific) for 20min at 37ºC, followed by removal of oligodendrocyte progenitor cells by shaking at 160rpm at 37ºC overnight. The remaining monolayer was treated with 20μM arabinofuranosyl cytidine (Ara-C,

Sigma) for 72h and washed with DMEM containing 1% [v/v] PS and 1% [v/v] N2-supplement (Invitrogen). 24h later, fresh DMEM containing 1% [v/v] PS was added for a further 48h. Media was then collected, filtered through 0.45μm filter unit (Nalgene) aliquoted and stored at -20ºC for later use.

2.2.4 Mouse fetal NSC culture

2.2.4.1 Striatal dissection

All surgical instruments were cleaned and sterilised in the laminar flow hood. Pregnant wild-type (WT) and galanin-Knockout (*Gal*-KO) mice were mated and plug-checked in house. At 14.5 days *post coitum* (dpc = E14.5), mice were anesthetised by isoflurane inhalation, sacrificed by cervical dislocation and swabbed with 70% [v/v] EtOH before an incision through the abdominal wall performed to expose the uterus. The embryos were then harvested and terminated by decapitation. The heads were then placed on a 90mm-Petri dish containing 10ml of DMEM. Tissue dissection was performed under a *MZ6 microscope* (Leica) with a *K1500 electronic light source* (Schott). The skin and soft bone tissue were discarded using forceps and the brain transferred into another dish containing 10ml fresh DMEM. The cerebellum was then removed and the meninges discarded. The striata were exposed and collected by a small incision through the cortex using fine dissection scissors and finally placed into fresh DMEM medium on ice. At this point the tissue was transferred into a laminar flow hood and all work performed under sterile conditions. Once all striata were collected, DMEM was removed and the tissue treated with 500μl of Accutase (Sigma) at 37°C for 10-20min. Following centrifugation at 1,000 RCF at room

temperature for 5min (*Megafuge-20R*, Heraeus Sepatech), the pellet was carefully resuspended in fresh culture medium and triturated to obtain a single-cell suspension using a *Gilson p200* pipette. Cell number and viability were assessed by Trypan blue exclusion (Sigma) using Neubauer Haemocytometer as described in 2.2.1.4.

2.2.4.2 Expansion of mouse fetal NSCs

A single-cell suspension was prepared as described above, $2 \cdot 10^5$cells·ml^{-1} were grown in DMEM:F12$^{B27\text{-}FH}$. This consisted in a 3:1 mixture of high glucose DMEM (Sigma) and F12-nutrient mixture (Gibco), supplemented with 2% [v/v] B27 supplement (Gibco); 20ng·ml^{-1} basic fibroblast-growth factor (FGF-b, Peprotech); 5mg·l^{-1} heparin (Sigma) and 100U·ml^{-1} penicillin, 0.1g·l^{-1} streptomycin (Sigma). NSCs were grown in 25cm^2 or 75cm^2 Nunc culture flasks (Thermo-Fisher). The cultures were fed every 3-4 days by replacing 50% of the culture medium with fresh DMEM:F12$^{B27\text{-}FH}$.

2.2.4.3 Passaging of mouse fetal NSCs

Under our culture conditions, NSCs proliferate as free-floating cell aggregates also known as neurospheres. When neurospheres become oversized (>0.5-1mm) diffusion of nutrients and mitogens to the neurosphere core is compromised and spontaneous differentiation can occur. To prevent this, every 7 days, cultures were transferred into 15ml-polypropylene tubes and centrifuged at 1,000 RCF at room temperature for 5min (Megafuge-20R, Heraeus Sepatech). The resulting pellet was treated with 300µl of Accutase at 37ºC for 10-20min, re-spun as above,

carefully resuspended in fresh DMEM:F12$^{B27\text{-}FH}$ and triturated to obtain a single-cell suspension. Cell density was determined as described previously (2.2.1.4) and $2{\cdot}10^5$cells·ml^{-1} were seeded into a mixture 50% fresh DMEM:F12$^{B27\text{-}FH}$ and 50% culture medium from the previous passage.

2.2.4.4 Differentiation of mouse fetal NSCs

To allow the differentiation of the multipotent NSCs into the different neural lineages, mitogens were withdrawn from the culture medium and single cells were plated on a permissive substrate (PDL). PDL-coated coverslips were prepared as described previously (2.2.1.3) and neurospheres were collected and dissociated as explained above, but were, in this case, resuspended in DMEM:F12$^{B27\text{-}DIFF}$ {3:1 mixture of high glucose DMEM (Sigma) and F12-nutrient mixture (Gibco); 2% [v/v] B27 supplement (Gibco); 1% [v/v] FCS (Gibco); and 100U·ml^{-1} penicillin, 0.1mg·ml^{-1} streptomycin (Sigma)}. Cell concentration was adjusted to $1.7{\cdot}10^6$cells· ml^{-1} before 30µl of the cell suspension were placed on the centre of each coverslip. To allow cells to settle, plates were incubated for 1h in a 5% CO_2 and 20% O_2 humidified atmosphere at 37ºC, before 500µl of DMEM:F12$^{B27\text{-}DIFF}$ were added to each well. Half of the medium was replaced with fresh DMEM:F12$^{B27\text{-}DIFF}$ after 3-4 days and the cells were allowed to differentiate for 7 days.

2.2.4.5 MTT-assays

Primary E14.5 striatal NSCs were seeded on 96-well plates at a density of $2.5{\cdot}10^4$cells·well^{-1} in 100µl of DMEM:F12$^{B27:FH}$. The plates were fed after 3-4

days by adding 100µl of fresh DMEM:F12$^{B27:FH}$. On day 7, 25µl of a 5g·l^{-1} solution of methyl-thiazolyl-diphenyl-tetrazolium bromide (MTT, Sigma) in ddH_2O were added per well. Following a 2h-incubation at 37ºC, the medium of each well was carefully removed and replaced by 150µl of acidified isopropanol (Fisher). To maximize the dissolution of the formazan product, plates were incubated at 37ºC overnight. Formazan formation was measured as 570nm absorbance with an MRX TC revelation spectrophotometer.

2.2.5 Mouse adult SVZ-NSC culture

2.2.5.1 Dissection of SVZ-NSCs

8-10 week-old adult mice culled as described previously (2.2.2.1) and decapitated. The scalp was withdrawn and the dorsal surface of the skull removed to expose the brain, this was carefully detached and transferred into a 50ml-polypropylene tube containing 20ml DMEM and placed on ice. Tissue from four to five mice was pooled for each culture. The brains were then placed into a 90mm-Petri dish containing 10ml of DMEM and tissue dissection was performed under a MZ6 microscope (Leica) with a K1500 electronic light source (Schott). The cerebellum and the olfactory bulbs were removed and the meninges discarded. The remaining of the brain was cut in three blocks by two coronal sections (one caudal to the hypothalamus and one rostral to the optic chiasm) and placed horizontally into a new 90mm-Petri dish containing 10ml of DMEM. The subventricular zone (SVZ) of the lateral ventricles (≈1mm from the lumen) was carefully collected using fine dissecting scissors into fresh DMEM on ice. At this point the tissue was transferred into a laminar flow hood and all work performed under sterile

conditions. Once all SVZ were collected, DMEM was removed and the tissue treated with 500µl of *Trypsin solution* {200U·ml^{-1} Trypsin (Worthington Laboratories); 240U·ml^{-1} DNAse I (Sigma); 0.6% [w/v] *D*-glucose (Melford) in sterile PBS pH7.4} for 10min at 37°C. The reaction was stopped by adding 250µl of *Trypsin inhibitor solution* {0.1% [w/v] trypsin inhibitor (Sigma) in HBSS (Gibco)} and 250µl of *DNAse I solution* {240KU·l^{-1} DNAse I (Sigma); 0.6% [w/v] *D*-Glucose (Melford) in sterile PBS pH7.4}. The cells were gently triturated with a *p1000 Gilson* pipette, sieved through a *40µm-cell nylon cell strainer* (BD-Falcon), followed by centrifugation at 1,000 RCF at room temperature for 5min (Megafuge-20R, Heraeus Sepatech). The resulting pellet was carefully resuspended in fresh culture medium and triturated to obtain a single-cell suspension using a *p200 Gilson* pipette. Cell number and viability were assessed by Trypan blue exclusion (Sigma) using Neubauer Haemocytometer as described in 2.2.1.4.

2.2.5.2 Expansion of adult SVZ-NSCs

Adult SVZ-NSCs are less expandable and grow at lower rates than fetal NSCs. For this reason, SVZ-NSCs were grown in a similar DMEM:F12 based medium but with both *epidermal growth factor* (EGF) and FGF-b as mitogens. This was done as follows: a single-cell suspension was prepared as described above, $2{\cdot}10^5$cells·ml^{-1} were grown in DMEM:F12$^{B27:EFH}$ {3:1 mixture of high glucose DMEM (Sigma) and F12-nutrient mixture (Gibco); 2% [v/v] B27 supplement (Gibco); 20ng·ml^{-1} EGF (Sigma); 20ng·ml^{-1} FGF-b (Peprotech); 5µg·ml^{-1} heparin (Sigma) and 100U·ml^{-1} penicillin, 0.1g·l^{-1} streptomycin (Sigma). NSCs were

grown in 25cm^2 or 75cm^2 Nunc culture flasks (Thermo-Fisher). The cultures were fed every 3-4 days by replacing 50% of the culture medium with fresh DMEM:F12$^{B27\text{-}EFH}$.

2.2.5.3 Passaging of adult SVZ-NSCs

In order to obtain enough material to proceed with our experiments, adult SVZ-NSCs were expanded for 10 days in DMEM:F12$^{B27\text{-}EFH}$ before passaging as previously described (2.2.4.3) and all experiments were carried out with P1-P2 cells (passage 1 or passage 2) as opposed to cells from P0-P1 in the mouse fetal NSC studies.

2.2.5.4 Differentiation of adult SVZ-NSCs

Adult SVZ-NSC neurospheres were harvested, disaggregated and seeded into PDL-coated plates and differentiated for 7 days as described in 2.2.4.4

2.2.6 Human fetal NSC culture

Human ventral-mesencephalon and cortex (8–10 weeks) were collected following routine terminations of pregnancies. The methods of collection conformed to arrangements recommended by the Polkinghorne Committee (1989) and the United Kingdom Department of Health guidelines (1995).

2.2.6.1 Expansion of human fetal NSCs

Human tissue was collected and dissected at the University of Cardiff and transported to our laboratory on ice. Upon arrival, the tissue was diced using a

scalpel blade, washed once in DMEM and treated with 500µl of Accutase (Sigma) at 37°C for 20min. Following centrifugation at 1,000 RCF at room temperature for 5min (*Megafuge-20R*, Heraeus Sepatech), the pellet was carefully resuspended in fresh culture medium and triturated to obtain a single-cell suspension using a *Gilson p200* pipette. Cell number and viability were assessed by Trypan blue exclusion (Sigma) using Neubauer Haemocytometer as described in 2.2.1.4. $2{\cdot}10^5$cells·ml^{-1} were seeded into 75cm^2 Nunc culture flasks (Thermo-Fisher). Cells were grown as neurospheres in DMEM:F12$^{B27\text{-}EFH}$ (see section 2.2.5.2). Passaging was carried out every two weeks or whenever the neurospheres became oversized (>1mm). Human fNSCs have poorer survival to mechanical or enzymatic passaging than rodent fNSCs and their growth is enhanced if cell to cell contact is preserved (Svendsen et al., 1998). For these reasons, neurospheres were cut into ≈0.06mm^2 pieces using a McIlwain tissue chopper (Mickle Engineering). This was done as follows: cultures were transferred into 15ml-polypropylene tubes and centrifuged at 1,000 RCF at room temperature for 5min. The resulting pellet was transferred onto the lid of a 50mm-Petri dish (BD-Falcon) and attached to the stage of the apparatus. A sterile razor blade was inserted into the arm of the tissue chopper. Sections were automatically taken through the spheres every 250µm, the lid was then rotated 90º and the spheres re-sectioned at 250µm as before. The resulting pieces of tissue were carefully washed in culture medium and reseeded into new 75cm^2 Nunc culture flasks containing 50% DMEM:F12$^{B27\text{-}EFH}$ from the previous passage and 50% fresh DMEM:F12$^{N2\text{-}EFH}$ {where 2% [v/v] B27-supplement (Gibco) is replaced by 1% [v/v] N2-supplement (Gibco)}. This progressive switch from B27-supplement to N2-supplement is due to the fact that although B27-supplement is required for

optimum growth of primary human fNSCs, it can be replaced by the chemically defined N2-supplement once the neurosphere cultures are established. After one month in culture, EGF was progressively removed from the medium (by replacing DMEM:F12$^{N2\text{-}EFH}$ with DMEM:F12$^{N2\text{-}FH}$} as EGF and FGF-b no longer had a synergistic effect on fNSC growth after this period.

2.2.6.2 Differentiation of human fetal NSCs

Whole neurospheres were plated on PDL/laminin-coated chamber slides. This was done as follows: 300µl of PDL solution (0.1g·l^{-1}; Sigma) was added to each well of an *8-well CultureSlide* (glass slide with polystyrene vessel, BD-Falcon) and incubated at 4ºC overnight. PDL was then recovered, washed and the *CultureSlides* dried as described in 2.2.1.3. The wells were then coated with 300µl of 10mg·l^{-1} laminin (Sigma) and incubated for at least 10min at 37ºC. Laminin was recovered, washed once with fresh DMEM and 300µl of *hfNSC-Differentiation medium* {3:1 mixture of high glucose DMEM (Sigma) and F12-nutrient mixture (Gibco), supplemented with 1% [v/v] N2-supplement (Gibco); 1mg·l^{-1} bovine serum albumin (BSA, Sigma); 0.6mg·l^{-1} *N*-acetyl-cysteine (Sigma); 5nM forskolin (Sigma) and 100U·ml^{-1} penicillin, 0.1g·l^{-1} streptomycin (Sigma)} added to each well. One or two neurospheres were carefully placed on the centre of each well, using a *p200 Gilson* pipette and the *CultureSlides* gently transferred into the incubator. Cultures were allowed to differentiate for 7 days or one month and fed every 3-4 days by replacing half of the medium with fresh *hfNSC-Differentiation medium.*

2.3 Recombinant lentiviral vectors

2.3.1 Third generation lentiviral system

This system was adapted from Dull et al. 1998 to generate self-inactivating lentiviral vectors derived from the human immunodeficiency virus (HIV). To minimise the risk of recombination, all essential viral elements were encoded by four separated plasmids and only transiently expressed in the producing cell line. Figure 2—1 shows a schematic of the helper plasmids used in a third generation system. All plasmids contained an ampicillin resistance cassette and a bacterial replication origin. pRSV-Rev plasmid encoded the HIV protein REV - essential for nuclear translocation of the viral transcripts - under the Rous-Sarcoma Virus (*Rsv*) promoter. pMD2-env-VSVG plasmid encoded the envelope glycoprotein of the vesicular stomatitis virus G (VSVG) under a recombinant cytomegalovirus promoter (r*cmv*). pMDLg/pRRE gag/pol contained a REV response element (RRE) and the gag/pol genes under r*cmv* that encoded for structural viral proteins {MA-membrane associated protein, CA-capsid and nucleoproteins} and those involved in viral integration {RT-*reverse transcriptase* and INT-*integrase*) (Dull et al., 1998).

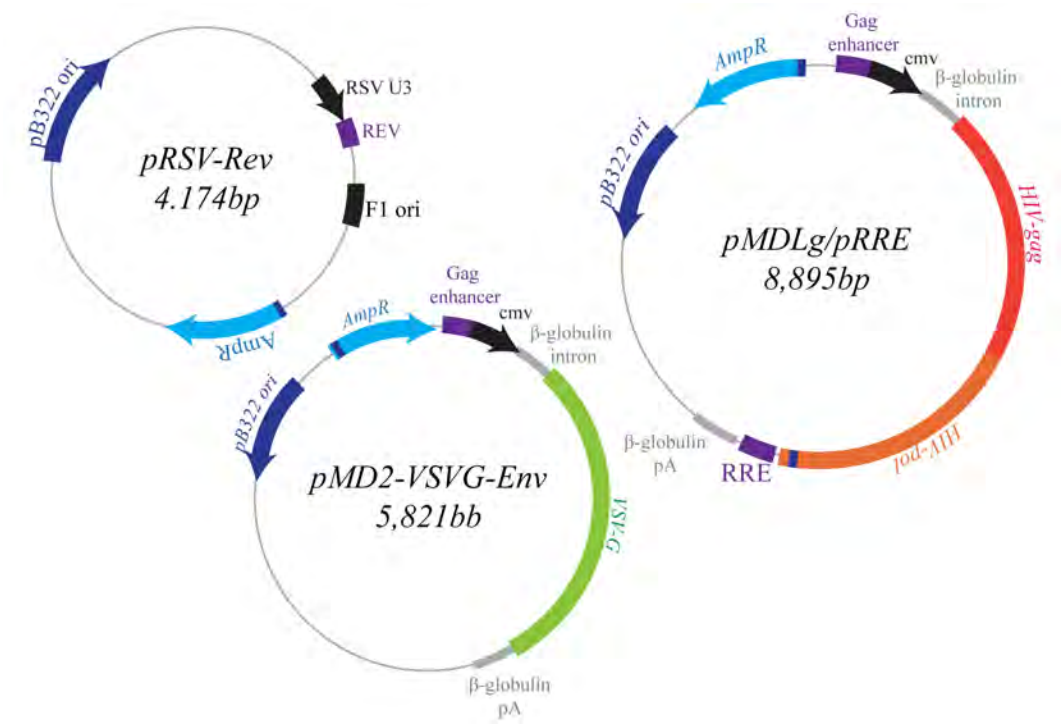

Figure 2—1 Third generation lentiviral helper plasmids
Elements required for viral replication and assembly are encoded in three separated plasmids. AmpR, ampicillin resistance; cmv, cytomegalovirus promoter; pA, polyadenylation signal; RRE, rev response element; rsv, Rous-sarcoma virus promoter; VSV-G, vesicular stomatitis virus glycoprotein gene.

2.3.2 Co-transfection of HEK-293T cells

Low passage (<40) human embryonic kidney cells (HEK293T) were maintained and passaged as described in 2.2.1.1 and 2.2.1.2. For co-transfection, $8{\cdot}10^6$ cells were plated onto $150cm^2$ plates (12 plates were required per virus) in 20ml DMEM*. After 24h, each plate was co-transfected with 10µg of lentiviral backbone containing the gene of interest, 10µg of pMDLg/pRRE gag/pol, 3.4µg of pMD2-env-VSVG and 2µg of pRSV-Rev. These four plasmids were added to a sterile 50ml-polypropylene tube and the final volume was made up to 1.1ml with ddH_2O. 140µl of 2M $CaCl_2$ were added to the DNA solution and mixed.

1.1ml of HEPES-buffered saline (HBS) {50mM 4-(2-hydroxyethyl)-1-piperazineethanesulfonic acid (HEPES, Sigma); 280mM NaCl (Melford); 1.5mM Na_2HPO_4 (Sigma); pH7.05} were added to the DNA drop-wise and the solution incubated at room temperature for 30min. This reaction mixture was scaled up for 12 plates as described in Table 2-8.

$CaCl_2$ Co-transfection mixture		
	1 PLATE	12.5 PLATES
Genome	**10µg**	**125µg**
Gag/pol	**10µg**	**125µg**
Env	**3.4µg**	**42.5µg**
Rev	**2µg**	**25µg**
ddH_2O	**Up to 1.1ml**	**Up to 13.75ml**
2M $CaCl_2$	**140µl**	**1.75ml**
HBS (added drop-wise)	**1.1ml**	**13.75ml**
30min at room temperature		

Table 2-8 HEK293T $CaPO_4$ co-transfection with genome and helper-plasmids

The transfection mixture (2.4ml per plate) was added evenly to the cells and plates incubated overnight in a 5% CO_2 and 20% O_2 humidified atmosphere at 37ºC.

2.3.3 Harvesting and concentration of lentiviral particles

24h after co-transfection with the lentiviral backbone and the three helper plasmids, culture medium was replaced with fresh DMEM* containing 10mM sodium butyrate (NaBut). Medium was harvested 6h later and replaced with 16ml of fresh DMEM*. Cells were returned to the incubator and the harvested medium was stored at 4˚C.

The following day, medium was carefully collected and pooled together with the first harvest (total volume of 384ml) and transferred into 500ml-centrifuge tubes (Corning). Culture plates were discarded at this point. Harvested medium was

centrifuged for 5min at 2,000 RCF (Megafuge-20R; Heraeus Sepatech) and the supernatant was filtered through a 0.45μm filter unit (Nalgene) using a vacuum pump. Cell-free supernatant was centrifuged at 6,000 RCF over night at 4ºC (SLA 3000 Rotor, Sorval Evolution RC). To further concentrate the viral particle suspension, the resulting pellet was resuspended in 5ml of ice-cold PBS and transferred into a 14ml-*Thinwall Polyallomer* tube (Beckman-Coulter) and centrifuged at 20,000 rpm (RCF = 70951.8; SW40 Ti ultra-Rotor, Beckman) for 90min. The supernatant was discarded and pellets left to drain for several minutes. 100μl of TSSM buffer {20mM tromethamine (Sigma); 100mM NaCl (Melford); $10g \cdot l^{-1}$ sucrose (Sigma) and $10g \cdot l^{-1}$ *D*-mannitol (Sigma)} was added to the pellet and left on ice for 2h. The pellet was then resuspended by gently pipetting and the final volume adjusted to 192μl with TSSM (this corresponds to a 2,000 fold concentration of the original culture medium). The concentrated viral preparations were aliquoted and stored at -80ºC.

2.3.4 Lentiviral titering by fluorescence activated cell sorting (FACS).

HEK293T cells were seeded at a density of $7.5x10^4$ cells per well in a 12-well plate in DMEM* and left to grow overnight. The following day, one representative well was used to determine the cell number at the time of transduction as described in section 2.2.1.4. The rest of the wells were transduced with serial dilutions (No virus, 10^{-3}, 10^{-4}, 10^{-5} and 10^{-6}) of the lentiviral vectors in a volume of 500μl per well and left at 37˚C for 3-4h before medium was topped up to 1ml. After 72h, the culture medium was aspirated and cells washed with PBS, followed by incubation with 200μl of Trypsin-EDTA per well for 2-4min. Trypsin was neutralised by adding 800μl of DMEM* and any cell clumps

dissociated using a *p200 Gilson* pipette. Once a single-cell suspension was obtained, the cells were transferred into 5ml-polystyrene tubes (12 x 75mm, BD-Falcon) and kept on ice.

Samples were then loaded onto the flow-cytometer (*FacsCalibur*, BD-Scientific) to determine the percentage of the population with green fluorescence emission. Briefly, particles were gated according to their complexity/granularity (side-scattered laser) and size/shape (forward-scattered laser) to exclude cell debris and aggregates from further analysis. At least 20,000 gated-events were recorded and the percentage cells emitting fluorescence through the FL1 filter (band pass 530nm) recorded. The viral titer (defined as the number of transducing viral particles per millilitre) was calculated according to the following mathematical expression:

$$\frac{TU}{ml} \equiv \frac{1}{n} \sum_{\substack{i=3 \\ \forall\, \%GFP^{+} \in [5\text{-}60]}}^{i=6} \frac{\left(\%\ GFP^{+}\ cells\right)_i \times \left(\begin{matrix}Total\\ number\\ of\ cells\end{matrix}\right) \times 100}{0.5\ ml \times 10^{-i}}$$

Transduced Volume

Viral preparation dilution factor

Equation 3 Viral titer estimation by fluorescence activated cell sorting

2.4 Protein analysis

2.4.1 Protein extraction

When possible, cells were washed once with ice-cold PBS and lysed in RIPA (radio-immunoprecipitation assay) on ice. This consisted of: 1X PBS, 1% [v/v] Igepal CA-630 (Sigma); 0.5% [w/v] sodium deoxycholate (Sigma); 0.1% [w/v], SDS (Melford) and one tablet per 10ml of *Complete Mini EDTA-free protease inhibitor* (ROCHE). Samples were homogenised using a *p200 Gilson* pipette and centrifuged at 12,000 RCF for 10 min at 4ºC (*Eppendorf Centrifuge 5430R*, Eppendorf). Finally, the supernatant was collected and stored at -80ºC.

Conditioned medium (without RIPA) was centrifuged at 1,200 RCF (Heraeus Pico 17, bench-top centrifuge, Thermo-Fisher) to eliminate any cell debris and snap-frozen on dry ice. All protein samples were kept at -80ºC.

2.4.2 Protein quantification

Bicinchoninic acid assay (BCA, Pierce) was performed according to the manufacturer's instructions. Briefly, protein standards were prepared by serial dilutions of $2g \cdot l^{-1}$ BSA to concentrations ranging from $2g \cdot l^{-1}$ to $25mg \cdot l^{-1}$. Protein samples from cell lines were typically diluted 1:5 before assay whereas samples from primary cell cultures were used neat. BCA working reagent is prepared by diluting 2% [v/v] *BCA-reagent B* (containing 4% [w/v] $CuSO_4$) in *BCA reagent A* (a highly alkaline buffer). 5µl of each sample and standard were added to a 96-well plate followed by 95µl of the BCA *Working Reagent*. The reaction was incubated at 37ºC until a suitable coloration developed (approximately 30min).

Plates were read in a plate spectrophotometer (*xMark*, Biorad) at 590nm. Protein concentration of the standards was plotted against their respective absorbance at 590nm (Abs^{590}) to generate a standard graph. The slope of the graph (*m*) was calculated by linear regression and the concentrations of the samples extrapolated using the following relationship.

$$[\text{Protein}]_{\text{sample}} = m \cdot Abs^{590}$$

2.4.3 SDS-polyacrylamide gel electrophoresis

Unless otherwise stated, protein samples were run on a 10% [w/v] denaturing SDS-polyacrylamide gel (SDS-PAGE). Typically, a *minigel* (10cm *x* 10cm *x* 1.5mm) was casted between two glass plates, consisting of a *resolving gel* (bottom) and a protein *stacking gel* (top). These were made up as follows:

Resolving gel mix

	CONCENTRATION	SUPPLIER
30% [w/v] acrylamide (29:1 acrylamide:bis-acrilamide)	**10%**	**Sigma**
1.5M Tris-HCl pH8.8	**375mM**	**Sigma**
10% [w/v] SDS)	**0.1%**	**Sigma**
10% [w/v] Ammonium persulfate (APS)	**0.1%**	**Sigma**
Tetramethylethylenediamine (TEMED)	**0.04%**	**Fisher**

Stacking gel mix

	CONCENTRATION	SUPPLIER
30% [w/v] acrylamide (29:1 acrylamide:bis-acrilamide)	**5%**	**Sigma**
1M Tris-HCl pH6.8	**125mM**	**Sigma**
10% [w/v] SDS)	**0.1%**	**Sigma**
10% [w/v] APS	**0.1%**	**Sigma**
TEMED	**0.1%**	**Fisher**

Table 2-9 Composition of SDS-PAGE gels

The resolving gel was cast first and overlaid with a thin layer of butanol (in order to prevent oxygen from inhibiting acrylamide polymerization). Once set, the butanol was removed and the gel surface washed with ddH_2O. Typically, 3ml of the *stacking gel* were cast on top of the *resolving gel*. Immediately after, an appropriately sized comb was placed between the forming plates and the gel allowed to set. When gels with different poly-acrylamide percentage were required, the resolving mixture was adjusted as follows:

Resolving gel mix

	6%	8%	12%	15%
30% [w/v] acrylamide (29:1 acrylamide:bis-acrilamide)	**6%**	**8%**	**12%**	**15%**
1.5M Tris-HCl pH8.8	**375mM**	**375mM**	**375mM**	**375mM**
10% [w/v] SDS)	**0.1%**	**0.1%**	**0.1%**	**0.1%**
10% [w/v] APS	**0.1%**	**0.1%**	**0.1%**	**0.1%**
TEMED	**0.08%**	**0.06%**	**0.04%**	**0.04%**

Table 2-10 Composition of SDS-PAGE resolving gels
Gel percentages as high as 15% were used to separate low molecular weight proteins (3-40KDa) whereas low percentage gels were used to resolve high molecular weight proteins.

The protein concentration of the samples (from 2.4.1) was determined as described in 2.4.2 and equal amounts (between 15-50µg) were loaded per lane. Samples were prepared by mixing with 0.25 volumes of *5X-loading dye* {300mM Tris-HCl (Melford) pH6.8; 50% [v/v] Glycerol (Sigma); 10% [w/v] SDS (Sigma); 0.5% [w/v] Bromophenol blue (Sigma) and freshly added 100mM DTT (Sigma)} followed by incubation at 100ºC for 4min. Samples and molecular weight markers (*Precision Plus Protein Kaleidoscope Standards*, Biorad) were then loaded into the SDS-acrylamide gel and run at a constant voltage of $8V \cdot cm^{-1}$ in *1X running buffer* {25mM Tris base, pH8.3 (Melford); 190mM Glycine (Melford) and 0.05% [w/v] SDS}. Once the bromophenol blue dye had reached the *resolving gel*

boundary, the voltage was increased to 15V·cm^{-1} and the gel run until the protein of interest reached the middle of the *resolving gel* (determined by the migration of the coloured protein standards).

2.4.4 Transfer of proteins to PVDF membranes

Proteins separated by SDS-PAGE were transferred to poly-vinylidene difluoride membranes (PVDF, Roche) by a *wet-transfer* method. Briefly, the SDS-PAGE gel and the PVDF membrane (soaked in methanol) were "sandwiched" between to foam pads (Biorad) and two sheets of Whatman 3MM paper (Whatman) soaked in *1X transfer buffer* {50mM Tris base pH8.3 (Melford); 40mM Glycine (Melford); 0.04% [w/v] SDS and 20% [v/v] methanol}. A *Trans-Blot^{TM} Cell* (Biorad) was assembled following manufacturer's instructions and protein transfer was carried out in *1X transfer buffer* for 90min on ice, under a constant electric current of 2mA·cm^{-2} of polyacrylamide gel.

2.4.5 Immunodetection of the protein of interest

The presence of the coloured molecular weight markers on the PVDF membrane was used to confirm the efficiency of the transfer step. Following wet transfer, the PVDF membrane was moved to a 50ml-polypropylene tube and washed twice with TBS-0.1%Tw$_{20}$ {20mM Tris-HCl (Melford); 0.1% [v/v] polyethylene glycol sorbitan monolaurate (Tween$_{20}$, Sigma); 154mM NaCl (Melford)}. The membrane was incubated with 10ml of *blocking solution* {TBS-0.1%Tw$_{20}$ containing 10% [w/v] dried skimmed milk (Marvel) and 0.01% [w/v] NaN_3}, on a horizontal roller at 4ºC for at least 2h. Followed by incubation with the primary antibody at the appropriate dilution (typically 1:1000) in 5ml of blocking solution

at 4ºC on a horizontal roller overnight. On the next day, the primary antibody preparation was recovered and kept at 4ºC (these were re-used for a maximum of 10 times), the PVDF membrane washed with TBS-0.1%Tw20 at least 5 times and incubated with the appropriate horseradish peroxidase (HRP)-conjugated secondary antibody (typically used at 1:5000) diluted in 5ml of blocking solution for 90min at room temperature on a horizontal roller. Unbound antibodies were washed with TBS-0.1%Tw20 at least 5 times followed by one last wash in ddH2O before protein detection.

2.4.6 Enhanced chemiluminescence (ECL) detection

Membranes were incubated in 1ml of *Supersignal West Pico* chemiluminescent substrate (Pierce) for 2-3min at room temperature. Excess substrate was removed and an autoradiographic film (Amersham, GE-Healthcare) was exposed to the membrane. The film was developed using a Kodak X-OMAT 1000 autoprocessor.

Membranes were often re-probed using a different primary antibody; this was done by incubation with 5ml of *restore western blot stripping buffer* (Pierce) for 10-20min at room temperature, followed by three washes in TBS-0.1%Tw_{20}. At this stage the membrane was re-blocked and re-probed as described above.

2.4.7 Densitometric analysis of western-blot bands

Densitometric analysis was carried out using ImageJ, a free image processing software available at http://rsbweb.nih.gov/ij/. The film was scanned using a grey scale mode and saved as a tiff file. The image background was eliminated using ImageJ's *subtract background* tool. Each protein band was individually selected

and using the tools in the *Analyse/gel* menu. Once all the bands were highlighted, a histogram was generated using the tool *Analyse/gel/plot/lanes*. Areas under the density peak were processed using the tool *Analyse/gel/label peaks* which generated the desired densitometry values; these were then imported onto an Excel file and processed for normalization and statistical analysis.

2.4.8 Immunocytochemistry

2.4.8.1 Immunofluorescence on cell monolayers

Cells grown as a monolayer on PDL-coated glass coverslips (prepared as described in 2.2.1.3) or chamber slides (section 2.2.6.2) were processed as follows: culture medium was aspirated and the monolayer washed once with PBS followed by incubation with 4% [w/v] PFA (paraformaldehyde, Sigma) for 20min at room temperature. PFA was then removed and the cells washed twice with PBS and permeabilised with ice-cold methanol at -20ºC for 20min. The methanol was then washed twice with PBS and the coverslips blocked in PBS containing 10% [v/v] serum (of the same species as the secondary antibodies used) at 4ºC for at least 3h. The cells were then incubated with primary antibodies diluted in PBS with 5% [v/v] serum and 0.01% [w/v] NaN_3 at 4ºC, overnight. The next day, unbound primary antibodies were washed thoroughly with PBS (3-5 washes) before incubating with the appropriate secondary antibodies at room temperature for 90min. These were diluted (typically 1:500) in PBS containing 5% [v/v] serum and 0.01% [w/v] NaN_3. Unbound secondary antibodies were washed three times with PBS and, if required, cell nuclei were counterstained by incubating with 1mg·l^{-1} Hoechst (Sigma) for 10min at room temperature before mounting. Finally,

coverslips were carefully removed from the wells using dissecting forceps, mounted into glass slides in Fluorsave (Calbiochem) and allowed to dry before imaging. Stained slides were kept at 4ºC in the dark for at least 3 months.

2.4.8.2 Immunofluorescence on free-floating sections

Brain sections were obtained as described in 2.5.7. Before immunostaining, the sections were gently transferred to *15ml-multiporpose pots* (Greine Bio-one) using a paintbrush. To allow quick removal of the staining solutions, the pots were covered with a nylon-mesh (Fabricland). Anti-freeze solution was washed twice with PBS before blocking with 1ml of PBS-0.1%Tx^{100} {PBS; 0.1% [v/v] 4-(1,1,3,3-Tetramethylbutyl)-phenyl-polyethylene glycol (Triton-X^{100}, Sigma)} containing 10% [v/v] serum (of the same species as the secondary antibodies used), 2% [w/v] BSA (Sigma) and 0.01% [w/v] NaN_3. Sections were blocked on a horizontal rocker at 10rpm (Stuart Scientific), 4ºC overnight. The following day, the blocking solution was decanted and sections incubated with primary antibodies diluted in 500µl of PBS-0.1%Tx^{100} containing 5% [v/v] serum, 1% [w/v] BSA and 0.01% [w/v] NaN_3, on a horizontal rocker at 10rpm 4ºC overnight. On the next day, the primary antibody preparation was recovered and kept at 4ºC (these were re-used for a maximum of 5 times); the sections were washed with PBS-0.1%Tx^{100} three times and incubated with the appropriate secondary antibodies on a horizontal rocker at 10rpm 4ºC overnight. Secondaries were diluted -typically at 1:500- in 500µl of PBS-0.1%Tx^{100} containing 5% [v/v] serum, 1% [w/v] BSA Unbound secondary antibodies were washed three times with PBS-0.1%Tx^{100} and, if required, cell nuclei were counterstained by incubating with 1mg·l^{-1} Hoechst for 20min at room temperature before mounting.

Sections were then transferred to a 90mm-Petri dish containing 10ml of PBS, carefully collected using a paintbrush and extended onto Superfrost^{+} slides (Fisher). These were allowed to dry for 5-10min and mounted in Fluorsave (Calbiochem). Stained slides were kept at 4ºC in the dark for at least 3 months.

2.4.8.3 DAB staining on free-floating sections

Brain sections were transferred into staining pots and washed as described in 2.4.8.2. To eliminate endogenous peroxidase activity, sections were quenched with 10% [v/v] MetOH and 3% [v/v] H_2O_2 for 5min at room temperature. Blocking, incubation with primary antibodies and washes were identical to 2.4.8.2 but were done using TBS {100mM Tris-HCl (Melford); 154mM NaCl (Melford)} instead of PBS as the presence of phosphate groups can inhibit the activity of the HRP. Once bound to primary antibody, the sections were incubated with a biotinylated secondary antibody diluted -typically at 1:400- in 500µl of TBS-0.1%Tx^{100} containing 5% [v/v] serum and 1% [w/v] BSA. Sections were incubated on a horizontal rocker at 10rpm (Stuart Scientific), at 4ºC, overnight. The following day, sections were washed with TBS-0.1%Tx^{100} three times and treated with HRP-conjugated avidin (ABC-Kit, Vector Labs) following manufacturer recommendations. Briefly, 0.5% [v/v] *solution A* and 0.5% [v/v] *solution B* were pre-mixed in 500µl of TBS and placed on ice for 30min, then added to the pots and incubated on a horizontal rocker at 10rpm at 4ºC for 2h. ABC-solution was then washed twice with TBS and once with TNS (Tris non-saline buffer, 100mM, Melford). The HRP-substrate 3-3'-diaminobenzidine (*DAB Substrate Kit for peroxidase*, Vector Laboratories) was prepared following manufacturer's instructions. Briefly, two drops of *buffer solution* were added to

5ml of ddH_2O and mixed, followed by four drops of *DAB solution* and two drops of *H_2O_2 solution*. 750µl of this mixture were added to each pot and incubated on a horizontal shaker at 40rpm at room temperature until a suitable staining developed (usually between 5 to 10min). The sections were then washed once in ddH_2O and kept in TBS at 4ºC until mounting.

STEP	REAGENT	TIME	SUPPLIER
1	Xylol 100%	10min	Sigma
2	Xylol 100%	10min	Sigma
3	Xylol:EtOH (1:1)	5min	Sigma:Fisher
4	EtOH 100%	5min	Fisher
5	EtOH 95%	5min	Fisher
6	EtOH 70%	5min	Fisher
7	EtOH 50%	5min	Fisher
8	ddH_2O	5min	
9	haematoxylin	10min	Sigma
10	H_2O (running)	5min	
11	70% EtOH 0.2N HCl	5-20s	Fisher:VWR
12	H_2O (running)	5min	
13	Li_2CO_3 saturated H_2O	30s	Sigma
14	H_2O (running)	5min	
15	EtOH 95%	dip	Fisher
16	Eosin	1min	Sigma
17	H_2O (running)	5min	
18	EtOH 50%	5min	Fisher
19	70% EtOH 0.2N HCl	5min	Fisher
20	EtOH 95%	5min	Fisher
21	EtOH 100%	5min	Fisher
22	Xylol 100%	5min	Sigma
23	Xylol 100%	5min	Sigma

Table 2-11 Haematoxylin-Eosin staining

2.4.8.4 Mounting and counterstaining of DAB-stained sections

Before mounting, sections were transferred to a 90mm-Petri dish containing 10ml of TBS, carefully collected using a paintbrush and extended onto Superfrost^{+} slides (Fisher). These were allowed to dry overnight and counterstained using a standard Hematoxylin:Eosin protocol. Washes and incubation times are detailed in Table 2-11. Slides were mounted in DPX-medium (VWR) and allowed to dry.

2.5 In vivo animal work

2.5.1 Animals

Galanin knockout (*Gal*-KO) mice were obtained as described in (Wynick et al., 1998). Briefly, mice homozygous for a targeted deletion of exons 1-5 of the galanin gene were generated using the E14 cell line. Mutation was kept inbred on the 129OlaHsd strain.

Adult Wistar male rats were obtained from Charles-River, all animals were between 280-310g at the time of surgery.

Pregnant female Wistar rats at E18 gestation day were obtained from the central animal facility (University of Bristol).

2.5.2 Adult neurogenesis study

In the short-term group, adult (8 to 10 weeks old) WT males and *Gal*-KO mice were given a single intraperitoneal injection (IP) of BrdU (Sigma) 100mg·Kg^{-1} in saline. Animals were sacrificed and perfused 2h later and their brains harvested as

described in 2.5.6. In the long-term study, animals were given one daily intraperitoneal injection (IP) of 100mg·Kg^{-1} BrdU for four consecutive days and sacrificed after 21 days.

2.5.3 Stereotactic surgery

All surgical procedures were carried out with sterile instruments, drapes, gloves and solutions. Animals were anaesthetized with a mixture of 1mg·Kg^{-1} medetomidine (*Dormitor*, Pfizer) and 75mg·Kg^{-1} ketamine (*Vetalar*, Pfizer) by IP injection, adequate anaesthesia was determined by footpad pinching and eye-blinking tests. Animals were shaved and mounted on a stereotaxic frame on a flat-skull position. The scalp was cut and held back with skin retractors to expose the dorsal surface of the skull. Craniotomies were made at the appropriate stereotactic coordinates relative to bregma and dura, according to the brain atlas of Paxinos and Watson (1998), injections were then performed using a Hamilton syringe fitted with a 33G gauge-15mm needle. Viral vectors were infused at a rate of 0.2µl·min^{-1} and the syringe was left in place for 5min after the injection. At the end of the procedure, the wound was closed using re-absorbable sutures and the animal recovered by subcutaneous administration of 0.2mg· Kg^{-1} atipamezole (*Antisedan*, Pfizer).

2.5.4 Nigro-striatal lesions

6-Hydroxydopamine (6-OHDA Sigma) was made up in deoxygenated sterile ddH_2O (bubbled with N_2) to a final concentration of 5g·l^{-1}. This was aliquoted under sterile conditions and kept at -80ºC for later use. To prevent the rapid

oxidation of 6-OHDA a new aliquot was used for every two animals. Injections were performed using a Hamilton syringe fitted with a 33G gauge-15mm needle as above. 6-OHDA was infused at a rate of $0.4\mu l \cdot min^{-1}$ and syringe was left in place for 2min after the injection.

2.5.5 Rotational behaviour

In order to assess the functional integrity of the nigro-striatal dopaminergic system, animals were injected with $2.5mg \cdot Kg^{-1}$ *D*-amphetamine sulphate (Sigma) IP or subcutaneously with $0.25mg \cdot Kg^{-1}$ *R*-apomorphine hydrochloride hemihydrate (Sigma). Amphetamine solutions were made up fresh on the day of turning whereas for apomorphine, a 10X stock {apomorphine 2.5g·l-1; 0.1% [w/v] ascorbic acid} was made up in deoxygenated-sterile ddH_2O and kept at -80ºC. Immediately after injection of the drugs, animals were placed inside 30cm-rotameters (kind gift from Oxford Biomedica) and attached to the revolution counter using an elastic corset. Ipsilateral and contralateral rotations were recorded every 5min using the *rotarod software* (purposely-designed in Oxford-Biomedica). Animals were monitored for up to 70min in apomorphine-induced rotations or up to 90min in amphetamine-induced rotations and returned to their cages.

2.5.6 Transcardial perfusions and brain harvesting

Animals were terminally anaesthetized with $150mg \cdot Kg^{-1}$ pentobarbital (*Euthatal*, Merial animal Health Ltd), adequate anaesthesia was determined by footpad pinching and eye-blinking tests. Once breathing had stopped, an incision was

performed through the sternum, the rib cage retracted and the heart exposed after removal of pericardium. A blunted needle (19gauge for rats and 23gauge for mice) was introduced into the left ventricle and clamped in place using a pair of mosquito-haemostats. The right atrium was pierced to allow the drainage of the perfusate. PBS-Heparin ($1U \cdot ml^{-1}$, Sigma) was injected using a peristaltic pump. 200ml at a rate of $40ml \cdot min^{-1}$ were used for rats and 20ml at $4ml \cdot min^{-1}$ for mice. This was followed by perfusion with 4% [w/v] PFA, again, 200ml at $40ml \cdot min^{-1}$ for rats and 20ml at $4ml \cdot min^{-1}$ for mice. The animals were then decapitated, the brains harvested, post-fixed in 4% [w/v] PFA overnight and transferred into a 30% [w/v] sucrose solution until sectioning.

2.5.7 Brain sectioning

Sucrose-equilibrated brains from section 2.5.6, were embedded in *OCT-matrix* (Thermo-Fisher), frozen and sectioned at -20ºC using a *Leica CM1900* cryostat (Leica). The brains were sectioned coronally or sagittally at 40µm and the sections transferred into 12-well plates (Nunc) containing an *antifreeze solution* {30% [v/v] ethylene glycol (Sigma); 30% [v/v] glycerol (Sigma); 3.8mM Na_2HPO_4 (Sigma); 1.3mM NaH_2PO_4 (Sigma); 0.01% [w/v] NaN_3 (Sigma)} and kept at -20ºC until analysed.

2.6 Image acquisition

Fluorescence staining was viewed under a Leitz DMRD fluorescent microscope attached to a Leica DFC340FX digital high-sensitivity monochrome camera and visualized using Leica Application suite 3.3.1. DAB-stained sections were viewed

under a Leitz DMRD microscope attached to a Leica DC500 42bit-color digital camera and visualized using the Leica IM50 4.0 software. Full-brain panels were obtained by taking low magnification images (10X) across the brain and carefully overlapping them using Adobe Photoshop CS3 software. Cell counts were performed using ImageJ and the cell counting plugin from Kurt De Vos at the University of Sheffield.

2.7 Statistical analysis

Statistical analysis was performed using the Graph Pad Prism software V4. When only two groups were studied, means were compared by Student's t-tests. For comparisons between more than one group with only one factor as source of variance, data were analysed by one-way ANOVA followed by Dunnett post test (if only compared to a control group) or a Newman-Keuls post-hoc test (for all possible comparisons). For studies with more than one group with two factors as source of variance, data were analysed by two-way ANOVA followed by Bonferroni post-hoc. N numbers were greater than or equal to three. The null hypothesis was rejected if $p < 0.05$.

Chapter 3

Chapter 3

Astrocyte secreted clusterin enhances neuronal differentiation from human neural precursor cells

Getting older is no problem. You just have to live long enough.
Groucho Marx

3.1 Introduction

3.1.1 Regional astrocytes

Astrocytes are essential regulators of neuronal function; they help to maintain the metabolic homeostasis in the brain (Walz, 2000; Bröer and Brookes, 2001) and to preserve the integrity of the brain-blood barrier (Liedtke et al., 1996). Astrocyte projections encapsulate neuronal synapses (Araque et al., 1999), promote synaptogenesis (Ullian et al., 2001) and can respond to neuronal activity (Wang et al., 2006). Reciprocally, astrocytes can also produce and release gliotransmiters to modulate neuronal activity, although the physiological relevance of this phenomenon remains controversial (Smith, 2010). Furthermore, astrocytes can promote neuronal differentiation itself (Song et al., 2002; Nakayama et al., 2003) and can protect neurons against insults such as ischemia (Lin et al., 2006). Indeed, neurons are so dependent on astrocytic support that it is not possible to generate viable neuronal populations in the complete absence of astrocytes (perhaps with the exception of retinal ganglion cells (Pfrieger and Barres, 1997) and evolutionary increases in neuronal number or complexity are associated with increased astrocyte to neuron ratios (Sherwood et al., 2006).

Astrocytes have classically been divided in three main subtypes according to their morphology: radial astrocytes surrounding the ventricles, protoplasmic astrocytes in grey matter and fibrous astrocytes in the white matter (Chen and Swanson, 2003); or in two types according to cellular markers – glial fibrillary acidic protein (GFAP) or S-100β (Ludwin et al., 1976). However, recent evidence challenges this simplistic view: astrocytic populations from the cerebellum, neocortex and brainstem have remarkably different transcriptomes (Yeh et al., 2009). Cortical and midbrain astrocytes have different trophic requirements (Wagner et al., 2006). Furthermore, hippocampal astrocytes (but not astrocytes from non-neurogenic areas like the cortex or spinal cord) are potent inductors of neurogenesis and neuronal fate commitment (Song et al., 2002). But not only is there a gross regional segregation of astrocytes, Hochstim et al. have shown that in the spinal cord, astrocyte diversity is generated following the same homeodomain transcription factor code as their neuronal counterparts. At least three positionally distinct astrocytic subtypes within the same spinal cord segment can be identified (Hochstim et al., 2008), for review see (Freeman, 2010). More recently Krencik et al. have successfully generated immature astrocytes from human pluripotent cells that carry distinct homeodomain transcription factors and display rostro-caudal and dorso-ventral patterning in vitro (Krencik et al., 2011). This was confirmed in the brain by Tsai et al., who showed that astrocytes generated from the developing neural tube migrate only radially and that astrocytic populations from different neural tube segments do not overlap spatially. Remarkably, the loss of a specific astrocytic subtype caused the loss of specific neuronal populations and could not be compensated by astrocytes from other regions (Tsai et al., 2012). This suggests that astrocytes could perhaps be as

diverse as the neurons they support, a concept already put forward by B. Barres in his wonderful review "The mystery and magic of glia" (Barres, 2008)

Furthermore, just one astrocytic subtype releases a myriad of factors into the brain parenchyma. These include neurotrophic factors such as glial derived neurotrophic factor (GDNF) (Appel et al., 1997), ciliary neurotrophic factor (CNTF) (Kamiguchi et al., 1995), or nerve growth factor (NGF) (reviewed in Ridet et al., 1997) and numerous interleukins (reviewed in Dong and Benveniste, 2001). Astrocytic secretomes have been profiled by a combination of proteomics and bioinformatics (Greco et al., 2010; Dowell et al., 2009) or by two-gel electrophoresis followed by mass-spectrometry in mouse postnatal astrocytes. (Lafon-Cazal et al., 2003). These studies have detected hundreds of proteins with multiple biological effects. Among the most abundant of these proteins are: apolipoprotein E, cystatin C, α2-macroglobulin, secreted protein and rich in cysteine (SPARC) and apolipoprotein J – also known as clusterin.

3.1.2 Clusterin

Clusterin (apolipoprotein J) was first isolated from human plasma as a 70KDa highly glycosylated protein (de Silva et al., 1990). In the full-length clusterin a signal peptide at the N-terminus forces endoplasmic reticulum (ER) translocation and consequent secretion. Immediately before secretion immature clusterin is cleaved in the Golgi apparatus (GA) and secreted as heterodimer (Burkey et al., 1991). This secreted form is the most abundant (95%) and is designated sCLU. Interestingly, clusterin contains a second start codon at position 34. Translation from this position produces a truncated form (43KDa) that cannot be secreted as it

lacks a signal peptide but is instead translocated to the nucleus due its nuclear localization signal between amino acids 52 to 58. This form is designated nCLU (Reddy et al., 1996). Furthermore, glycosylated but uncleaved sCLU is also found in the cytosol. Retro-translocation from the ER is a rare event but can be induced by inhibition of the proteasome (Harshman et al., 1999). Subcellular localization is critical for clusterin function as sCLU has anti-apoptotic effects whereas nCLU can sequester the anti-apoptotic factors BCL-2 and BCL-Xl through its BH3 domain (Lee et al., 2011a) and is considered to be pro-apoptotic (for review see Nayoung Kim, 2011) .

Clusterin is generally up-regulated in stress conditions. *Drosophila melanogaster* flies overexpressing human clusterin are more resistant to heat shock and oxidative stress. Remarkably, these flies have reduced levels of reactive oxygen species and increased life span (Lee et al., 2012). Michel et al. discovered a highly conserved domain in the clusterin promoter (clusterin element or *Cle*). *Cle* is very similar to the consensus sequence of the heat shock response element in mammals, it can recruit heat-shock transcription factors like heat shock factor-1 (HSF-1) and confers heat shock dependent transcriptional activation (Michel et al., 1997). Other stressors such as irradiation or topoisomerase poisons can also induce clusterin expression (Goetz et al., 2011). It has been suggested that sCLU could act as an extracellular ATP-independent co-chaperone, with similar roles to the intracellular heat shock protein-25 (*Hsp25*) (Poon et al., 2000). Indeed, sCLU can prevent heat-induced denaturing and precipitation of ovotransferrin, lysozyme and arginine-vasopressin in vitro. sCLU does not prevent the loss of protein activity but keeps the unfolded protein in a competent state for refolding by

ATP-dependent chaperones like heat shock protein-70 (*Hsp70*). This process is not dependent on ATP and no ATPase activity is found in clusterin (Poon et al., 2000).

Clusterin displays an impressive array of biological functions. Clusterin mRNA is up-regulated in the regenerating pancreas: following pancreatectomy, *Clu*-KO mice have reduced proliferation in the epithelial cells of pancreatic ducts, reduced number of insulin producing cells and fewer endocrine islets. This results in decreased endocrine and exocrine tissue differentiation and impaired glucose tolerance (Lee et al., 2011b). In the heart, clusterin mRNA is induced after autoimmune myocarditis and *Clu*-KO mice are more susceptible to myocardial damage with increased inflammation and myocyte necrosis compare to wild-type (WT) controls (McLaughlin et al., 2000). In the kidney, *Clu*-KO mice develop glomerulopathy at old age, associated with abundant collagen and the deposition of immune complexes in glomerular lesions (Rosenberg et al., 2002). In the testis, clusterin is involved in spermatogenesis. *Clu*-KO mice are fertile but have accelerated germ-cell apoptosis and delayed tissue reorganization after testicular heat shock (Bailey et al., 2002).

3.1.2.1 Clusterin and cancer

There is a strong association between clusterin expression and tumorigenicity. Clusterin is up-regulated in genetically unstable cells and after double stranded DNA breaks (Goetz et al., 2011). The clusterin promoter contains a *B-myb* binding site - a transcription factor involved in cell cycle progression and tumorigenesis (reviewed in Oh and Reddy, 1999). Overexpression of clusterin in

the neuroblastoma line LAN-5 reduces the apoptotic cell death caused by the antitumor drug doxorubicin. This protection is lost if an antibody raised against clusterin is added to the culture medium, confirming that the anti-apoptotic effect of clusterin is due to its extracellular form (Cervellera et al., 2000). Similarly, clusterin overexpression induces chemoresistance against etoposide in fibrosarcoma cell lines (Zhang et al., 2005). Moreover, in non-small-cell lung cancer cell lines, the levels of sCLU are inversely correlated to chemosensitivity to several antitumor drugs. Accordingly, cell viability is reduced after clusterin knock-down and increased with conditioned medium containing clusterin (Cheng et al., 2012). In intestinal tumours isolated from mice with multiple intestinal neoplasia, clusterin immunoreactivity is elevated and generally absent from apoptotic cells (Chen et al., 2003). Furthermore, high levels of clusterin are found in multiple prostate cancer cell lines (Zhang et al., 2005) and antisense RNA constructs specific for sCLU mRNA are now in phase II/III clinical trials in combination with standard chemotherapies for prostate cancer.

In summary, clusterin expression in cancer cells is associated with increased survival and resistance to antitumor drugs. This chemoresistance is generally conferred by the secreted form sCLU. Although in some cases, high levels of nCLU (but not sCLU) are found in some highly metastatic cancer cell lines and are associated with chemoresistance to antitumor drugs. (Zhang et al., 2005)

3.1.2.2 Clusterin expression in the brain

Pasinetti et al. found clusterin mRNA by in situ hybridisation in all brain regions of the adult rat brain. Intense labelling appeared in neurons from the CA1 and

CA3 regions of the hippocampus and astrocytes throughout the brain (Pasinetti et al., 1994). During brain development in mouse, clusterin mRNA increases after embryonic day 14 (E14) when is localized in the ependymal cells of the choroid plexus and periventricular zones. By E16, neuronal populations throughout the brain express clusterin. From E18, intense clusterin labelling appears in hippocampal astrocytes and astrocytic populations across the cortex. Brain protein levels continue to increase with age, peaking around postnatal day 14 (P14) (Charnay et al., 2008). Clusterin is also up-regulated after stress in the brain: after treatment with transforming growth factor-β (TGF-β) in cortical astrocytes in vivo and in mixed glial cultures in vitro (Morgan et al., 1995); after kainic acid treatment in the cortex and hippocampus (Montpied et al., 1998); after lipopolysaccharide (LPS) treatment in mixed glial cultures (Saura et al., 2003) and in the post-ischemic hippocampus (Han et al., 2001).

3.1.2.3 Clusterin in Alzheimer's disease

Alzheimer's disease (AD) is characterized by three pathological features: presence of intracellular inclusions of hyperphosphorylated tau [named neurofibrillary tangles (NTF)], extracellular deposits of amyloid [named amyloid plaques (AP)] and vascular amyloidosis. Amyloid-β (Aβ) aggregates are the main component of extracellular APs. Aβ is produced by enzymatic cleavage of the transmembrane amyloid precursor protein (APP). γ-secretase is one of the enzymes involved in APP processing and can produce both Aβ1-40 or Aβ1-42 depending on the cleavage site. Increased production of Aβ caused by mutations in the *App* gene or by gene triplication (Down's Syndrome) trigger early onset

AD. Conversely, alterations in Aβ metabolism or clearance are associated with late-onset AD (LOAD).

Levels of hippocampal clusterin are increased in AD and correlate with the number of apoE4 alleles present (Bertrand et al., 1995). Interestingly, clusterin is present in surviving NFT-containing neurons in AD (Giannakopoulos et al., 1998). Early studies showed that clusterin can bind to Aβ1-40 with higher affinity than to aggregated forms of amyloid (Matsubara et al., 1995) and that clusterin inhibits aggregation Aβ1-42 in vitro (Oda et al., 1995). More recent and refined methodologies have confirmed that clusterin forms very stable complexes with Aβ oligomers, robustly inhibiting further aggregation into fibrils (Narayan et al., 2012). Furthermore, pre-fibrillated Aβ1-42 induces up-regulation of clusterin in human astrocytes in vitro (Nuutinen et al., 2007). Accordingly, loss of clusterin leads to a marked increase in amyloid burden and deposition in the hippocampus and cortex in a mouse model of AD (DeMattos et al., 2004).

In addition to preventing the aggregation of Aβ, clusterin also has a role in clearing Aβ from the brain across the BBB (Shayo et al., 1997). Once translocated across the BBB, complexes between clusterin and misfolded or aggregated proteins are rapidly cleared from the circulation by the liver and degraded by lysosomal proteases (Wyatt et al., 2011).

The translocation process is mediated by the clusterin receptor megalin (Zlokovic et al., 1996), for review see (Bu, 2009). Megalin has four times higher affinity for Aβ-clusterin complexes than free clusterin (Zlokovic et al., 1996) and binding to megalin causes receptor internalisation in vitro (Kounnas et al., 1995), a process

that is stimulated by insulin growth factor 1 (IGF1) (Carro et al., 2005). In the adult brain, megalin is only expressed in the choroid plexus and ventral regions of the lateral ventricles (Assémat et al., 2005). Interestingly, down-regulation of megalin causes cortical accumulation of Aβ1-40 and Aβ1-42 in mice and compromises water maze performance (Carro et al., 2005). Furthermore, megalin levels are reduced with age and in AD (Dietrich et al., 2008) and a single nucleotide polymorphism (SNP) in the megalin promoter that reduces its activity is associated with a small increase in the risk of LOAD (Vargas et al., 2010).

Despite all this experimental evidence, the importance of the association between clusterin and AD was only recently vindicated by a large genome-wide association study (GWAS) in American and European populations. In this study, only three SNPs reached genome-wide significance: rs1048699 (corresponding to the well-known LOAD risk-factor *APOE*) and two newly identified loci: rs3851179 in the *PICALM* gene and rs11136000 in an intron of the clusterin gene (Harold et al., 2009). This association was validated in data pooled from three studies in the Chinese population (Ma et al., 2011) and one study in the Taiwanese population (Lin et al., 2012). In this model, rs1113600 follows a recessive inherited model with TT genotype carriers having a reduced LOAD risk (Ma et al., 2011). After genotyping the entire coding region of the clusterin gene in a Texas cohort, 18 polymorphisms were identified. Interestingly, mutations leading to a loss of clusterin function were only found in AD patients (Ferrari et al., 2012). Furthermore, patients from the Danish 1905 cohort study carrying the T allele in the rs11136000 SNP had better cognitive composite scores than other

genotypes (Mengel-From et al., 2011). This highlights the importance of clusterin as a protective factor in LOAD.

Remarkably, clusterin has also been associated with other neurodegenerative diseases such as Parkinson's disease (Gao et al., 2011) or prion-disease (Freixes et al., 2002; Sasaki et al., 2002). This suggests not only the existence of a shared underlying mechanism for these diseases but also the potential for a common therapeutical approach and the importance of studying clusterin in neurodegeneration and repair.

3.2 Aims

To confirm the regional properties of astrocytes by studying the effect of astrocyte conditioned medium (ACM) on human neural stem cells. In order to do this we will obtain pure astrocytic cultures from several regions of the postnatal rat brain and collect their conditioned medium after culture in vitro. We will then test the ability of regional ACMs to promote neuronal differentiation and / or survival of NSCs isolated from the developing human midbrain and expanded in vitro. We will next analyse the protein composition of the ACMs by mass spectrometry in order to discover factors with differential expression in regional ACMs. To confirm the involvement of a given factor, this will be removed from ACM by immunodepletion. We will then test the ability of ACM immunodepleted of the factor of interest or the ability of the purified factor itself to recapitulate the effects of native ACM. We will also determine if components of ACM can activate pro-survival signalling pathways within the cell by imaging the intracellular levels of phosphorylated second messengers using high content microscopy. Finally, we will test if the effects of ACM / ACM components are restricted to MB-ACM or are also applicable to NSCs from other areas of the developing human brain.

3.3 Author contribution

Production of ACM and phospho-neurofilament cell counts were done by Dr Sarah Scott at the Centre for Brain Repair at Cambridge University. Mass-spectrometry analysis was performed by Dr Ruma Raha-Chowdhury at Cambridge University.

3.4 Materials and methods

3.4.1 Preparation of astrocyte conditioned medium

Mixed glial cultures from P0-P3 rat pups were prepared as previously described in 2.2.3 (McCarthy and De Vellis, 1980). Glia from midbrain (MB), cortex (CTX) and hippocampus (HPC) were plated on *PDL* and cultured in Dulbecco's Modified Eagle's Medium (DMEM), 1% [v/v] penicillin G/streptomycin/ amphotericin (Sigma) and 10% [v/v] fetal calf serum (FCS). Medium was changed 24h after platting and twice weekly thereafter until the cells reached confluence (8–10 days). Microglia were removed by vigorous shaking of the cultures at 240rpm for 20 min, followed by removal of oligodendrocyte progenitor cells by shaking at 160rpm, overnight. The remaining monolayer was treated with 20μM arabinofuranosyl cytidine (Ara-C, Sigma) for 72h, and washed with DMEM containing 1% [v/v] PS and 1% [v/v] N2-supplement (Invitrogen). 24h later, fresh DMEM containing 1% [v/v] PS was added for a further 48h. Medium was then collected, filtered with a 0.45μm filter unit (Nalgene) aliquoted and stored at -20ºC for later use.

3.4.2 MALDI tandem MS analysis and protein identification

Proteins in 200ml of media were precipitated with acetone, resolubilized in 0.3% [w/v] sodium dodecyl sulphate (SDS, Sigma), reduced and alkylated with S-methyl methanethiosulfonate and digested with trypsin (Promega) at 37ºC overnight. The peptide mixture was zip-tipped (C18; Waters) and analysed by nanoLC-MALDI. MS analysis was achieved using a MALDI-TOF/TOF instrument (4700 Proteomics Analyzer, Applied Biosystems). The MS/MS spectra

were searched against all species in the National Centre for Biotechnology Information (NCBI) database using GPS software (Applied Biosystems) running Mascot search algorithm (Matrix Science) for peptide and protein identification. A mass tolerance of 100ppm and 0.25Da was used for precursors and fragment ions, respectively. The data searches were performed with the following criteria: variable modifications with methionine oxidation, S-methyl methanethiosulfonate derivation of cysteine and N-terminal pyroglutamate. Two missed cleavages were allowed. At least 95% confidence interval threshold was used for peptide identification and manual validation was also performed for each MS/MS spectrum.

3.4.3 Immunodepletion of clusterin from midbrain ACM

Pansorbin-A beads (Millipore) were incubated in either rabbit anti-clusterin (0.1mg) or normal rabbit serum (Invitrogen, Renfrew, UK) overnight at 4ºC. Following three washes with phosphate buffered saline (PBS, Invitrogen); beads with absorbed IgGs were incubated with 5ml of MB-ACM for 6h at 4ºC. Beads were pelleted by centrifugation 14,000 RCF for 20min at 4ºC. ACM was collected for neuronal differentiation and beads were boiled for 5min in lysis buffer {50mM Tris (Melford), 150mM NaCl (Melford), 1mM ethylene glycol tetra acetic acid, (EGTA, Sigma)} containing a cocktail of protease inhibitors (Complete Mini, Roche). Released clusterin and beads were separated by centrifugation at 14,000 RCF for 20min at 4ºC.

3.4.4 Human fNSCs culture

Human ventral mesencephalon (VM) or CTX (8–10 weeks post conception) was collected following routine terminations of pregnancies. The methods of collection conformed to arrangements recommended by the Polkinghorne Committee (1989) and the United Kingdom Department of Health guidelines (1995). Human CTX or VM fNSCs were expanded and passaged as described in 2.2.6.

3.4.5 Differentiation of human fNSCs

To induce differentiation, CTX and VM neurospheres were plated on poly-D-lysine/laminin coated (2.2.1.3) 8-well glass chamber-slides (BD-Scientific). One or two neurospheres were transferred into each well using a sterile plastic pipette tip. Differentiation medium consisted in {DMEM (Sigma), 1% (v/v) N2 (Invitrogen), 1 $g \cdot l^{-1}$ BSA (Sigma), 0.6$g \cdot l^{-1}$ *N*-acetyl-cysteine (Sigma), 5nM forskolin (Sigma), 1% [v/v] PS (Sigma) and 1% [v/v] *L*-glutamine (Sigma)}. 250µl of medium were added in the control wells. 125µl of differentiation medium-containing 2% [v/v] N2-supplement and 125µl of ACM from the CTX, HPC or MB were added to designated wells. In clusterin-only wells, purified clusterin (ProspectBIO) was added to the differentiation medium to a final concentration of 5nM or 10nM. Cells were fed by replacing 50% of the medium every 4 days with fresh culture medium. 0.2mM bromodeoxyuridine (BrdU, Sigma) was added to the medium on plating day and kept in the cultures for 7 days. After 7 days cells were fixed in 4% [w/v] *para*-formaldehyde (PFA, Sigma) and processed for immunohistochemistry.

3.4.6 Imaging and quantification of cultured cells

Cultures were viewed under a Leitz DMRD fluorescent microscope attached to a Leica DFC340FX digital camera and visualized using Leica Application suite 3.3.1. Images were taken from a minimum of four random fields (20x magnification) per coverslip from four coverslips per culture from at least four independent cultures. Results were analysed by one-way ANOVA followed by Newman–Keuls post hoc test.

3.4.7 Immunocytochemistry and TUNEL assay

Standard immunocytochemistry was performed as described previously (2.4.8.1). Primary and secondary antibodies are detailed in Table 3-1. For Terminal deoxynucleotidyl transferase dUTP Nick End Labelling (TUNEL), the standard protocol was modified as follows: cells were permeabilised by with 0.1% [w/v] sodium citrate and 0.1% [v/v] polyethylene glycol tert-octylphenyl ether (Tx^{100}, Sigma) for 2min on ice. As a positive control, some wells were treated with 50U of DNAse I (Roche) for 20min at 37ºC. After three washes with PBS, 50µl of TUNEL reaction mixture (*In Situ Cell-death detection Kit*, ROCHE) were added per coverslip. As a negative control, some wells were stained with a TUNEL reaction mixture without the terminaldeoxynucleotidyl transferase enzyme. Plates were placed for 60min at 37ºC in a humidified incubator, washed twice with PBS, blocked in 10% [v/v] normal goat serum (NGS) (Vector Laboratories) and 1% [w/v] BSA for 3h and stained with anti-TUJ1 antibody overnight. Our TUNEL kit is fluorescein based, which has a maximum emission wavelength at 521nm.

Therefore *Alexa fluor* 568 (Table 3-1) with maximum emission wavelength at 603nm was used as secondary antibody.

3.4.8 Deglycosilation of conditioned media

A volume of 18µl of MB-ACM or HPC-ACM was incubated for 10min at 100ºC with 2µl of denaturing buffer (NEB). Denatured ACMs were treated with 500U of peptide: *N*-glycosidase F (PNGase F, NEB) to remove *N*-linked oligosaccharides; 40,000U of endo-*a*-*N*-acetylgalactosaminidase (*O*-glycosidase, NEB) and 50U of neuramidase (NEB) to eliminate *O*-linked oligosaccharides. Reactions were carried out in 1% [v/v] NP40 (NEB) and 1X G7 reaction buffer at 37ºC overnight. Deglycosylated extracts were run in 12% [w/v] SDS–Tris–glycine gels and probed for clusterin.

3.4.9 SDS-polyacrylamide gel electrophoresis and western blot analysis

After electrophoretical separation of protein extracts in 10% [w/v] SDS-Tris-glycine gels, proteins were blotted onto 0.45mm polyvinylidene difluoride (PVDF) membranes as described previously (2.4.3 & 2.4.4). Membranes were blocked with 10% [w/v] skimmed dry milk (Marvel) and 0.05% [v/v] polyoxyethylenesorbitan monolaurate (Tween 20, Sigma) in Tris buffered saline (TBS, Melford). After incubation with primary antibody (anti-Rat clusterin, 1:1000 in blocking buffer) followed by the horseradish-peroxidase (HRP)-conjugated secondary antibody anti-rabbit IgG (1:2000 Jackson Labs in blocking buffer) protein bands were visualized with ECL plus chemiluminescence developing agent (Amersham ECL plus, GE Healthcare) as described previously (2.4.6).

3.4.10 Semi-automated image acquisition and analysis

15,000 cells were plated on poly-*D*-lysine coated 96-well plates. After 24h, cells were stimulated with 10nM clusterin (Prospecbio) from 5min to 6h. Cells were washed once with ice-cold PBS and fixed with 4% [w/v] PFA for 20min. Immunohistochemistry was performed as described previously (2.4.8.1). Briefly, cells were blocked in 10% [v/v] NGS and 1% [w/v] BSA for 3h and stained with anti-p44/42 MAP kinase and anti-phospho p44/42 MAP kinase overnight. Appropriate secondary antibodies were used (Table 3-1). Cell nuclei were counterstained with $0.1 mg \cdot l^{-1}$ Hoechst. Image acquisition and analysis were performed on an IN Cell Analyzer workstation (GE Healthcare) using a multi-target analysis algorithm to quantify fluorescence intensity in nuclear and cytoplasmic compartments (in total and ppERK1/2 image channels).

ANTIBODY	SPECIES	DILUTION	SUPPLIER
Alexa fluor 488 anti mouse IgG	Goat	1:500	Invitrogen
Alexa fluor 488 anti rabbit IgG	Goat	1:500	Invitrogen
Alexa fluor 488 anti rat IgG	Goat	1:500	Invitrogen
Alexa fluor 568 anti rabbit IgG	Goat	1:500	Invitrogen
IgG anti BrdU	Rat	1:400	Abcam
IgG anti Clusterin	Rat	1:1000	BioVendor
IgG anti GFAP	Rabbit	1:1000	DAKO
HRP-conjugated anti rat	Goat	1:2000	Jackson Labs
IgG anti p44/42 MAP Kinase	Rabbit	1:400	Cell Signalling
IgG anti Phospho-p44/42 MAP Kinase (Thr202/Tyr204)	Mouse	1:400	Cell Signalling
Tuj1	Mouse	1:500	Covance

Table 3-1 List of antibodies used, species raised in, dilutions and suppliers.

3.5 Results

3.5.1 ACM from the hippocampus and midbrain, but not cortex increase the number of neurons from VM-hfNSCs.

To determine if regional ACM had an effect on the number of VM-hfNSC-derived neurons, VM-hfNSCs were expanded for one month in FGF-b + Hep before plating in control, CTX, HPC or MB ACM. MB-ACM increased the number of neurons after a week and month of differentiation (Newman-Keuls, $p<0.05$; N=4, Figure 3—1a). HPC-ACM had a similar effect that became statistically significant after a month (Newman-Keuls, $p<0.05$; N=4, $p<0.05$). Interestingly CTX-ACM had no effect on neurogenic potential. We next examined ACMs effects on morphology and specifically on neurofilament phosphorylation using SMI312. This antibody is specific for phospho-epitopes in neurofilaments, and was used as readout for axonal integrity. The results show that MB-ACM significantly increased the number of SMI312 neurons (Newman-Keuls; N=4, Figure 3—1a and b) after one week ($p<0.01$) and one month ($p<0.01$). Again, HPC-ACM showed a similar increase that became statistically significant after a month ($p<0.05$; Figure 3—1a). To determine whether regional ACM had an effect on neurite length, neurite lengths in SMI312-expressing neurons were measured.

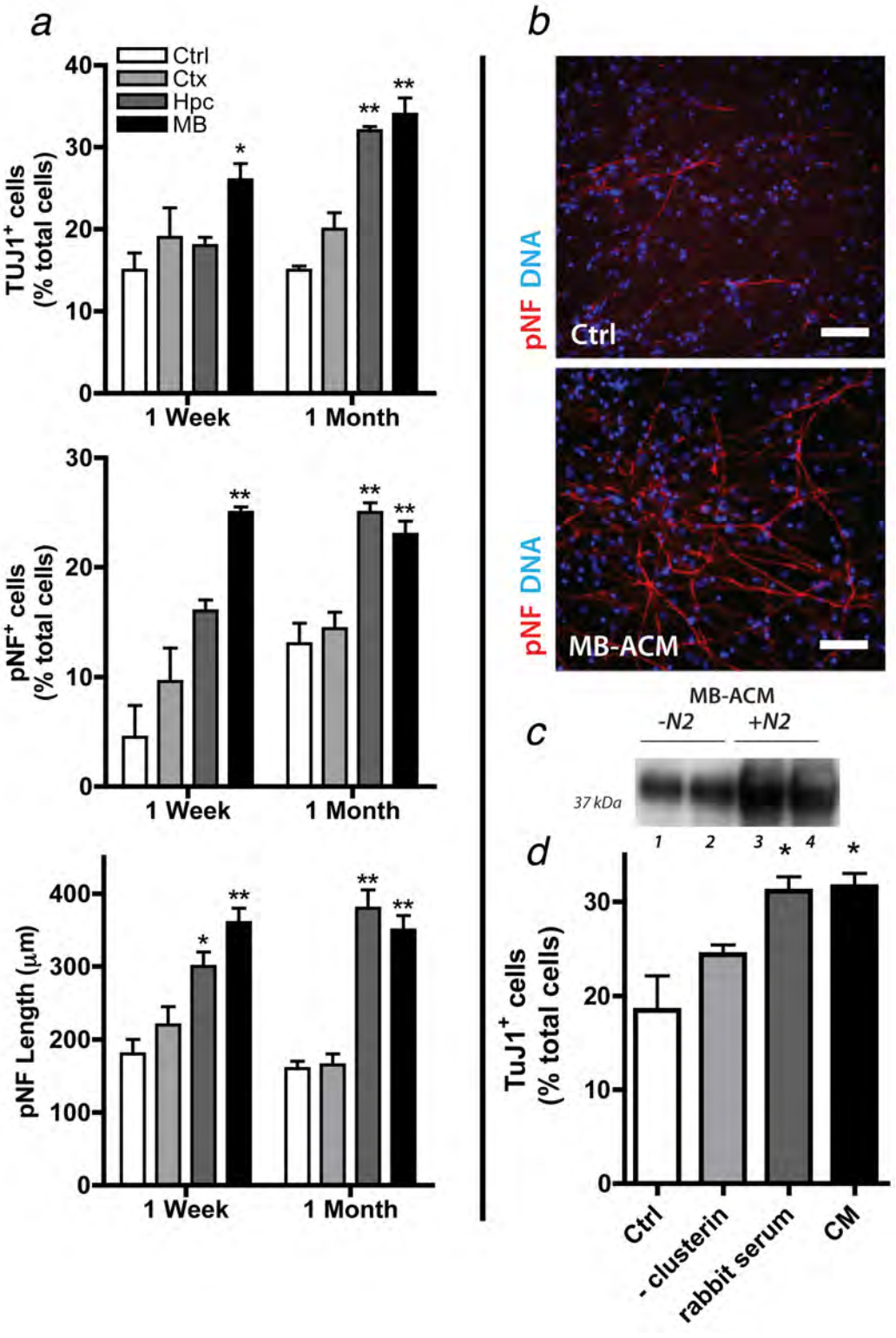

Figure 3—1 ACM increases neuronal differentiation from VM derived hfNSCs. Midbrain ACM increases TuJ1 after 1 week, and both hippocampal and midbrain ACM increase TuJ1 after 1 month of differentiation. Midbrain ACM increases phosphorylated neurofilaments (pNF) neurons after 1 week, and both hippocampal and midbrain increase pNF after 1 month of differentiation, Both

hippocampal and midbrain ACM increase neurite lengths after 1 week and 1 month. (b) Photomicrograph of pNF in control and cells treated with midbrain ACM after 1 month. (c) Western blot showing clusterin immunodepletion from midbrain ACM. Lanes 1, 2 ACM without N2, lanes 3, 4 ACM with N2. (d) VM-hfNSCs differentiated for a month under control conditions, ACM immunodepleted of clusterin (-sClu), with rat anti-clusterin–IgG substituted for rabbit serum during immunodepletion (RS) and with ACM. There is a reduction in the number of Tuj1 and pNF-positive neurons when clusterin is immunodepleted from the media (-sClu) compared with rabbit serum control or ACM. *p<0.05, **p<0.01 versus Ctrl and CTX ACM; Newman Keuls, N=4 per group. Scale bars = 50μm.

Both HPC and MB ACM significantly increased neurite length (Figure 3—1a). Again CTX-ACM had no effect. Cultures were also stained for the astrocyte marker GFAP, but none of the ACMs had an effect on astrocyte numbers (Figure 3—2), revealing a neuronal specific effect for the ACM.

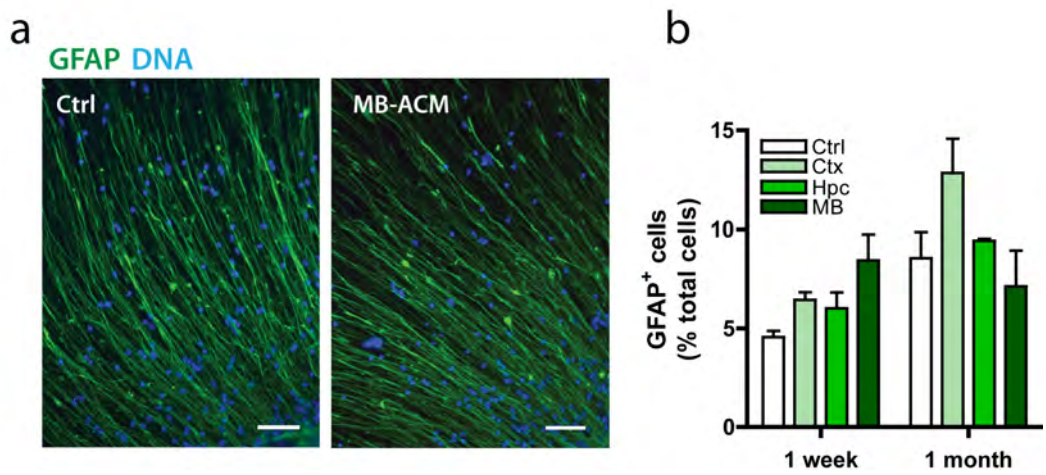

Figure 3—2 Regional ACMs do not influence astrocytic numbers Photomicrographs of GFAP$^+$ cells untreated (Ctrl) or treated with midbrain ACM. Scale bars=50μm

3.5.2 Protein identification by MS

To determine the major protein components secreted by the regional astrocytes, nanoLC-MALDI-TOF/TOF-MS/MS analyses were carried out on peptides produced from tryptic digestion of proteins in the ACM. ACM was collected in minimal phenol-free medium containing high glucose and glutamine without N2 or B27 cell media supplements, which are known to contain significant amounts of potentially confounding proteins. Five main proteins were identified by mass spectrometry in all tested ACMs (Table 3-2). All of these proteins are well known components of the astrocytic secretome (Lafon-Cazal et al., 2003; Dowell et al., 2009; Greco et al., 2010). Interestingly, clusterin was one of the major proteins found in MB and HPC ACM. However, the MALDI-TOF/TOF-MS/MS database search software was not able to identify clusterin in the cortical ACM, suggesting that this protein, if present at all, was secreted at very low levels.

Protein	MW (KDa)	Midbrain		Hippocampus		Cortex	
		Peptides	Coverage (%)	Peptides	Coverage (%)	Peptides	Coverage (%)
α-2-Macroglobulin	164	10	8.7	6	6	3	3
Clusterin	51	4	11	4	11	-	-
Cystatin C	13	3	39	3	30	3	39
Extracellular matrix protein 2	70.5	2	6	-	-	4	10
Vimentin	53.7	2	6	8	22	11	27

Table 3-2 Proteins identified in the conditioned medium of cultured astrocytes from various brain regions.
The number of peptides observed by MALDI-TOF/TOF tandem mass spectrometry and the percentage of amino acid sequence covered for each protein are indicated.

3.5.3 Clusterin in ACM is the highly glycosylated secreted form (sCLU)

Clusterin was detected by immunoblotting in MB-ACM from astrocytes grown with or without N2 supplement (Figure 3—1c). Untreated ACM gave a *smeared* band with an apparent size of 39KDa. Smearing in western-blot bands of secreted proteins is suggestive of the existence of protein species with different degrees of glycosylation. This can affect the electrophoretic mobility of the protein of interest, masking the presence of species with different molecular weight. Figure 3—3 shows that removal of *N*-linked oligosaccharides with PNGase or *O*-linked oligosaccharides with *O*-glycosydase results in a reduction of the apparent molecular weight of clusterin. Complete deglycosylation (PNGase + *O*-glycosydase) resulted in more than 30% reduction of the molecular weight of clusterin and the appearance of two different subunits. Similar glycosylation extent was found in clusterin secreted by HPC and MB astrocytes. These results confirmed that clusterin present in ACM corresponded to the highly glycosylated heterodimeric (sCLU) form described in the literature.

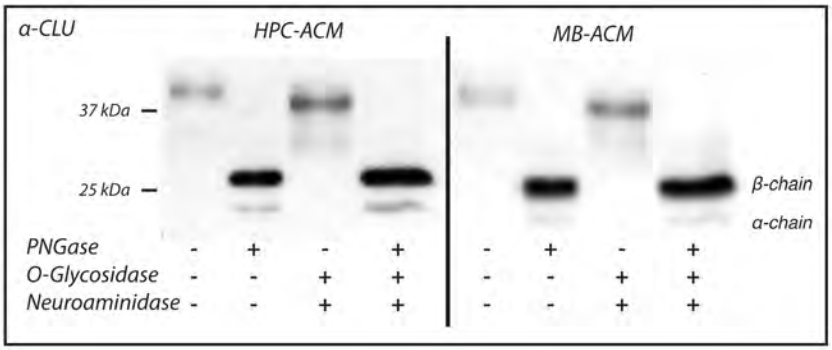

Figure 3—3 Secreted clusterin is a highly glycosylated heterodimeric protein. HPC-ACM or MB-ACM (lanes 1 & 5) were treated with PNGase to remove N-linked oligosaccharides (lanes 2 & 6); with O-glycosidase to remove O-linked oligosaccharides (lanes 3 & 7). Complete deglycosilation of clusterin is shown in lanes (4 & 8).

3.5.4 Removal of sCLU from ACM reduces neuronal differentiation from VM-derived fNSCs.

To determine the effect of sCLU on neuronal differentiation, VM-hfNSCs were differentiated in untreated MB-ACM and MB-ACM immunodepleted of clusterin (-sCLU). Figure 3—1d shows that MB-ACM or MB-ACM immunodepleted with unspecific rabbit IgGs (RS) significantly increased the number of $Tuj1^+$ cells after differentiation ($p<0.05$ vs. Ctrl; Newman-Keuls, N=4). However, when sCLU was removed from MB-ACM, this lost its pro-neuronal effect, suggesting that sCLU was, at least partly, responsible for the effect on neuronal differentiation of MB-ACM.

3.5.5 Purified clusterin recapitulates the effects of MB-ACM

Clusterin in plasma (Burkey et al., 1992; Hennessy et al., 1997) and cerebro-spinal fluid (CSF) (LaDu et al., 1998; Koch et al., 2001) is part of lipoprotein complexes. Therefore, sCLU immunoprecipitation could also deplete ACM from other apolipoproteins or factors present in lipoproteins or modify the lipid composition of the medium. In order to confirm that the loss of the pro-neuronal effect of MB-ACM after sCLU depletion is due specifically to clusterin and not to the co-immunoprecipitation of other components of ACM, we tested wether purified clusterin, alone, could mimic the effect of untreated MB-ACM. Figure 3—4a shows that this was indeed the case, 10nM sCLU added to the medium increased the number of $Tuj1^+$ neurons to a similar extent than MB-ACM.

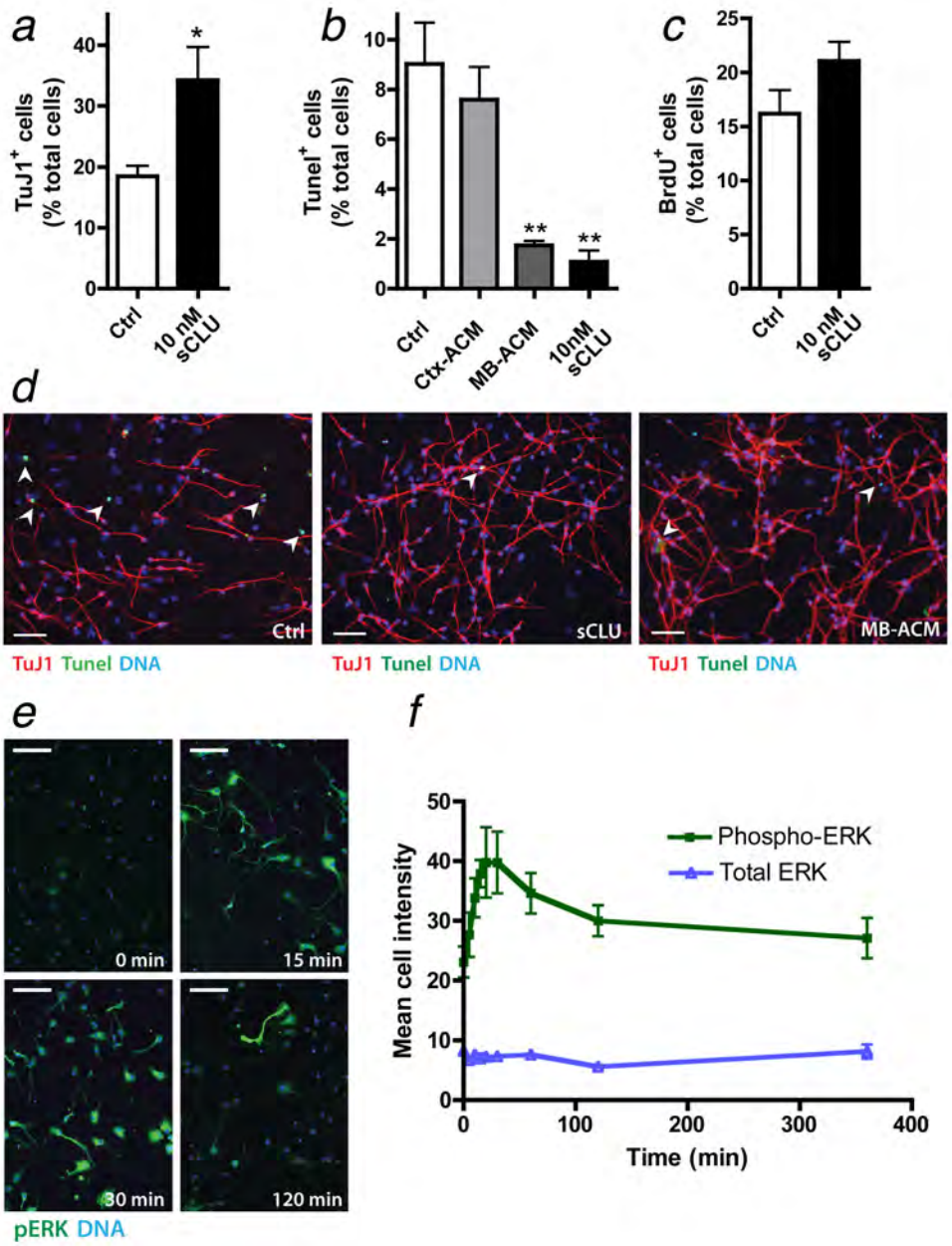

Figure 3—4 Clusterin promotes neuronal differentiation from VM derived hfNSCs by increasing cell survival.
(a) sCLU increases the number of Tuj1$^+$ neurons. (b) sCLU decreases TUNEL$^+$ nuclei to a greater extent than CTX-ACM and similarly to MB-ACM. (c) sCLU does not increase proliferation of hfNSCs (d) Photomicrograph of Tuj1$^+$ cells (red), TUNEL$^+$ nuclei (green) and DNA (blue) in cultures treated with control-ACM, 10nM sCLU or MB-ACM; scale bars = 50µm; white arrowheads point to TUNEL$^+$ nuclei (e) Photomicrographs of ERK activation after 10nM sCLU at the indicated times; scale bars = 100µm. (f) 10nM sCLU increases phospho-ERK (green squares) but not total ERK (blue triangles). *p<0.05,**p<0.01 vs. Ctrl; Newman Keuls, N=4 per group.

3.5.6 sCLU is a pro-survival factor for VM-hfNSCs but has no proliferative effect

To determine whether the increase in the neuronal number caused by sCLU was due to enhanced proliferation or survival of VM-hfNSCs, TUNEL and BrdU incorporation analysis were performed. To confirm the specificity and sentivity of our TUNEL assay methodology we performed the positive and negative controls recommended by the manufacturer (Figure 3—5). More interestingly, (Figure 3—4b & d) show that sCLU reduced the number of $TUNEL^+$ nuclei to a similar extent than MB-ACM and that CTX-ACM had no significant effect on the number of apoptotic nuclei. However, no significant change in the number of $BrdU^+$ cells was observed after the addition of 10nM sCLU (Figure 3—4c & Figure 3—6). This suggests that sCLU was not enhancing the proliferation of VM-hfNSCs but was instead increasing the amount of $Tuj1^+$ cells by reducing the number of cells lost by apoptotic death.

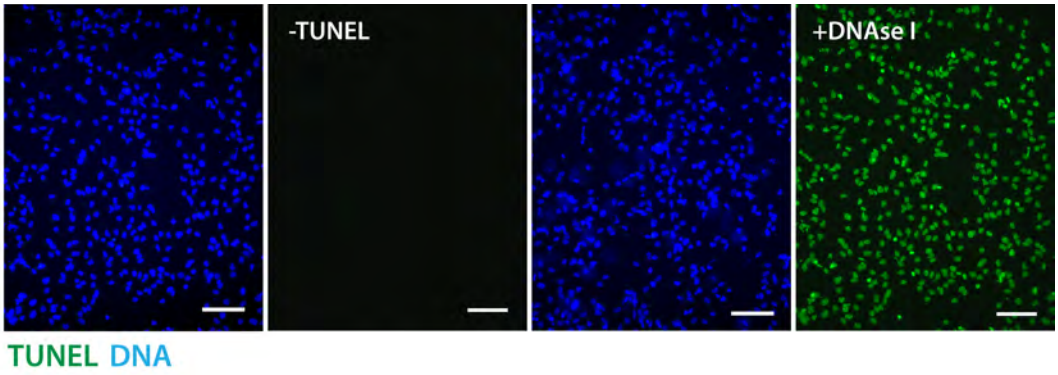

Figure 3—5 Specificity of the TUNEL method to label apoptotic cells. No fluorescein signal is detected if no Terminal Deoxynucleotidyl transferase is added to the TUNEL labelling mixture. All nuclei are labelled if the cells are pre-treated with DNAse I that introduces double stranded DNA breaks. Scale bars = 50μm.

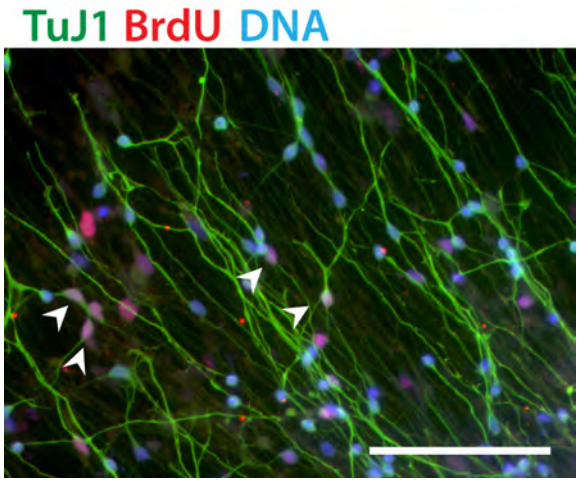

Figure 3—6 Representative photo-micrograph of BrdU$^+$ VM-hfNSCs BrdU staining (red), Tuj1 (green) and DNA (blue). White arrow-heads point to BrdU+ nuclei. Scale bar=50μm

3.5.7 Extracellular clusterin can induce intracellular ERK activation in VM-hfNSCs

To provide a possible mechanism for the pro-neuronal action of sCLU we studied the effect of acute stimulation with sCLU on AKT and ERK signalling pathways – as both are known to control cell fate and survival. We used the IN-Cell Analyser for semi-automated image acquisition and analysis. The software detects the nuclear compartment based on Hoechst staining of the DNA and then delineates the cytoplasmic compartment using a top-hat algorithm. This allows fluorescence-intensity measurements in thousands of cells within minutes. (Figure 3—4e & f) show a fast increase of ERK activation (given by phospho-ERK staining) in VM-hfNSCs after sCLU stimulation but no change on the total amount of ERK protein within the cells. Interestingly, sCLU-induced ERK activation was sustained and did not return to basal levels even after 6 hours (Figure 3—4f). No effect was found on AKT phosphorylation (data not shown).

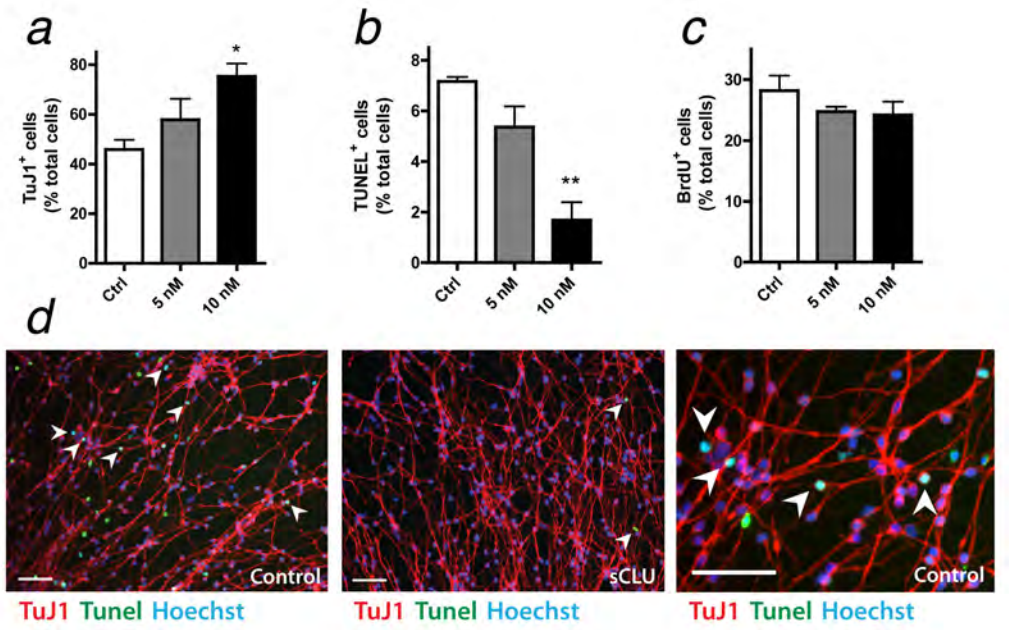

Figure 3—7 Clusterin increases neuronal differentiation from cortical-derived hfNSCs by promoting cell survival.
(a) 10nM sCLU increases the number of Tuj1$^+$ neurons. (b) sCLU has no effect on CTX-hfNSC proliferation. (c) sCLU decreases TUNEL$^+$ nuclei. (d) photomicrographs of Tuj1$^+$ (red), TUNEL$^+$ and DNA (blue) in control and sCLU treated cultures. White arrowheads point to TUNEL$^+$ nuclei. Scale bars = 50µm. *p<0.05, **p<0.01 vs. Ctrl; Newman Keuls, N=4 per group.

3.5.8 Clusterin effects are not limited to VM-hfNSCs

To test whether the pro-neuronal effect of sCLU is specific to hfNSCs derived from the VM or is common to hfNSCs from other brain regions, hfNSCs derived from the developing CTX were expanded under identical conditions as described for VM-hfNSCs cultures. In agreement with previous results from our lab (Ostenfeld et al., 2002) cortical hfNSCs are more neurogenic than VM-hfNSCs (number of Tuj1$^+$ neurons from CTX-hfNSCs doubles the number of neurons obtained from VM-hfNSCs). Remarkably, the pro-neuronal effect of sCLU is maintained also in CTX-hfNSCs: 10nM sCLU increased the number of Tuj1$^+$ neurons (Figure 3—7a), decreased the number of TUNEL$^+$ nuclei (Figure 3—7b) but had no effect on proliferation (Figure 3—7c). This demonstrated that the effects of sCLU are not region specific.

3.6 Discussion

In this study we sought to exploit the regional properties of astrocytes to discover novel neurotrophic factors. We have shown that ACM derived from the HPC and MB increases neuronal differentiation from expanded hfNSCs, as assessed by TuJ1 and SMI312 staining. SMI312 identifies neurofilaments and has previously been shown to be axon specific (Lubetzki et al., 1993). Phosphorylation of neurofilaments during development is fundamental to maturation and stabilization of the neuronal cytoskeleton, as well as an increase in axonal diameter (Carden et al., 1987). We show that HPC and MB ACM also increase the neurite length of pNF-positive neurons, indicating their role in neuronal maturation. CTX-ACM had no such effects. MALDI-TOF analysis revealed a number of proteins were present in all ACMs tested. Cystatin C is a low-molecular weight protein (13KDa), which is expressed in the brain of rat, monkey and human and is localized predominately in astrocytes but also in some neurons (Yasuhara et al., 1993). Interestingly, it has been purified from the conditioned medium of adult hippocampal neural stem cell cultures, and has been shown to be required for the mitogenic activity of FGF-b (Taupin et al., 2000). In addition, its combined delivery with FGF-b in vivo to the adult dentate gyrus resulted in increased neurogenesis in this brain region (Taupin et al., 2000). Moreover, cystatin C has been shown to have a role in neuroprotection in vivo, for example, Olsson et al. demonstrated that focal ischemia resulted in significantly greater brain infarcts in a cystatin C gene-knockout mouse (Olsson et al., 2004). Furthermore, cystatin C has been shown to prevent the degeneration of rat substantia nigra dopamine neurons both in vitro and in vivo (Wu et al., 2005). Taken together, these results confirm the importance of this protein in cell survival. Other proteins were found

in ACM, α-2 macroglobulin and extracellular matrix protein 2, both have been implicated in neurite outgrowth. The α-2 macroglobulin is a major serum glycoprotein found in adult and fetal brain cells (Dziegielewska et al., 1986) including astrocytes (Gebicke-Haerter et al., 1987). It has been shown to bind neurotrophic factors, such as NGF and neurotrophin-3 (NTF-3), which are secreted by astrocytes (Lin et al., 2006). We have previously shown that hfNSCs express the tropomyosin-receptor-kinase C (*TrkC*)-receptor (Caldwell et al., 2001), so binding of α-2 macroglobulin to NTF-3 secreted by astrocytes may be having a role in the neurite outgrowth seen with HPC and MB ACM. In addition, extracellular matrix glycoprotein, falls into the family of neurite promoting factors, so this too may be having a role in neurite outgrowth (Lee and Koo, 2000).

The other major protein found in MB and HPC ACM was clusterin. Clusterin is a multifunctional protein and can present in three different forms. The most abundant is the full length clusterin or sCLU; this isoform is readily secreted from the producing cells (Burkey et al., 1991) and has generally anti-apoptotic or pro-survival functions. A truncated form of clusterin, nCLU, is confined to the nuclear compartment (Reddy et al., 1996) and is considered to be pro-apoptotic (Nayoung Kim, 2011). The third form corresponds to a full-length sCLU that is retrotranslocated into the cytoplasm upon ER stress and proteasomal inhibition but its functions are not completely understood (Nizard et al., 2002). In agreement with its pro-survival properties, sCLU confers chemoresistance to anti-tumour drugs to multiple types of cancer cells (Cervellera et al., 2000; Chen et al., 2003; Zhang et al., 2005; Cheng et al., 2012) and it is involved in pancreas (Lee et al.,

2011b), myocardium (McLaughlin et al., 2000) and testis regeneration (Bailey et al., 2002). Additionally clusterin has a role in lipid transportation and metabolism and appears in lipoprotein particles in plasma (Burkey et al., 1992; Hennessy et al., 1997; Navab et al., 2005) and CSF (LaDu et al., 1998; Fagan et al., 1999; Koch et al., 2001). This ability to interact with hydrophobic substances also allows clusterin to bind to misfolded proteins preventing their complete denaturation or aggregation. Indeed, clusterin is also considered an extracellular ATP-independent co-chaperone (Poon et al., 2000).

These results demonstrated the importance of clusterin in cell survival and regeneration. This lead us to hypothesise that clusterin present in MB and HPC ACM was responsible for the increased neuronal differentiation and neurite outgrowth observed in our VM-hfNSCs cultures. This was indeed the case and clusterin immunodepletion from MB-ACM suppressed its pro-neuronal action. However, as clusterin is part of lipoprotein complexes (Burkey et al., 1992; Hennessy et al., 1997; LaDu et al., 1998; Koch et al., 2001) clusterin pull-downs could effectively remove other pro-neuronal factors from the MB-ACM. For this reason we tested if purified clusterin could recapitulate the effects of full ACM. This was also the case. We then showed that astrocyte-secreted clusterin has no effect on the proliferation of VM-hfNSCs, but it does promote their differentiation by sustaining ERK phosphorylation and decreasing the number of apoptotic nuclei. Interestingly, an increase in phosphorylated ERK has been associated with increased cell survival (for review see Nishida and Gotoh, 1993), so our data suggest that astrocyte-sCLU is promoting both cell survival and differentiation of VM-hfNSCs. Furthermore, a similar pro-neuronal effect of clusterin was observed

with CTX-hfNSCs, indicating that clusterin is a general trophic factor for NSCs across brain regions.

Interestingly, clusterin is profoundly linked with the neurodegenerative mechanisms that lead to AD. Clusterin was one of the only three genes associated with LOAD in a large GWAS and carriers of the TT genotype for an SNP in the clusterin gene have reduced risk of LOAD (Harold et al., 2009). Clusterin levels are increased in AD (Bertrand et al., 1995) and its expression is up-regulated by Aβ (Nuutinen et al., 2007). Extracellular clusterin can bind to Aβ (Matsubara et al., 1995), preventing the formation of fibrils and further aggregation (Oda et al., 1995; Narayan et al., 2012) that would eventually lead to plaque formation. Furthermore, clusterin-Aβ complexes can be eliminated from the brain by the clusterin receptor megalin (Zlokovic et al., 1996) reducing the amyloid burden in the brain (DeMattos et al., 2004).

APOE and *PICALM* – the other two risk genes from the 2009 Harold et al. study - are also involved in Aβ clearance. APOE binds to Aβ (Martel et al., 2002) and Aβ-APOE complexes can be removed from the brain by the lipoprotein receptor-1 (LRP1) receptor expressed by endothelial cells or by megalin in the choroid plexus (Bell et al., 2007). Furthermore, double clusterin and *ApoE*-KO mice have a dramatic and premature increase in Aβ deposition (DeMattos et al., 2004). PICALM is involved in receptor endocytosis by endothelial cells (Tebar et al., 1999). These three genes highlight the importance of Aβ clearing in LOAD and suggest that enhancing the elimination of Aβ from the brain or its transport into the blood can be a successful strategy for AD treatment. Indeed, the "peripheral

sink" approach (DeMattos et al., 2001) is already being developed in clinical trials (Gilman et al., 2005).

This is the first study to corroborate the effect of clusterin on neurogenesis from hNSCs. To date, no publication has associated clusterin and NSCs (from any species) and whether neurogenesis is affected in *Clu*-KO mice is not known. Interestingly, clusterin is up-regulated in AD and we could expect some effect on endogenous NSCs. However, it is unclear how neurogenesis is affected by AD. Jin et al. showed that protein levels of neurogenic markers such as doublecortin (DCX), poly-sialated neural cell adhesion molecule (PSA-NCAM), TUC-4, NeuroD were increased in AD brains and correlated with AD severity. They also found that AD patients had higher numbers of hippocampal NSCs (Jin et al., 2004). Confoundingly, Boekhoorn et al. found no evidence of enhanced generation of neurons in AD. They did however find increased proliferation assessed by Ki67 staining (a histone marker in dividing cells) in the hippocampus of AD patients, but attributed this to increased gliosis and not neurogenesis (Boekhoorn et al., 2006). Animal models of AD give an even less clear picture. Dozens of publications have analysed the effect on neurogenesis by AD-like pathology. However, the results are often contradictory and highly dependent on the animal model or methodology used (for review see Lazarov and Marr, 2010). In light of our results, it is possible that the up-regulation of clusterin seen in AD could trigger an increase in the generation, differentiation and survival of new neurons but this would be, in any case, unable to compensate for the severe neuronal loss found in AD. Alternatively, in the AD brain, an excess of Aβ could

effectively sequester the available clusterin depriving neurons and NSCs of its trophic support and thus compromising both neurogenesis and neuronal survival.

Could clusterin be used as a therapy for AD?

Systemic administration of clusterin could act as a peripheral sink for amyloid and reduce the amyloid brain burden. However transport of clusterin into the brain is already saturated at physiological concentrations (Shayo et al., 1997), therefore peripheral clusterin cannot stimulate brain neurogenesis. Furthermore, higher systemic levels of clusterin could increase the risk of tumour development, strongly arguing against this approach. On the other hand, intracerebral administration of clusterin could enhance both Aβ clearance and endogenous neurogenesis (from our results) and it is perhaps worth investigating further.

Finally, there is an unexplored implication of the current literature and our results: APP and the presenilins are considered neuronal genes and mutations in these genes are associated with early onset AD (Suh and Checler, 2002). However, none of the three genes associated with LOAD are neuronal. *Picalm* is mainly expressed in endothelial cells from blood vessels in the brain, whereas clusterin and *ApoE* (Xu et al., 2006) are typically astrocytic genes. This suggests, perhaps, that the first alterations that lead to LOAD do not occur in neurons but elsewhere.

Indeed soluble Aβ causes vasoconstriction and endothelial damage (Thomas et al., 1996) and early vasculature changes in endothelial permeability are thought to precede any neurological symptom (for review see Carmeliet and De Strooper, 2012). These changes could compromise Aβ transport across the BBB (for review

see Sagare et al., 2012), limit the entry of trophic factors like IGF-1 (Carro et al., 2002) or lead to brain inflammation and gliosis (for review see Lucin and Wyss-Coray, 2009) in the brain triggering AD-like pathology. However, most of the Aβ in the brain and CSF originates within the brain itself (Siemers et al., 2005). Therefore, before it reaches the pericytes or endothelial cells in the BBB, Aβ must interact first with the astrocytes that surround the blood vessels.

Could astrocytes be the primary target of Aβ toxicity?

Remarkably, Aβ treatment caused dramatic intracellular increases of calcium in astrocytes but not neurons. These calcium increases were blocked by zinc or clioquinol – a Ca^{2+} chelator agent and inhibitor of Aβ oligomerisation (Abramov et al., 2003). Interestingly Aβ oligomers have been shown to form pore-like structures in artificial membrane preparations allowing the flow of ions (Arispe et al., 1993) that can be blocked by Zn^{2+} or Ca^{2+} absence (Lin et al., 2001). Indeed, Aβ leads to glutathione depletion and astrocytic death followed only indirectly by neuronal loss (Abramov et al., 2003). Furthermore, Aβ causes astrocyte activation with release of inflammatory cytokines (IL-1β, IL-6 and IFN-γ) (Garwood et al., 2011) potentially leading to the brain inflammation and gliosis observed in AD. Additionally, astrocyte secreted APOE is essential to maintain BBB permeability (Bell et al., 2012) and astrocyte dysfunction could compromise BBB function due to the close cross-talk between astrocytes and endothelial cells (Abbott, 2002), leading to the early vascular changes that precede neuronal loss.

The hypothesis that Aβ is primarily harmful for astrocytes is supported by the arsenal of Aβ-controlling machinery that astrocytes release even when they do not

produce Aβ themselves. Besides APOE and clusterin, cystatin C and α-2 macroglobulin are some of the most abundant proteins in astrocytic secretomes (Lafon-Cazal et al., 2003; Dowell et al., 2009; Greco et al., 2010) and were also found in our study. Remarkably, cystatin C can also bind to Aβ (Sastre et al., 2004) and reduce aggregation and brain amyloid burden (Mi et al., 2007). Loss of cystatin C causes vascular amyloidosis affecting mainly the cerebral arteries (Levy, 1989). Similarly, α-2-macroglobulin can bind to Aβ and trigger lipoprotein receptor-mediated clearance (Qiu et al., 2002) and has been associated with a small risk of LOAD (Kovacs, 2000). Furthermore, astrocytes also produce amyloid cleaving enzymes such as neprelysin, endothelin converting enzyme-2 and angiotensin-converting enzyme-1 (Pihlaja et al., 2011) that have been shown to degrade amyloid (Carson and Turner, 2002). Although, there is no gross astrocytic loss in AD - but profound gliosis - it is possible that regional specific populations of astrocytes are lost or affected in AD and that the activated or migrating astrocytes that surround the amyloid plaques and degrade Aβ (Wyss-Coray et al., 2003) fail to provide the appropriate neurotrophic support for regional neurons.

In conclusion, our study and others highlight the importance of astrocytes and astrocyte-released factors for normal brain function and disease. We have also shown regional differences in astrocyte secretion and how MB and HPC but not CTX astrocytes can promote neuronal differentiation and survival from NSCs. Finally, we have shown that astrocyte-secreted clusterin is a novel multifunctional NTF that increases neurogenesis and neurite outgrowth from NSCs. This may have implications for neurodegeneration and repair.

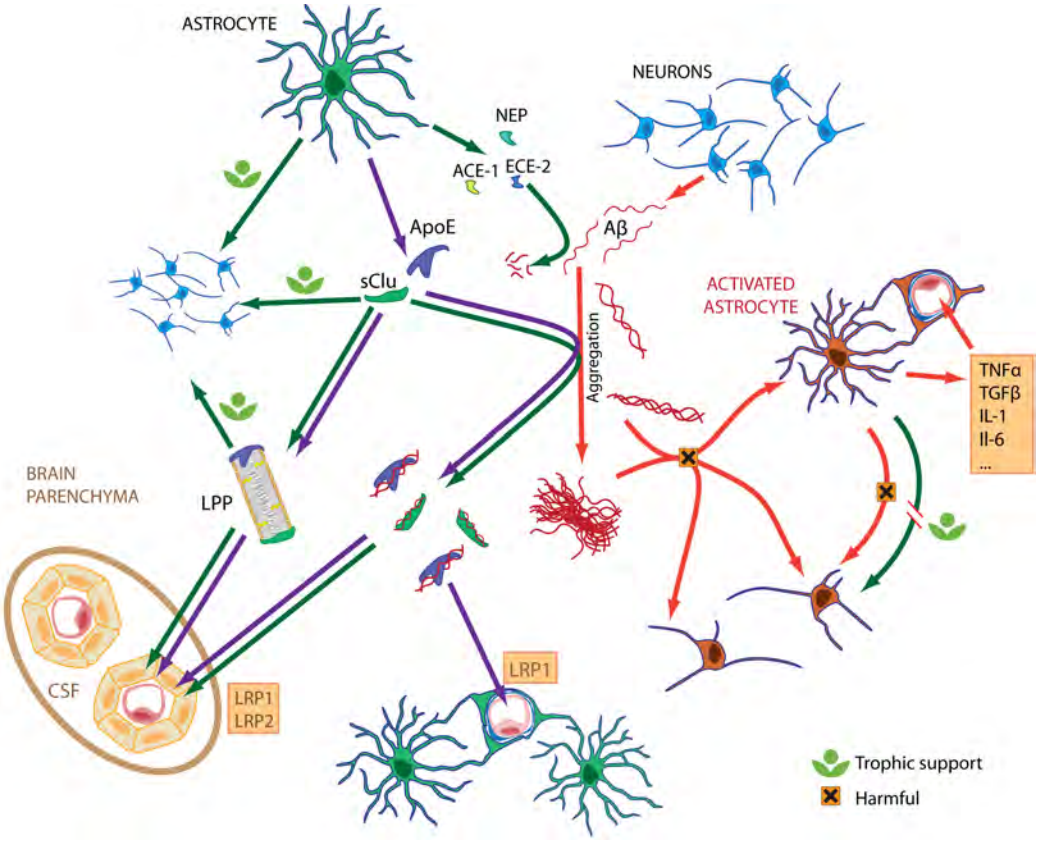

Figure 3—8 Astrocytes as a target for Aβ toxicity.
Astrocytes provide trophic support to neurons and release amyloid clearing machinery. Clusterin can bind to Aβ and acts as trophic factor (directly and in the form of lipoproteins) Aβ oligomers or aggregates primarily affect astrocytes leading to astrocyte activation / death. Astrocytic dysfunction could cause secondary changes in vascular permeability, inflammation and loss of trophic support for neurons leading to Alzheimer's disease

Chapter 4

Chapter 4

Galanin, a neurotrophic factor for neural stem cells

I don't like it and I am sorry I ever had anything to do with it.
Erwin Shrödinger
(on quantum physics)

4.1 Introduction

Galanin is one of the 70 neuropeptides described in the mammalian brain (Burbach, 2010). These are small peptidergic molecules that are produced by neurons and bind to specific neuronal receptors. Unlike classical neurotransmitters, neuropeptides are released extra-synaptically and do not have re-uptake mechanisms but are instead cleared by enzymatic cleavage. They are biologically active in the nanomolar range and can diffuse over long distances. These properties make them ideal candidates for neuroendocrine and neuromodulatory regulation and enable them to have pleiotropic functions.

Galanin was first isolated from porcine intestine (Tatemoto et al., 1983) and has a highly conserved sequence with 29 aminoacids or 30 in humans (Schmidt et al., 1991). Galanin is highly expressed in the gastrointestinal tract and in the brain (Kaplan et al., 1988). Within the brain, there is widespread immunoreactivity in the olfactory bulb, cerebral cortex, basal forebrain and circumventricular organs (Pérez et al., 2001). Galanin is synthesised and released from dopamine, acetyl-choline (ACh), serotonin, GABA neurons suggesting a role as a neuromodulator of synaptic transmission (Melander et al., 1986). Indeed galanin has been shown to regulate serotonin and noradrenaline release in the hippocampus (Yoshitake et

al., 2004) and to inhibit ACh release (Wang et al., 1999). In the pituitary galanin modulates the secretion of luteinizing hormone (LH) (López et al., 1991), growth hormone (GH) (Davis et al., 1987) and prolactin (PRL) (Koshiyama et al., 1987).

Three specific galanin receptors have been cloned so far. Galanin receptor-1 (*GalR1*) was first cloned from a brain cDNA library (Burgevin et al., 1995). In the brain, *GalR1* receptor shows particularly high expression in the lateral olfactory tract and hippocampus (HPC) but it is also present in the hypothalamus, brain stem and many other areas (Gustafson et al., 1996). *GalR2* was originally cloned from the rat pituitary (Fathi et al., 1997). *GalR2* shows a remarkably high expression in dorsal-root ganglia (DRG) neurons but it is also present centrally in dentate gyrus (DG) of the HPC, mammillary cortex, cerebellar cortex, olfactory bulb (OB) and olfactory tubercle (O'Donnell et al., 1999). *GalR3* was the last galanin receptor to be cloned and has a restricted distribution in the brain (Mennicken et al., 2002). These receptors differ in their pharmacological properties and their affinity for galanin fragments or chimeric peptides, for review see (Branchek et al., 2000; Florén et al., 2000; Lang et al., 2007).

Early studies focused on the effects of galanin in the hypothalamic-pituitary axis. Galanin levels in the para-ventricular nucleus (PVN) correlate with body weight gain and fat ingestion (Akabayashi et al., 1994), though high levels of galanin do not induce sustained obesity and produce complex changes in daily caloric intake and fat deposition depending on fat and carbohydrate composition of the diet (Hohmann et al., 2003; Adams et al., 2008). In the pituitary galanin is required for PRL release (Wynick et al., 1993) and acts as a trophic factor for lactotroph cells

(Wynick et al., 1998; Cai et al., 1999). Accordingly, galanin expression is increased post-parturition and suckling in the pituitary, suggesting that galanin plays an important role in lactation and maternal behaviour (Ren et al., 1999).

One of the most remarkable features of galanin is that its levels are greatly up-regulated after nerve injury. Facial nerve lesions cause profound galanin up-regulation in the facial nucleus (Burazin and Gundlach, 2002) whereas sciatic nerve crush enhances galanin expression in the DRG by more than two orders of magnitude (Hökfelt et al., 1987). This property is conferred by an axotomy-responsive element in the galanin promoter (Bacon et al., 2007) and suggests that galanin is important for neuroregeneration and repair. Supporting this view, knock out of galanin reduces nerve regeneration and neurite outgrown from adult DRG in vitro (Holmes et al., 2000; Sachs et al., 2007) via activation of GALR2 (Mahoney et al., 2003). Similar results were found in *GalR2*-KO mice (Hobson et al., 2006), suggesting that galanin binding and signalling to GALR2 are required for nerve regeneration following axotomy in DRGs.

Galanin has also been shown to play a protective role in the HPC: galanin reduces glutamate or staurosporin excitotoxicity in hippocampal cultures (Elliott-Hunt et al., 2004) via GALR2 (Elliott-Hunt et al., 2007) and attenuates seizure sensitivity and kainic acid (KA)-induced hippocampal cell death (Haberman et al., 2003; Elliott-Hunt et al., 2004; Mazarati et al., 2004a). Accordingly, *Gal*-KO mice have increased propensity to develop status epilepticus (after perforant-path stimulation, KA or Li-pilocarpine administration) (Mazarati et al., 2004a; 2004b). This seems to be mainly mediated by GALR2 (Mazarati et al., 2004a; Elliott-Hunt et al., 2007). However, *GalR1*-KO also have remarkable KA-induced cell death in

the CA1 and CA3 regions of the HPC (Schauwecker, 2010) indicating that both receptors could be necessary for the neuroprotective effect of galanin.

Supporting its function as a neuroprotective factor, galanin has also been associated with neurodegeneration. In multiple sclerosis (MS), galanin is up-regulated in microglial cells surrounding MS lesions in humans. Interestingly, loss of galanin or *GalR2* leads to accelerated and more profound pathology in a mouse model of experimental autoimmune encephalitis, whereas galanin overexpression, greatly attenuates the disease progression in this model (Wraith et al., 2009). Accordingly, galanin overexpression alleviates oligodendrocyte loss and demyelination in the cuprizone-model of MS (Zhang et al., 2012).

In Alzheimer's disease (AD) the role of galanin is still controversial. Galanin immunoreactivity can be detected in the medial septum, nucleus basalis of Mainhart and HPC in mice (Pérez et al., 2001) and galanin and ACh-esterase colocalise in HPC-projecting fibres present in the medial septum and diagonal band (Melander et al., 1985). Galanin is up-regulated in mouse models of AD (Diez et al., 2000) and in the cerebral cortex of AD patients (Gabriel et al., 2008) associated with senile amyloid plaques (Kowall and Beal, 1989). This evidence indicates that galanin is expressed in areas that undergo neurodegeneration in AD and suggests a possible role for galanin in disease progression. Interestingly, galanin reduces long-term potentiation (LTP) and CREB (cyclic AMP response element biding protein) activation in the DG (Badie-Mahdavi et al., 2005). Furthermore, galanin overexpressing mice (*Gal*-OE) have reduced number of cholinergic neurons in the diagonal band and compromised performance in the water maze test for spatial memory (Steiner et al., 2001), suggesting that the

increase in galanin observed in AD might exacerbate the memory deficits in these patients.

However, Wrenn et al. found no consistent correlation between the levels of galanin in the HPC and frontal cortex with compromised cognitive performance for several behavioural tests (Wrenn et al., 2002). Furthermore, galanin expressing neurons in the locus coeruleus are preserved in AD (Miller et al., 2002) and nerve growth factor (NGF) promotes both galanin and choline acetyl-transferase (ChAT, the main enzyme involved in the synthesis of ACh) expression in the basal forebrain (Planas et al., 1997). Accordingly, Counts et al. have shown by single-cell PCR-analysis that in cholinergic neurons in the nucleus basalis of AD patients, galanin expression correlates with levels of ChAT (Counts et al., 2008). Remarkably, galanin is required for the survival specific ChAT septohippocampal neurons and *Gal*-KO mice have compromised ACh release and water maze performance (O'Meara et al., 2000). Interestingly, galanin via GALR2 reduces amyloid-beta (Aβ)-induced cell death in basal forebrain neurons (Ding et al., 2006) and in cholinergic cell lines (Pirondi et al., 2009; Elliott-Hunt et al., 2011). In conclusion galanin seems to have conflicting roles in AD, it can inhibit ACh release and impede memory processes but can also support and protect hippocampal and forebrain neurons against amyloid toxicity. This balance between negative neuromodulation and neuroprotection is not completely understood and will require further study.

In summary galanin is up-regulated after injury in the nervous system, it is involved in neuroregeneration and is a neuroprotective factor in the HPC and forebrain. Furthermore galanin is required for the postnatal survival of specific

neuronal populations in the DRG (Holmes et al., 2000), ChAT neurons in the forebrain (O'Meara et al., 2000) and is a potent trophic factor for hypophyseal neurons.

Despite its importance for neuroregeneration and repair, very few publications have considered or studied galanin in stem cell biology. However, galanin and its receptors are present in neural crest cells during embryogenesis (Jones et al., 2009) and in bone marrow mesenchymal stem cells (Louridas et al., 2009). Galanin is one of the most highly expressed transcripts in mouse R1-ES cells, at levels comparable with pluripotency factors (Anisimov et al., 2002). In the adult brain galanin and *GalR1& 2* are expressed in neural stem cells (NSCs) in all neurogenic areas: in the DG, in the subventricular zone (SVZ), in the rostral migratory stream (RMS) and in the OB (Shen et al., 2003). Interestingly, galanin, via GALR2, is required for seizure-induced hippocampal neurogenesis (Mazarati et al, 2004), although its role on basal neurogenesis is not yet established. In conclusion, galanin is present in stem cells and in locations that could modulate NSC biology and this could be a contributing factor to the neuroprotective and neuroregenerative functions described above. This hypothesis will be tested in this chapter.

4.2 Aims

To establish a role for galanin in NSCs in the adult and fetal mouse brain.

Fetal NSCs:

We will isolate striatal NSCs from Gal-KO and WT E14.5 embryos as at this developmental stage Str-NPCs are FGF-b and EGF responsive and can generate both neurons and glia upon differentiation. We will first determine the expression of galanin and its receptors by qPCR on primary Gal-KO and WT Str-NSCs. Using high content microscopy we will then test whether these receptors are functional and galanin stimulation can activate intracellular signalling pathways known to be important in cell survival and fate determination. We will next profile the changes in expression in pro-survival and lineage specific genes following galanin stimulation of Str-NSCs. We will use MTT assays to measure mitochondrial reductase activity – a proxy variable for cell number on expanding cell populations – to study the effect of galanin and galanin disruption on cell growth. This will be complemented by analysis of BrdU incorporation as marker of dividing cells. Finally, we will determine if galanin or galanin disruption has any effect on NSC fate determination by quantifying the number of astrocytes, oligodendrocytes and neurons upon differentiation in vitro.

Adult NSCs:

We will study adult neurogenesis and the effect of galanin KO in vivo by profiling short-term and long-term BrdU incorporation in adult Gal-KO and

WT Str-NSCs. We will quantify the number of dividing cells in the subventricular zone and the dentate gyrus and we will determine the number of these cells that migrates towards the olfactory bulb and granular cell layer of the hippocampus respectively. We will also study the effect of galanin and galanin KO on the proliferation and differentiation profile of adult NSCs in vitro.

4.3 Materials and Methods

4.3.1 Animals

Gal-KO mice were generated in Prof. David Wynick's laboratory as described in (Wynick et al., 1998). Briefly, mice homozygous for a targeted deletion of exons 1-5 of the galanin gene were generated using the E14 cell line. The mutation and a strain matched WT line have remained inbred on the 129OlaHsd strain.

4.3.2 MTT-assays

Primary striatal (Str)-NSCs were harvested from *Gal*-KO and WT embryos at 14.5 days *post coitum* (E14.5) as described previously (2.2.4.1). Briefly, striata from 4-6 embryos were dissected, pooled together and treated with Accutase (Sigma) at 37°C for 10-20min. Following centrifugation at 1,000 RCF, the pellet was carefully resuspended in fresh culture medium and triturated to obtain a single-cell suspension. Cell number and viability were assessed by trypan blue exclusion (Sigma) using a Neubauer haemocytometer as described in (2.2.1.4). $2.5 \cdot 10^4$cells were seeded on 96-well plates in 100µl of DMEM:F12^{B27} with 20ng·ml^{-1} epidermal growth factor (EGF, Sigma) or 20ng·ml^{-1} basic fibroblast-growth factor (FGF-b, Peprotech) with 5µg·ml^{-1} Heparin (Hep, Sigma) as mitogens. 1nM, 10nM, 50nM, 100nM or 1µM galanin (Sigma) was added to the wells. No galanin was added to control wells. After seven days, 25µl of a 5g·l^{-1} solution of methylthiazolyldiphenyl-tetrazolium bromide (MTT, Sigma) in ddH_2O were added per well. The reaction was incubated for 2h at 37ºC and the medium of each well was carefully removed and replaced by 150µl of acidified

isopropanol (Fisher). Formazan formation was measured as 570nm absorbance with an MRX TC revelation spectrophotometer.

4.3.3 Fetal NSC culture

Primary Str-NSCs were harvested from *Gal*-KO and WT embryos at E14.5 as described previously. $2{\cdot}10^5$cells·ml^{-1} were grown in DMEM:F12$^{B27\text{-}FH}$ (for detailed composition see 2.2.4.2) supplemented with 100nM galanin. No galanin was added to control flasks. NSCs were cultured in 25cm^2 culture flasks (Nunc) and fed every 3-4 days by replacing 50% of the culture medium with fresh DMEM:F12$^{B27\text{-}FH}$. Str-NSCs were passaged after seven days as described previously 2.2.4.3.

4.3.4 Adult SVZ-NSC culture

Adult SVZ-NSCs were harvested from 8-10 week-old WT and *Gal*-KO male mice as described previously 2.2.5.1. Briefly, tissue from 4-5 mice was pooled for each culture. The SVZ of the lateral ventricles (≈1mm from the lumen) was carefully collected and treated with 0.1% [v/v] trypsin (Worthington Biochemical) for 7min at 37°C. Digestion was stopped with a mixture of 0.1% [v/v] trypsin inhibitor and 0.008% [v/v] DNAse (Worthington Biochemical) at 37°C for 5min. The cells were gently triturated and sieved through a *40μm-cell nylon cell strainer* (BD-Falcon). Cell number and viability were assessed by trypan blue exclusion (Sigma) as in 2.2.1.4. $2{\cdot}10^5$cells·ml^{-1} were grown in DMEM:F12$^{B27:EFH}$ {3:1 mixture of high glucose DMEM (Sigma) and F12-nutrient mixture (Gibco); 2% [v/v] B27 supplement (Gibco); 20ng·ml^{-1} EGF (Sigma); 20ng·ml^{-1} FGF-b (Peprotech);

5μg·ml^{-1} Hep and 100U·ml^{-1} penicillin, 0.1g·l^{-1} streptomycin (Sigma). SVZ-NSCs were grown in 25cm^2 Nunc culture flasks (Thermo-Fisher).

Adult SVZ-NSCs are less expandable and grow at lower rates than fetal NSCs. For this reason, SVZ-NSCs were grown in a similar DMEM:F12 based medium than fetal-NSCs but with both *epidermal growth factor* (EGF) and FGF-b + Hep as mitogens. To generate enough cells for our studies, primary SVZ-NSCs were initially expanded for 10 days, passaged and expanded for 7 additional days, with or without 100nM galanin, prior to differentiation.

4.3.5 Differentiation of fetal and adult NSCs

To label dividing cells, 0.2μM BrdU (Sigma) was added to NSC-cultures from 4.3.3 and 4.3.4, before plate-downs (-24h in fetal-NSC and -72h in adult-NSC). Before plating, neurospheres were collected, dissociated and resuspended in DMEM:F12^{B27} supplemented with 1% [v/v] fetal calf serum (FCS, Gibco)}. $5x10^4$ cells were seeded on the centre of each coverslip and 500μl of DMEM:F12$^{B27\text{-}DIFF}$ were added to each well. Half of the medium was replaced with fresh DMEM:F12$^{B27\text{-}DIFF}$ after 3-4 days. For those cultures expanded in the presence of galanin, 100nM galanin was also kept in the differentiation medium, whereas control cultures were not supplemented with galanin at any stage. Cells were allowed to differentiate for seven days before fixation.

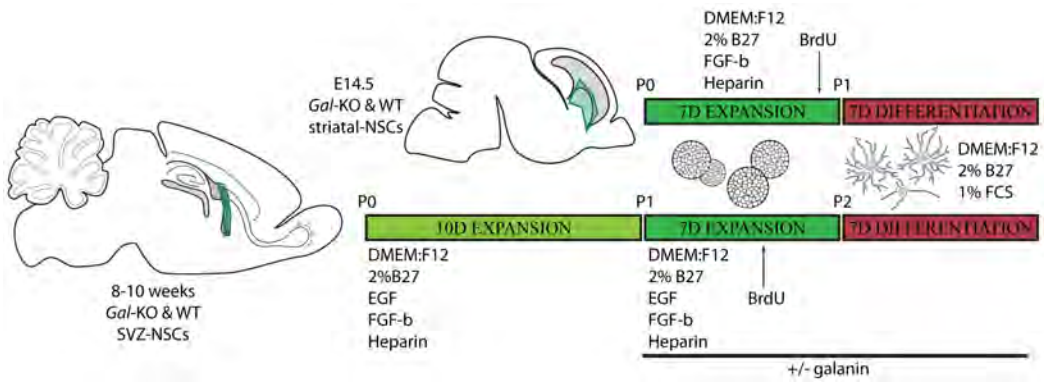

Figure 4—1 Expansion and differentiation of E14.5-striatal and adult-SVZ NSCs

4.3.6 Semiquantitative RT-PCR

NSCs expanded for seven days and hitherto untreated with galanin were exposed to 100nM of the peptide 6 or 12 hours before RNA extraction. Galanin untreated samples were used as controls. Cultures were then pelleted and RNA isolated according to the Trizol-Reagent protocol (Invitrogen): briefly, cells were lysed with Trizol followed by a phase separation with chloroform and precipitation with isopropanol; the precipitate was then washed with 75% [v/v] ethanol, allowed to dry and resuspended in RNAse/DNAse-free water (Gibco). RNA samples were treated with DNAse I and reprecipitated as described in 2.1.13. Final RNA concentration was measured using a Pearl nanophotometer and equal amounts of RNA were added to the reverse transcription mixture. This was set up as follows:

RT-reaction		
	AMOUNT	SUPPLIER
RNA	**150ng**	
Random Primers	**300ng**	*Invitrogen*
10mM dNTPs	**2µl**	*Invitrogen*
ddH_2O	**Up to 25µl**	*Sigma*
5min at 65ºC **5min at 4ºC**		
5X First-Strand Buffer	**5µl**	*Invitrogen*
RNAse out	**1µl**	*Invitrogen*
0.1M DTT	**1µl**	*Invitrogen*
Superscript III	**1µl**	*Invitrogen*
5min at 25ºC **60min at 50ºC**		

Table 4-1 Semi-quantitative PCR I: reverse transcription step
In order to facilitate annealing, primers and sample RNAs were pre-incubated at 65ºC for five minutes followed by another period of 5 minutes at 25ºC prior to addition of the remaining components of the RT mixture. No Superscript III was added to "RT-negative" tubes. The RT reaction was allowed to take place at 47ºC for 1 hour.

RT products were then distributed into PCR reactions for four sets of primers: *Bcl-XL*, *Bcl-2*, *Mash-1* and *Olig-2* (all primers were designed against the *Mus musculus* sequence). Primer sequences are detailed in Table 4-2. PCRs were set up as described in Table 4-3. Final PCR products were run on a 1% [w/v] agarose (Melford) gel with 0.5mg·l^{-1} of ethidium bromide and visualised under a UV lamp as described in 2.1.1.

Gene Expression primers (5'⟶3')	
mm-Bcl-xl forward	*GGCAGGAAGAAGAGCCTGGA*
mm-Bcl-xl reverse	*CAAGCCAGCAGCTCCTCACA*
mm-Bcl-2 forward	*TCTCATGCCAACGGGGAAAC*
mm-Bcl-2 reverse	*CATCTCCAGCATCCCACTCG*
mm-Mash-1 forward	*ACAAGAGCTGGACTTTACC*
mm-Mash-1 reverse	*CAGTCACTCTTCTCGTGTCTGG*
mm-Olig2-1 forward	*TATTACAGACCGAGCCAACACC*
mm-Olig2-1 reverse	*CTGGAGGAAGATGACTTGAAGC*

Table 4-2 Semi-quantitative RT-PCR, primer sequences

Semi-quantitative-PCR		
	AMOUNT	SUPPLIER
cDNA	**3µl**	
Forward primer (10µM)	**0.5µl**	*Sigma*
Reverse primer (10µM)	**0.5µl**	*Sigma*
25mM $MgCl_2$	**1.2µl**	*Promega*
10mM dNTPs	**2µl**	*Invitrogen*
5X Green reaction buffer	**5µl**	*Promega*
GoTaq DNA polymerase	**0.5µl**	*Promega*
ddH_2O	**Up to 25µl**	*Sigma*
5min at 95°C		
30s at 94°C	**X 35 cycles**	
30s at 60°C		
45s at 72°C		
10min at 72°C		

Table 4-3 Semi-quantitative PCR parameters

4.3.7 Real time quantitative RT-PCR (*Taqman*)

mRNA from primary E14.5 Str-NSCs was extracted, DNAse-I treated and quantified as described previously. 1μg of mRNA was added to 50μl of reverse transcription reaction and amplified using random hexamers (Taqman Reverse Transcription Reagents Kit, Applied Biosystems). The reaction was set up as follows:

RT-Taqman

	AMOUNT	SUPPLIER
RNA	**1 μg**	
Random primers	**300ng**	*Taqman*
10mM dNTPs	**5μl**	*Taqman*
Reverse transcriptase	**1μl**	*Taqman*
10X Buffer	**5μl**	*Taqman*
RNAse inhibitor	**1μl**	*Taqman*
25mM $MgCl_2$	**10μl**	*Taqman*
ddH_2O	**Up to 25μl**	*Sigma*

10min at 25ºC
30min at 48ºC
5min at 95ºC

Table 4-4 qPCR, RT reaction

Each total RNA sample was used for two duplicate reactions containing reverse transcriptase (RT+), and one without enzyme (RT−) as a control for the RT-dependence of the product. 1μl of the RT reaction was added to 50μl of PCR mixture containing the appropriate primers and probes, Table 4-5. Replicate 25μl qPCRs included 12.5μl Taqman Universal PCR Master Mix (Applied Biosystems), water (Sigma), primers, probe and template in a 96-well microtitre plate (Applied Biosystems). Standard cycling conditions (95 °C for 10min, followed by 95°C for 15s and 60°C for 1min, for 50 cycles) were used in an ABI PRISM 7900 Sequence Detection System (Applied Biosystems).

Real-time qPCR (TaqMan)	*(5'⟶3')*
mm-galanin forward	*CTGGCTCCTGTTGGTTGTGA*
mm-galanin reverse	*CCAACCTCTCTTCTCCTTTGCA*
mm-galanin probe	*CATCCCAAGTCCCAGAGTGGCTGACA*
mm-GalR1 forward	*GTCAAAAAAGTCTGAAGCATCCAA*
mm-GalR1 reverse	*GCCAGGATATGCCAAATACTACAA*
mm-GalR1 probe	*ACCACCAGGACGGTCTGTGCAGTCTT*
mm-GalR2 forward	*TCTGCAAGGCCGTTCATTTC*
mm-GalR2 reverse	*TAGCGGATGGCCAGATACCT*
mm-GalR2 probe	*CGCTGGCCGCTGTCTCCCTG*
mm-GalR3 forward	*GCTGGCGGCGCTCTTT*
mm-GalR3 reverse	*TAGCCTGCGGCGAAGGT*
mm-GalR3 probe	*ACGGCACGGTGCGCTACGG*
mm-Gapdh forward	*GCAGTGGCAAAGTGGAGATTG*
mm-Gapdh reverse	*CTGGAACATGTAGACCATGTAGTTGA*
mm-Gapdh probe	*CCATCAACGACCCCTTCATTGAC*

Table 4-5 Real-time qPCR primers and probes

4.3.8 Adult neurogenesis

In the short-term study, WT and *Gal*-KO adult male mice (8-10 weeks old) were given a single intraperitoneal injection (IP) of 100mg·Kg^{-1} BrdU (Sigma) in 0.9% [w/v] saline and sacrificed after two hours. In the long-term study, animals were given one daily intraperitoneal injection (IP) of 100mg·Kg^{-1} BrdU for four consecutive days and sacrificed after 21 days. All mice were culled by injection of terminal anaesthetic and transcardially perfused with phosphate buffered saline (PBS, pH7.4) followed by fixation with 4% [w/v] para-formaldehyde (PFA) as

described in 2.5.6. Brains were harvested and post-fixed in 4% [w/v] PFA overnight. The following day brains were transferred to a 30% [w/v] sucrose solution and left overnight at 4ºC. 40μm-brain sections were prepared as described in 2.5.7 and processed for immunohistochemistry.

4.3.9 Immunocytochemistry

One week after plate-downs, differentiated NSCs were processed for immunocytochemistry following the standard protocol described in 2.4.8.1, but adapted to allow O4 staining and retrieval of the BrdU antigen. This was done as follows:

Primary antibody against olygodendrocytic marker O4 was added prior to fixation: culture medium was replaced by a 1:4 dilution of O4 antibody (kind gift from Dr Siddharthan Chandrari; University of Edinburgh) in preheated DMEM and incubated at 37ºC for 30min. Unbound O4 antibody was washed twice with DMEM and with PBS (pH 7.4, Gibco). The cells were then fixed with 4% [w/v] PFA (pH 7.4) for 20min and washed once with PBS. Permeabilisation of cellular membranes was achieved by treatment with ice-cold methanol for 20min at -20ºC, followed by two washes in PBS. Incubation with 2N HCl for 30min at room temperature was used to retrieve the BrdU antigen followed by three washes in PBS for 10min to allow the neutralisation of the pH. Preparations were blocked with 10% [v/v] normal goat serum (NGS, Vector Laboratories) in PBS and treated with the remaining primary antibodies overnight. The following day, primary antibodies were recovered and cells incubated with the appropriate secondary antibodies. Cell nuclei were counterstained with 0.1mg·l^{-1} Hoechst (Sigma).

Finally, coverslips were mounted with Fluorsave (Calbiochem) and allowed to dry before imaging. Primary and secondary antibodies used are detailed in Table 4-6.

ANTIBODY	SPECIES	DILUTION	SUPPLIER
Alexa fluor 488 anti mouse IgG	Goat	1:500	Invitrogen
Alexa fluor 488 anti rabbit IgG	Goat	1:500	Invitrogen
Alexa fluor 568 anti mouse IgG	Goat	1:500	Invitrogen
Alexa fluor 568 anti rabbit IgG	Goat	1:500	Invitrogen
Alexa fluor 568 anti rat IgG	Goat	1:500	Invitrogen
IgG2a anti BrdU (monolayer)	Mouse	1:100	Hybridoma Bank
IgG anti BrdU (monolayer)	Rat	1:500	Abcam
Fluorescein-conjugated anti mouse IgM	Goat	1:200	Vector Labs
IgG anti AKT	Rabbit	1:400	Cell Signalling
IgG Phospho-AKT (Ser473) (Thr202/Tyr204)	Mouse	1:400	Cell Signalling
IgG anti p44/42 MAP Kinase	Rabbit	1:400	Cell Signalling
IgG anti Phospho-p44/42 MAP Kinase (Thr202/Tyr204)	Mouse	1:400	Cell Signalling
IgG anti GFAP	Rabbit	1:1000	DAKO
IgM anti O4	Mouse	1:4	S.Chandrari
IgG anti Tuj1	Mouse	1:500	Covance
IgG anti DCX	Rabbit	1:500	Abcam

Table 4-6 List of antibodies used, species raised in, dilutions and suppliers

4.3.10 Imaging and quantification of cultured cells and sections

Fluorescence staining was viewed under a Leitz DMRD fluorescent microscope attached to a Leica DFC340FX digital high-sensitivity monochrome camera and visualized using Leica Application suite 3.3.1. DAB-stained sections were viewed under a Leitz DMRD microscope attached to a Leica DC500 42bit-color digital camera and visualized using the Leica IM50 4.0 software. Full-brain panels were obtained by taking low magnification images (10X) across the brain and carefully overlapping them using Adobe Photoshop CS3 software. Cell counts were

performed using ImageJ and the cell counting plugin from Kurt De Vos at the University of Sheffield.

4.3.11 Semi-automated image acquisition and analysis

Primary Str-NSCs from *Gal*-KO and WT (4.3.3) were plated on poly-*D*-lysine coated 96-well plates at density of $6.5x10^4$cells·cm^{-2} in $DMEM:F12^{B27\text{-}DIFF}$. After 24h, cells were stimulated with 100mM galanin (Sigma) from 5min to 2h. Cells were washed once with ice-cold PBS and fixed with 4% [w/v] PFA for 20min. Immunohistochemistry was performed as described previously (2.4.8.1.). Briefly, cells were permeabilised with ice-cold methanol, blocked in 10% [v/v] NGS and 1% [w/v] BSA for 3h and stained for AKT (or protein kinase B) and phospho-AKT (Ser473) or p44/42 MAP kinase and phospho p44/42 MAP kinase overnight. Appropriate secondary antibodies were used (Table 4-6). Cell nuclei were counterstained with 0.1mg·l^{-1} Hoechst. Image acquisition and analysis were performed on an IN Cell Analyzer workstation (GE Healthcare) using a multi-target analysis algorithm to quantify fluorescence intensity in nuclear and cytoplasmic compartments.

4.3.12 Fluorescence immunohistochemistry

40μm-brain sections were prepared as described in 2.5.7 and stained as free-floating sections as in 2.4.8.2. Briefly, sections were incubated with 2N HCl for 30min at room temperature inn order to retrieve the BrdU antigen followed by three washes in PBS for 10min to allow the neutralisation of the pH. Sections were then blocked overnight in PBS-0.1%Tx^{100} containing 10% [v/v] NGS, 2%

[w/v] BSA (Sigma) and 0.01% [w/v] NaN_3. The following day, sections were incubated with primary antibodies diluted in PBS-0.1%Tx^{100} containing 5% [v/v] NGS, 1% [w/v] BSA and 0.01% [w/v] NaN_3, washed and incubated with the appropriate secondary antibodies. Cell nuclei were counterstained by incubating with 0.1mg·l^{-1} Hoechst. Finally sections were mounted onto Superfrost$^+$ slides (Fisher), briefly allowed to dry and mounted in Fluorsave. Stained slides were kept at 4ºC in the dark for at least 3 months.

4.3.13 DAB-staining

For 3-3'-diaminobenzidine (DAB) staining, brain sections were quenched and treated with 2N HCl blocked and incubated with primary antibodies as above but were done using TBS instead of PBS. Once bound to the primary antibody, sections were incubated overnight with a biotinylated secondary antibody diluted in TBS-0.1%Tx^{100} containing 5% [v/v] serum and 1% [w/v] BSA. The following day, sections were treated with HRP-conjugated avidin, washed and incubated with DAB until a suitable staining developed (5-10min) . Sections were then washed once in ddH_2O and mounted on Superfrost$^+$ slides. These were dehydrated overnight, delipidated by serial washes in xylene, counterstained with Hematoxylin:Eosin and mounted with DPX-medium (see 2.4.8.4).

4.3.14 Statistical analysis

MTT data were screened with 1-way ANOVAs followed by Newman-Keuls as post-hoc test. Data from immunostaining analysis and the adult neurogenesis study were compared using t-tests. Statistical significance was accepted when $p<0.05$. For in vitro studies, N numbers were greater than or equal to three. For in

vivo studies 8 animals were analysed per group. The null hypothesis was rejected if $p < 0.05$.

4.4 Results

4.4.1 Galanin and galanin receptors are expressed in Str-NSCs

To confirm the expression of galanin and the galanin receptors in Str-NSCs, mRNA was extracted from primary Str-NSCs from WT and *Gal*-KO mice and the expression levels of galanin, *GalR1*, *GalR2* and *GalR3* compared by Taqman-qPCR. Figure 4—2 shows that, as expected, galanin was expressed in WT Str-NSCs but not in *Gal*-KO Str-NSCs. Both *GalR1* and *GalR2* mRNA were present at similar levels in *Gal*-KO and WT mice. The lower ΔCt value for *GalR1* (WT-*GalR1* 10.56±0.13 vs. WT-*GalR2* 19.39±0.22) indicated that this receptor is expressed at higher levels than *GalR2*. No *GalR3* mRNA could be detected, suggesting that this receptor is not expressed in E14.5 Str-NSCs.

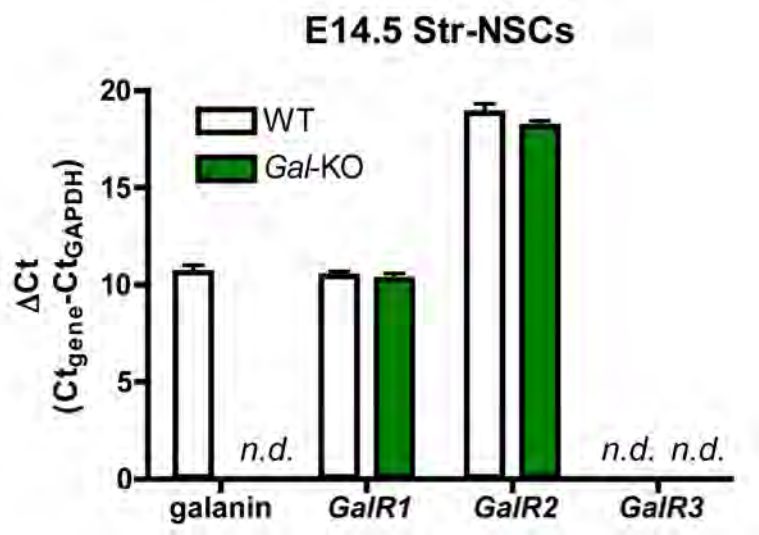

Figure 4—2 Expression of galanin and GalRs in E14.5 Str-NSCs
Detection of mRNA expression levels in primary Str-NSCs by real-time qPCR. Similar levels of galanin receptor 1 (GalR1) and 2 (GalR2) mRNA were present in Gal-KO (green bars) and WT (white bars) NSCs. No galanin mRNA was detected in Gal-KO NSCs. Galanin receptor 3 (GalR3) mRNA was not present in Str-NSCs. Bars represent the mean of three independent experiments ± SEM.

4.4.2 Galanin induces AKT activation in Str-NSCs

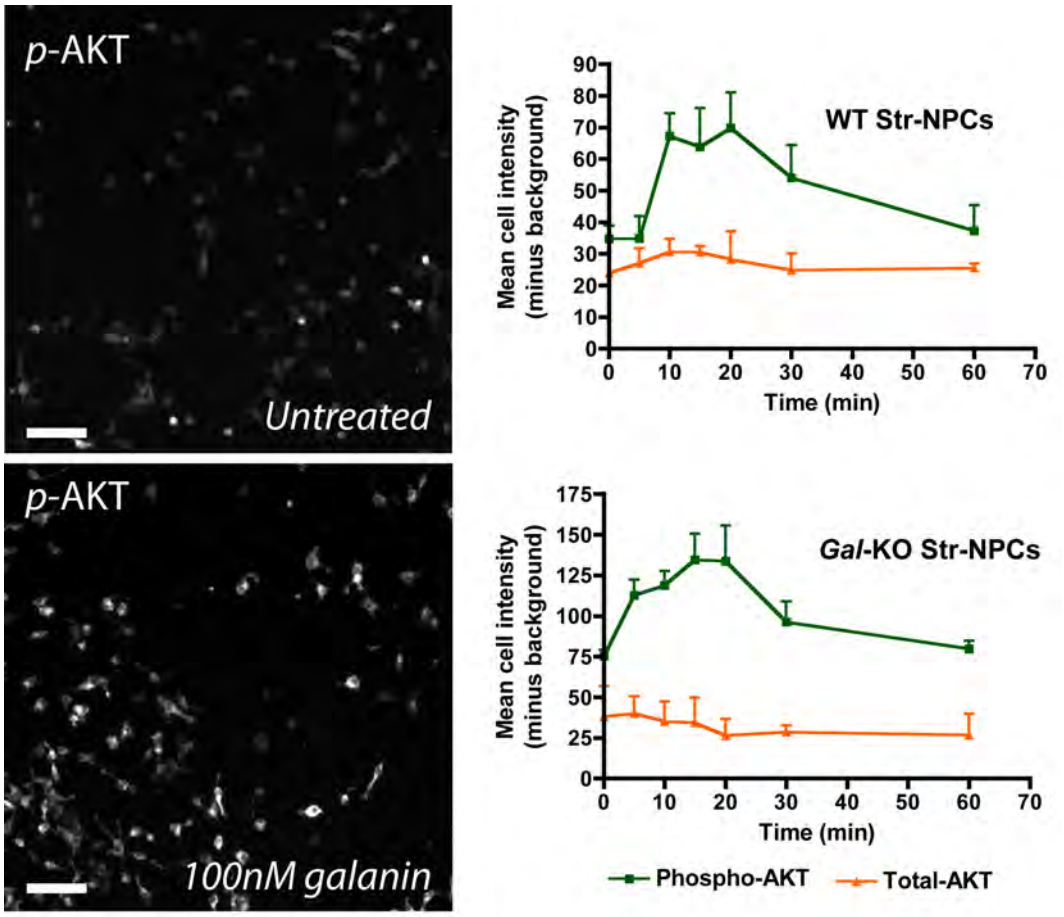

Figure 4—3 Galanin induces AKT activation in Str-NSCs
Photomicrographs of AKT activation with 10mM galanin after 20min; scale bars = 50µm. 100nM galanin increases phospho-AKT labelling (green squares) but not total AKT levels (orange triangles) both in WT and Gal-KO Str-NSCs. Graphs represent the mean of three independent experiments ± SEM.

To demonstrate that galanin receptors are functionally active in Str-NSCs we studied the effect of acute stimulation with galanin on AKT and ERK signalling pathways – as both are known to control cell fate and survival and can be activated by GALRs. We used an IN-Cell Analyser for semi-automated image acquisition and analysis. The software detects the nuclear compartment based on Hoechst staining of the DNA and then delineates the cytoplasmic compartment using a top-hat algorithm. Figure 4—3 shows a rapid increase in AKT activation (given by phospho-AKT staining) in Str-NSCs after galanin stimulation but no

change on the total amount of AKT protein within the cells. This agrees with the current literature that shows that AKT activation is one of the downstream mediators of galanin stimulation (Elliott-Hunt et al., 2004; Ding et al., 2006; Hobson et al., 2006; Elliott-Hunt et al., 2007). No effect on ERK phosphorylation was detected (data not shown).

4.4.3 Galanin increases the growth of Str-NSCs

Given that functional galanin receptors are expressed on Str-NSCs, we sought to determine the effect of addition of exogenous galanin on NSCs cultures and the optimal concentration of galanin to be used in further experiments. Primary, E14.5 NSCs from WT and *Gal*-KO embryos were expanded for seven days, in the presence of 0, 1, 10, 50, 100 and 1000nM of galanin with EGF or FGF-b + Hep as mitogens. On day seven, MTT assays were performed on the cultures. Galanin did not induce cell growth on WT-EGF cultures (Figure 4—4a) but significantly increased MTT activity when the same NSCs were expanded with FGF-b + Hep (Figure 4—4b). 10nM galanin was the lowest concentration to produce this effect (control 1.51±0.05 vs. 10nM galanin 1.94±0.03, Newman-Keuls post-hoc test, $p<0.05$, $N=3$).

Similar results were obtained for *Gal*-KO NSCs: galanin failed to induce cell growth in EGF cultures (Figure 4—5a) but significantly increased MTT activity when these NSCs were expanded with FGF-b + Hep (Figure 4—5b). 50nM galanin was the lowest concentration to produce this effect (control 1.58±0.02 vs. 50nM galanin 1.99±0.06; Newman-Keuls, $p<0.01$; $N=3$). Thereafter, Str-NSCs

cultures were expanded with FGF-b + Hep as mitogens and 100mM galanin was used for all further experiments.

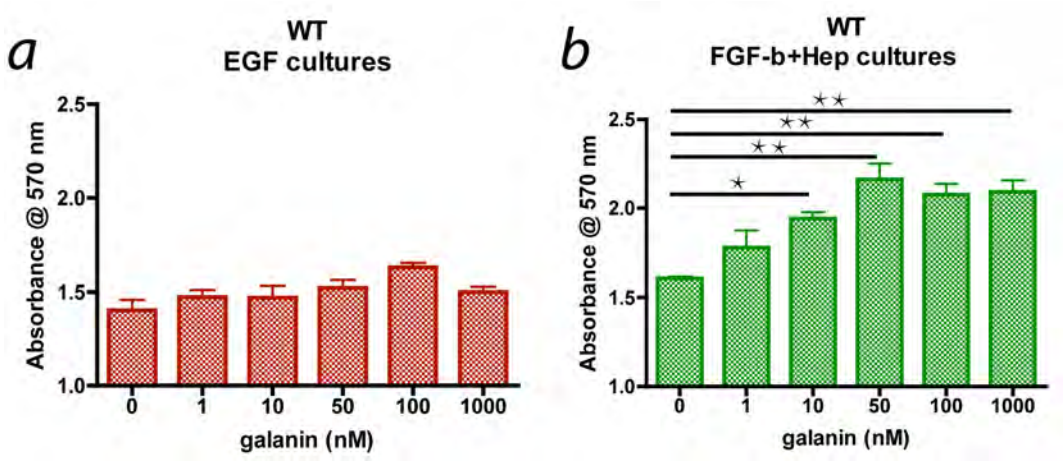

Figure 4—4 MTT assay I

WT E14.5 NSCs, after 7D expansion in the presence of 0, 1, 10, 50, 100 and 1000nM galanin. a) Cultures expanded with EGF. b) Cultures expanded with FGF-b + Hep. * p<0.05; **p<0.01; Newman-Keuls post-hoc test, N=3 per group.

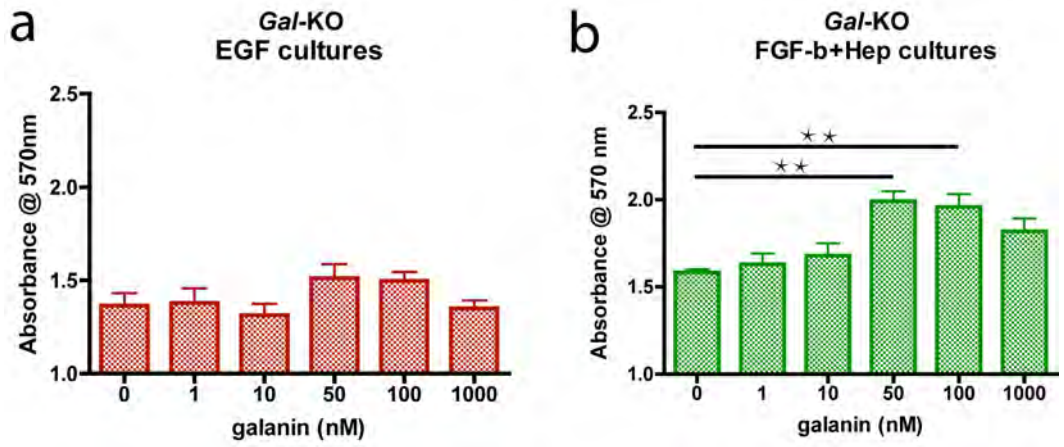

Figure 4—5 MTT assay II

Gal-KO E14.5 NSCs, after 7D expansion in the presence of 0, 1, 10, 50, 100 and 1000nM galanin. a) Cultures expanded with EGF. b) Cultures expanded with FGF-b + Hep. * p<0.05; **p<0.01; Newman-Keuls post-hoc test, N=3 per group.

4.4.4 Galanin induces expression of anti-apoptotic and pro-neuronal genes in Str-NSCs

Cell growth is a function of cell proliferation, survival and death. We have shown that galanin increased cell growth from Str-NSCs. This could reflect an increase of cell proliferation or cell survival. We therefore sought to determine if galanin stimulation could result in up-regulation of anti-apoptotic genes and thus increase cell survival. Str-NSCs were expanded for one week in vitro in the presence of FGF-b + Heparin. On day seven, cultures were treated with 100nM galanin for 6 or 12 hours, their RNA was extracted and analysed by semi-quantitative RT-PCR.

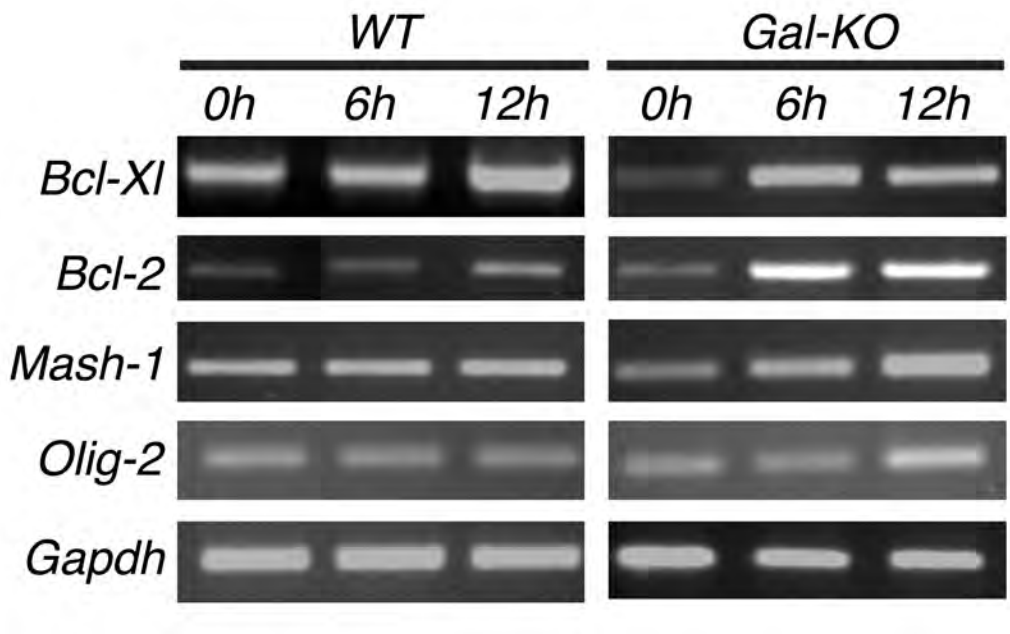

Figure 4—6 Short-term stimulation with galanin, semi-quantitative RT-PCR Gal-KO and WT E14.5 NSCs, after 7D expansion in the presence of FGF-b + Hep, were stimulated with 100nM galanin for 6 or 12h. Rows 1 & 2, anti-apoptotic genes Bcl-Xl and Bcl-2. Rows 3 & 4, lineage specific transcription factors. Row 5, endogenous control.

Figure 4—6 shows that addition of 100nM galanin caused an up-regulation of the anti-apoptotic genes *Bcl-Xl* and *Bcl-2*. In WT Str-NSCs, this effect was observed 12h post-stimulation whereas *Gal*-KO showed earlier gene induction, with up-regulation becoming obvious after 6h. Interestingly, *Bcl-Xl* and *Bcl-2* have been shown to direct NSCs towards a neuronal phenotype. This effect is independent of their anti-apoptotic actions (Chang et al., 2007). Therefore, we also profiled the lineage specific transcription factors *Mash-1* and *Olig-2*. *Mash-1* and *Olig-2* expression were up-regulated by galanin stimulation in *Gal*-KO Str-NSCs 6h after *Bcl-2* and *Bcl-Xl* up-regulation. This suggests that that these genes could be downstream of *Bcl-Xl* and *Bcl-2* signalling and partly responsible for the pro-neuronal of anti-apoptotic genes described by Chang et al. In WT Str-NSCs, *Bcl-Xl* and *Bcl-2* response is delayed compared to *Gal*-KO NSCs, becoming up-regulated only 12h following galanin stimulation. Accordingly, no increases in *Mash-1* or *Olig-2* expression were found within these time points. This suggests that the increase in pro-neuronal genes is secondary to up-regulation of the pro-survival *Bcl-Xl* and *Bcl-2* gens and could require longer galanin stimulation in WT-NSCs.

4.4.5 Galanin increases the number of neurons after fetal Str-NSC differentiation

We next studied if galanin could affect the differentiation potential of Str-NSCs. In order to test this, E14.5 Str-NSCs were expanded for seven days in vitro (DIV) in the presence of 0 or 100nM of galanin with FGF-b + Hep as mitogens. To assess the effect of galanin on neuroblast proliferation, BrdU was added to cultures 24h prior to plating. After seven days, Str-NSCs were plated on PDL and

mitogens withdrawn. The cells were allowed to differentiate for seven days before analysis. In WT Str-NSCs (Figure 4—8b), addition of galanin throughout the expansion and differentiation stages resulted in a 13% increase in the number of neurons given by $Tuj1^+$ cells (100nM: 48.8±4.3% $Tuj1^+$ vs. Ctrl: 35.9±1%; $p<0.05$, *t-test*; N=3). Number of astrocytes ($GFAP^+$ cells), oligodendrocytes ($O4^+$ cells) or neuroblasts $Tuj1^+ \cap BrdU^+$ cells) was not changed by treatment with galanin. There was also a 17% increase in total number of proliferating NSCs ($BrdU^+$) that agrees with our MTT data but did not reach the significant threshold (100nM: 58.7.1±5.32% $BrdU^+$ vs. Ctrl 41.52±4.23; $p= 0.06$, *t-test*; N=3).

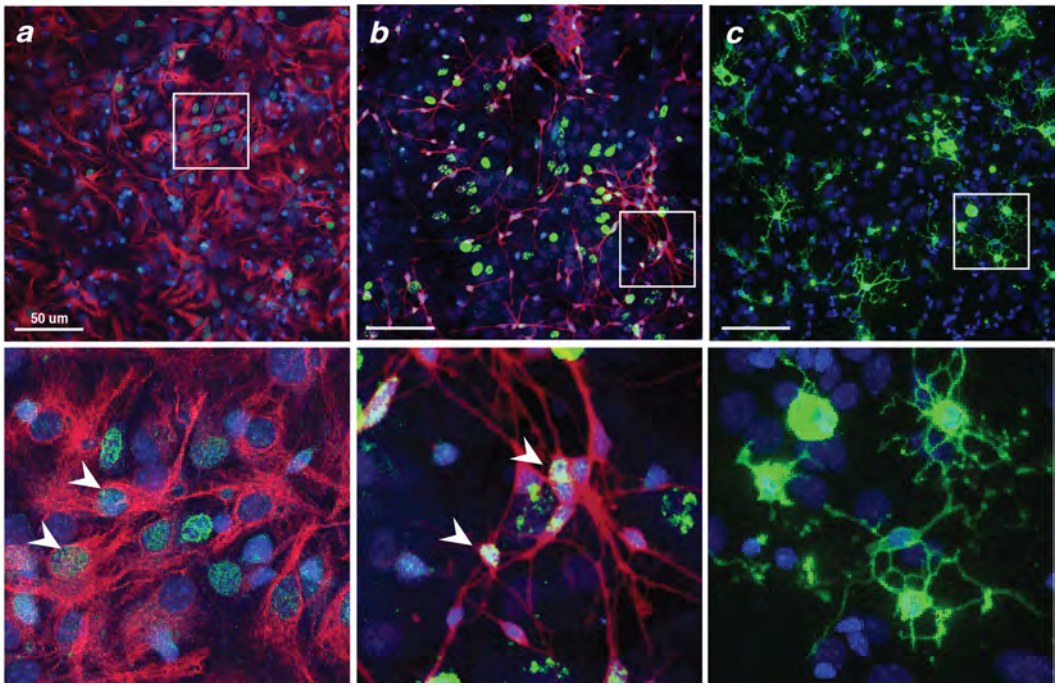

***Figure 4—7 Immunofluorescent characterisation of differentiated Str-NSCs** Representative images of Gal-KO NPCs + 100nM galanin after 7D differentiation. A) Astrocytic marker GFAP (red), BrdU (green) and higher magnification depicting $GFAP^+/BrdU^+$ cells (arrowheads). B) Neuronal marker Tuj1 (red), BrdU (green) and higher magnification depicting $Tuj1^+/BrdU^+$ cells (arrowheads). C) Oligodendrocytic marker O4. DNA staining, Hoescht is shown in blue in all images. Scale bars = 50 µm.*

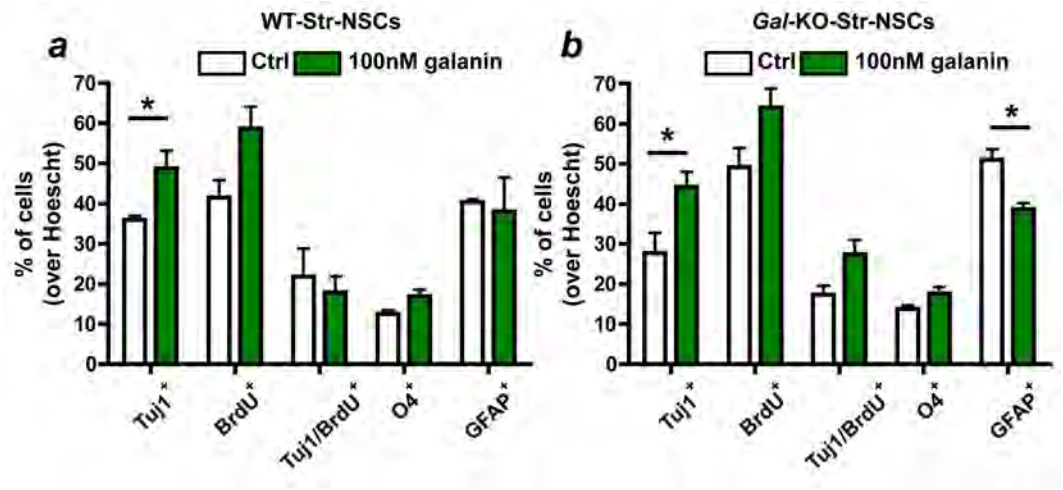

Figure 4—8 Effect of galanin on Str-NSC differentiation
Str-NSCs from WT (a) and Gal-KO (b) litters after 7D differentiation in vitro. White bars represent control cultures where no galanin was added. Green bars represent cultures supplemented with 100nM of galanin. Percentages of neurons, proliferating NSCs, neuroblasts, oligodendrocytes and astrocytes are given by $Tuj1^+$, $BrdU^+$, $Tuj1BrdU^+$, $O4^+$ and $GFAP^+$ cells, respectively. *p<0.05; Student t-test, N=3 per group.

Similarly, *Gal*-KO Str-NSCs (Figure 4—8a) yielded 17% more neurons given by $Tuj1^+$ cells upon differentiation when exposed to galanin (100nM: 44.24±5.04% $Tuj1^+$ vs. Ctrl: 27.7±3.45%; p=0.057 *t-test*, N=3). Number of oligodendrocytes ($O4^+$ cells) was unaffected by galanin treatment but number of astrocytes was significantly reduced (100nM: 52.2±1.13% $GFAP^+$ vs. Ctrl: 38.7±1.; p<0.05 *t-test*, N=3). As with WT, a trend towards an increase in proliferating cells (in this case both for NSCs and neuroblasts) was observed, but these differences were not significant. Interestingly, although galanin was able to increase neuronal numbers from both WT and *Gal*-KO Str-NSCs, untreated *Gal*-KO and WT cultures did not have significantly different neuronal yields (WT: 35.9±1% vs. *Gal*-KO: 27.7±3.45%; p=0.084 *t-test*, N=3). This suggests that galanin enhances neurogenesis but it is not required for basal fetal NSCs differentiation.

4.4.6 Galanin increases the number of neurons after adult SVZ-NSC differentiation

In the adult striatum, NSCs are restricted to the SVZ. From this area, newly generated neuroblasts migrate along the RMS towards the OB where they differentiate into OB-interneurons. From our previous results, we wondered if the effect of galanin was specific to fetal Str-NSCs or could also affect adult SVZ-NSCs. To test this, we harvested SVZ-NSCs from 8-10 week-old *Gal*-KO and WT mice and expanded and differentiated in vitro. SVZ-NSCs were initially expanded for 10 days with EGF and FGF-b + Hep as mitogens. At this point the cells were passaged, expanded in the presence of 100nM galanin for seven additional days, no galanin was added to control cultures. BrdU was added to cultures 72h prior to plating. On day 17, SVZ-NSCs were plated on PDL and mitogens withdrawn. Cells were allowed to differentiate with or without galanin for seven days before analysis.

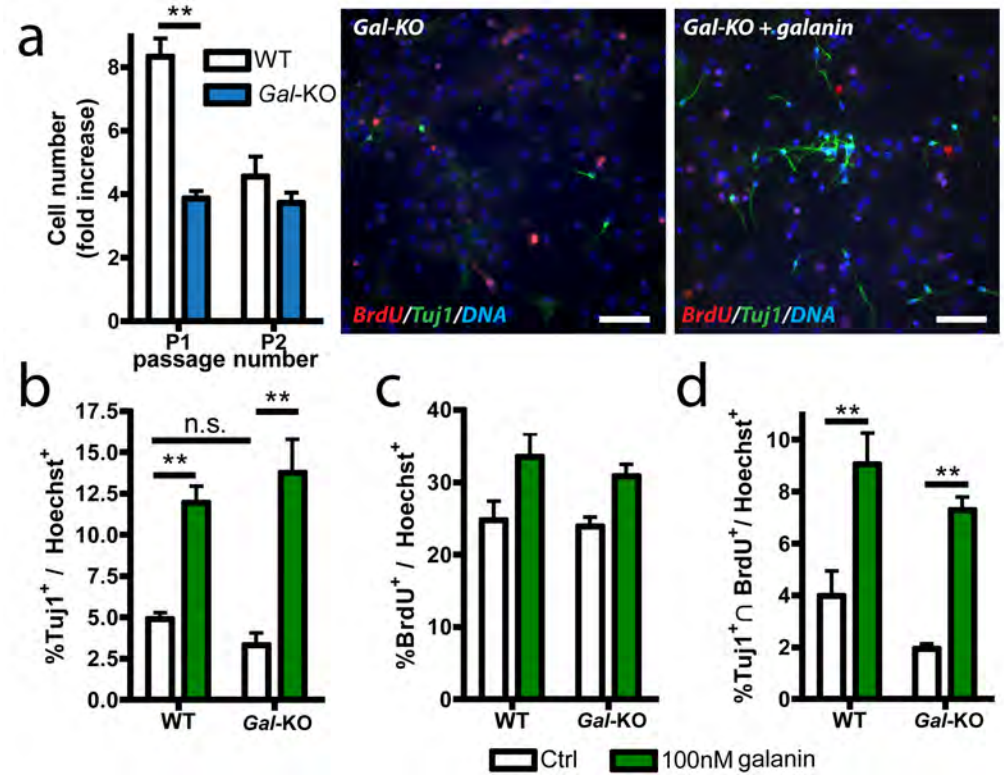

Figure 4—9 Effect of galanin on adult SVZ-NSCs.
a) In vitro expansion of SVZ-NSCs from WT and Gal-KO adult mice. b, c & d) Percentages of neurons, proliferating NSCs and neuroblasts are given by Tuj1$^+$, BrdU$^+$, Tuj1∩BrdU$^+$ cells, respectively. Cells were differentiated for 7DIV, white bars represent control cultures where no galanin was added. Green bars represent cultures supplemented with 100nM of galanin. * p<0.05; **p<0.01; Student t-test, N=3 per group. Scale bars = 50 µm.

Gal-KO SVZ contained fewer proliferating cells compared to WT and gave rise to fewer NSCs after 10DIV (Figure 4—9a, *P1*). After 17D in vitro, selection and normalisation of NSCs due to passaging and loss of self-renewal potential typical of adult-NSCs resulted in similar values for *Gal*-KO and WT (Figure 4—9a, *P2*). Following differentiation, galanin-treated cultures showed a marked increase in the number of neurons given by Tuj1$^+$ cells, both in WT cultures (WT: Ctrl 4.91±0.35% vs. 100nM galanin 11.94±0.99%; *t-test* $p<0.01$; N=3) and in *Gal*-KO cultures (*Gal*-KO: Ctrl 3.31±0.73% vs. 100nM galanin 13.77±2.00%, *t-test* $p<0.01$; N=3). The number of neuroblasts was also increased by galanin in both cultures (WT: Ctrl 4.00±0.95% vs. 100nM galanin 9.1±1.18% and *Gal*-KO:

Ctrl 1.94 ± 0.19% vs. 100nM galanin 7.28 ± 0.49%; *t-test* $p<0.01$; N=3). Higher numbers of $BrdU^+$ NSCs were observed after galanin treatment, indicating a general increase in NSC-proliferation. However, this difference was not statistically significant. Similarly to our result with Str-NSCs, untreated *Gal*-KO and WT SVZ-NSC cultures did not have significantly different neuronal yields (WT: 4.91±0.36% vs. *Gal*-KO: 3.31±0.73%; $p=0.084$ *t-test*; N=3). This suggests that SVZ-NSCs are galanin responsive and that galanin can enhance neurogenesis from this cells but it is not necessary for basal SVZ-NSCs differentiation.

4.4.7 The brain of adult *Gal*-KO mice contains reduced numbers of proliferating NSCs

Given the ability of galanin to promote NSC survival and neurogenesis in vitro, we then wondered if loss of galanin could compromise NSC function in the adult brain. In order to label dividing cells in adult mice, 8 to 10 week-old male mice were given an IP injection of 100 $mg \cdot Kg^{-1}$ BrdU and sacrificed after two hours. Brain cells that had incorporated BrdU into their DNA were visualised and counted by DAB staining on sagital sections (Figure 4—10). Identity of these cells as NSCs was confirmed by double-staining with the immature neuronal marker doublecortin (DCX) (Figure 4—11 and Figure 4—12).

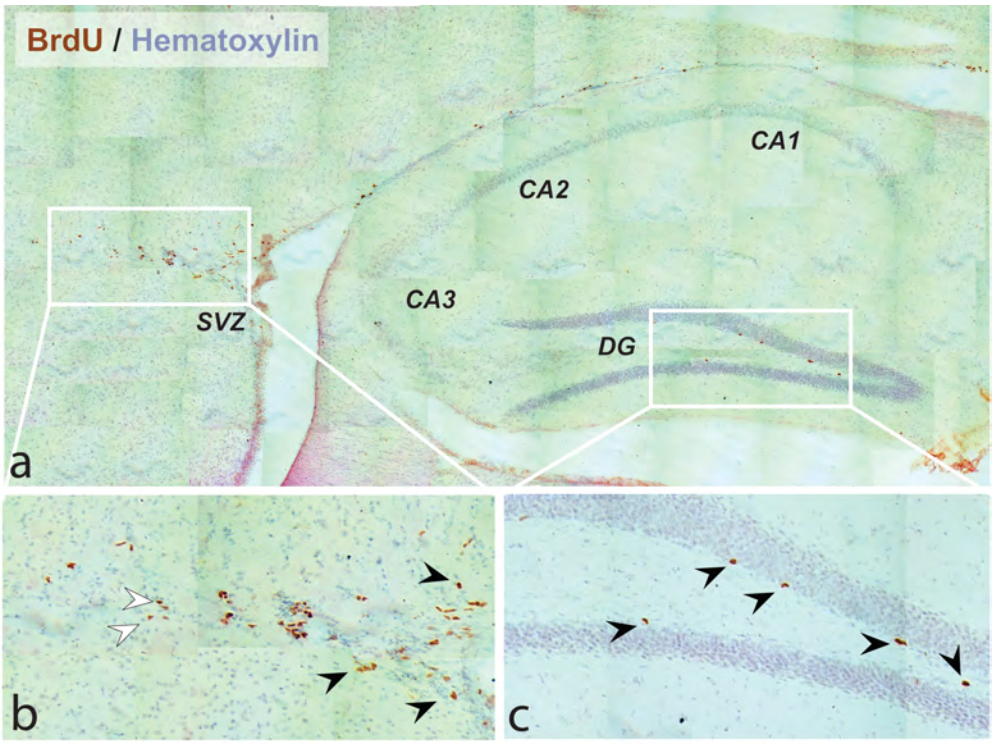

Figure 4—10 Brain distribution of DAB-BrdU$^+$ cells.
a) Two hours post BrdU injection proliferating cells (BrdU$^+$, DAB$^+$) are located in three areas: DG of the hippocampus, SVZ and RMS. b) Higher magnification shows dividing NSCs in the SVZ (black arrowheads) and neuroblasts starting migration along the RMS (white arrowheads). c) Dividing cells in the hippocampus. Sections were counterstained with Haematoxylin.

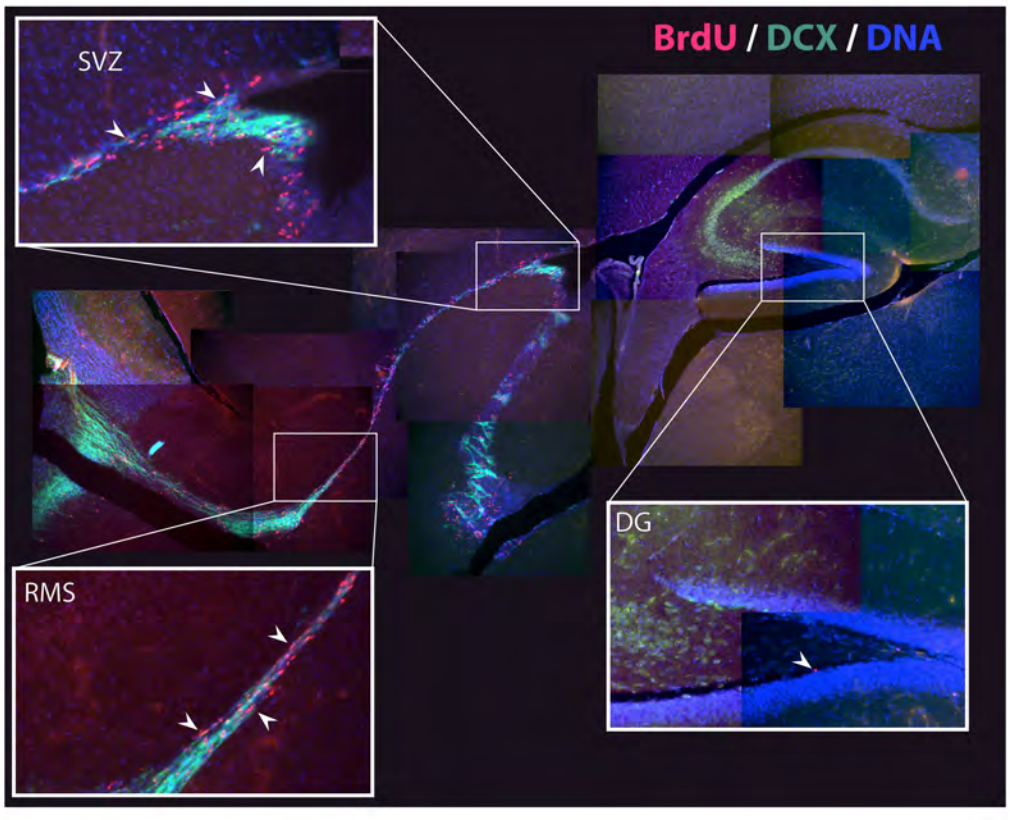

Figure 4—11 Neurogenic areas in the adult brain.
distribution of BrdU+ cells (two hours post-injection) and DCX+ cells: Immunohistochemistry on 40µm sagital sections for BrdU (red), DCX (green) and DNA (Blue). Rectangles show dividing cells on the main neurogenic areas of the adult mouse brain. DG: dentate gyrus; RMS: rostral-migratory stream; SVZ: sub-ventricular zone.

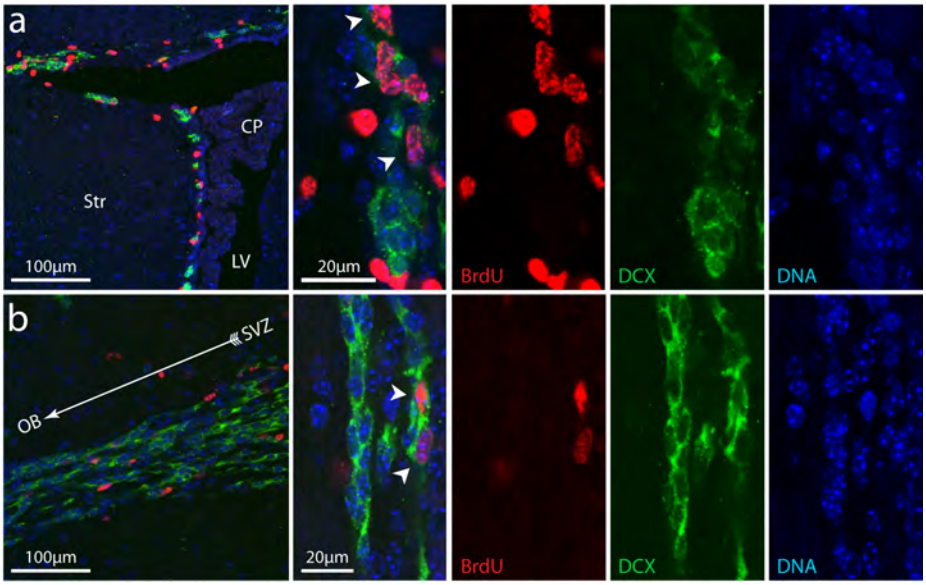

Figure 4—12 Confocal microscopy of SVZ and RMS neuroblasts
a) SVZ neuroblasts. (CP: Choroid plexus, LV: Lateral ventricle, Str: Striatum). b) Migrating neuroblasts in the RMS (OB: olfactory bulb, SVZ: subventricular zone). White arrowheads BrdU+ neuroblasts.

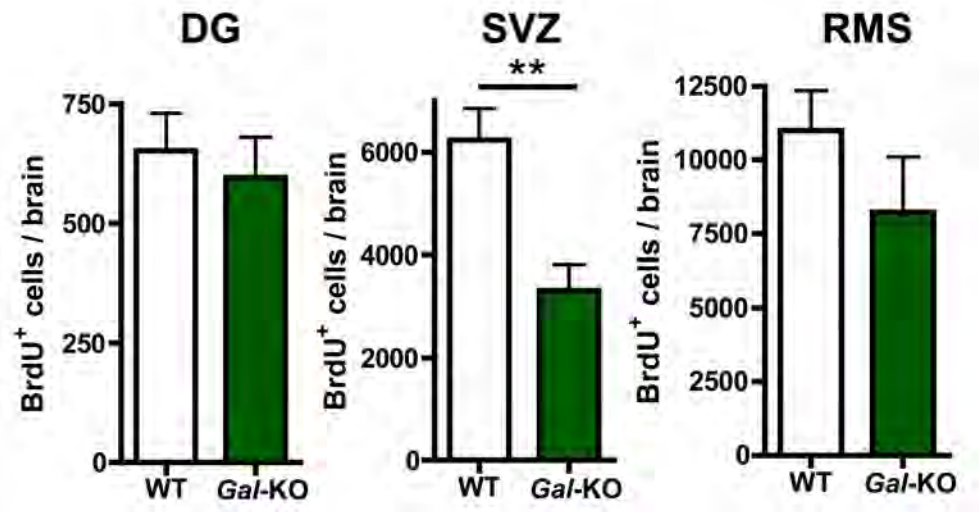

Figure 4—13 Adult neural proliferation (Short term)
Total number of BrdU$^+$ in the dentate gyrus (DG), sub-ventricular zone (SVZ) and rostral migratory stream (RMS) of adult WT and Gal-KO mice. **p<0.01; Student t-test, N=8 per group.

Figure 4—13 shows that *Gal*-KO mice had a marked reduction in proliferation in the SVZ. This trend was significantly pronounced in the SVZ neurogenesis, were galanin disruption resulted in 46% reduction in the number of $BrdU^+$ NSCs (WT: 6384.95± 541 $BrdU^+$cells vs. *Gal*-KO: 3423.33±475.57 $BrdU^+$cells, *t-test* $p<0.01$; N=8). This agreed with our results in vitro and confirmed that galanin is an important in-vivo modulator of SVZ-NSC function.

4.4.8 Fewer migrating neuroblasts reach the olfactory bulb in *Gal*-KO mice

To allow newly generated neuroblasts in the SVZ to reach their destination at the OB, animals were injected with 100 $mg \cdot Kg^{-1}$ BrdU for four consecutive days and sacrificed after 21 days from the last BrdU injection. Figure 4—14 shows that at this time point, the granular cell layer of the OB in *Gal*-KO mice contained 52% less $BrdU^+$ cells per cubic millimetre than the WT controls (WT 3881.12 ± 337.54 $BrdU^+cells \cdot mm^{-3}$ vs. *Gal*-KO 1869.77±318.91 $BrdU^+cells \cdot mm^{-3}$, *t-test* $p<0.01$; N=8). This confirmed our previous result, indicating that not only less neuroblasts are originated in the SVZ of *Gal*-KO mice but that a smaller percentage of these reach the OB and survive after 21 days.

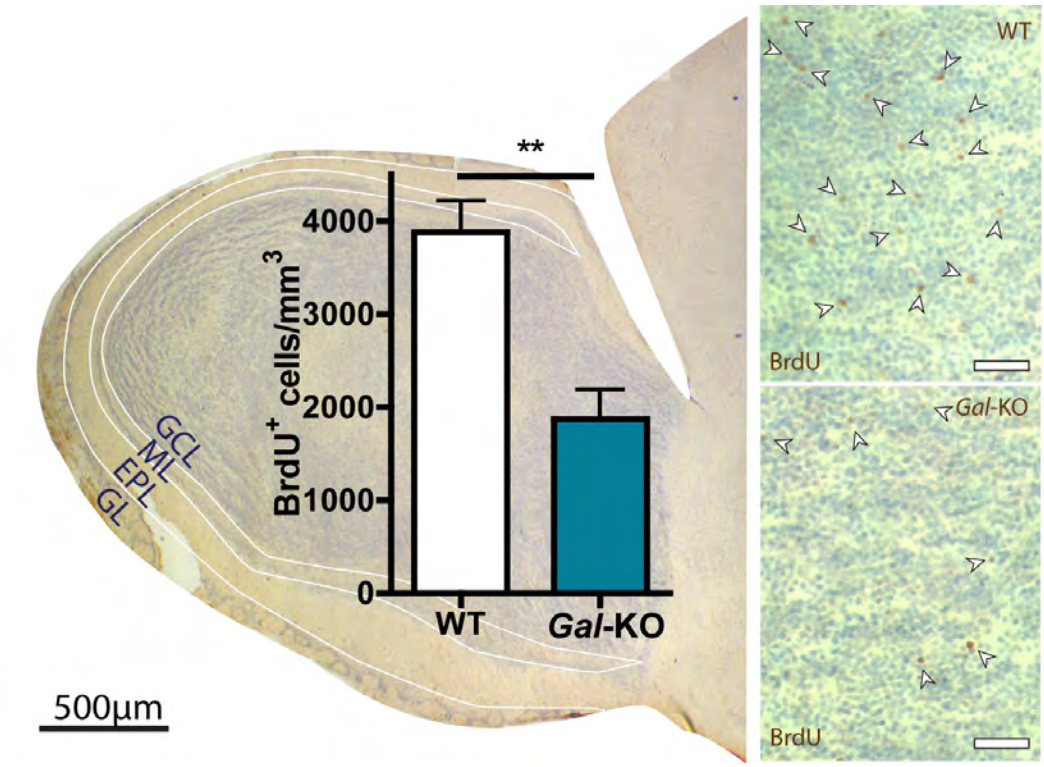

Figure 4—14 Density of BrdU+ cells in the olfactory bulb (Long term). ***The olfactory bulb is organised in distinct layers: glomerular layer (GL), external plexiform layer (EPL), mitral layer (ML) and granular cell layer (GCL). Graph represents the mean number ± SEM of BrdU+ cells per mm^3 in the GCL, 21 days post BrdU-administration. Data compared with t-test (**p<0.01, N=8 per group). Images correspond to BrdU$^+$ cells (white arrow heads) in the GCL in WT and Gal-KO mice, white scale bars = 50µm.***

4.5 Discussion

Galanin is a pleiotropic neuropeptide that is up-regulated after injury in the nervous system, is involved in neuroregeneration and is a neuroprotective factor in the hippocampus and forebrain. It is also a trophic factor for specific neuronal populations in the forebrain (O'Meara et al., 2000), pituitary (Wynick et al., 1998) and DRG (Holmes et al., 2000). Galanin and its receptors are expressed in NSCs and in the neurogenic niche in the adult brain (Tarasov et al., 2002; Shen et al., 2003). However, little is known to date of the effect of galanin in NSCs.

We have shown that fetal Str-NSCs express galanin and both *GalR1* and *GalR2*. We could not detect any mRNA for the *GalR3* suggesting that this receptor is present at very low levels in Str-NSCs if expressed at all. Although Tarasov et al. reported relatively high expression of *GalR3* in mouse ES cells (Tarasov et al., 2002), this receptor has a very restricted distribution in the CNS (Mennicken et al., 2002) and might be down-regulated in pluripotent stem cells once they commit to the neural lineage. Loss of galanin did not alter the expression levels of its receptors in agreement with published observations from the Wynick lab (Hobson et al., 2006). We have then shown that GALRs in Str-NSCs are functional and lead to AKT activation when stimulated with galanin AKT is a well-known modulator of cell survival and has been shown to act downstream of galanin signalling (Elliott-Hunt et al., 2004; Ding et al., 2006; Hobson et al., 2006; Elliott-Hunt et al., 2007).

Given that galanin is a trophic factor for the CNS, we next wondered if addition of exogenous galanin could promote cell growth from Str-NSCs. MTT-assays

showed that this was indeed the case and that galanin treatment resulted in increased MTT activity after seven days in vitro. Cell growth is a function of cell division, survival and death, therefore galanin could be enhancing growth by affecting any of these parameters. Analysis of BrdU incorporation into the DNA of dividing cells, showed only a marginal increase in cell proliferation after galanin treatment, suggesting that this was not the main mechanism by which galanin was promoting cell growth. We next wondered if galanin could be promoting cell survival by up-regulating anti-apoptotic genes. Indeed, galanin stimulation resulted in a marked increase in the anti-apoptotic genes Bcl-2 and Bcl-xl suggesting that galanin was promoting cell survival and viability of our Str-NSC cultures.

Shen el al. have previously preformed a similar experiment to ours assessing NSC growth by MTT assay. Surprisingly, they reported that galanin reduced NSC growth and they hypothesised that this was due to galanin inducing NSC apoptosis via GALR2 (Shen et al., 2005). Shen et al. used rat E14 NSC for their experiments, so it is possible that this discrepancy is due a different response to galanin at different developmental stages or in different species. Of note, this paper was published as a review and the methodologies used, such as the regional origin of the NSCs, were not fully described. Furthermore, Shen et al. did not perform any additional characterisation of the effect of galanin on NSCs and NSC- differentiation, nor did they provide a mechanism for the pro-apoptotic galanin.

In our hands, galanin treated Str-NSCs gave rise to more neurons, indicated by the number of $Tuj1^{+}$ cells upon differentiation. This effect was neuronal specific and

no increases in the number of astrocytes (given by $GFAP^+$ cells) or oligodendrocytes (given by O4+ cells) were found. Furthermore, no changes in the number of neuroblasts (given by $Tuj1^+ \cap BrdU^+$ cells) were noted. This indicates that galanin did not induce growth of Str-NSCs in general, as this would lead to increases of other neural cell types. Furthermore, galanin did not induce the proliferation of neuronal progenitors, as this would lead to an increase in the number of dividing neuroblasts. Taken together, these data indicate that galanin promotes the growth of Str-NSCs by inducing AKT activation and up-regulation of the anti-apoptotic genes *Bcl-2* and *Bcl-Xl*. This results in the survival of newly-formed neurons and their progenitors, leading to increased neuronal numbers upon NSC differentiation. Interestingly, BCL-2 and BCL-XL are also instructive factors for neuronal differentiation and this is independent of their anti-apoptotic properties (Chang et al., 2007). Accordingly, we have showed that *Mash-1* up-regulation (a well-known pan-neuronal homeobox transcription factor) and *Olig2* (a motor neuron transcription factor) follow *Bcl-Xl* and *Bcl-2* up-regulation, at least in *Gal*-KO Str-NSCs. This suggests that galanin is not only promoting Str-NSC survival but could also direct their differentiation towards the neuronal fate.

We next wondered if the pro-neuronal effect of galanin was specific to fetal NSCs or was also recapitulated in NSCs from the adult brain. In adult mice, striatal NSCs are confined to the SVZ of the lateral ventricles, for this reason we studied the effect of galanin on SVZ-NSCs. Remarkably, *Gal*-KO-SVZ contained fewer expandable NSCs than WT-SVZ, resulting in only four population doublings after 10DIV. In agreement with our results in fetal NSCs, untreated adult *Gal*-KO and WT SVZ-NSCs did not differ in the number of neurons they generated upon

differentiation. However, galanin treatment almost doubled this number in the adult cultures. Furthermore, the number of proliferating neuroblasts (given by Tuj1+ ∩ BrdU+ cells) was also more than doubled after galanin treatment. This indicates that in adult SVZ-NSCs, galanin enhances neurogenesis by specifically promoting the proliferation of neuronal precursors. Interestingly, Abbosh et al. have recently shown that galanin also induces proliferation of postnatal HPC-NSCs, increasing the number of neuroblasts and granular layer neurons upon differentiation in vitro (Abbosh et al., 2011). This suggests that the trophic role of galanin on adult NSCs is not restricted to the SVZ.

The ability of galanin to enhance SVZ and HPC NSC neurogenesis in vitro lead us to hypothesise that *Gal*-KO mice could have compromised neurogenesis in vivo. Indeed, this proved to be the case:

We have showed that in the *Gal*-KO DG, basal neurogenesis was not affected in the absence of galanin. However, galanin enhances neurogenesis from HPC-NSCs (Abbosh et al., 2011) and Mazarati et al. have demonstrated that galanin is required for KA-induced neurogenesis in the hippocampus (Mazarati et al., 2004b). This indicates that although galanin is not required for basal NSC function and neurogenesis, situations when galanin expression is elevated (such as injury or neurodegeneration) could result in NSC activation and generation of new hippocampal neurons. This highlights the importance of galanin as neurotrophic factor for the hippocampus.

Shen et al. have demonstrated that galanin and its receptors are expressed in the SVZ and the RMS of adult mice (Shen et al., 2005), suggesting a role for galanin

in the neurogenesis in this area. We have shown that the SVZ of *Gal*-KO mice contains 46% less proliferating NSCs than age-matched WT controls. NSCs in the SVZ give rise to neuroblasts that then migrate along the RMS towards the OB were they differentiate into neurons. As expected, the number of newly formed neuroblasts that manage to reach the OB and survive after 21 days was dramatically reduced in *Gal*-KO mice.

Adult neurogenesis and integration of new neurons in neuronal circuits are thought to contribute to brain plasticity – for review see (Lledo et al., 2006). Furthermore, in rodents, survival of newly integrated neurons is dependent on olfactory activity suggesting that OB circuits are generated based on olfactory experience (Petreanu and Alvarez-Buylla, 2002). Sakamoto et al. have shown that continuous SVZ neurogenesis is required for innate predator avoidance and sex-specific behaviours that require olfaction (Sakamoto et al., 2011). Thus, our results might imply abnormal olfaction in *Gal*-KO mice. Although extensive galanin immunoreactivity has been described in the mitral and glomerular layers in the OB (Stanic et al., 2010), to our knowledge, only Wrenn et al. have studied galanin and olfactory behaviour. They have shown that overexpressing galanin under the dopamine β-hydroxylase promoter in mice affects the social transmission of food preference (STFP) (Wrenn et al., 2003). STFP is a very complex behavioural task, including social interaction, memory processes, olfaction, taste and appetite. Additionally, the dopamine β-hydroxylase promoter would ectopically induce galanin overexpression in the SVZ and therefore a definite role for galanin in olfaction cannot be inferred from this experimental design. Interestingly, *Gal*-KO mice have decreased ethanol and high-fat

preference compared to WT mice (Karatayev et al., 2010) and although food intake is controlled centrally in the hypothalamus, Kinney et al. have shown that anosmic mice also have decreased preference for high-fat foods (Kinney and Antill, 1999). This supports our hypothesis that olfaction might be compromised in *Gal*-KO mice due to insufficient SVZ-neurogenesis, which could partially explain the differences in food and alcohol preferences described in *Gal*-KO mice. However, to date, no formal study of olfaction in *Gal*-KO mice has been undertaken.

Galanin is increased in the pituitary post-parturition and during suckling, suggesting an important role in lactation and maternal behaviour (Ren et al., 1999). Furthermore, *Gal*-KO mice have reduced levels of circulating PRL (Wynick et al., 1998), as galanin is a trophic factor for lactotroph cells and is required for oestrogen-induced lactotroph hyperplasia (Wynick et al., 1993). PRL-receptors are expressed in the vicinity of the SVZ (Roky et al., 1996) and Shingo et al. have showed that pregnancy or PRL administration causes a marked increase in SVZ proliferation and doubles the number of newly generated OB interneurons after four weeks (Shingo et al., 2003). Similarly to our findings, PRL also induced SVZ-NSC proliferation and neuronal differentiation in vitro (Shingo et al., 2003). Furthermore, *PrlR*-KO mice have deficits in olfactory-dependent maternal behaviour to fostered pups (Lucas et al., 1998) similar to the decreased ability to nurture pups described in *Gal*-KO mice (Wynick et al., 1998). Sakamoto et al. demonstrated that disruption of SVZ neurogenesis leads to severe deficits in maternal behaviour, including pup abandonment and insufficient nurturing (Sakamoto et al., 2011). Taken together, these data highlight the importance of the interplay between galanin and PRL in modulating SVZ neurogenesis and

olfaction-related maternal behaviour. This suggests that neurogenesis in *Gal*-KO female mice SVZ could be compromised to a greater extent than in male *Gal*-KO mice, which could in part explain the deficits of these mice in lactation.

Finally, it is worth noting that galanin is not the only neuropeptide that has been shown to affect NSCs in the brain and SVZ neurogenesis in particular. Neuropeptide Y (NPY) was - like galanin - initially isolated by Tatemoto et al. from pig intestine (Tatemoto et al., 1985). NPY acts as a paracrine factor in the SVZ and similarly to galanin induces proliferation of SVZ-NSCs and promotes their neuronal differentiation (Thiriet et al., 2011). *Npy* and its receptors (*Y1R* and *Y2R*) are expressed in the SVZ and RMS in mouse (Stanic et al., 2008). Interestingly, *Npy*-KO mice have a reduced number of neurons in the olfactory epithelium (Doyle et al., 2012) whereas *Npy1r*-KO or *Npy2r*-KO mice showed reduced SVZ-NSC proliferation and fewer migrating neuroblasts, which results in lower numbers of granular and glomerular OB interneurons (Stanic et al., 2008). This could represent a shared evolutionary strategy by which orexigenic neuropeptides not only modulate central neuroendocrine and hypothalamic functions but also control SVZ neurogenesis and OB plasticity, resulting in complex behavioural responses such as feeding preferences.

In conclusion, we have shown that galanin enhances survival and neuronal differentiation from fetal Str-NSCs. This effect is magnified in adult SVZ-NSCs where galanin directly promotes neuroblast proliferation and neurogenesis in vitro. Accordingly, *Gal*-KO mice have reduced NSC-proliferation in the SVZ, which results in a dramatic loss of newly generated granular cells in the OB.

Abnormal olfactory behaviour could explain some of the complex phenotypes described in *Gal*-KO mice.

Chapter 5

Chapter 5

Lentiviral-mediated delivery of *CDNF* and *MANF* fails to prevent dopaminergic cell loss in the 6-OHDA model of PD

5.1 Introduction

Parkinson's disease (PD) is the second most common neurodegenerative disease affecting one person in every 500 of the total population and around 127,000 in the UK alone (www.parkinsons.org.uk). PD is a slowly progressive and debilitating disease, characterised by tremor, bradykinesia, rigidity and postural instability but also by non-motor symptoms including cognitive disturbances. The hallmark of PD is the degeneration of dopaminergic neurons in the substantia nigra and the loss of dopaminergic neurotransmission in the corpus striatum, which causes the motor symptoms (Dauer and Przedborski, 2003). Although in advanced stages, the pathology also spreads towards cortical areas and causes cognitive decline and psychiatric symptoms (Maetzler et al., 2009).

Most forms of PD are characterised by the presence of α-synuclein inclusions in neurites (Lewy neurites) or neuronal somas (Lewy Bodies) (Spillantini et al., 1997). Indeed, mutations (Polymeropoulos et al., 1997; Krüger et al., 1998) or triplications of the α-synuclein gene (Singleton et al., 2003) are known to cause early-onset PD. However, these mutations are rare and even if other more common mutations in risk genes such leucin-rich repeat kinase (*LRRK2,* Zimprich et al., 2004), parkin (Shimizu et al., 1998) or PTEN-induced kinase 1 (*PINK1,* Valente et al., 2004) are considered, only about 15% of PD patients have a first-

degree relative with the disease (Samii et al., 2004) and in most of the cases the cause of PD remains unknown. Interestingly, according to Braak and colleagues, during the first asymptomatic stages of the disease, α-synuclein inclusions appear in anterior olfactory structures (olfactory bulb, stalk and nucleus) or in the medulla oblongata (mainly in the motor nucleus of the vagus nerve). From these areas, the pathology progresses through the brainstem, amygdala and finally reaches the substantia nigra (SN) (Braak et al., 2006). Braak and colleagues hypothesised that a neurotropic agent entering the body by the gastric or nasal route could eventually lead to nigro-striatal degeneration (Hawkes et al., 2009). Supporting this theory, intragastric administration of rotenone - a commonly used pesticide - in mice causes inflammation and α-synuclein phosphorylation in the enteric nervous system and the motor nucleus of the vagus. These mice develop α-synuclein aggregation and partial neuronal loss in the SN after three months (Pan-Montojo et al., 2010). Furthermore, nasal inoculation with the H5N1 influenza virus in mice causes microglia activation and α-synuclein aggregation that persist even after the infection is resolved. Remarkably, 60 days post-infection, these mice show a 17% reduction of dopaminergic neurons in the SN (Jang et al., 2009). It is not clear, however, how the pathology can spread from the olfactory epithelium or the enteric nerves towards the CNS but a prion-like propagation of α-synuclein (Desplats et al., 2009; Angot et al., 2010), oxidative stress, inflammation, excitotoxicity or loss of neurotrophic support have been proposed as possible mechanisms (Brundin et al., 2008). Importantly, ageing remains, to date, the greatest risk factor for PD and it has even been suggested that all these genetic and environmental factors are simply accelerating the normal process of ageing (Collier et al., 2011).

Due to our lack of understanding of the ethiology of PD, to date only symptomatic treatment is available and is predominantly based upon dopaminergic stimulation, either via dopamine precursors such as *L*-3,4-dihydroxyphenylalanine (L-DOPA) or dopamine agonists. At late stages of the disease, the systemic administration of L-DOPA becomes less effective in treating the impairments in movement and has marked deleterious side effects (for review see LeWitt, 2008). Gene therapy is a promising alternative to the present gold standard treatment L-DOPA. This aims to offer neuroprotection by delivering neurotrophic factors such as glial derived growth factor (*GDNF*) (Björklund et al., 2000; Déglon et al., 2000; Kordower et al., 2000) and neurturin (Kordower et al., 2006; Gasmi et al., 2007); or to replace dopamine loss in the striatum by delivery of dopamine synthesising enzymes – such as aromatic *L*-amino acid decarboxylase (*AADC*) in primates (Bankiewicz et al., 2006) and clinical trials (Muramatsu et al., 2010; Mittermeyer et al., 2012) or combined delivery of *AADC*, tyrosine hydroxylase (*TH*) and GTP-cyclohydrolase-1 (Azzouz et al., 2002; Muramatsu et al., 2002; Jarraya et al., 2009). A different gene therapy approach is aimed at restoring the levels of gamma-aminobutyric acid (GABA) in the subthalamic nucleus by delivering glutamic decarboxylase, the rate limiting enzyme for the synthesis of GABA, a strategy that is currently being tested in clinical trials (LeWitt, 2011).

Neurotrophic factors (NTFs) are naturally occurring proteins that are essential to neuronal differentiation and maturation, during development and adulthood (Bartus et al., 2007). It is now well established that *GDNF* can protect dopamine neurons from several insults and restore function in animal models of PD (for review see Evans and Barker, 2008). More recently, another member of the *Gdnf* family, neurturin has also been shown to be neuroprotective in animal models of

PD (Kordower et al., 2006; Gasmi et al., 2007). Both GDNF (Gill et al., 2003; Nutt et al., 2003; Lang et al., 2006) and neurturin (Marks et al., 2008; 2010) have been tested in clinical trials but, so far, the results are unsatisfactory. Furthermore, *Gdnf*, the prototypical NTF for dopaminergic neurons failed to prevent dopamine-neuron degeneration in the rat α-synuclein model of PD (Decressac et al., 2011). This suggests that, although extremely effective in toxin-based models, *Gdnf* - perhaps even all members of the *Gdnf* family - might not be applicable in models more relevant to the pathology of PD and that alternative NTFs are needed.

The newest candidate growth factor for dopamine neurons is conserved dopamine neurotrophic factor (*Cdnf*) (Lindholm et al., 2007). It is a vertebrate specific paralogue of the recently identified human mesencephalic astrocyte-derived-neurotrophic Factor (*Manf*) (Petrova et al., 2003). *Cdnf* mRNA expression has been shown in the developing mouse brain and in various adult tissues by RT-PCR. *Cdnf* mRNA transcripts were detected in the midbrain and striatum both in the embryonic and brain (Lindholm et al., 2007). Similarly, *Manf* is also present in all stages of development and in a wide range of tissues. In the brain, MANF protein is found in neurons throughout the cortex, the cerebellum, hippocampus, and midbrain where it colocalises partially with TH (Lindholm et al., 2008). Interestingly, disruption of the *Manf* gene in *Drosophila melanogaster*, leads to a striking loss of TH^+ neurites - but not dopaminergic cell bodies - and reduced dopamine levels (Palgi et al., 2009).

More importantly, like GDNF and neurturin, CDNF and MANF are neurorestorative when given after intra striatal 6-hydroxydopamine (6-OHDA)

lesion in the rat. CDNF treatment into the striatum before 6-OHDA lesion was able to dose dependently prevent the loss of TH neurons in the SN. In addition, CDNF administered four weeks following 6-OHDA lesion, was able to increase the number of TH^+ neurons in the SN by preventing the death of remaining neurons, when measured twelve weeks post-lesion (Lindholm et al., 2007). In this study, one single dose of the purified CDNF protein was afforded significant neuroprotection. Similarly, one single dose of MANF into the rat striatum was also neuroprotective as well as neurorestorative (Voutilainen et al., 2009).

Human *CDNF* and human *MANF* have 59% sequence homology; both have eight cysteine (Cys) residues with conserved spacing (Lindholm et al., 2007) and both have structures dominated by α-helices. Their N-terminus domain is similar to the saposin-like proteins and might be involved in interaction with phospholipids or cellular membranes while their C-terminal domain could be involved in protein folding by its Cys-X-X-Cys domains (Parkash et al., 2009). Invertebrates have only one member of this family: *DmManf* (Palgi et al., 2009), so it is possible that the two genes present in vertebrates are duplicated genes with somehow redundant functions. However, growing evidence suggests that *Cdnf* and *Manf* have differential and specific characteristics. CDNF is a secreted glycosylated protein (Sun et al., 2011). Like GDNF, CDNF injected into the striatum is retrogradely transported into nigral dopaminergic neurons (Voutilainen et al., 2011). In contrast, MANF is not retrogradely transported towards the SN but to the frontal cortex (Voutilainen et al., 2008). Furthermore, MANF is not N-glycosylated and its secretion is controversial: although, initially isolated from conditioned medium (Petrova et al., 2003), MANF has an endoplasmic reticulum (ER) retention motif and can be co-purified with other ER resident proteins

(Mizobuchi et al., 2007); some of MANF functions require intracellular localisation (Hellman et al., 2011), although its localisation could be modified by ER stress or pathological conditions (Airavaara et al., 2009). Moreover, *Manf* - but not *Cdnf* - is upregulated upon oxidative stress or ER-accumulation of misfolded proteins(Mizobuchi et al., 2007). Remarkably, MANF modulates DA release by increasing GABAergic transmission (Zhou et al., 2006) while no neuromodulative properties have been reported for CDNF.

It is still not clear what mechanisms underlie the neuroprotective properties of *Cdnf* and *Manf*. However, structural analysis suggests that CDNF and MANF could be involved in protein folding in the ER (Parkash et al., 2009). Interestingly, several insults that cause ER stress lead to Manf upregulation: Treatment with tunicamycin (N-glycosylation inhibitor) (Yu et al., 2010), thapsigargin (ER-Ca^{2+}/ATPase inhibitor), or dithiothreitol, a reducing agent (Mizobuchi et al., 2007) result in *Manf* upregulation. Furthermore, MANF could reduce cellular apoptosis following insult by inhibiting BAX (Bcl-2-associated X protein) via its Ku70-like domain (Hellman et al., 2011). This evidence suggests that CDNF and MANF could minimise the oxidative damage in DA neurons following 6-OHDA lesion by reducing protein misfolding and apoptotic cell death. However, a potential effect on nigrostriatal neurogenesis or other possible mechanisms cannot be excluded.

In this chapter, we will test if *Cdnf* are *Manf* are protective in the 6-OHDA rat model of PD as suggested by Voutilainen et al. and Lindholm et al. We will deliver these NTFs using lentiviral-vectors, which are suitable for long-term, stable transduction of neural cells (for review see Lundberg et al., 2008).

5.2 Aims

In this chapter we aim to confirm the ability of *Cdnf* and *Manf* to protect dopaminergic neurons in the 6-OHDA rat model of PD as reported by Voutilainen et al. and Lindholm et al. and to test whether long-term overexpression of these NTFs results in enhanced neuroprotection than has been reported for one single dose of the purified proteins.

In order to do this, we will use lentiviral vectors as these can efficiently be used for long-term delivery of transgenes in the CNS. We will generate three lentiviral vectors that allow the expression of *CDNF*, *MANF* or both. We will compare the efficacy of these vectors against a negative control lentvirus (GFP-only), as a positive control we will use a GDNF expressing lentivirus, as this factor is considered the gold standard in the 6-OHDA model.

We will initially compare to two lentiviral vector pseudotypes (rabies and VSVG) and their ability to transduce the nigro-striatal dopaminergic system. We will select the optimal pseudotype for nigro-striatal deliver

and we will use a GFP-only Third, to test if *Cdnf* and *Manf* act in a synergistic manner and thus combined overexpression of *Cdnf* and *Manf* results in enhanced neuroprotection compared to either of the two factors alone. To compare the efficacy of *Cdnf* and *Manf* against the gold-standard neuroprotective factor in this model, *GDNF* (Kirik et al., 2004).

5.3 Author contribution

All surgical procedures in this chapter were done side by side with Dr Benjamin Houghton at the University of Bristol. The *sffv*-eGFP control virus with an empty *cmv* expression cassette was also designed and cloned by Dr Benjamin Houghton.

5.4 Materials and methods

5.4.1 Generation of lentiviral inserts

5.4.1.1 cDNA clones

cDNA clones for human *CDNF* (*hsCDNF*), human *MANF* (*hsMANF*) and human *GDNF* (*hsGDNF*) were purchased from *Gene Service* (Source BioScience). Bacterial clones were spread in solid Luria-Bertani Medium [LB, Fisher; 15g·l^{-1} granulated agar (Difco); 1mM NaOH] with 100mg·l^{-1}Kanamycin (Sigma) as selection antibiotic as described in (2.1.9). Individual colonies were picked and their plasmid DNA minipreped as detailed in (2.1.10). DNA plasmids containing the cDNA of the human gene of interest were stored as -20ºC later use. Bacterial clones were kept as glycerol stocks for long-term storage (2.1.11).

5.4.1.2 Generation of NTF DNA-inserts

To amplify and purify the cDNA of the gene of interest, cDNA plasmids from 5.4.1.1 were used as templates for high fidelity polymerase chain reactions (hfPCR). To enable directional cloning, forward hfPCR-primers included a XhoI restriction site (*CTCGAG*) at the 5' end whereas reverse primers contained a SpeI restriction site (*ACTAGT*) at the 3' end. To facilitate the initiation of translation on target cells and therefore, the expression levels of the gene of interest, a *kozak* consensus sequence (*GCCACC*) was introduced immediately upstream of the translation start codon (*ATG*). Additional bases were included upstream of the restriction sites to facilitate enzymatic cleavage and optimise the melting

temperature of primers. Desalted DNA oligonucleotides were purchased from Sigma, resuspended to a final concentration of 10μM and kept at -20ºC. hfPCRs were set up as described previously. Table 5-1 details the primer design.

Table 5-1 hfPCR cloning primers

Cloning primers I (5'⟶3')	
hsCDNF forward	*GA CTCGAG (XhoI) GCCACC (kozak) **ATG**TGGTGCGCGAGCCCA*
hsCDNF reverse	*CCCCAAAACAGAGCTC**TGA** ACTAGT (SpeI) GCC*
hsGDNF forward	*GA CTCGAG (XhoI) GCCACC (kozak) **ATG**AAGTTATGGGATGTC*
hsGDNF reverse	*GCTAAAAGGTGTGGATGTATC**TGA** ACTAGT (SpeI) GC*
hsMANF forward	*GAATT CTCGAG (XhoI) GCCACC (kozak) **ATG**TGGGCCACGCAGGGGC*
hsMANF reverse	*GTGCACGGACCGATTTG**TAG** ACTAGT (SpeI) GCGCCGCG*

Forward primers contain 17-22bp complementary to the beginning of the target gene and the consensus kozak sequence with a XhoI restriction site immediately upstream of the starting codon (green). Reverse primers contain 17-22bp complementary to the end of the target gene and a SpeI restriction site immediately after the stop codon (red). For illustrative purposes, the sequence of reverse primers in the table is the reverse-complement of the actual hfPCR primers.

5.4.1.3 Generation of CDNF-t2a-MANF insert

An overlap-extension hfPCR strategy was used to generate a DNA insert containing *hsCDNF* and *hsMANF* separated by a self-cleaving peptide. This strategy involved three hfPCR steps, outlined in Figure 5—1. *First*: (Primers I & II) a XhoI restriction site was introduced upstream of the *hsCDNF* gene. The *hsCDNF* stop codon was replaced by four glycine codons followed by the first 2/3 of the t2a sequence. *Second*: (Primers III & IV) the last 2/3 of the t2a sequence followed by four glycine codons was introduced upstream of the *hsMANF* gene

and a SpeI restriction site immediately after the *hsMANF* stop codon. hfPCR products were run on an agarose gel as described in 2.1.1, gel-extracted and quantified as explained in 2.1.7. *Third*: (Primers I & IV) 10ng of the XhoI-*hsCDNF*-t2a construct and 10ng of the t2a-*hsMANF*-SpeI construct were used as template for a final overlap-extension-hfPCR. Primer sequences are detailed in Table 5-2. hfPCR parameters are explained in Table 5-3. hfPCR I & hfPCR II had standard cycle settings (2.1.15) whereas the final hfPCR had one initial 10min annealing-elongation cycle before the amplification cycles begun to allow the amplification of the initial double-stranded templates.

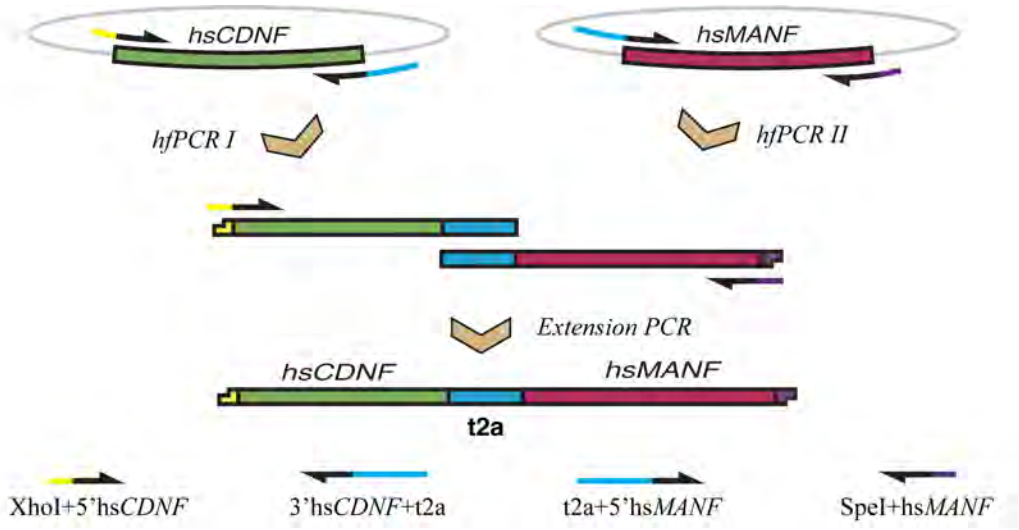

Figure 5—1 Schematic of the CDNF-t2a-MANF overlap-extension hfPCR hfPCR-I: (primers I & II) a XhoI restriction site and the sequence of the t2a self-cleaving peptide are introduced by hfPCR flanking the hsCDNF gene. hfPCR-II: (primers III & IV) a SpeI restriction site and the sequence of the t2a self-cleaving peptide are introduced by hfPCR flanking the hsMANF gene. Extension hfPCR: (primers I & IV) XhoI-hsCDNF-t2a and t2a-hsMANF-SpeI are used as a template for a final hfPCR yielding the full-length DNA construct.

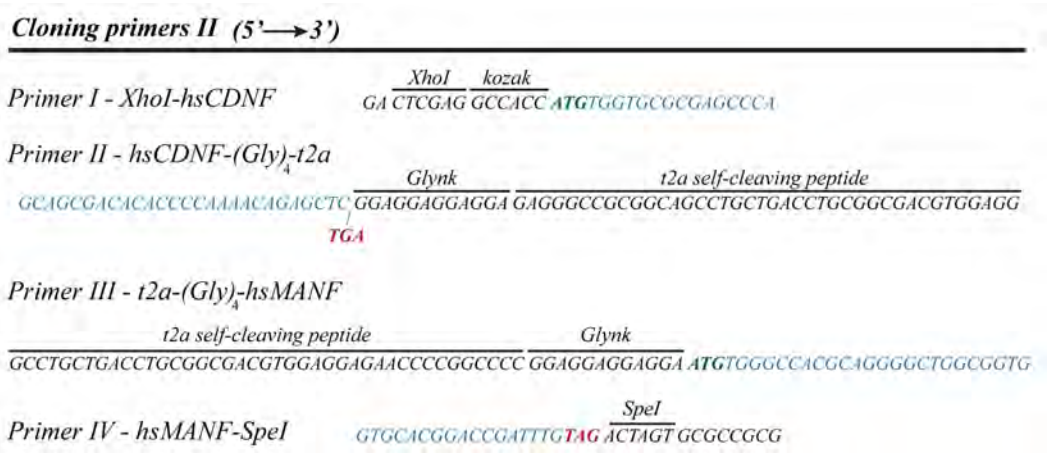

Table 5-2 Overlap-Extension hfPCR primers
Primer I contains 18bp complementary to the beginning of hsCDNF (blue) and the consensus kozak sequence with a XhoI restriction site immediately upstream of the starting codon (green). Primer II contains 27bp complementary to the end of hsCDNF (blue) but the stop codon has been replaced by four glycine codons (Glynk) followed by 42bp of the t2a sequence. Primer III contains the last 40bp of the t2a sequence followed by four glycine codons (Glynk) and 27bp complementary to the beginning of hsMANF (blue). Primer IV contains 20bp complementary to the end of hsMANF followed by a SpeI restriction site immediately after the stop codon (red). For illustrative purposes, the sequence of primers II & IV in the table is the reverse-complement of the actual hfPCR primers.

Overlap-extension hfPCR

	hfPCR1	*hfPCR2*	*Extension PCR*
Template	**hs*CDNF* cDNA**	**hs*MANF* cDNA**	**XhoI-hs*CDNF*-t2a t2a-hs*MANF*-SpeI**
Forward primer	**I**	**III**	**I**
Reverse primer	**II**	**IV**	**IV**
$(CH_3)_2SO$	**0%**	**0%**	**2.5%**

2 min at 95ºC		***2 min at 95ºC***
30s at 95ºC		***30s at ∇48-60ºC***
30s at ∇55-65ºC	***X35***	***10 min at 72ºC****
50s at 72ºC		***30s at 95ºC***
10 min at 72ºC		***30s at ∇48-60ºC***
		50s at 72ºC
		20 min at 72ºC

X35

Table 5-3 Overlap-extension hfPCR, cycle parameters
****additional pre-extension cycle***

5.4.2 Lentiviral Dual-promoter backbone

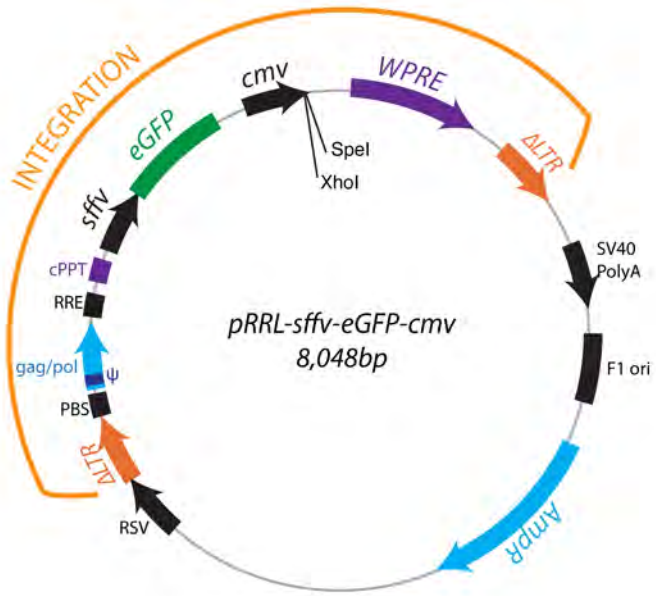

Figure 5—2 Dual promoter, third generation and HIV-derived backbone. AmpR, ampicillin resistance; cPPT, central polypurine tract; cmv, cytomegalovirus promoter; ΔLTR, truncated long terminal repeat; eGFP, enhance green fluorescent protein; PBS, primer binding site; RRE, rev-response element; RSV, Rous sarcoma virus promoter; sffv, spleen focus-forming virus promoter; SV40 polyA, Simian vacuolating virus 40 poly-adenylation signal; WPRE, woodchuck hepatitis virus post-trancriptional regulatory element.

All DNA inserts were cloned into a dual promoter, third generation and human immunodeficiency virus (HIV)-derived lentiviral backbone, which was a kind gift from Dr Liang Fong-Wong at the University of Bristol. The pRRL-sffv-eGFP-cmv backbone contained the eGFP reporter gene downstream of the spleen focus-forming virus (*sffv*) promoter, an empty expression cassette with a multiple cloning site after the cytomegalovirus (*cmv*) promoter, a bacterial replication origin, the ampicillin resistance gene and a minimal viral genome enclosed within the two truncated long-terminal repeat regions (LTRs). Most of the original HIV genome was removed from the construct as viral machinery required for replication and packaging was encoded by the helper plasmid system

(Dull et al., 1998). The viral genome contained the following features: a reduced gag/pol gene including a packaging signal (ψ), a primer binding site (*PBS*) essential for reverse transcription initiation, a Rsv-response element (*RRE*) that allows nuclear translocation of the viral transcript, a central polypurine tract (*cPPT*) to enhance viral transduction and transgene expression (Barry et al., 2001) and a post-trancriptional regulatory element from the woodchuck hepatitis virus (*WPRE*), known to promote transgene transcription (Zufferey et al., 1999). For enhanced biosafety, the HIV promoter was removed from the endogenous 5'LTR. Transcription of the viral genome is instead driven by the Rous-sarcoma virus promoter, upstream of 5'ΔLTR. Additionally the endogenous poly-adenylation signal within HIV-3'LTR was deleted and stability of the viral transcript provided by the simian vacuolating virus 40 polyA downstream of 3'ΔLTR.

5.4.3 Generation of NTF lentiviral constructs

XhoI-*hsCDNF*-SpeI, XhoI-*hsMANF*-SpeI, XhoI-*hsGDNF*-SpeI and XhoI-*hsCDNF*-t2a-*hsMANF*-SpeI inserts generated by hfPCR were run on 1% [w/v] agarose gels as explained in (see 2.1.1); gel-extracted using *QIAquick Gel Extraction Kit* (see 2.1.6), quantified using a *Pearl nanophotometer* (2.1.7); digested with XhoI and SpeI on NEB buffer 4 (see 2.1.2) and purified using the *QIAquick PCR Purification Kit.* The lentiviral backbone was also digested with XhoI and SpeI as above, followed by removal of 5' phosphate groups with Antarctic phosphate to avoid vector re-circularisation (see 2.1.4), run on 1% [w/v] agarose gel and the 8,046bp band was gel-extracted as above.

Gene inserts were ligated into lentiviral backbones downstream of the cmv promoter using the Takara mighty mixture (see 2.1.8) and transformed into *NEB-5-α* supercompetent cells (section 2.1.9). Bacterial clones were grown overnight in solid-LB medium with 100mg·l^{-1} ampicillin (Sigma) as selection antibiotic. The following day, individual colonies were picked and inoculated into 5ml of LB-medium with ampicillin, grown overnight and their plasmid DNA extracted using the *QIAprep kit (2.1.10)*. To verify the correct ligation of the constructs, plasmids were digested with the appropriate restriction enzymes and the length of the restriction fragments determined after agarose electrophoresis.

At this stage, plasmids were sent to Source BioScience (Oxford) and candidate clones confirmed by sequencing downstream of the cmv promoter using a *cmv* forward primer (5'-GAGCTCGTTTAGTGAACCGTC-3'). Sequence-verified constructs were transformed into *One Shot Stbl-3 Chemically competent E. coli* (see *2.1.9*) and grown overnight on solid-LB with ampicillin. The following day, individual colonies were inoculated into 5ml of LB-medium with ampicillin and grown for 16h at 37ºC at 150rpm. In order to confirm the identity of transformed clones, 1ml of these *minipreps* was used for plasmid-DNA extraction as above and check-digested. 1ml of confirmed-cultures was used for long-term storage as glycerol-stocks (section 2.1.11). The remaining *miniprep* was inoculated into 500ml of LB-medium with ampicillin and grown overnight at 37ºC at 200rpm. Large scaled purification of plasmid DNAs was performed as described in 2.1.12.

5.4.3.1 Generation of lentiviral control construct

To generate a lentiviral backbone with an empty expression cassette downstream of the *cmv* promoter, the lentiviral backbone was digested with XhoI and SpeI as in 5.4.3. Fragments were then blunted using the klenow fragment of DNApol I from *E. coli* (see 2.1.5), run on 1% [w/v] agarose gel and the 8,038bp band, gel-extracted as previously. The fragment was then re-ligated with Takara mighty mix (see 2.1.8), transformed into *One Shot Stbl-3 Chemically competent E. coli* (section 2.1.9) and grown overnight on solid-LB. The following day, individual colonies were inoculated into 5ml of LB-medium and grown as above. Cultures were check-digested and aliquoted into glycerol-stocks (see 2.1.11). The remaining culture was used to inoculate 500ml of LB-medium with ampicillin and grown overnight at 37ºC at 200rpm. Large scaled purification of plasmid DNAs was performed as described in 2.1.12.

5.4.4 Production of VSVG-pseudotyped lentiviral vectors

Vesicular stomatitis virus glycoprotein (VSVG)-pseudotyped lentiviral vectors were produced as described in (2.3). Briefly, lentiviral backbones were co-transfected with three lentiviral helper plasmids into HEK293T cells using the $CaPO_4$ method. Cell supernatants were collected after 12 and 48h and concentrated by ultracentrifugation. Lentiviral particles were resuspended in TSSM buffer, aliquoted and stored at -80ºC.

Lentiviral preparations were tittered by fluorescence activated cell sorting (FACS, see 2.3.4). Only viral preparations with titers above $10^8 TU \cdot ml^{-}1$ were deemed suitable for in vivo experiments.

5.4.5 Production of rabies-pseudotyped lentiviral vectors

In order to generate rabies-pseudotyped lentiviruses, the pMD2-env-*VSVG* helper plasmid was replaced by a plasmid codifying for the rabies virus glycoprotein (kind gift from Dr Liang Fong-Wong at the University of Bristol). Production of rabies-pseudotyped lentiviral vectors was optimised by testing several transfection methods and modifying the ratios of the packaging plasmids as detailed below.

Low passage (<40) HEK293T were maintained and passaged as described previously (2.2.1). For co-transfection, $8 \cdot 10^6$cells were plated onto 150cm^2 plates (two plates were prepared for each condition) in 20ml DMEM* without antibiotics. After 24h, each plate was co-transfected with the lentiviral backbone containing the gene of interest, pMDLg-Prpe (gag/pol), Rabies-G (env) and rev. Co-transfection amounts for each 150cm^2 plate are detailed in Table 5-4.

Co-transfection ratios

	$CaPO_4$	*Lipofectamine*	*Fugene*	*PEI*
Genome	**10µg**	**6.5µg**	**10µg**	**10µg**
Gag/pol	**10µg**	**6.5µg**	**3.2µg**	**3.2µg**
Rev	**2µg**	**1.6µg**	**2.5µg**	**2.5µg**
Rabies-G	**2/3.4/5µg**	**0.5/2/5µg**	**0.5/2/5µg**	**1.2/2.3/4.6µg**

Table 5-4 Rabies-pseudotyped lentiviral vector transfection optimisation

5.4.5.1 $CaPO_4$ transfection

The four plasmids were added to a sterile 50ml polypropylene tube. Amounts were adjusted for 2.5X 150cm^2 plates. Three different ratios of rabies-G plasmid were used (5, 8.5 or 12.5µg). The final volume was made up to 2.75ml with

ddH_2O. 350µl of 2M $CaCl_2$ were added to the DNA solution and mixed followed by 2.75ml of HEPES-buffered saline and the solution incubated at room temperature for 30min. 2.5ml of transfections mixtures were added per plate.

5.4.5.2 Fugene transfection

The four plasmids were added to a sterile 50ml polypropylene tube. Amounts were adjusted for 2.5X 150cm^2 plates. Three different ratios of rabies-G plasmid (1.25, 5 or 12.5µg) and two different *Fugene* (Roche) ratios were used (2.5µl or 5µl Fugene per 1µg of DNA). The final volume was made up to 5.5ml with *Optimem medium* (Invitrogen). DNA was added first to *Optimem* followed by the *Fugene* reagent. Transfection mixtures were incubated for 20min at room temperature and 2.5ml of these were added per transfection plate.

5.4.5.3 Lipofectamine 2000 transfection

16.25µg of lentiviral backbone were mixed with 16.25µg of gap/pol, 6.25µg of rev at three different ratios of rabies-G plasmid (1.25, 5 or 12.5µg). 2.5µl·(µg of $DNA)^{-1}$ *Lipofectamine 2000* (Invitrogen) were added to 2.75ml of *Optimem* and incubated at room temperature for 5min. This was combined with 2.75ml of *Optimem* containing the DNA mixture and incubated at room temperature for 20min. 2.5ml of transfection mixtures were added per plate.

5.4.5.4 PEI transfection

25µg of lentiviral backbone were mixed with 7.5µg of gap/pol, 4µg of rev and three different ratios of rabies-G plasmid (3, 5.5 or 11.5µg) were added to 1.6ml

of 0.15M NaCl in a 50ml polypropylene tube. On a separate tube, 1ml of polyethylenimine (PEI) solution (kind gift from Dr Liang Fong-Wong) was mixed with 550µl of 0.15M NaCl. PEI and DNA were combined, incubated at room temperature for 20min and 1.2ml of transfection mixtures were added per plate.

5.4.5.5 Harvesting of unconcentrated rabies-lentiviral preparations

24h after co-transfections, culture medium was replaced with fresh DMEM* containing 10mM sodium butyrate (NaBut). Medium was replaced with 16ml of fresh DMEM* after 6h and the plates returned to the incubator. The following day, culture media were harvested, centrifuged and filtered to discard any cellular debris (see 2.3.3). Unconcentrated preparations were kept at 4ºC for less than one week.

5.4.5.6 Titering of unconcentrated rabies-lentiviral preparations

HEK293T cells were seeded at a density of $7.5x10^4$ cells per well in a 12-well plate in DMEM* and left to grow overnight. The following day, one representative well was used to determine the cell number at the time of transduction. The rest of the wells were transduced with serial dilutions (no virus, neat preparation, 10^{-1}, 10^{-2} and 10^{-3}) of the unconcentrated supernatants from 5.4.5.5. 500µl were added per well and left at 37˚C for 3-4h before the culture medium was topped up to 1ml. After 72h, the percentages of GFP-expressing cells were determined by FACS as described previously (2.3.4).

5.4.6 Transduction of primary rat E18 cortical neurons

Rat primary E18 neuronal cultures were prepared as described in 2.2.2. Five days after plating, culture medium was removed and replaced with 250µl of *cortical neuron feeding medium* containing $3.75 \cdot 10^5$ lentiviral particles (Multiplicity of infection, MOI=5). Cells were kept in reduced medium for 3-4 hours before adding 250µl of fresh *feeding medium*. Five days post-transduction, the cells were fixed and processed for immunohistochemistry.

5.4.7 Transduction of HEK293T cells

HEK293T cells were seeded at a density of 7.5×10^4 cells per well in a 12-well plate in DMEM* and left to grow overnight. The following day, one representative well was used to determine the cell number at the time of transduction. The rest of the wells were transduced at MOI (0.1, 1 or 5) with the appropriate lentiviral vector in 500µl of DMEM* and left 3-4h before wells were topped up with 500µl of fresh DMEM*. After 72h, the culture supernatants were collected, centrifuged at 2,000 RCF for 5min and snap-frozen. Half of the wells were collected in RIPA buffer for western and the other half was fixed with 4% [w/v] *para*-formaldehyde (PFA) and processed for immunocytochemistry.

5.4.8 Immunoblotting

Protein samples from 5.4.6-5.4.7 were separated by SDS-polyacrylamide electrophoresis as previously described (2.4.3). Briefly, 25µg of cell extracts or 40µl of culture medium were mixed with an appropriate volume of *6X loading dye*, run in a 10% [w/v] polyacrylamide gel and transferred onto a PVDF

membrane (see 2.4.4). Membranes were then blocked in 10% [w/v] milk in TBS-0.1%Tw_{20} probed with primary antibodies (anti-MANF, anti-GDNF or anti-CDNF), washed and incubated with an HRP-conjugated antibody. Bound secondaries were detected using the *Supersignal West Pico* chemiluminescent substrate. Autoradiographic films were developed using a Kodak autoprocessor.

ANTIBODY	SPECIES	DILUTION	SUPPLIER
CDNF	Rabbit	1:1000	Prospecbio
GDNF	Mouse	1:1000	Abcam
MANF	Rabbit	1:1000	Sigma
α-tubulin	Mouse	1:2000	Sigma
HRP-conjugated anti rabbit	Goat	1:2000	Jackson Labs
HRP-conjugated anti mouse	Goat	1:2000	Jackson Labs

Table 5-5 Western-blot: list of antibodies, species, dilutions and suppliers.

5.4.9 Animals

Adult Wistar male rats were obtained from Charles-Rivers, all animals were between 280-310g at the time of surgery. A minimum of six animals was used per experimental group. For E18 neuronal cultures, pregnant female Wistar rats at E18 gestation day were obtained from the central animal facility (University of Bristol).

5.4.10 Stereotactic surgery

Stereotactic surgery was performed as described previously (2.5.3). 2µl of concentrated lentiviral-vector preparations were injected unilaterally into the SN or the corpus striatum. Stereotactic coordinates relative to Bregma are detailed in Table 5-6). 6-OHDA (SIGMA) was injected unilaterally in two sites of the cortex striatum (see Table 5-6) on the same day as lentiviral-vectors. 10µg of 6-OHDA

were given per site. Animals were sacrificed at eight weeks post-lesion and their brains harvested for immunohistochemistry.

Stereotactic coordinates (mm)				
		AP	ML	DV
RabiesG-Virus	*Intrastriatal I*	**0**	**-3.5**	**-4.8**
	Intrastriatal II	**+1**	**-3.5**	**-4.8**
VSVG-Virus	*Intranigral*	**-5.3**	**-2.2**	**-7.2**
	Intrastriatal	**-0.6**	**-3.3**	**-5**
6-OHDA	*Intrastriatal I*	**0**	**-2.6**	**-5**
	Intrastriatal II	**-1.2**	**-3.9**	**-5**

Table 5-6 Stereotactic coordinates for intranigral or intrastriatal delivery All coordinates are given in millimetres, relative to Bregma: AP, anteroposterior and ML, mediolateral or dura: DV, dorso-ventral.

5.4.11 Behavioural analysis

Integrity of the nigro-striatal dopaminergic system was assessed at 2, 4, 6 and 8 weeks post-lesion. Animals were injected subcutaneously with 0.25mg·Kg^{-1} *R*-apomorphine hydrochloride or 2.5mg·Kg^{-1} *D*-amphetamine sulphate. Ipsilateral or contralateral rotations to the lesioned hemisphere were recorded for 70-90min as described in 2.5.5.

5.4.12 Immunostaining on cell monolayers

Standard immunocytochemistry was performed as in 2.4.8.1. Briefly, cells were fixed, permeabilised with methanol, blocked in 10% [v/v] normal goat serum, incubated with primary antibodies, washed with PBS and incubated with appropriate secondary antibodies (see Table 5-7). Cell nuclei were counterstained by incubating with 0.2mg·l^{-1} Hoechst. Coverslips were mounted in *Fluorsave* and allowed to dry before imaging.

5.4.13 Fluorescence immunohistochemistry

40μm-brain sections were prepared as described in 2.5.7 and stained as free-floating sections as in 2.4.8.2. Briefly, sections were blocked overnight in PBS-0.1%Tx^{100} containing 10% [v/v] normal goat serum (NGS), 2% [w/v] bovine serum albumin (BSA) and 0.01% [w/v] NaN_3. The following day, sections were incubated with primary antibodies diluted in PBS-0.1%Tx^{100} containing 5% [v/v] NGS, 1% [w/v] BSA and 0.01% [w/v] NaN_3, washed and incubated with the appropriate secondary antibodies (see Table 5-7). Cell nuclei were counterstained by incubating with 0.1mg·l^{-1} Hoechst. Finally sections were mounted onto *Superfrost*$^+$ slides, briefly allowed to dry and mounted in *Fluorsave*. Stained slides were kept at 4ºC in the dark for up to 3 months.

5.4.14 TH-DAB-staining

For 3-3'-diaminobenzidine (DAB) staining, brain sections were quenched, blocked and incubated with primary antibodies as above but were done using TBS instead of PBS. Once bound to the mouse-anti-TH primary antibody, the sections were incubated overnight with a biotinylated goat-anti mouse IgG secondary antibody diluted in TBS-0.1%Tx^{100} containing 5% [v/v] NGS and 1% [w/v] BSA. The following day, sections were treated with HRP-conjugated avidin, washed and incubated with DAB until a suitable staining developed (5-10min). Sections were then washed once in ddH_2O and mounted on *Superfrost*$^+$ slides. These were dehydrated overnight, delipidated by serial washes in xylene (see 2.4.8.4) and mounted with DPX-medium.

ANTIBODY	SPECIES	DILUTION	SUPPLIER
Alexa fluor 488 anti chicken IgG	Goat	1:500	Invitrogen
Alexa fluor 568 anti mouse IgG	Goat	1:500	Invitrogen
Alexa fluor 568 anti rabbit IgG	Goat	1:500	Invitrogen
HRP-conjugated anti rabbit	Goat	1:2000	Jackson Labs
IgG anti CDNF	Rabbit	1:1000	Prospecbio
IgG anti GDNF	Rabbit	1:1000	Abcam
IgG anti MANF	Rabbit	1:1000	Sigma
IgG1 anti TH	Mouse	1:500	Millipore

Table 5-7 List of antibodies used, species raised in, dilutions and suppliers

5.4.15 Image acquisition and statistical analysis

Fluorescence staining was viewed under a Leitz DMRD fluorescent microscope attached to a Leica DFC340FX digital high-sensitivity monochrome camera and visualized using Leica Application suite 3.3.1. DAB-stained sections were viewed under a Leitz DMRD microscope attached to a Leica DC500 42bit-color digital camera and visualized using the Leica IM50 4.0 software. Full-brain panels were obtained by taking low magnification images (10X) across the brain and carefully overlapping them using Adobe Photoshop CS3 software. For neuronal counts, images were taken from at least four sections (20X magnification) from each animal and quantified using ImageJ and the cell counting plugin from Kurt de Vos at the University of Sheffield. For striatal densitometry, DAB-stained sections were scanned using Epson-Scan2480 and the manufacturers software; optical densitometry was quantified using ImageJ as described in 2.4.7. Results were analysed by one-way ANOVA followed by Dunnett post-hoc test or two-way ANOVA followed by Bonferroni post-hoc test when appropriate.

5.5 Results

5.5.1 Validation of lentiviral vectors

5.5.1.1 Generation of inserts

The DNA inserts XhoI-*hsCDNF*-SpeI, XhoI-*hsMANF*-SpeI, XhoI-*hsGDNF*-SpeI were generated by hfPCR as described previously (Figure 5—3a & b). XhoI-*hsCDNF*-T2A-*hsMANF*-SpeI DNA insert was generated using an overlap-extension hfPCR strategy (Figure 5—3c & d). All fragments were ligated into the pRRL-*sffv*-eGFP-*cmv* dual promoter backbone and transformed into recombination deficient *E. coli*. Bacterial clones were screened by treatment with the appropriate restriction endonucleases (Figure 5—3e & f) and their sequence verified. Lentiviral particles containing the desired construct (Figure 5—1) were generated, titered and concentrated as described in section 2.3.

5.5.1.2 Validation of lentiviral vectors on HEK293T cells

To ensure that the lentiviral vectors generated in 5.5.1.1 were able to infect target cells and induce the expression of the gene of interest, concentrated lentiviral preparations were used to transduce HEK293T cells at increasing MOI (0, 0.1, 1, 2 and 5). 72h post-transduction, the culture medium and cell pellets were collected and analysed by immunoblotting or the cells fixed and processed for immunocytochemistry. Figure 5—5a shows that increasing the MOI results on higher expression levels of the gene of interest (GFP). Immunocytochemistry (Figure 5—5b) and immunoblotting (Figure 5—5d) on HEK293T cells, show that these cells have high endogenous MANF expression but that overexpression can

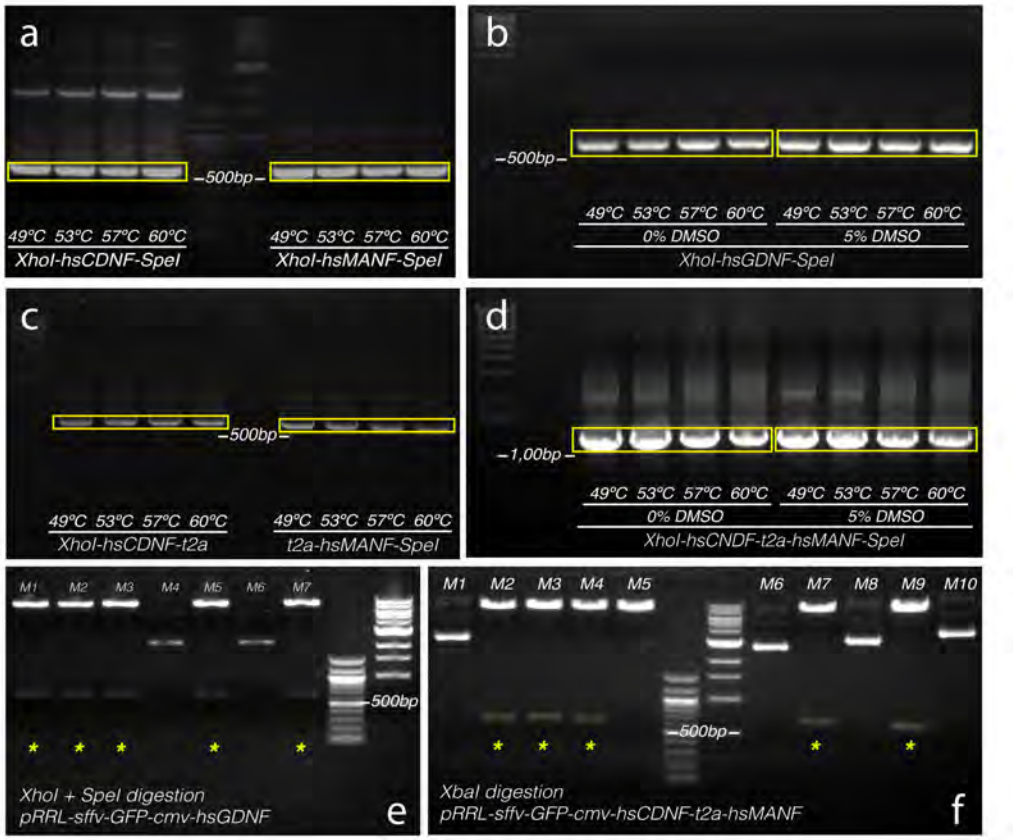

Figure 5—3 Cloning of lentiviral constructs

a) Generation of XhoI-hsCDNF-SpeI and XhoI-hsMANF-SpeI by hfPCR. b) Generation of XhoI-hsGDNF-SpeI by hfPCR. c) Generation of XhoI-hsCDNF-t2a and T2A-hsMANF-SpeI by hfPCR. d) Generation of XhoI-hsCDNF-t2a-hsMANF-SpeI by overlap-extension hfPCR. e) Screening of pRRL-sffv-GFP-cmv-hsGDNF bacterial clones (M1-M7) by double digestion with XhoI and SpeI f) Screening of pRRL-sffv-GFP-cmv-hsCDNF-T2A-hsMANF bacterial clones (M1-M10) by digestion with XbaI. Positive clones are indicated by *.

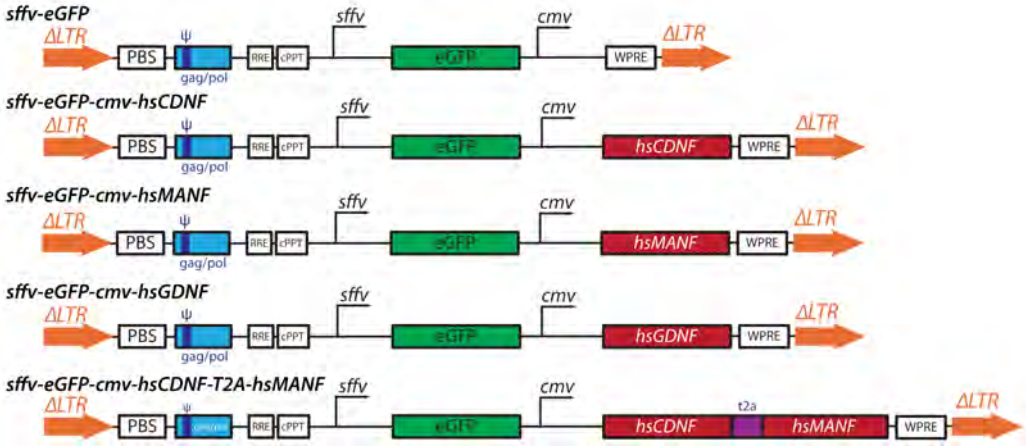

Figure 5—4 Lentiviral vector design

be effectively achieved by using *sffv*-GFP-*cmv*-*hsMANF* at high MOIs. No MANF expression could be detected in the conditioned medium from control or transduced cells, indicating that MANF is not secreted under these experimental conditions. In contrast, Figure 5—5c & d show that no CDNF was detected in control cells but that transduction with *sffv*-GFP-*cmv*-*hsCDNF* resulted in robust intracellular and secreted expression of CDNF.

Figure 5—5f shows that transduction with *sffv*-GFP-*cmv*-*hsCDNF*-t2a-*hsMANF* lentivirus effectively induced the expression of both CDNF (intracellular and secreted) and MANF (intracellular) in HEK293T cells. It should be noticed that CDNF-t2a had a higher molecular weight than native CDNF (+ lane) whereas t2a-MANF and native MANF (+ lane) had identical molecular weights. These sizes correspond to the theoretical fragments illustrated in Figure 5—6. With our design, the *hsCDNF*-t2a-*hsMANF* gene is translated as one single polypeptide chain that is then cleaved into two fragments by the autocatalytic properties of t2a (Szymczak et al., 2004). Both MANF and CDNF contain signal peptides at the amino-terminal region that are removed by endogenous ER signal peptidases. The final CDNF mature protein is 19 aminoacids longer that native CDNF as a small fragment of the t2a peptide remains attached to it. This explains the difference in size observed in (Figure 5—5f). In contrast, after removal of the signal peptide, the final MANF protein is indistinguishable from endogenous MANF. Intermediate forms - with CDNF still attached to MANF - would appear as high molecular weight bands (>50KDa) in (Figure 5—5f). However, no such forms were detected, indicating that the t2a-self cleavage was extremely effective.

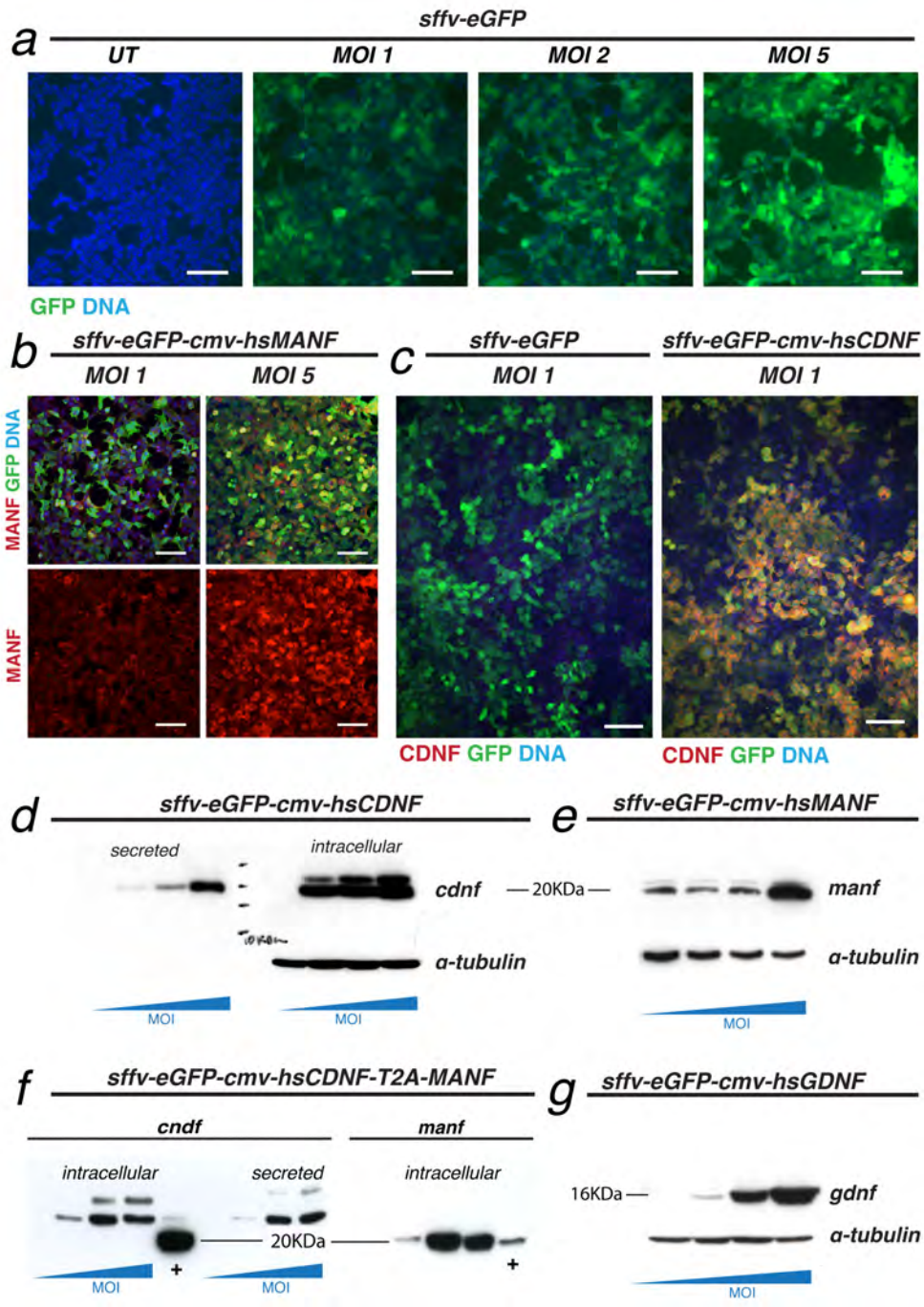

Figure 5—5 Lentiviral vector validation in HEK293T cells.
a) Increased MOI results in increased expression of the gene of interest (GFP). Immunocytochemistry: b) Transduction with sffv-eGFP-cmv-hsMANF MOI5 induces MANF overexpression. c) Transduction with sffv-eGFP-cmv-hsCDNF induces CDNF overexpression. Immunoblotting: d) Increased CDNF expression in culture supernatants and cell pellets with higher sffv-eGFP-cmv-hsCDNF MOI. e) Increased MANF expression in cell pellets with sffv-eGFP-cmv-hsMANF MOI=5. f) Increased intracellular CDNF and MANF as well as secreted CDNF with higher sffv-eGFP-cmv-hsCDNF-t2a-hsMANF MOI (+ = positive control). g) Increased GDNF expression with higher sffv-eGFP-cmv-hsGDNF MOI. Scale bars = 100μm. α-tubulin was used as an endogenous loading control.

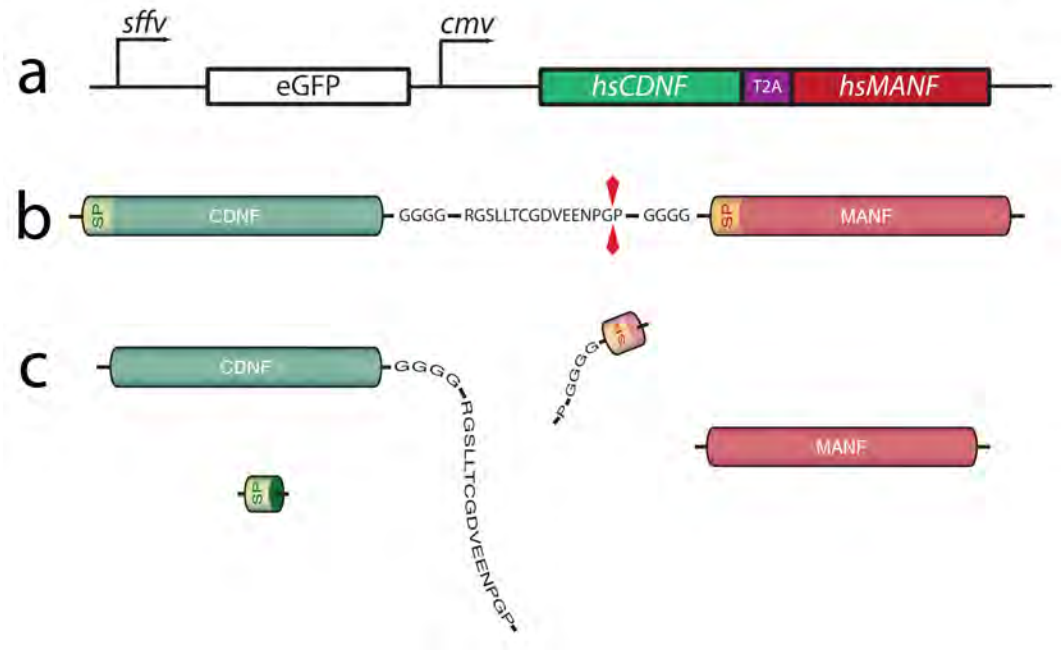

Figure 5—6 Processing of hsCNDF-t2a-hsMANF
a) DNA construct. b) Translation of the hsCDNF-T2A-hsMANF gene as one single polypeptide. c) Removal of signal peptides (SP) and t2a-induced self-cleaving yields four peptidic fragments, including CDNF+19aas and native MANF.

Similarly, transduction with the *sffv*-GFP-*cmv-hsGDNF* lentiviral vector enabled GDNF overexpression in HEK293T cells, as shown by western-blot on Figure 5—5g.

5.5.1.3 Validation of lentiviral vectors in E18 cortical neurons

To ensure that our lentiviral vector could effectively transduce and induce the expression of the gene of interest in neuronal cells, E18 rat cortical neurons were transduced at an MOI=5 with the appropriate vector. Cells were processed for immunocytochemistry five days post-transduction. Figure 5—7 shows that this was indeed the case, confirming that our lentivirus can be used successfully to induce the overexpression of our NTFs on post-mitotic neurons.

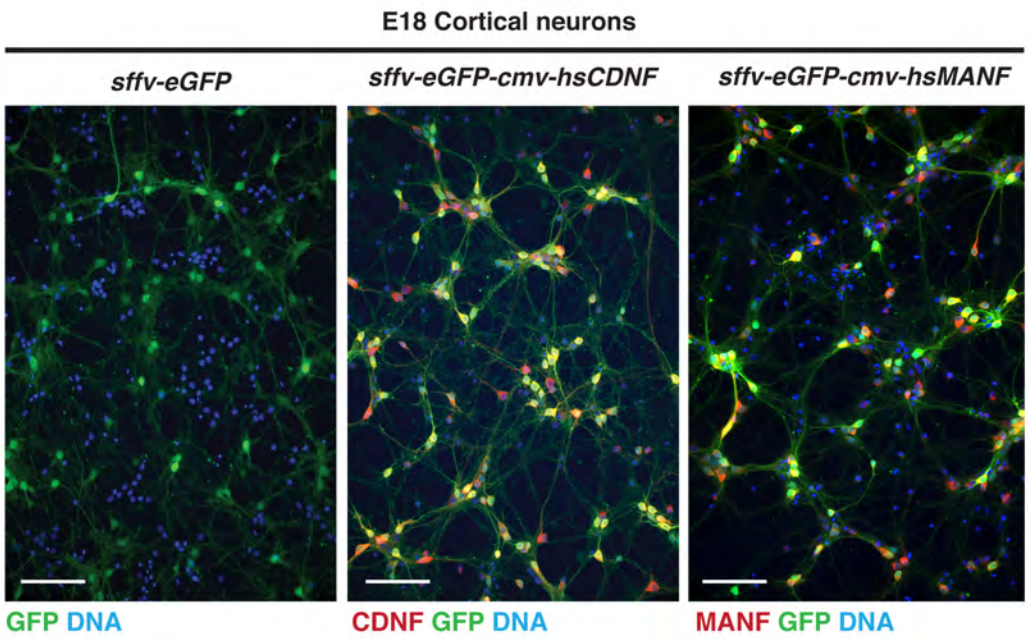

Figure 5—7 Lentiviral vector validation on neuronal cells
Immunocytochemistry on transduced E18 rat cortical neurons (MOI=5). Left: control virus sffv-eGFP. Middle: transduction with sffv-eGFP-cmv-hsCDNF virus stained for CDNF (red), GFP (green) and DNA (blue). Right: transduction with sffv-eGFP-cmv-hsMANF stained MANF (red), GFP (green) and DNA (blue). Scale bars = 50µm

5.5.2 Generation of rabies-pseudotyped lentiviral vectors

5.5.2.1 Rabies-pseudotyped lentiviral vector production

Lentiviral vectors pseudotyped with the envelope glycoprotein from the rabies virus are retrogradely transported from nerve terminals to neuronal cell bodies. If delivered intrastriatally, a rabies-pseudotyped lentivirus transduces local cells and axons but is also transported to the projecting dopaminergic neurons in the substantia nigra (Mazarakis et al., 2001). This approach is very attractive as it can potentially be utilised to deliver a gene of interest to the whole nigro-striatal dopaminergic system from a reduced number of injection sites. For this reason, we decided to test the feasibility of using this type of envelope for the in vivo delivery of our lentiviral-vectors.

In our experience, the standard protocol for the production of VSGV-lentiviral vectors yields relatively low titer preparations (10^6-10^7 TU·ml^{-1}) when directly applied for the production of rabies-pseudotyped lentivirus. These low titers are unsuitable for experiments in vivo. To solve this problem, we decided to improve the transfection efficiency of our standard $CaPO_4$ method, by using different commercially available transfection reagents – as this could, in theory, increase the number of virus-producing cells (those transfected with the four lentiviral-plasmids) and therefore, increase the final lentiviral titer.

Unconcentrated lentiviral preparations were obtained as described in 5.4.5 using different packaging plasmid ratios (Table 5-4) and Fugene (Roche), Lipofectamine (Invitrogen) or PEI as transfection reagents. Unconcentrated preparations were used to transduce HEK293T cells and the number of GFP$^+$ cells - directly proportional to the viral titer - was determined by FACs after 72 hours.

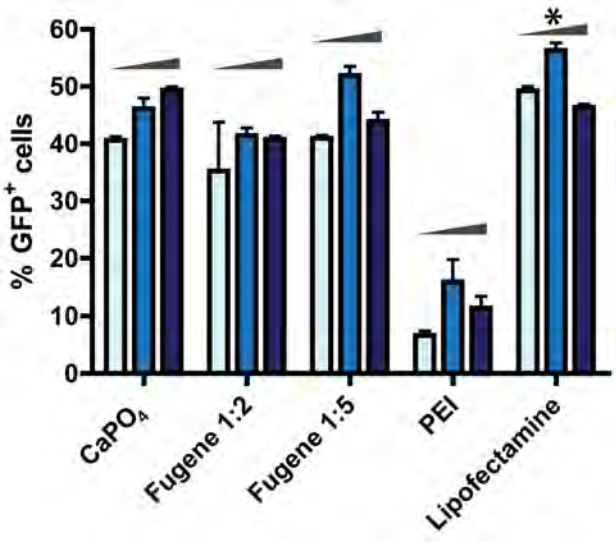

Figure 5—8 Rabies-pseudotyping optimisation
Production of rabies-pseudotyped lentiviruses by 4 different transfection methods with increasing amounts of Rabies-coding plasmid. Graph illustrates the percentages of transduced cells with unconcentrated 1:2 lentiviral-preparations. (Bars represent the mean of 2 independent experiments ± SEM). * selected transfection method.

The highest titer (Figure 5—8 indicated with *) was obtained with the ratio 6.5 PRRL-backbone / 6.5 gap/pol / 1.6 Rev / 2 Rabies-G, in combination with Lipofectamine. This protocol was subsequently used to generate full-scale concentrated rabies-lentiviral preparations. The titers of these preparations were reliably over 10^8 TU·ml^{-1}, which were deemed suitable for in vivo use.

5.5.2.2 Selection of lentiviral vector

To test the ability of intrastriatal rabies-lentivirus delivery to transduce nigral dopaminergic neurons, 2µl of a concentrated sffv-GFP Rabies-lentivirus preparation were injected in two separate sites in the corpus striatum (Table 5-6) of three adult Wistar male rats. In parallel, 2µl of an *sffv*-GFP VSVG-pseudotyped lentivirus were injected in one site directly into the SN of three adult male rats. To allow appropriate expression and retrograde transport, animals were perfused two weeks post injections and their brains processed for immunohistochemistry.

As expected, intrastriatal delivery of rabies-pseudotyped lentiviral vector provided widespread striatal transduction (Figure 5—9a & sagittal section Ia). Furthermore, this vector was indeed retrogradely transported to the SN. However, the efficiency of this process was low and very few dopaminergic neurons were transduced (Figure 5—9 & sagittal section Ib). Furthermore, similar numbers of transduced neurons were also found in other brain areas like the cortex (Figure 5—9c & e) and thalamus (Figure 5—9d). In contrast, direct injection of a VSVG-lentiviral vector results in robust expression in dopaminergic neurons (Figure 5—9f & sagittal section II) with negligible spread to other brain areas.

The poor nigral transduction obtained with our rabies-lentiviral vector and the relatively high numbers of transduced cells in other areas, which could have undesirable side effects when delivering novel neurotrophic factors, precluded the use of this approach in our experimental model.

For these reasons, more traditional VSVG-pseudotyped lentiviral-vectors (Dull et al., 1998) were used in the remaining experiments of this thesis. These vectors were utilised to deliver NTFs into the striatum, as purified CDNF and MANF have been shown to be protective from this area in the 6-OHDA model (Lindholm et al., 2007; Voutilainen et al., 2009). Intranigral neurotrophic delivery was also performed in parallel as direct protection of dopaminergic-neurons using CDNF or MANF has not been attempted before.

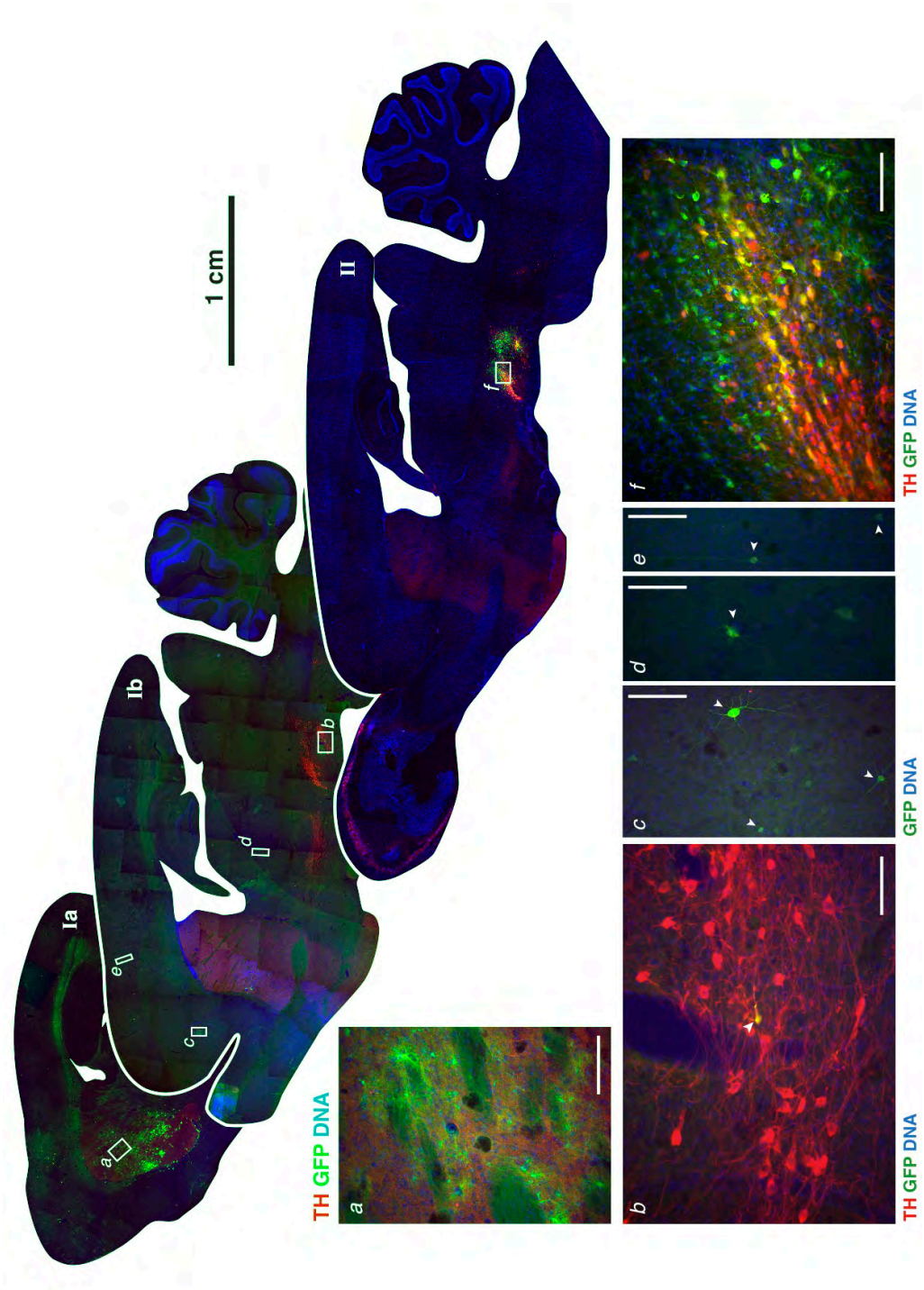

Figure 5—9 Intranigral VSVG-lentivirus vs. intrastriatal rabies-lentivirus *Immunohistochemistry on 40µm-sagittal sections (3 weeks post viral injections): Sections Ia & Ib) Instrastriatal injection of rabies-pseudotyped lentivirus: a) Striatal spread; b) Retrograde transport to the substantia nigra and transduction of TH neurons (given by GFP^+ cells); c) GFP^+ cortical neurons; d) GFP^+ thalamic neurons; e) GFP^+ cortical pyramidal neurons. Section II) Intranigral injection of VSVG-pseudotyped lentivirus: f) Nigral spread and GFP^+ TH neurons. White arrowheads point to transduced (GFP^+) neurons. White scale bars = 50µm*

5.5.3 6-OHDA lesions

The ability of our NTF lentiviral-mediated delivery to protect the nigro-striatal dopaminergic system was tested in the 6-OHDA model of PD. Adult Wistar male rats were lesioned unilaterally by injecting 10µg of 6-OHDA in two sites in the corpus striatum. VSVG-pseudotyped lentiviral vectors were delivered unilaterally in one site in the corpus striatum (stNTF) or one site in the SN (niNTF) on the same day as the 6-OHDA neurotoxin.

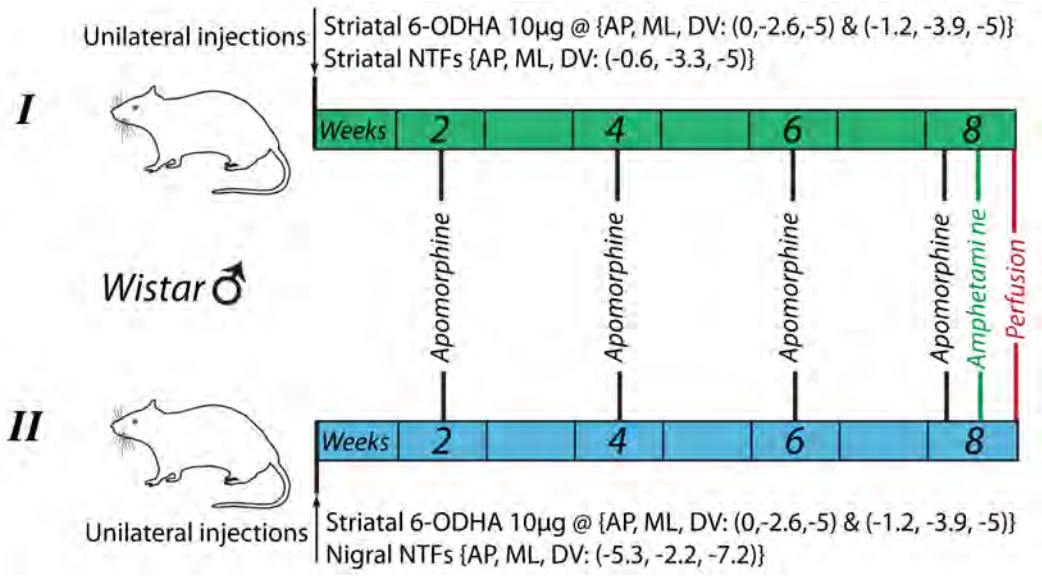

Figure 5—10 Experimental design
Group I: Striatal 6-OHDA lesion and intrastriatal NTF, VSVG-lentivirus mediated delivery. Group II: Striatal 6-OHDA lesion and intranigral NTF VSVG-lentivirus mediated delivery. Animals are sacrificed after 8 weeks and their harvested.

NTF-delivery at the time of lesion allows the NTF-expression at phase I (0-7days) of the 6-OHDA-induced neurodegeneration - a period of axonal loss and atrophy of dopamine neuron cell bodies - and also at phase II (1-4 weeks) when TH-downregulation and rapid dopaminergic cell death occur (Kirik et al., 1998). In addition, this timeframe falls within the therapeutic window reported for CDNF and MANF (Lindholm et al., 2007; Voutilainen et al., 2009).

5.5.3.1 Rotational behaviour

To assess the functional integrity of the nigro-striatal dopaminergic system, animals were injected with the dopamine agonist apomorphine, which induces contralateral rotations to the lesioned hemisphere and amphetamine, which induces ipsilateral rotations (see Figure 5—11). Apomorphine-induced rotations were analysed at 2, 4, 6 & 8 weeks; animals were monitored for 70min and the cumulative turns recorded in 5min intervals. Amphetamine-induced rotations were analysed on week 8; animals were monitored for 90min and the cumulative turns recorded in 5min intervals.

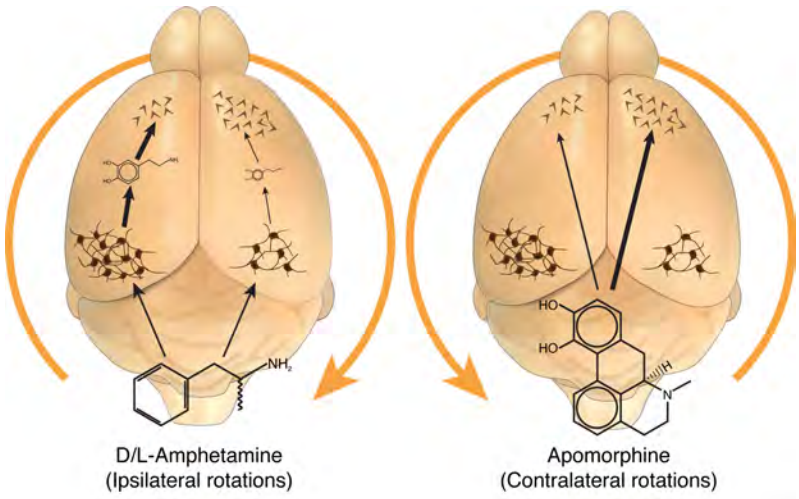

Figure 5—11 Drug-induced rotations in the hemilesioned rat.
Left: Amphetamine induces dopamine release from surviving dopaminergic neurons. DA release is higher in the intact hemisphere and this imbalance results in ipsilateral rotations. Right: lesioned hemisphere is hyper-responsive to dopamine. Apomorphine, a dopamine receptor agonist causes overactivation in the lesioned hemisphere and leads to contralateral rotations. Right hemisphere: lesion side.

5.5.3.2 Intrastriatal lentiviral-vector delivery.

In the striatal-delivery groups, analysis of apomorphine-induced rotations (Figure 5—12b) revealed no major differences across experimental groups and time post-lesion. A general reduction in the number of contralateral rotations was found in striatal-*GDNF* overexpressing animals (*stGDNF*) when compared to the GFP-control group, whereas rotations were increased in the *MANF*-overexpressing group. However, none of these differences reached statistical significance. No differences in the number of amphetamine-induced rotations were found either for *CDNF* (*stCDNF* 529±93.36 turns·90min^{-1}) or *MANF* (*stMANF* 573.83±165.68 turns·90min^{-1}) overexpressing animals when compared to the GFP-control animals. In contrast, lentiviral vector mediated *GDNF*-overexpression in the striatum resulted in a marked decrease in the number of ipsilateral turns compared to controls (*stGDNF* 181.2±66.67 turns·90min^{-1} vs. stGFP 667.83±137.93 turns·90min^{-1}; Dunnett post-hoc test, $p<0.05$; N=6).

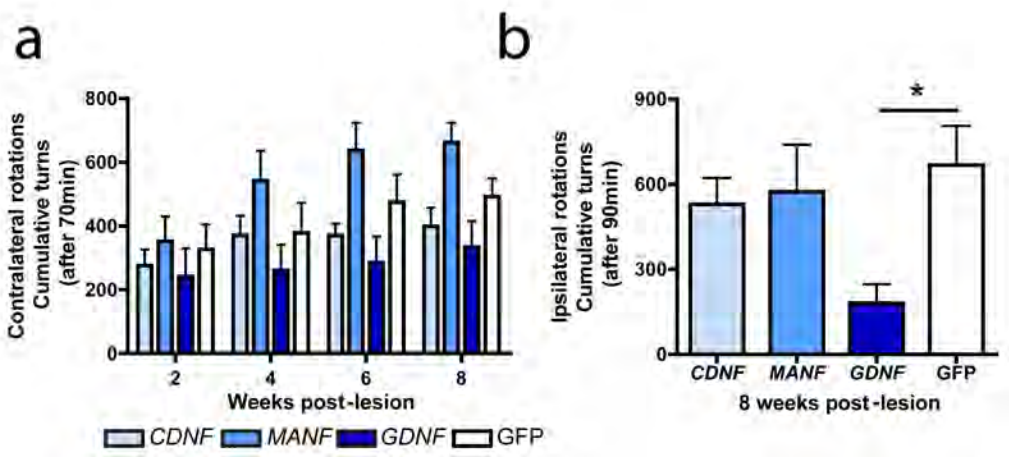

Figure 5—12 Striatal delivery, rotational behaviour
a) Apomorphine-induced rotations at 2, 4, 6 & 8 weeks post-lesion. b) Amphetamine-induced rotations at 8 weeks post-lesion. *p<0.05, Dunnett post-hoc test; N=6 per group.

5.5.3.3 Intranigral lentiviral-vector delivery.

Similarly to the striatal delivery group, analysis of apomorphine-induced rotations (Figure 5—13a) revealed no significant differences across experimental groups and time post-lesion, although *niGDNF* animals generally rotated less and *niMANF* animals more than other groups. In contrast, lentiviral vector-mediated *CDNF* overexpression in the SN, especially in combination with *MANF* resulted in a marked decrease in the number of amphetamine-induced ipsilateral turns compared to controls (*niCDNF* 404.33±35.57 turns·90min^{-1} and *niCDNF*-t2a-*MANF* 110.5±34.8 turns·90min^{-1} vs. niGFP 655.4±78.70 turns·90min^{-1}; Dunnett post-hoc test, $p<0.05$; N=6).

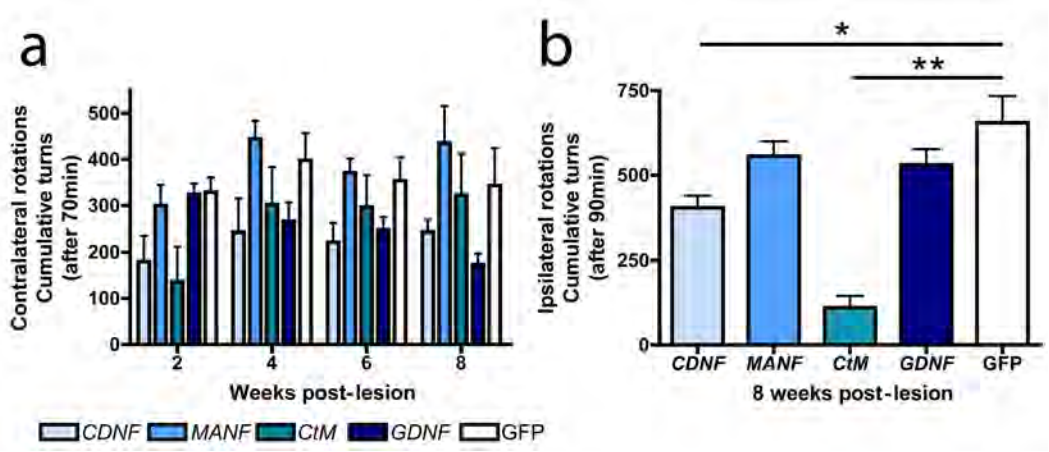

Figure 5—13 Intranigral delivery, rotational behaviour
a) Apomorphine-induced rotations at 2, 4, 6 & 8 weeks post-lesion. b) Amphetamine-induced rotations at 8 weeks post-lesion. * p<0.05,** p<0.01 Dunnett post-hoc test; N=6 per group.

5.5.4 Intrastriatal delivery of *CDNF* or *MANF* does not protect striatal TH-fibres against 6-OHDA toxicity

To determine if lentiviral-mediated overexpression in the striatum could reduce the loss of striatal dopaminergic innervation, coronal sections (Bregma 0.6±0.1mm) were stained for TH-DAB (see 5.4.14) and the optical density of TH-staining in the striatum measured. Densitometric analysis was carried out using ImageJ, slides were scanned using a grey scale mode and saved as a tiff file. Each hemisphere was individually selected and using the tools in the *Analyse/gel* menu. A histogram was generated using the tool *Analyse/gel/plot/lanes*. Areas under the density peak were processed using the tool *Analyse/gel/label peaks* which generated the desired densitometry values; these were then imported onto an Excel file and processed for normalization and statistical analysis. Values were expressed as percentage of the optical density in the contralateral non-lesioned hemisphere.

Figure 5—14a & b show that striatal overexpression of *CDNF* (*stCDNF* 32.84±2.83%) or *MANF* (*stMANF* 29.31±5.76%) did not protect striatal dopaminergic fibres against 6-OHDA toxicity. In contrast, in *GNDF*-overexpressing animals, TH-density was significantly higher than in GFP-control animals (*stGDNF* 47.66±1.45% vs. stGFP 33.16±1.65%; $p<0.05$, Dunnett post-hoc test; N=6), indicating that *stGDNF* but not *stCDNF* or *stMANF* reduced the dopaminergic deafferation in this model.

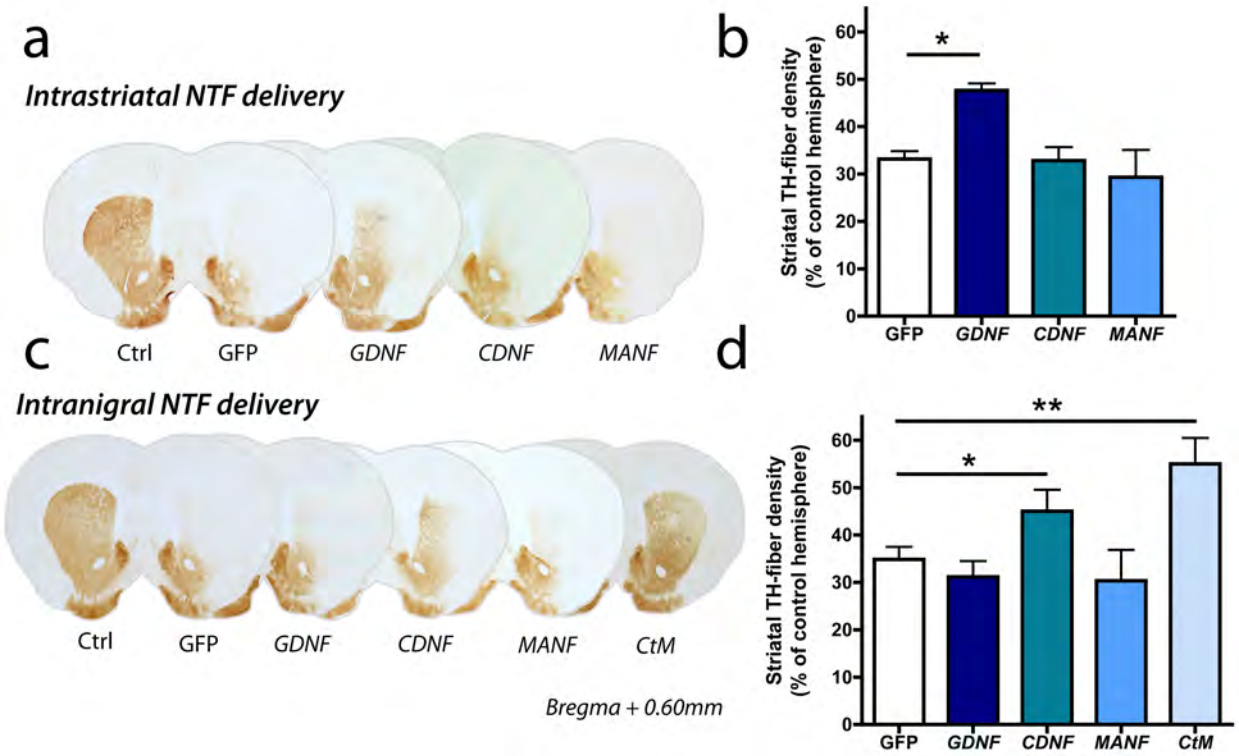

Figure 5—14 Striatal TH-fibre density. TH-DAB immunohistochemistry on coronal sections of the corpus striatum (Bregma +0.6). a) Representative sections of GFP, GDNF, CDNF or MANF delivered into the striatum. b) Quantification of TH-fibre density by optical densitometry. c) Representative sections of GFP, GDNF, CDNF, MANF or CDNF-t2a-MANF delivered into the substantia nigra. d) Quantification of TH-fibre density by optical densitometry. Bars represent the percentage of fibre preservation relative to the control hemisphere. (p*<0.05; **p<0.01 Dunnett post-hoc test, N≥6).

5.5.5 Intranigral delivery of *CDNF* prevents the loss of striatal TH-innervation after 6-OHDA lesion.

Figure 5—14c & d show that intranigral overexpression of *CDNF*, alone or in combination with *MANF*, significantly reduced the loss of TH-innervation to the striatum when compared to GFP overexpressing animals (*niCDNF* 45.05±4.49%; *niCDNF*-t2a-*MANF* 55±5.49% vs. niGFP 34.86±2.64%; $p<0.05$, Dunnett post-hoc test; N=6). In contrast, no differences in the striatal TH-innervation were found in nigral-*GDNF* (*niGDNF* 31.19±3.3%) or nigral-*MANF* (*niMANF* 30.36±6.48%) overexpressing animals, indicating that only *CNDF* was able to reduce the loss striatal dopaminergic afferents when overexpressed from the SN.

5.5.6 Intrastriatal delivery of *CDNF* or *MANF* does not protect TH neurons Against 6-OHDA toxicity.

To test whether the loss of dopaminergic innervation in the striatum was accompanied by the loss of dopaminergic cell bodies in the SN, coronal sections were stained for TH-DAB and the number of surviving dopaminergic neurons (given by TH^+ cells) quantified. Values were expressed as percentage of the TH^+ numbers in the contralateral non-lesioned hemisphere. Figure 5—15 shows that our 6-OHDA lesion results in a dramatic reduction in the number nigral dopaminergic neurons (given by TH^+ cells), with almost 90% neuronal loss in the lesioned hemisphere. This reduction could not be prevented by striatal overexpression of *CDNF* (*stCDNF* 7.78±1.89%) or *MANF* (*stMANF* 8.7±0.6%) but was notably reduced by striatal *GDNF*-overexpression (*stGDNF* 56.52±5.39% vs. stGFP 8.07%±1.15; Dunnett post-hoc test, $p<0.001$; N=6) (Figure 5—15).

5.5.7 Intranigral delivery of *CDNF* or *MANF* does not protect TH neurons against 6-OHDA toxicity.

Similarly to the striatal delivery group, nigral overexpression of *CDNF* (*niCDNF* 20.42±4.87%), *MANF* (*niMANF* 27.17±7.38%) or both (*niCDNF*-t2a-*MANF* 22.21±4.43%) did not prevent the loss of nigral TH^+ neurons in the lesioned hemisphere. In contrast, nigral *GDNF*-overexpression resulted in a robust protection of dopaminergic cell bodies in the SN (*niGDNF* 66.80±4.13% vs. niGFP 18.24±1.83%; Dunnett post-hoc test, $p<0.001$; N=6). This is in agreement with Kirik et al. who have shown that although nigral *GDNF* can prevent the dopaminergic cell loss caused by 6-OHDA, only striatal delivery provides functional improvement and preservation of dopaminergic terminals (Kirik et al., 2000).

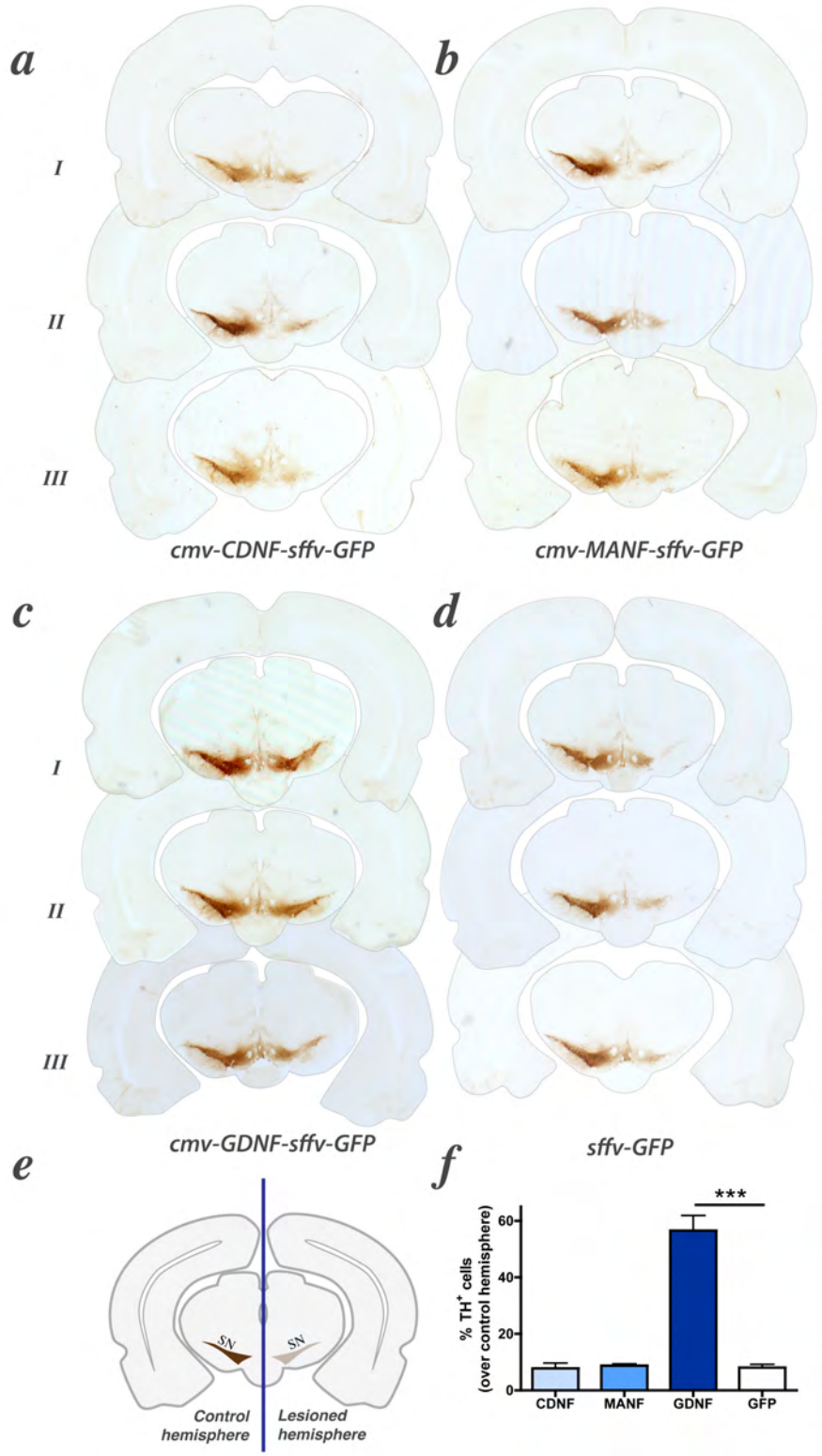

Figure 5—15 Intrastriatal delivery CDNF or MANF fails to protect nigral TH$^+$-neurons against 6-OHDA toxicity.
DAB immunohistochemistry on coronal sections at 8 weeks post-lesion. Instrastriatal lentivirus-mediated delivery GDNF (c) but not CDNF (a) or MANF (b) protects nigral-TH$^+$ neurons against 6-OHDA toxicity compared to control animals (d) (p<0.001; Newman-Keuls post-hoc test, N=6 per group).***

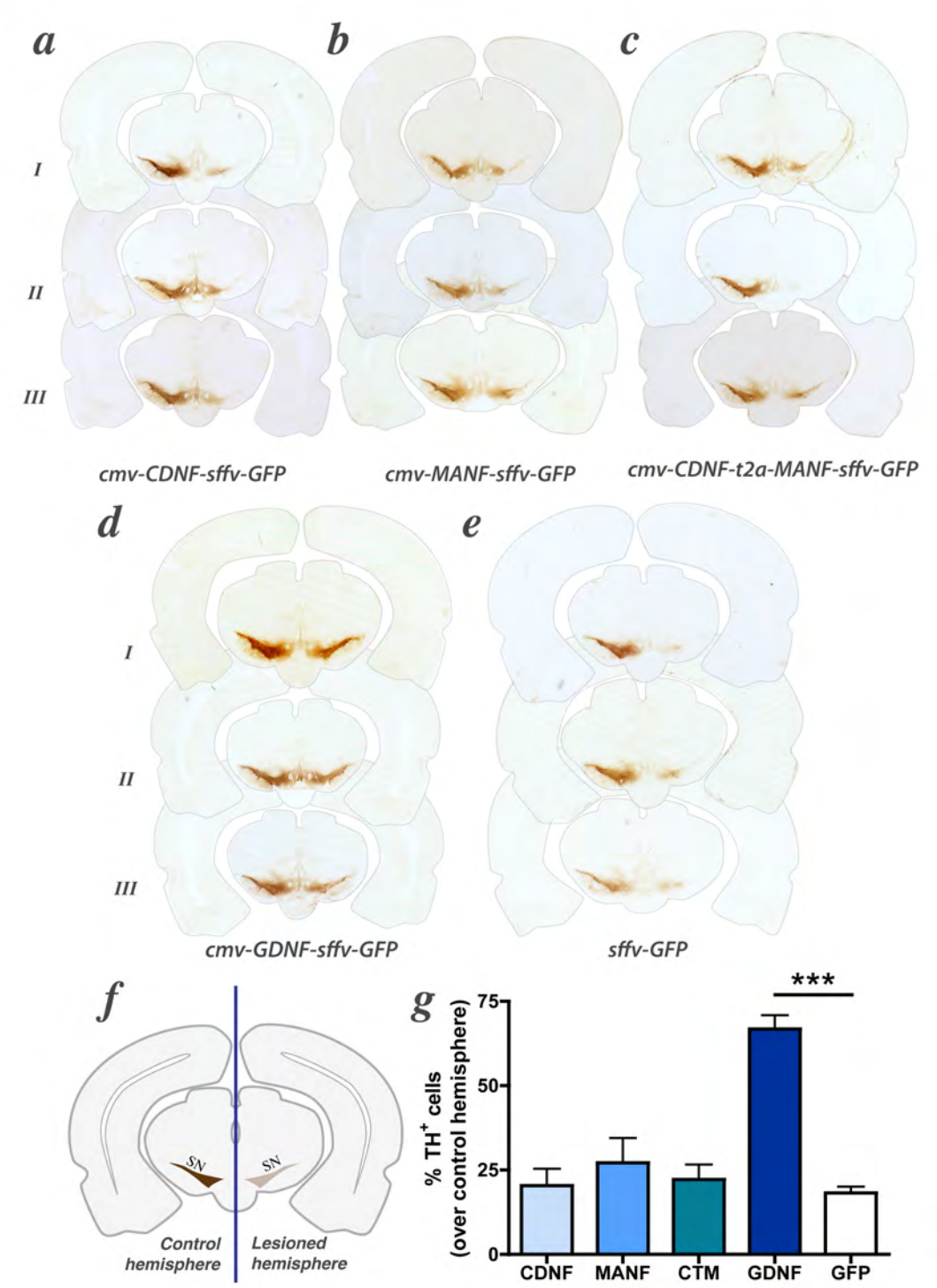

Figure 5—16 Intranigral delivery of CDNF or MANF fails to protect nigral TH$^+$-neurons against 6-OHDA toxicity.
DAB immunohistochemistry on coronal sections at 8 weeks post lesion. Instrastriatal lentivirus-mediated delivery GDNF (d) but not CDNF (a) MANF (b) or both (c) protects nigral-TH$^+$ neurons against 6-OHDA toxicity compared to control animals (e) (p<0.001; Newman-Keuls post-hoc test, N=6).***

5.6 Discussion

Cdnf and *Manf* are members of a novel family of NTFs for dopaminergic neurons (Petrova et al., 2003; Lindholm et al., 2007). Both *Cdnf* and *Manf* are expressed in the developing and adult brain (Lindholm et al., 2007; 2008). Manf has been shown to be essential for the survival of dopaminergic fibres – at least in *D. melanogaster* (Palgi et al., 2009) and to protect embryonic dopaminergic neurons in vitro (Petrova et al., 2003). Interestingly both CDNF and MANF can protect the nigro-striatal dopaminergic system when injected into the striatum six hours prior to the lesion in the 6-OHDA model of PD (Lindholm et al., 2007; Voutilainen et al., 2009). Furthermore, when injected four weeks after lesion, both CDNF and MANF can restore dopaminergic function and partially revert the loss of nigral dopaminergic neurons (Lindholm et al., 2007; Voutilainen et al., 2009). Remarkably, in these studies, neuroprotection was achieved with one single injection (3-10μg) of the purified protein, which led us to hypothesise that a more prolonged treatment with these NTFs could enhance their efficacy. This goal can be achieved by lentiviral-vectors, which have successfully been used for long-term overexpression of target genes in the central nervous system (CNS) with minimal immune reaction (Lundberg et al., 2008). For these reasons, we decided to test the ability of lentiviral-vector delivery of *Cdnf* and *Manf* as neuroprotective factors in the 6-OHDA model.

We designed three third generation lentiviral-vectors that allow the expression of human *CDNF*, human *MANF* or combined expression of both – as one single polypeptide chain separated by a self-cleaving peptide. In our study, we also included a *GDNF*-overexpressing lentivirus – used as a positive control given its

well-established efficacy in this model (for review see Kirik et al., 2004) and a GFP-only lentiviral vector as a negative control. We confirmed the ability of these vectors to induce the expression of the genes of interest in mammalian and neuronal cells. We then pseudotyped our vectors with the rabies virus envelope glycoprotein as this allows the vectors to be retrogradely transported from nerve terminals to cell somas (Mazarakis et al., 2001). This would enable both striatal and nigral overexpression of our NTFs from one delivery site, which would be advantageous in terms of surgery time and difficulty. However, in our hands, very few nigral dopaminergic neurons were transduced after delivery of rabies-pseudotyped lentivirus into the striatum. Furthermore, expression of the transgene was detected in other brain areas, which could complicate the interpretation of our results and could lead to un-wanted side effects. These observations lead us to a more traditional approach by which VSVG-pseudotyped lentiviral vectors are used to transduce cells in the vicinity of dopaminergic nerve terminals in the striatum or to directly transduce dopaminergic neurons in the SN.

To test the ability of our vectors to prevent the dopaminergic cell loss caused by 6-OHDA, we performed a two-site preterminal lesion by injecting 10μg of 6-OHDA in two striatal sites. This leads to around 70% loss in dopaminergic neurons and 40-60% reduction in striatal innervation (Kirik et al., 1998), sparing a significant portion of the nigro-striatal system which could then serve as base for regeneration and functional recovery induced by our NTFs. We chose to deliver our vectors at the same time of the lesion as this falls within the therapeutic window of opportunity for CDNF and MANF [-6hours, 4weeks] (Lindholm et al., 2007; Voutilainen et al., 2009) and simplifies the surgical procedure while also reducing the animal suffering.

We have shown that striatal overexpression of *CDNF* or *MANF* does not result in any behavioural improvement (assessed by apomorphine and amphetamine-induced rotations). Furthermore, striatal *CDNF* or *MANF* overexpression afforded no protection to the dopaminergic innervation in the striatum or to the dopaminergic cell bodies in nigra. In contrast, striatal *GDNF* significantly reduced the number of amphetamine-induced turns and resulted in a marked preservation of dopaminergic neurons and their terminals. This lack of effect of *CDNF* and *MANF* was an unexpected finding and it is in direct contradiction with the results from Lindholm et al. and Voutilainen et al. There are several possible explanations for this discrepancy:

First: we have not found any evidence of MANF secretion (whether endogenous *MANF*, overexpressed *MANF* or overexpressed *CDNF*-t2a-*MANF*); this suggests that MANF is not a secreted protein. Indeed MANF has an ER retention motif, co-purifies with ER resident proteins (Mizobuchi et al., 2007) and has intracellular functions (Hellman et al., 2011). However, Voutilainen et al. injected the purified protein into the striatal parenchyma, indicating that MANF is neuroprotective in the extracellular space. Since our lentiviral-vector does not induce MANF secretion, our results are not directly comparable to those of Voutilainen et al. and it remains possible that MANF is protective when present ectopically in the brain parenchyma.

Second: The 6-OHDA model used by these authors consists in one single 6-OHDA injection (8μg) into the striatum, which leads, to a 30-35% TH-loss. Our model results in a much harsher lesion (75-90% TH-loss). Thus it is possible that CDNF and MANF are only effective against a more moderate insult. Indeed,

when the same lab at the University of Helsinki used a lesion model more similar to ours - 2 sites at similar coordinates, 10μg of 6-OHDA per site and leading also to 75% TH loss - the effects of CDNF and MANF were far less clear (Voutilainen et al., 2011). In this paper, striatal CDNF but not GDNF or MANF reduced amphetamine-induced rotations but only when the cumulative number across all weeks is added and this only for one of CDNF doses used - a rather unorthodox analysis. Surprisingly, CDNF but not GDNF protected dopaminergic neurons against 6-OHDA - again unorthodox. Furthermore, no protective effect of MANF was found in any of the parameters analysed for any of the MANF doses used (Voutilainen et al., 2011). This suggests that CDNF or MANF might not be as robust NTFs as initially reported.

Third: CDNF appears to be retrogradely transported from the striatum to the SN less readily than GDNF (Voutilainen et al., 2011). Furthermore, only high amounts of CDNF (over 3μg) afforded significant protection in the original Lindholm et al. paper. It is possible that the CDNF released by lentiviral overexpression in the striatum does not reach that protective threshold. It is also possible that even less CDNF reaches the dopaminergic cell bodies in the SN. This could account for the discrepancies between lentiviral-overexpression and injections of the purified protein. The case is even stronger for a non-secreted MANF, as it might not be able to interact with TH terminals, let alone with cells several centimetres apart.

This third possibility led us to hypothesise that a direct nigral overexpression of *CDNF* or *MANF* could be more efficacious than striatal delivery. Additionally, to exploit any synergistic effect between these two factors, we also attempted a

combined lentiviral-mediated intranigral delivery of both *CDNF* and *MANF*. However, *MANF* overexpression in the SN did not lead to any improvements in rotational behaviour or protection of the nigro-striatal system. No protection to dopaminergic cell bodies was afforded by nigral *CDNF*-overexpression either.

Interestingly, nigral *CDNF* did result in a remarkable preservation of dopaminergic fibres, even when the numbers of surviving TH neurons were not different from controls. Furthermore, this was accompanied by a significant reduction in the number of amphetamine-induced rotations, indicating that *CDNF* did improve the functionality of the nigro-striatal system after 6-OHDA lesion. This is perhaps, counterintuitive, however it seems that *CDNF* is more efficacious at protecting the striatal afferents than *GDNF* and that more dopaminergic terminals are preserved from the fewer surviving neurons. Alternatively, it is also possible that nigral *CDNF* induces sprouting and reinnervation of the deafferated striatum – again from the fewer surviving neurons.

As a final consideration, we should highlight that no significant differences in the number of apomorphine-induced rotations were found in any of the groups analysed in our study (including *strGDNF*). Of note, Kirik et al. and Georgievska et al. have similarly found that *Gdnf* overexpression has no effect on apomorphine-induced turning despite a marked reduction in amphetamine-induced rotations and robust preservation of dopaminergic neurons and their terminals (Kirik et al., 2000; Georgievska et al., 2002). This is not surprising as apomorphine-induced rotations do not directly reflect the integrity of the nigro-striatal system and might not be an accurate measurement of functional-recovery.

The main aim of this chapter was to confirm that *CDNF* and *MANF* can prevent the loss of dopaminergic neurons in the 6-OHDA model of PD. From this, our main conclusion is clear: they cannot, whether from nigra or from the striatum. Even if a protective effect of these genes exists beyond the statistical power of our experimental numbers, this would be, in any case, far weaker than the effect of *GDNF*. However, the *Gdnf* family and the *Cdnf/Manf* family appear to have different mechanisms of action. Thus *Cdnf* and *Manf* could be protective where *Gdnf* is not (and vice versa) and testing the efficacy of this novel family in other models of PD or neurodegeneration – such as the α-synuclein model (Decressac et al., 2011) - should not be precluded by our results.

Chapter 6

Chapter 6

Final Discussion

> It is a capital mistake to theorise before one has data. Insensibly, one begins to twist facts to suit theories, instead of theories to suit facts...
>
> ***Sherlock Holmes***

6.1 Introduction

In this thesis I have presented three independent results chapters or *tales of neurotrophism*. In these chapters I have sought to identify, characterise and validate novel neurotrophic factors (NTFs), which can promote the differentiation, maturation and survival of neuronal cells. This is part of a broader search for strategies aiming either at the generation of specific neuronal populations in vitro (as a platform for basic research or as a possible source of tissue for cell replacement approaches) or at halting or reversing the neuronal loss characteristic of neurodegenerative diseases.

In the introduction of this thesis I have explained the origin of neural stem cells (NSCs) and attempted to highlight the intricate spatio-temporal patterning mechanisms that transform these cells into the remarkably complex mammalian brain. I have also described how NSCs remain active throughout life and how a continuous stream of new neurons and glia is added to active neural circuits in the adult brain. I concluded my introduction with several examples of important neurotrophic factors (NTFs) that are required for the development and maintenance of such brain. In the first results chapter I have utilised human fetal NSCs (hfNSCs) to establish the role of clusterin as an astrocyte-secreted protein and novel neurotrophic factor for hfNSCs in vitro. In the second results chapter I

have studied the effects of galanin - a pleiotropic neuropeptide with neuroprotective and neuroregenerative properties - on neural differentiation of fetal and adult mouse NSC in vitro and the consequences of galanin disruption on adult neurogenesis in vivo. In the third results chapter, I have tested the ability of lentivirus-mediated delivery of conserved dopamine neurotrophic factor (*Cdnf*) and mesencephalic astrocyte-derived neurotrophic factor (*Manf*) to prevent the dopaminergic cell loss in the 6-hydroxy-dopamine (6-OHDA) rat model of Parkinson's disease (PD).

In this final chapter I will recapitulate my findings and discuss future research possibilities uncovered by these results.

6.2 Clusterin

I have shown that astrocyte conditioned medium (ACM) from the hippocampus (HPC) and midbrain (MB), but not from the cortex (CTX) increases neuronal differentiation, neuronal maturation and neurite length from expanded hfNSCs isolated from the developing mesencephalon. I have used MALDI-TOF analysis to compare the composition of regional ACMs and discovered that clusterin - a highly glycosylated heterodimeric protein - was present at high levels in MB and HPC-ACM but could not be detected in cortical ACM. This led me to hypothesise that clusterin was responsible for the pro-neuronal properties of MB and HPC-ACM. I then demonstrated that clusterin immunodepletion suppressed this pro-neuronal effect and that treatment with purified clusterin fully recapitulated the effects of MB-ACM. I next showed that astrocyte-secreted clusterin did not increase the proliferation of NPCs, but instead promoted their neuronal

differentiation by sustaining extracellular signal-regulated kinase (ERK) activation and decreasing the number of apoptotic nuclei. This indicated that astrocyte-secreted clusterin promoted both cell survival and differentiation of NPCs. I concluded this section by demonstrating that the pro-neuronal effects of clusterin are not limited to midbrain-hfNPCs but that clusterin also enhances neuronal differentiation from cortical hfNPCs. This indicated that the effects of clusterin were not regional specific even when clusterin secretion was. My study was the first to demonstrate the effect of clusterin on NSCs in any species.

Clusterin KO (*Clu*-KO) mice have been available for more than a decade and have been used to study pancreas regeneration (Lee et al., 2011b), myocardial damage (McLaughlin et al., 2000), spermatogenesis (Bailey et al., 2002), glomerulopathy (Rosenberg et al., 2002) and neurodegeneration in models of Alzheimer's Disease (AD) (DeMattos et al., 2004). However no stem cell studies have been conducted with these mice to date. Based on my results, it would be interesting to test if adult neurogenesis is affected in *Clu*-KO mice. Given the high levels of clusterin detected in HPC-ACM in my study but also because hippocampal neurogenesis may be affected in AD, it would be of particular interest to study hippocampal neurogenesis in these mice.

In my study, I have proven the regional-specific properties in astrocytes derived from the rat brain. However, it would be important to confirm that these effects are conserved in human astrocytes. Dr. Federica Rinaldi in the Caldwell lab has recently developed (based on Krencik et al., 2011) two neuralisation protocols that allow the generation of midbrain specific and forebrain specific regional astrocytes from human pluripotent stem cells. It would be interesting to revisit my

experiments with ACM collected from these two astrocytic populations and characterise their effect in neuronal differentiation (confirming also the presence of clusterin). Furthermore, a single nucleotide polymorphism (SNP) in the clusterin gene (rs1113600) has been associated with an increase in the risk of late-onset AD (LOAD) (Harold et al., 2009). However, the effects of this SNP in clusterin function are not known. The recent development of the induced pluripotent stem cell (iPSCs) technology allows the reprogramming of human somatic cells into pluripotent cells and thus the generation of patient specific iPS Using Dr Rinaldi's protocol I would generate and characterise regional astrocytic populations from patients with different genotypes in the rs1113600 SNP in the clusterin gene. I would then used these astrocytes to investigate their neuroprotective effects in different models of neuronal insult, which would clarify if a particular genotype in the rs1113600-SNP is associated with enhanced neuronal vulnerability or susceptibility and therefore an increased risk of LOAD. I have also hypothesised that differences in regional astrocytic properties could account for the stereotypical neuronal loss observed in several neurodegenerative diseases. This idea would be easily tested in iPS derived regional astrocytes. For example, Abramov et al. have shown that amyloid beta (Aβ) causes glutathione depletion and death in astrocytes (Abramov et al., 2003). A sensible experiment would be to determine if this is true for all astrocytes or only for hippocampal or cortical astrocytes, which could explain why these areas are particularly affected in AD.

6.3 Galanin

Galanin is a multitalented neuropeptide ubiquitously expressed in the central nervous system that has neurotrophic, neuroprotective, neuromodulatory and neuroregenerative properties (Hökfelt and Tatemoto, 2008). Prior to my study, only Shen et al. had linked this neuropeptide with stem cell physiology and neurogenic areas in the adult brain (Shen et al., 2005). I have extended these results by demonstrating that galanin and its receptors were expressed in mouse striatal NSCs during development. I have also shown that stimulation with galanin led to activation of the AKT signalling pathway and up-regulation of pro-survival genes in these cells. This resulted in enhanced cell-growth and neuronal differentiation from striatal NSCs. I then confirmed that these effects were not restricted to fetal NSCs but that galanin also increased the number of neuroblasts and neuronal differentiation in NSCs isolated from the adult subventricular zone (SVZ). Furthermore, galanin KO (*Gal*-KO) mice showed a dramatic reduction in the number of proliferating NSCs in SVZ in vivo, accompanied by a reduction in the number of migratory neuroblasts that reach the olfactory bulb. This indicated that adult SVZ-neurogenesis is severely compromised in the absence of galanin signalling.

I have detected the expression of two galanin receptors in these NSCs, *GalR1* and *GalR2*. The next logical experiment would be to determine which one of these receptors mediates the pro-neuronal effects of galanin. This would be easily done by repeating our experiments using the galanin fragment GAL2-29, which has 50-100 fold less affinity for GALR1 than full-length galanin (Florén et al., 2000). If the involvement of GALR2 was confirmed, I would then revisit our

experiments using NSCs isolated from *GalR2*-KO (Elliott-Hunt et al., 2007) mice available in the Wynick's laboratory.

With regards to effect of galanin in adult neurogenesis, several research avenues are now open. At present, it is not known if the reduction in SVZ proliferation is due to depletion of type B quiescent progenitors or to a reduced proliferation of type C rapidly proliferating progenitors. I could answer this question by quantifying the number of $Nestin^+$ proliferating cells (type C) or $GFAP^+$-$Nestin^+$ proliferating cells (type B) in the SVZ (Doetsch et al., 1999) of adult *Gal*-KO mice. If galanin loss led to a reduction in the number of type B quiescent progenitors, then I would expect a further reduction of SVZ neurogenesis with age. Therefore, it would be interesting to study the rate of adult neurogenesis in older *Gal*-KO mice. Also, from our results, I would anticipate an increase in SVZ neurogenesis in galanin-overexpressing mice (*Gal*-OE); this hypothesis could be easily tested, as these mice are also available in the Wynick's laboratory. Finally, one of the most exciting functional implications of my findings is that olfaction could be compromised in *Gal*-KO mice, explaining some of the complex phenotypes in these mice. I am currently exploring this hypothesis by studying olfactory learning in *Gal*-KO mice in collaboration with Dr Peter Brennan at the University of Bristol.

6.4 CDNF and MANF

Conserved dopamine neurotrophic factor (*Cdnf*) and mesencephalic astrocyte-derived neurotrophic factor (*Manf*) (Lindholm et al., 2007) are members of a novel family of NTFs for dopaminergic neurons (Petrova et al., 2003; Lindholm

et al., 2007). In this chapter I sought to validate the ability of these two NTFs to prevent the dopaminergic cell loss in the rat 6-OHDA model of PD (as reported in Lindholm et al., 2007; Voutilainen et al., 2009). In order to do this, I designed, cloned and validated three lentiviral vectors that allow the expression of human *CDNF*, human *MANF* or both *CDNF* and *MANF*. I delivered these lentiviral vectors at the same time of the 6-OHDA neurotoxin, since this was within the window of opportunity suggested by Lindholm et al. and Voutilainen et al. I injected these vectors in the corpus striatum as this is the optimal delivery site for glial derived neurotrophic factor (GDNF) (Kirik et al., 2004) and injection of purified CDNF or MANF had previously been shown to be effective from this location. Surprisingly, striatal overexpression of *CDNF* or *MANF* did not result in any improvement in rotational behaviour. Furthermore, I found no protection to striatal dopaminergic nerve terminals or to dopaminergic cell bodies in the substantia nigra with *CDNF* or *MANF* overexpression. In contrast, lentiviral-mediated overexpression of *GDNF* in the striatum led to a remarkable preservation of dopaminergic neurons and their projections, accompanied by significant reduction amphetamine-induced rotations. This was in agreement with the current literature on *Gdnf* and confirmed the validity of my experimental methodology.

I then hypothesised that the lack of neuroprotection could be due to an insufficient amount of CDNF or MANF reaching the nigral dopaminergic cell bodies. For this reason, I next injected our lentiviral-vectors directly in the substantia nigra. From this location, lentiviral-mediated delivery of *GDNF* was again extremely effective in preventing the dopaminergic cell loss caused by 6-OHDA. However, nigral overexpression of *MANF* failed to protect the nigro-striatal dopaminergic system

and had no effect on apomorphine or amphetamine-induced rotations. Interestingly, nigral-overexpression of *CDNF* did lead to a significant reduction in the numbers of amphetamine-induced rotations and enhanced preservation of dopaminergic fibres. This was not accompanied by protection of the dopaminergic neurons themselves. Taken together, these results indicate that lentiviral-mediated delivery of *MANF* is not protective in this model and that lentiviral-mediated delivery of *CDNF* is only partially effective and only if expressed from the substantia nigra.

Interestingly, overexpression of *Gdnf* in the intact nigro-striatal system leads to a 70% downregulation in the levels of tyrosine hydroxylase (TH), while other dopaminergic markers remain unchanged (Georgievska et al., 2004). If *CDNF* or *MANF* overexpression had a similar effect on TH levels, then my dopaminergic neuronal counts (based on the number of TH^+ cells) could be an underestimation of the surviving dopaminergic neurons, which would in turn underestimate the neuroprotective potential of these two factors. This hypothesis could be tested by repeating our neuronal counts using other dopaminergic markers such as vesicular monoamine transporter 2 (VMAT-2).

Based on these findings and on the unconvincing results of chronic administration of CDNF and MANF (Voutilainen et al., 2011), I consider that the efficacy of these two factors in the rat 6-OHDA model of PD must be taken with caution. At least until other members of the scientific community succeed in validating the results of Lindholm et al. and Voutilainen et al. However, there are several possibilities that cannot be excluded from our results:

In my experimental design, *CDNF* and *MANF* expression is only achieved 24-48 hours post-lesion. At this stage, axonal damage and atrophy have already begun in this model (Kirik et al., 1998). Thus it is possible that earlier delivery of my lentiviruses would have been more efficacious. However, this could not have been anticipated as both Lindholm et al. and Voutilainen et al. claimed that direct injection of CDNF and MANF was effective even when administered four weeks post-lesion.

One of the biggest caveats of this study is that overexpression of *MANF* – unlike injection of purified MANF - does not deliver the protein to the brain parenchyma. Therefore, I cannot rule out a neuroprotective effect of extracellular MANF. If this were the case, then other delivery approaches – such as infusion pumps – could be more appropriate.

From a strictly academic point of view, I wish to highlight that although *GDNF* was the most effective NTF in protecting dopaminergic cell bodies in this study, nigral *CDNF*-t2a was the most effective NTF in protecting dopaminergic nerve terminals. Thus it would be interesting to test the efficacy of combined nigral delivery of *CDNF*-t2a-*GDNF* in this model. It is also theoretically possible to engineer the *MANF* gene so that it becomes a secreted protein, enabling its lentiviral delivery, but this is beyond the scope of this discussion.

I must emphasise that efficacy in the 6-OHDA model does not guarantee efficacy in other models of PD or even in the treatment of PD itself – as demonstrated by GDNF. Therefore, these results should not preclude the evaluation of *Cdnf* and *Manf* in other models of neurodegeneration.

6.5 Concluding remarks

I do not wish to conclude this thesis on a negative note for NTFs. After all, I have only demonstrated the inability of two NTFs (*Cdnf* and *Manf*) to prevent neuronal loss in one particular model of PD but I have also established a role for two novel NTFs (galanin and clusterin).

The ultimate goal for NTF research is to halt or reverse neurodegeneration not only in PD, but also in AD and other neurodegenerative diseases. Even if NTFs fail to achieve this goal, even if trying to prevent neurodegeneration turned out to be a vain attempt to prevent ageing, our research would not be meaningless. All the knowledge acquired along the way would make our journey worthwhile.

Bibliography

Bibliography

Aaku-Saraste E, Hellwig A, Huttner WB (1996) Loss of Occludin and Functional Tight Junctions, but Not ZO-1, during Neural Tube Closure—Remodeling of the Neuroepithelium Prior to Neurogenesis. Developmental Biology 180:664-679.

Abbosh C, Lawkowski A, Zaben M, Gray W (2011) GalR2/3 mediates proliferative and trophic effects of galanin on postnatal hippocampal precursors. J Neurochem 117:425–436.

Abbott NJ (2002) Astrocyte–endothelial interactions and blood–brain barrier permeability. Journal of Anatomy 200:629.

Abramov A, Canevari L, Duchen R (2003) Changes in Intracellular Calcium and Glutathione in Astrocytes as the Primary Mechanism of Amyloid Neurotoxicity. The Journal of Neuroscience 23:5088–5095.

Acampora D, Avantaggiato V, Tuorto F, Simeone A (1997) Genetic control of brain morphogenesis through Otx gene dosage requirement. Development 124:3639–3650.

Adams AC, Clapham JC, Wynick D, Speakman JR (2008) Feeding behaviour in galanin knockout mice supports a role of galanin in fat intake and preference. J Neuroendocrinol 20:199–206.

Airaksinen MS, Saarma M (2002) The GDNF family: signalling, biological functions and therapeutic value. Nat Rev Neurosci 383-394.

Airavaara M, Shen H, Kuo C-C, Peränen J, Saarma M, Hoffer BJ, Wang Y (2009) Mesencephalic astrocyte-derived neurotrophic factor reduces ischemic brain injury and promotes behavioral recovery in rats. J Comp Neurol 515:116-124.

Akabayashi A, Koenig JI, Watanabe Y, Alexander JT, Leibowitz SF (1994) Galanin-containing neurons in the paraventricular nucleus: a neurochemical marker for fat ingestion and body weight gain. PNAS 91:10375–10379.

Alexander T, Nolte C, Krumlauf R (2009) Hox genes and segmentation of the hindbrain and axial skeleton. Annual Reviews Cell and Developmental Biology 25:431–456.

Allen BL, Tenzen T, McMahon AP (2007) The Hedgehog-binding proteins Gas1 and Cdo cooperate to positively regulate Shh signaling during mouse development. Genes & Development 21:1244–1257.

Altaba ARI, Dahmane N, Lee J, Robins P, Heller P (1997) Gli Proteins in Developmental and Disease. Annual Review Cell Developmental Biology 389:876–881.

Altar CA, Cai N, Bliven T, Juhasz M, Conner JM (1997) Anterograde transport of brain-derived neurotrophic factor and its role in the brain. Nature 389:856-860.

Altman J, Das GD (1965) Autoradiographic and histological evidence of postnatal hippocampal neurogenesis in rats. J Comp Neurol 124:319–335.

Angot E, Steiner J, Hansen C, Li J-Y, Brundin P (2010) Are synucleinopathies prion-like disorders? The Lancet 9:1128–1138.

Anisimov SV, Tarasov KV, Tweedie D, Stern MD, Wobus AM, Boheler KR (2002) SAGE identification of gene transcripts with profiles unique to pluripotent mouse R1 embryonic stem cells. Genomics 79:169–176.

Appel E, Kolman O, Kazimirsky G, Blumberg PM, Brodie C (1997) Regulation of GDNF expression in cultured astrocytes by inflammatory stimuly. 8:3309–3312.

Araque A, Parpura V, Sanzgiri RP, Haydon PG (1999) Tripartite synapses: glia, the unacknowledged partner. Trends in Neurosciences 22:208–215.

Arispe N, Rojas E, Pollard HB (1993) Alzheimer disease amyloid beta protein forms calcium channels in bilayer membranes: blockade by tromethamine and aluminum. PNAS 90:567–571.

Assémat E, Châtelet F, Chandellier J, Commo F, Cases O, Verroust P, Kozyraki R (2005) Overlapping expression patterns of the multiligand endocytic receptors cubilin and megalin in the CNS, sensory organs and developing epithelia of the rodent embryo. Gene Expression Patterns 6:69–78.

Azzouz M, Martin-Rendon E, Barber RD, Mitrophanous KA, Carter EE, Rohll JB, Kingsman SM, Kingsman AJ, Mazarakis ND (2002) Multicistronic Lentiviral Vector-Mediated Striatal Gene Transfer of Aromatic l-Amino Acid Decarboxylase, Tyrosine Hydroxylase, and GTP Cyclohydrolase I Induces Sustained Transgene Expression, Dopamine Production, and Functional Improvement in a Rat Model of Parkinson's Disease. The Journal of Neuroscience 22:10302–10312.

Bacon A, Kerr NCH, Holmes FE, Gaston K, Wynick D (2007) Characterization of an enhancer region of the galanin gene that directs expression to the dorsal root ganglion and confers responsiveness to axotomy. J Neurosci 27:6573–6580.

Badie-Mahdavi H, Lu X, Behrens MM, Bartfai T (2005) Role of galanin receptor 1 and galanin receptor 2 activation in synaptic plasticity associated with 3′,5′-cyclic AMP response element-binding protein phosphorylation in the dentate gyrus: Studies with a galanin receptor 2 agonist and galanin receptor 1 knockout mice. Neuroscience 133:591–604.

Bailey RW, Aronow BJ, Harmony JAK, Griswold MD (2002) Heat Shock-Initiated Apoptosis Is Accelerated and Removal of Damaged Cells Is Delayed in the Testis of Clusterin/ApoJ Knock-Out Mice. Biology of Reproduction 66:1042–1053.

Baloh RH, Tansey MG, Lampe PA, Fahrner TJ, Enomoto H, Simburger KS, Leitner ML, Araki T, Johnson EM Jr, Milbrandt J (1998) Artemin, a Novel Member of the GDNF Ligand Family, Supports Peripheral and Central Neurons and Signals through the GFRα3–RET Receptor Complex. Neuron 21:1291–1302.

Bankiewicz KS, Forsayeth J, Eberling JL, Sanchez-Pernaute R, Pivirotto P, Bringas J, Herscovitch P, Carson RE, Eckelman W, Reutter B, Cunningham J (2006) Long-term clinical improvement in MPTP-lesioned primates after gene therapy with AAV-hAADC. Mol Ther 14:564–570.

Barde Y-A, David E, Thoenen H (1982) Purification of a new neurotrophic factor from mammalian brain. EMBO J 1:549.

Barres BA (2008) The mystery and magic of glia: a perspective on their roles in health and disease. Neuron 60:430–440.

Barry SC, Harder B, Brzezinski M, Flint LY, Seppen J, Osborne WRA (2001) Lentivirus Vectors Encoding Both Central Polypurine Tract and Posttranscriptional Regulatory Element Provide Enhanced Transduction and Transgene Expression. Human Gene Therapy 12:1103–1108.

Bell RD, Sagare AP, Friedman AE, Bedi GS, Holtzman DM, Deane RR, Zlokovic BV (2007) Transport pathways for clearance of human Alzheimer's amyloid β-peptide and apolipoproteins E and J in the mouse central nervous system. J Cereb Blood Flow Metab 27:909–918.

Bell RD, Winkler EA, Singh I, Sagare AP, Deane RR, Wu Z, Holtzman DM, Betsholtz C, Armulik A, Sallstrom J, Berk BC, Zlokovic BV (2012) Apolipoprotein E controls cerebrovascular integrity via cyclophilin A. Nature 485:512–516.

Bergami M, Rimondini R, Santi S, Blum R, Götz M, Canossa M (2008) Deletion of TrkB in adult progenitors alters newborn neuron integration into hippocampal circuits and increases anxiety-like behavior. PNAS 105:15570–15575.

Bertrand P, Rozovsky I, Oda T, Finch CE, Pasinetti GM (1995) Association of apolipoprotein E genotype with brain levels of apolipoprotein E and apolipoprotein J (clusterin) in Alzheimer disease. Molecular brain Research 33:174–178.

Björklund A, Kirik D, Rosenblad C, Georgievska B, Lundberg C, Mandel RJ (2000) Towards a neuroprotective gene therapy for Parkinson's disease: use of adenovirus, AAV and lentivirus vectors for gene transfer of GDNF to the nigrostriatal system in the rat Parkinson model. Brain Research 886:82–98.

Blurton-Jones M, Kitazawa M, Martinez-Coria H, Castello NA, Müller F-J, Loring JF, Yamasaki TR, Poon WW, Green KN, LaFerla FM (2009) Neural stem cells improve cognition via BDNF in a transgenic model of Alzheimer disease. PNAS 106:13594–13599.

Boekhoorn K, Joels M, Lucassen PJ (2006) Increased proliferation reflects glial and vascular-associated changes, but not neurogenesis in the presenile Alzheimer hippocampus. Neurobiol of Disease 24:1–14.

Bowenkamp KE, Hoffman AF, Gerhardt GA, Henry MA, Biddle PT, Hoffer BJ, Granholm A-CE (1995) Glial cell line-derived neurotrophic factor supports survival of injured midbrain dopaminergic neurons. J Comp Neurol 355:479–489.

Braak H, Bohl JR, Müller CM, Rüb U, de Vos RAI, Del Tredici K (2006) Stanley Fahn Lecture 2005: The staging procedure for the inclusion body pathology

associated with sporadic Parkinson's disease reconsidered. Mov Disord 21:2042–2051.

Branchek TA, Smith KE, Gerald C, Walker MW (2000) Galanin receptor subtypes. Trends in Pharmacological Sciences 21:109–117.

Bröer S, Brookes N (2001) Transfer of glutamine between astrocytes and neurons. J Neurochem 77:705–719.

Brundin P, Li J-Y, Holton JL, Lindvall O, Revesz T (2008) Research in motion: the enigma of Parkinson's disease pathology spread. Nat Rev Neurosci 9:741–745.

Bu G (2009) Apolipoprotein E and its receptors in Alzheimer's disease: pathways, pathogenesis and therapy. Nat Rev Neurosci 10:333–344.

Burazin TCD, Gundlach A (2002) Inducible Galanin and GalR2 Receptor System in Motor Neuron Injury and Regeneration. J Neurochem 71:879–882.

Burbach JPH (2010) Neuropeptides from concept to online database www.neuropeptides.nl. Eur J Pharmacol 626:27–48.

Burgevin MC, Loquet I, Quarteronet D, Habert-Ortoli E (1995) Cloning, pharmacological characterization and anatomical distribution of a rat cDNA encoding for a galanin receptor. Journal of Molecular Neuroscience 6:33-41.

Burkey BF, Harshini V, Harmony JAK (1991) Intracellular processing of apolipoprotein J precursor to the mature heterodimer. Journal of lipid research 32:1039–1048.

Burkey BF, Stuart WD, Harmony JAK (1992) Hepatic apolipoprotein J is secreted as a lipoprotein. Journal of lipid research 33:1517–1526.

Cai A, Hayes D, Patel N, Hyde JF (1999) Targeted Overexpression of Galanin in Lactotrophs of Transgenic Mice Induces Hyperprolactinemia and Pituitary Hyperplasia. Endocrinology 140:4955–4964.

Caldwell MA, He X, Wilkie N, Pollack S, Marshall G, Wafford KA, Svendsen CN (2001) Growth factors regulate the survival and fate of cells derived from human neurospheres. Nat Biotechnol 19:475–479.

Cameron HA, McKay RD (2001) Adult neurogenesis produces a large pool of new granule cells in the dentate gyrus. J Comp Neurol 435:406–417.

Cameron HA, McKay RDG (1999) Restoring production of hippocampal neurons in old age. Nat Neurosci 2:894–897.

Carden MJ, Trojanowski JQ, Schlaepfer WW, Lee VM (1987) Two-stage expression of neurofilament polypeptides during rat neurogenesis with early establishment of adult phosphorylation patterns. The Journal of Neuroscience 7:3489–3504.

Carmeliet P, De Strooper B (2012) Alzheimer's disease: A breach in the blood–brain barrier. Nature 485:451–452.

Carro E, Spuch C, Trejo JL, Antequera D, Torres-Aleman I (2005) Choroid Plexus Megalin Is Involved in Neuroprotection by Serum Insulin-Like Growth Factor I. The Journal of Neuroscience 25:10884–10893.

Carro E, Trejo JL, Gomez-Isla T, LeRoith D, Torres-Aleman I (2002) Serum insulin-like growth factor I regulates brain amyloid-β levels. Nat Med 8:1390–1397.

Carson JA, Turner AJ (2002) β-Amyloid catabolism: roles for neprilysin (NEP) and other metallopeptidases? J Neurochem 81:1–8.

Cepko CL, Austin CP, Yang X, Alexiades M, Ezzeddine D (1996) Cell fate determination in the vertebrate retina. PNAS 93:589–595.

Cervellera M, Raschella G, Santilli G, Tanno B, Ventura A, Mancini C, Sevignani C, Calabretta B, Sala A (2000) Direct Transactivation of the Anti-apoptotic Gene Apolipoprotein J (Clusterin) by B-MYB. J Biol Chem 275:21055-21060.

Chanas-Sacre G, Rogister B, Moonen G, Leprince P (2000) Radial glia phenotype: Origin, regulation, and transdifferentiation. J Neurosci Res 61:357–363.

Chang M-Y, Sun W, Ochiai W, Nakashima K, Kim S-Y, Park C-H, Kang JS, Shim J-W, Jo A-Y, Kang C-S, Lee Y-S, Kim J-S, Lee S-H (2007) Bcl-XL/Bax proteins direct the fate of embryonic cortical precursor cells. Molecular and Cellular Biology 27:4293–4305.

Chao MV (2003) Neurotrophins and their receptors: A convergence point for many signalling pathways. Nat Rev Neurosci 4:299–309.

Charnay Y, Imhof A, Vallet P, Hakkoum D, Lathuiliere A, Poku N, Aronow BJ, Kovari E, Bouras C, Giannakopoulos P (2008) Clusterin expression during fetal and postnatal CNS development in mouse. Neuroscience 155:714–724.

Chen X, Halberg RB, Ehrhardt WM, Torrealba J, Dove WF (2003) Clusterin as a biomarker in murine and human intestinal neoplasia. PNAS 100:9530–9535.

Chen X, Tolkovsky AM, Herbert J (2011) Cell Origin and Culture History Determine Successful Integration of Neural Precursor Transplants into the Dentate Gyrus of the Adult Rat Baccei M, ed. PLoS ONE 6:e17072.

Chen Y, Swanson RA (2003) Astrocytes and Brain Injury. Nature 23:137–149.

Cheng C, Cherng S, Wu W, Yang T, Huan X-Y, Liao F-T, Wu M-F, She G-T (2012) Regulation of chemosensitivity and migration by clusterin in non-small cell lung cancer cells. Cancer Chemotherapy Pharmacology 69:145-154.

Choi BH (1981) Radial glia of developing human fetal spinal cord: Golgi, immunohistochemical and electron microscopic study. Developmental Brain Research 1:249–267.

Ciccolini F, Svendsen CN (1998) Fibroblast Growth Factor 2 (FGF-2) Promotes Acquisition of Epidermal Growth Factor (EGF) Responsiveness in Mouse Striatal Precursor Cells: Identification of Neural Precursors Responding to both EGF and FGF-2. The Journal of Neuroscience 18:7869–7880.

Cohen S, Levi-Montalcini R (1956) A Nerve Growth-stimulating factor isolated from snake venom. PNAS 42:571–574.

Collier TJ, Kanaan NM, Kordower JH (2011) Ageing as a primary risk factor for Parkinson's disease: evidence from studies of non-human primates. Nat Rev Neurosci 12:359–366.

Cooke JE, Moens CB (2002) Boundary formation in the hindbrain: Eph only it were simple…. Trends in Neurosciences 25:260–267.

Counts SE, He B, Che S, Ginsberg SD, Mufson EJ (2008) Galanin Hyperinnervation Upregulates Choline Acetyltransferase Expression in Cholinergic Basal Forebrain Neurons in Alzheimer's Disease. Neurodegenerative Dis 5:228–231.

Crossley PH, Martin GR (1995) The mouse Fgf8 gene encodes a family of polypeptides and is expressed in regions that direct outgrowth and patterning in the developing embryo. Development 121:439–451.

Crossley PH, Martinez S, Martin GR (1996) Midbrain development induced by FGF8 in the chick embryo. Nat Cell Biol 380:66–68.

Crowley C, Spencer SD, Nishimura MC, Chen KS, Pitts-Meek S, Armaninl MP, Ling LH, McMahon SB, Shelton DL, Levinson AD, Phillips HS (1994) Mice lacking nerve growth factor display perinatal loss of sensory and sympathetic neurons yet develop basal forebrain cholinergic neurons. Cell Cycle 76:1001–1011.

Dallner C, Woods AG, Deller T, Kirsch M, Hofmann H-D (2002) CNTF and CNTF receptor alpha are constitutively expressed by astrocytes in the mouse brain. Glia 37:374–378.

Dauer W, Przedborski S (2003) Parkinson's Disease. Neuron 39:889–909.

Davis T, Burrrin JM, Bloom SR (1987) Growth Hormone (GH) Release in Response to GH-Releasing Hormone in Man is 3-Fold Enhanced by Galanin. Journal of Clinical Endocrinology & Metabolism 65:1248–1252.

de Silva HV, Stuart WD, Park YB, Mao SJ, Gil CM, Wetterau JR, Busch SJ, Harmony JAK (1990) Purification and characterization of apolipoprotein J. J Biol Chem 265:14292–14297.

Decressac M, Ulusoy A, Mattsson B, Georgievska B, Romero-Ramos M, Kirik D, Björklund A (2011) GDNF fails to exert neuroprotection in a rat {alpha}-synuclein model of Parkinson's disease. Brain 134:2302–2311.

DeMattos RB, Bales KR, Cummins DJ, Dodart JC, Paul SM, Holtzman DM (2001) Peripheral anti-A beta antibody alters CNS and plasma A beta clearance and decreases brain A beta burden in a mouse model of Alzheimer's disease. PNAS 98:8850–8855.

DeMattos RB, Cirrito J, Parsadanian M, May P, A OM, Taylor JW, Harmony JAK, Aronow BJ, Bales KR, Paul SM, Holtzman DM (2004) ApoE and Clusterin Cooperatively Suppress Aβ Levels and Deposition: Evidence that ApoE Regulates Extracellular Aβ Metabolism In Vivo. Neuron 41:193–202.

Deppmann C, Mihalas S, Sharma N, Lonze BE, Niebur E, Ginty DD (2008) A Model for Neuronal Competition During Development. Science 320:ec145-ec145.

Desai AR, McConnell SK (2000) Progressive restriction in fate potential by neural progenitors during cerebral cortical development. Development 127:2863–2872.

Desplats P, Lee H-J, Bae E-J, Patrick C, Rockenstein E, Crews L, Spencer B, Masliah E, Lee S-J (2009) Is Parkinson's disease a prion disorder? PNAS 106:12571–12572.

Dessaud E, McMahon AP, Briscoe J (2008) Pattern formation in the vertebrate neural tube: a sonic hedgehog morphogen-regulated transcriptional network. Development 135:2489–2503.

Déglon N, Tseng JL, Bensadoun J-C, Zurn AD, Arsenijevic Y, Almeida LPD, Zufferey R, Trono D, Aebischer P (2000) Self-Inactivating Lentiviral Vectors with Enhanced Transgene Expression as Potential Gene Transfer System in Parkinson's Disease. Human Gene Therapy 11:179–190.

Dietrich M, Spuch C, Antequera D, Rodal I, Yébenes JG, Molina JA, Bermejo F, Carro E (2008) Megalin mediates the transport of leptin across the blood-CSF barrier. Neurobiology of Aging 29:902–912.

Diez M, Koistinaho J, Kahn K, Games D, Hökfelt T (2000) Neuropeptides in hippocampus and cortex in transgenic mice overexpressing V717F β-amyloid precursor protein — initial observations. Neuroscience 100:259-286.

Ding X, MacTavish D, Kar S, Jhamandas JH (2006) Galanin attenuates β-amyloid (Aβ) toxicity in rat cholinergic basal forebrain neurons. Neurobiol Dis 21:413–420.

Doetsch F, Caille I, Lim DA, Garcia-Verdugo J-M, Alvarez-Buylla A (1999) Subventricular Zone Astrocytes Are Neural Stem Cells in the Adult Mammalian Brain. Cell 97:703–716.

Dong Y, Benveniste EN (2001) Immune function of astrocytes. Glia 36:180–190.

Dowell JA, Johnson JA, Li L (2009) Identification of Astrocyte Secreted Proteins with a Combination of Shotgun Proteomics and Bioinformatics. J Proteome Res 8:4135–4143.

Doyle KL, Hort YJ, Herzog H, Shine J (2012) Neuropeptide Y and peptide YY have distinct roles in adult mouse olfactory neurogenesis. J Neurosci Res 90:1126–1135.

Dull T, Zufferey R, Kelly M, Mandel RJ, Nguyen M, Trono D, Naldini L (1998) A Third-Generation Lentivirus Vector with a Conditional Packaging System. Journal of Virology 72:8463–8471.

Dziegielewska KM, Saunders NR, Schejter EJ, Zakut H, Zevin-Sonkin D, Zisling R, Soreq H (1986) Synthesis of plasma proteins in fetal, adult, and neoplastic human brain tissue. Developmental Biology 115:93–104.

Egan MF, Kojima M, Callicott JH, Goldberg TE, Kolachana BS, Alessandro B, Zaitsev E, Gold B, Goldman D, Dean M, Lu B, Weinberger DR (2003) The BDNF val66met polymorphism affects activity-dependent secretion of BDNF and human memory and hippocampal function. Cell 122:257–269.

Eggert K, Schlegel J, Oertel W, Würz C, Krieg J-C, Vedder H (1999) Glial cell line-derived neurotrophic factor protects dopaminergic neurons from 6-hydroxydopamine toxicity in vitro. Neuroscience Letters 269:178–182.

Elliott-Hunt CR, Holmes FE, Hartley DM, Perez S, Mufson EJ, Wynick D (2011) Endogenous Galanin Protects Mouse Hippocampal Neurons Against Amyloid Toxicity in vitro via Activation of Galanin Receptor-2. Journal of Alzheimer's Disease 25:455–462.

Elliott-Hunt CR, Marsh B, Bacon A, Pope R, Vanderplank P, Wynick D (2004) Galanin acts as a neuroprotective factor to the hippocampus. PNAS 101:5105–5110

Elliott-Hunt CR, Pope RJP, Vanderplank P, Wynick D (2007) Activation of the galanin receptor 2 (GalR2) protects the hippocampus from neuronal damage. J Neurochem 100:780–789.

Eriksson PS, Perfilieva E, Björk-Eriksson T, Alborn A-M, Nordborg C, Peterson DA, Gage FH (1998) Neurogenesis in the adult human hippocampus. Nat Med 4:1313–1317.

Ernfors P, Lee K-F, Kucera J, Jaenisch R (1994) Lack of neurotrophin-3 leads to deficiencies in the peripheral nervous system and loss of limb proprioceptive afferents. Cell 77:503–512.

Evans JR, Barker RA (2008) Neurotrophic factors as a therapeutic target for Parkinson's disease. Expert Opin Ther Targets 12:437–447.

Fagan AM, Holtzman DM, Munson G, Mathur T, Schneider D, Chang LK, Getz GS, Reardon CA, Lukens J, Shah JA, LaDu MJ (1999) Unique Lipoproteins Secreted by Primary Astrocytes From Wild Type, apoE (−/−), and Human apoE Transgenic Mice. J Biol Chem 274:30001–30007.

Fariñas I, Jones KR, Backus C, Wang XY, Reichardt LF (1994) Severe sensory and sympathetic deficits in mice lacking neurotrophin-3. Nature 369:658-661.

Fathi Z, Cunningham AM, Iben LG, Battaglino PB, Ward SA, Nichol KA, Pine KA, Wang J, Goldstein ME, Iismaa TP, Zimanyi IA (1997) Cloning, pharmacological characterization and distribution of a novel galanin receptor. Molecular brain Research 51:49–59.

Ferrari R, Moreno J, Minhajuddin A, E OS, Reisch JS, Barber RC, Momeni P (2012) Implication of common and disease specific variants in CLU, CR1, and PICALM. Neurobiology of Aging.

Florén A, Land T, Langel Ü (2000) Galanin receptor subtypes and ligand binding. Neuropeptides 34:331–337.

Freeman M (2010) Specification and Morphogenesis of Astrocytes. Science 330:774–778.

Freixes M, Puig B, Rodríguez A, Torrejón-Escribano B, Blanco R, Ferrer I (2002) Clusterin solubility and aggregation in Creutzfeldt-Jakob disease. Acta neuropathologica 108:295–301.

Fukumitsu H, Ohtsuka M, Murai R, Nakamura H, Itoh K, Furukawa S (2006) Brain-derived neurotrophic factor participates in determination of neuronal

laminar fate in the developing mouse cerebral cortex. J Neurosci 26:13218-13230.

Gabriel SM, Bierer LM, Davidson M, Purohit DP, Perl DP, Harotunian V (2008) Galanin-Like Immunoreactivity Is Increased in the Postmortem Cerebral Cortex from Patients with Alzheimer's Disease. J Neurochem 62:1516-1523.

Gage FH, Coates PW, Palmer TD, Kuhn HG, Fisher LJ, Suhonen JO, Peterson DA, Suhr ST, Ray J (1995) Survival and differentiation of adult neuronal progenitor cells transplanted to the adult brain. PNAS 92:11879–11883.

Gao J, Huang X, Park Y, Hollenbeck A, Chen H (2011) An Exploratory Study on CLU, CR1 and PICALM and Parkinson Disease. PLoS ONE 6:e24211.

Gardell LR et al. (2003) Multiple actions of systemic artemin in experimental neuropathy. Nat Med 9:1383–1389.

Garwood C, Pooler A, Atherton J, Hanger DP, Noble W (2011) Astrocytes are important mediators of Aβ-induced neurotoxicity and tau phosphorylation in primary culture. Cell Death & Disease:e167.

Gash DM, Zhang Z, Ovadia A, Cass WA, Yi A, Simmerman L, Russell D, Martin D, Lapchak PA, Collins F, Hoffer BJ, Gerhardt GA (1996) Functional recovery in parkinsonian monkeys treated with GDNF. Nat Cell Biol 380:252–255.

Gasmi M, Brandon EP, Herzog CD, Wilson A, Bishop KM, Hofer EK, Cunningham JJ, Printz MA, Kordower JH, Bartus RT (2007) AAV2-mediated delivery of human neurturin to the rat nigrostriatal system: Long-term efficacy and tolerability of CERE-120 for Parkinson's disease. Neurobiol Dis 27:67–76.

Gavalas A (2002) ArRAnging the hindbrain. Trends in Neurosciences 25:61–64.

Gebicke-Haerter PJ, Bauer J, Brenner A, Gerok W (1987) Alpha 2-macroglobulin synthesis in an astrocyte subpopulation. J Neurochem 49:1139–1145.

Georgievska B, Kirik D, Björklund A (2004) Overexpression of Glial Cell Line-Derived Neurotrophic Factor Using a Lentiviral Vector Induces Time- and Dose-Dependent Downregulation of Tyrosine Hydroxylase in the Intact Nigrostriatal Dopamine System. The Journal of Neuroscience 24:6437-6445.

Georgievska B, Kirik D, Rosenblad C, Lundberg C, Björklund A (2002) Neuroprotection in the rat Parkinson model by intrastriatal GDNF gene transfer using a lentiviral vector. Neuroreport 13:75–82.

Giannakopoulos P, Kovari E, French LE, Viard I, Hof PR, Bouras C (1998) Possible neuroprotective role of clusterin in Alzheimer's disease: a quantitative immunocytochemical study. Acta neuropathologica 95:387-394.

Gill SS, Patel NK, Hotton GR, O'Sullivan K (2003) Direct brain infusion of glial cell line-derived neurotrophic factor in Parkinson disease. Nat Med 9:589-595.

Gilman S, Koller M, Black R, Jenkins L, Griffith SG, Fox NC, Eisner L, Boada Rovira M, Forette F, Orgogozo J-M (2005) Clinical effects of Aβ

immunization (AN1792) in patients with AD in an interrupted trial. Neurology 64:1553–1562.

Goetz EM, Shankar B, Zou Y, Morales JC, Luo X, Araki S, Bachoo R, Mayo LD, Boothman DA (2011) ATM-dependent IGF-1 induction regulates secretory clusterin expression after DNA damage and in genetic instability. Oncogene 30:3745–3754.

Gould E, Reeves A, Graziano M, Gross CG (1999) Neurogenesis in the Neocortex of Adult Primates. Science 286:548–552.

Granholm AC, Reyland M, Albeck D, Sanders L, Gerhardt G, Hoernig G, Shen L, Westphal H, Hoffer B (2000) Glial cell line-derived neurotrophic factor is essential for postnatal survival of midbrain dopamine neurons. J Neurosci 20:3182–3190.

Greco TM, Seeholzer SH, Mak A, Spruce L, Ischiropoulos H (2010) Quantitative Mass Spectrometry-based Proteomics Reveals the Dynamic Range of Primary Mouse Astrocyte Protein Secretion. J Proteome Res 9:2764–2774.

Gritti A, Parati EA, Cova L, Frolichsthal P, Galli R, Wanke E, Faravelli L, Morassutti DJ, Roisen F, Nickel DD, Vescovi AL (1996) Multipotential stem cells from the adult mouse brain proliferate and self-renew in response to basic fibroblast growth factor. The Journal of Neuroscience 16:1091-1100.

Grosskortenhaus R, Pearson BJ, Marusich A, Doe CQ (2005) Regulation of Temporal Identity Transitions in Drosophila Neuroblasts. Developmental Cell 8:193–202.

Grosskortenhaus R, Robinson KJ, Doe CQ (2006) Pdm and Castor specify late-born motor neuron identity in the NB7-1 lineage. Genes & Development 20:2618–2627.

Gustafson EL, Smith KE, Durkin MM, Gerald C, Branchek TA (1996) Distribution of a rat galanin receptor mRNA in rat brain. Neuroreport 7:953–957.

Haberman RP, Samulski RJ, McCown TJ (2003) Attenuation of seizures and neuronal death by adeno-associated virus vector galanin expression and secretion. Nat Med 9:1076–1080.

Han B, DeMattos RB, Dugan L, Kim-Han J, Brendza RP, Fryer JD, Kierson M, John C, Quick K, Harmony JAK, Aronow BJ, Holtzman DM (2001) Clusterin contributes to caspase-3−independent brain injury following neonatal hypoxia-ischemia. Nat Med 7:338-343.

Harold D et al. (2009) Genome-wide association study identifies variants at CLU and PICALM: associated with Alzheimer's disease. Nature Genetics. Nat Genet 41:1088–1095.

Harshman LG, Moore KM, Sty MA, Magwire MM (1999) Stress resistance and longevity in selected lines of Drosophila melanogaster. Neurobiology of Aging 20:521–529.

Hartfuss E, Galli R, Heins N, Götz M (2001) Characterization of CNS Precursor Subtypes and Radial Glia. Developmental Biology 229:15–30.

Hawkes CH, Del Tredici K, Braak H (2009) Parkinson's Disease: The Dual Hit Theory Revisited. Annals NY Acad Sci 1170:615–622.

Hellman M, Arumäe U, Yu L-Y, Lindholm P, Peränen J, Saarma M, Permi P (2011) Mesencephalic astrocyte-derived neurotrophic factor (MANF) has a unique mechanism to rescue apoptotic neurons. J Biol Chem 286:2675-2680.

Hennessy L, Kunitake S, Jarvis M, Hamilton RL, Endeman G, Protter A, Kane JP (1997) Isolation of subpopulations of high density lipoproteins: three particle species containing apoE and two species devoid of apoE that have affinity for heparin. Journal of lipid research 38:1859–1868.

Hébert JM, Mishina Y, McConnell SK (2002) BMP Signaling Is Required Locally to Pattern the Dorsal Telencephalic Midline. Neuron 35:1029–1041.

Hirabayashi Y, Suzki N, Tsuboi M, Endo TA, Toyoda T, Shinga J, Koseki H, Vidal M, Gotoh Y (2009) Polycomb Limits the Neurogenic Competence of Neural Precursor Cells to Promote Astrogenic Fate Transition. Neuron-63:600–613.

Hitoshi S, Tropepe V, Ekker M, van der Kooy D (2002) Neural stem cell lineages are regionally specified, but not committed, within distinct compartments of the developing brain. Development 129:233–244.

Hobson S-A, Holmes FE, Kerr NCH, Pope RJP, Wynick D (2006) Mice deficient for galanin receptor 2 have decreased neurite outgrowth from adult sensory neurons and impaired pain-like behaviour. J Neurochem 99:1000–1010.

Hochstim C, Deneen B, Lukaszewicz A, Zhou Q, Anderson DJ (2008) Identification of positionally distinct astrocyte subtypes whose identities are specified by a homeodomain code. Cell 133:510–522.

Hock C, Heese K, Hulette C, Rosenberg C, Otten U (2000) Region-Specific Neurotrophin Imbalances in Alzheimer DiseaseDecreased Levels of Brain-Derived Neurotrophic Factor and Increased Levels of Nerve Growth Factor in Hippocampus and Cortical Areas. Arch Neurol 57:846–851.

Hoffer BJ, Hoffman A, Bowenkamp K, Huettl P, Hudson J, Martin D, Lin L-FH, Gerhardt GA (1994) Glial cell line-derived neurotrophic factor reverses toxin-induced injury to midbrain dopaminergic neurons in vivo. Neuroscience Letters 182:107–111.

Hohmann JG, Krasnow SM, Teklemichael DN, Clifton DK, Wynick D, Steiner RA (2003) Neuroendocrine Profiles in Galanin-Overexpressing and Knockout Mice. Neuroendocrinology 77:354–366.

Holmes FE, Mahoney S, R King Von, Bacon A, Kerr NCH, Pachnis V, Curtis R, Priestley JV, Wynick D (2000) Targeted disruption of the galanin gene reduces the number of sensory neurons and their regenerative capacity. PNAS 97:11563–11568.

Horch HW, Katz LC (2002) BDNF release from single cells elicits local dendritic growth in nearby neurons. Nat Neurosci 5:1177–1184.

Horger BA, Nishimura MC, Armanini MP, Wang L-C, Poulsen KT, Rosenblad C, Kirik D, Moffat B, Simmons L, Johnson E, Milbrandt J, Rosenthal A,

Björklund A, Vandlen RA, Hynes MA, Phillips HS (1998) Neurturin Exerts Potent Actions on Survival and Function of Midbrain Dopaminergic Neurons. The Journal of Neuroscience 18:4929–4937.

Hou J-GG, Lin L-FH, Mytilineou C (2002) Glial Cell Line-Derived Neurotrophic Factor Exerts Neurotrophic Effects on Dopaminergic Neurons In Vitro and Promotes Their Survival and Regrowth After Damage by 1-Methyl-4-Phenylpyridinium. J Neurochem 66:74–82.

Hökfelt T, Tatemoto K (2008) Galanin – 25 years with a multitalented neuropeptide. Cell Mol Life Sci 65:1791–1795.

Hökfelt T, Wiesenfeld-Hallin Z, Villar M, Melander T (1987) Increase of galanin-like immunoreactivity in rat dorsal root ganglion cells after peripheral axotomy. Neuroscience Letters 83:217–220.

Hyman C, Hofer M, Barde YA, Juhasz M, Yancopoulos GD, Squinto SP, Lindsay RM (1991) BDNF is a neurotrophic factor for dopaminergic neurons of the substantia nigra. Nature 350:230–232.

Incardona JP, Gruenberg J, Roelink H (2002) Sonic Hedgehog Induces the Segregation of Patched and Smoothened in Endosomes. Current Biology 12:983–995.

Ip NY, Li YP, van de Stadt I, Panayotatos N, Alderson RF, Lindsay RM (1991) Ciliary neurotrophic factor enhances neuronal survival in embryonic rat hippocampal cultures. The Journal of Neuroscience 11:3124–3134.

Irving C, Mason I (2000) Signalling by FGF8 from the isthmus patterns anterior hindbrain and establishes the anterior limit of Hox gene expression. Development 127:177–186.

Jang H, Boltz D, Sturm-Ramirez K, Shepherd KR, Jiao Y, Webster R, Smeyne RJ (2009) Highly pathogenic H5N1 influenza virus can enter the central nervous system and induce neuroinflammation and neurodegeneration. PNAS 106:14063–14068.

Jarraya B, Boulet S, Ralph GS, Jan C, Bonvento G, Azzouz M, Miskin JE, Shin M, Delzescaux T, Drouot X, Hérard A-S, Day DM, Brouillet E, Kingsman SM, Hantraye P, Mitrophanous KA, Mazarakis ND, Palfi S (2009) Dopamine gene therapy for Parkinson's disease in a nonhuman primate without associated dyskinesia. Sci Transl Med 1:1–11.

Jin K, Peel AL, Mao XO, Xie L, Cottrell BA, Henshall DC, Greenberg DA (2004) Increased hippocampal neurogenesis in Alzheimer's disease. PNAS 101:343–347.

Jin KL, Mao XO, Greenberg DA (2000) Vascular endothelial growth factor: Direct neuroprotective effect in in vitro ischemia. PNAS 97:10242–10247.

Johansson CB, Momma S, Clarke DL, Risling M, Lendahl U, Frisén J (1999) Identification of a Neural Stem Cell in the Adult Mammalian Central Nervous System. Cell 96:25–34.

Jones M, Perumal P, Vrontakis M (2009) Presence of Galanin-Like Immunoreactivity in Mesenchymal and Neural Crest Origin Tissues During Embryonic Development in the Mouse. Anat Rec 292:481–487.

Kahn MA, Kumar S, Liebl D, Chang R, Parada LF, De Vellis J (1999) Mice lacking NT-3, and its receptor TrkC, exhibit profound deficiencies in CNS glial cells. Glia 26:153–165.

Kamiguchi H, Yoshida K, Sagoh M, Sasaki H, Inaba M, Wakamoto H, Otani M, Toya S (1995) Release of ciliary neurotrophic factor from cultured astrocytes and its modulation by cytokines. Neurochemistry Research 20:1187–1193.

Kaplan LM, Spindel ER, Isselbacher KJ, Chin WW (1988) Tissue-specific expression of the rat galanin gene. PNAS 85:1065–1069.

Kaplan M, Hinds JW (1977) Neurogenesis in the adult rat: electron microscopic analysis of light radioautographs. Science 197:1092–1094.

Karatayev O, Baylan J, Weed V, Chang S, Wynick D, Leibowitz SF (2010) Galanin Knockout Mice Show Disturbances in Ethanol Consumption and Expression of Hypothalamic Peptides That Stimulate Ethanol Intake. Alcoholism: Clinical and Experimental Research 34:72–80.

Kempermann G, Kuhn HG, Gage FH (1997) More hippocampal neurons in adult mice living in an enriched environment. Nature 386:493–495.

Kinney NE, Antill RW (1999) Role of olfaction in the formation of preferenence for high-fat foods in mice. Physiology and Behavior 59:475–478.

Kirik D, Georgievska B, Björklund A (2004) Localized striatal delivery of GDNF as a treatment for Parkinson disease. Nat Neurosci 7:105–110.

Kirik D, Rosenblad C, Björklund A (1998) Characterization of Behavioral and Neurodegenerative Changes Following Partial Lesions of the Nigrostriatal Dopamine System Induced by Intrastriatal 6-Hydroxydopamine in the Rat. Experimental Neurology 152:259–277.

Kirik D, Rosenblad C, Björklund A, Mandel RJ (2000) Long-Term rAAV-Mediated Gene Transfer of GDNF in the Rat Parkinson's Model: Intrastriatal But Not Intranigral Transduction Promotes Functional Regeneration in the Lesioned Nigrostriatal System. The Journal of Neuroscience 20:4686–4700.

Koch S, Donarski N, Goetze K, Kreckel M, Stuerenburg H-J, Buhmann C, Beisiegel U (2001) Characterization of four lipoprotein classes in human cerebrospinal fluid. Journal of lipid research 42:1143–1151.

Kordower JH et al. (2000) Neurodegeneration prevented by lentiviral vector delivery of GDNF in primate models of Parkinson's disease. Science 290:767–773.

Kordower JH, Herzog CD, Dass B, Bakay RAE, Stansell J III, Gasmi M, Bartus RT (2006) Delivery of neurturin by AAV2 (CERE-120)-mediated gene transfer provides structural and functional neuroprotection and neurorestoration in MPTP-treated monkeys. Ann Neurol 60:706–715.

Koshimizu H, Hazama S, Hara T, Ogura A, Kojima M (2010) Distinct signaling pathways of precursor BDNF and mature BDNF in cultured cerebellar granule neurons. Neuroscience Letters 473:229–232.

Koshiyama H, Kato Y, Inoue T, Murakami Y, Ishikawa Y, Yanaihara N, Imura H (1987) Central galanin stimulates pituitary prolactin secretion in rats: Possible involvement of hypothalamic vasoactive intestinal polypeptide. Neuroscience Letters 75:49–54.

Kotzbauer PT, Lampe PA, Heuckeroth RO, Golden JP, Creedon DJ, Johnson EM Jr, Milbrandt J (1996) Neurturin, a relative of glial-cell-line-derived neurotrophic factor. Nat Cell Biol 384:467–470.

Kounnas MZ, Loukinova EB, Stefansson S, Harmony JAK, Brewer BH, Strickland DK, Argraves WS (1995) Identification of Glycoprotein 330 as an Endocytic Receptor for Apolipoprotein J/Clusterin. J Biol Chem 270:13070–13075.

Kovacs DM (2000) Macroglobulin in late-onset Alzheimer's disease. Experimental Gerontology 35:473–479.

Kowall NW, Beal MF (1989) Galanin-like immunoreactivity is present in human substantia innominata and in senile plaques in Alzheimer's disease. Neuroscience Letters 98:118–123.

Krencik R, Weick JP, Liu Y, Zhang Z-J, Zhang S-C (2011) Specification of transplantable astroglial subtypes from human pluripotent stem cells. Nat Biotechnol 29:528–534.

Krüger R, Kuhn W, Müller T, Woitalla D, Graeber M, Kösel S, Przuntek H, Epplen JT, Schols L, Riess O (1998) Ala30Pro mutation in the gene encoding α-synuclein in Parkinson's disease. Nat Genet 18:106–108.

Kuhn HG, Dickinson-Anson H, Gage FH (1996) Neurogenesis in the dentate gyrus of the adult rat: age-related decrease of neuronal progenitor proliferation. The Journal of Neuroscience 16:2027–2033.

LaDu MJ, Gilligan SM, Lukens JR, Cabana VG, Reardon CA, Van Eldik LJ, Holtzman DM (1998) Nascent Astrocyte Particles Differ from Lipoproteins in CSF. J Neurochem 70:2070–2081.

Lafon-Cazal M, Adjali O, Galéotti N, Poncet J, Jouin P, Homburger V, Bockaert J, Marin P (2003) Proteomic Analysis of Astrocytic Secretion in the Mouse. J Biol Chem 278:24438–24448.

Lamb T, Knecht A, Smith W, Stachel S, Economides A, Stahl N, Yancopolous G, Harland R (1993) Neural induction by the secreted polypeptide noggin. Science 262:713–718.

Lang AE et al. (2006) Randomized controlled trial of intraputamenal glial cell line-derived neurotrophic factor infusion in Parkinson disease. Ann Neurol 59:459–466.

Lang R, Gundlach A, Kofler B (2007) The galanin peptide family: Receptor pharmacology, pleiotropic biological actions, and implications in health and disease. Pharmacology & Therapeutics 115:177–207.

Lazarov O, Marr RA (2010) Neurogenesis and Alzheimer's disease: At the crossroads. Experimental Neurology 223:267–281.

Lee D, Ha J, Kim Y, Bae K (2011a) Interaction of a putative BH3 domain of clusterin with anti-apoptotic Bcl-2 family proteins as revealed by NMR spectroscopy. Biochem Biophys Res Commun 408:541–547.

Lee J, Seroogy KB, Mattson MP (2002) Dietary restriction enhances neurotrophin expression and neurogenesis in the hippocampus of adult mice. J Neurochem 80:539–547.

Lee KJ, Dietrich P, Jessell TM (2000) Genetic ablation reveals that the roof plate is essential for dorsal interneuron specification. Nature 403:734–740.

Lee P, Koo PH (2000) Rat α1-Macroglobulin Enhances Nerve Growth Factor-Promoted Neurite Outgrowth, TrkA Phosphorylation, and Gene Expression of Pheochromocytoma PC12 Cells. J Neurochem 74:81–91.

Lee R, Kermani P, Teng KK, Hempstead BL (2001) Regulation of Cell Survival by Secreted Proneurotrophins. Science 294:1945–1948.

Lee S, Hong S, Min B, Shim Y, Lee KU, Lee IK, Bendayan M, Aronow BJ, Park IS (2011b) Essential role of clusterin in pancreas regeneration - Lee. Developmental Dynamics 240.

Lee Y-N, Shim Y-J, Kang B-H, Park J-J, Min B-H (2012) Over-expression of human clusterin increases stress resistance and extends lifespan in Drosophila melanogaster. Biochem Biophys Res Commun 420:851–856.

Levi-Montalcini R, Hamburger V (1953) A diffusible agent of mouse sarcoma, producing hyperplasia of sympathetic ganglia and hyperneurotization of viscera in the chick embryo. Journal of Experimental Zoology 123:233–288.

Levitt P, Rakic P (1980) Immunoperoxidase localization of glial fibrillary acidic protein in radial glial cells and astrocytes of the developing rhesus monkey brain. J Comp Neurol 193:815–840.

Levy E (1989) Stroke in Icelandic patients with hereditary amyloid angiopathy is related to a mutation in the cystatin C gene, an inhibitor of cysteine proteases. Journal of Experimental Medicine 169:1771–1778.

LeWitt PA (2008) Levodopa for the Treatment of Parkinson's Disease. The New England Journal of Medicine 359:2468–2476

Li H, He Z, Su T, Ma Y, Lu S, Dai C, Sun M (2003) Protective action of recombinant neurturin on dopaminergic neurons in substantia nigra in a Rhesus monkey model of Parkinson's disease. Neurological Research 25:263–267.

Li Y, Luikart BW, Birnbaum S, Chen J, Kwon C-H, Kernie SG, Bassel-Duby R, Parada LF (2008) TrkB Regulates Hippocampal Neurogenesis and Governs Sensitivity to Antidepressive Treatment. Neuron 59:399–412.

Li Y, Yui D, Luikart BW, McKay RM, Li Y, Rubenstein JL, Parada LF (2012) Conditional ablation of brain-derived neurotrophic factor-TrkB signaling impairs striatal neuron development. PNAS 109:15491–15496.

Liedtke W, Edelman W, Bieri PL, Chiu F-C, Cowan NJ, Kucherlapati R, Raine CS (1996) GFAP Is Necessary for the Integrity of CNS White Matter Architecture and Long-Term Maintenance of Myelination. Neuron 17:607-615.

Lillien L, Raphael H (2000) BMP and FGF regulate the development of EGF-responsive neural progenitor cells. Development 127:4993–5005.

Lim DA, Tramontin AD, Trevejo JM, Herrera DG, Garcia-Verdugo J-M, Alvarez-Buylla A (2000) Noggin Antagonizes BMP Signaling to Create a Niche for Adult Neurogenesis. Neuron 28:713–726.

Lin C, Cheng F, Lu Y, Chu L, Wang C, Hsueh C-M (2006) Protection of ischemic brain cells is dependent on astrocyte-derived growth factors and their receptors. Experimental Neurology 201:225–233.

Lin H, Bhatia R, Lal R (2001) Amyloid ß protein forms ion channels: implications for Alzheimer's disease pathophysiology. fasebjorg 5:2433–2444

Lin L, Doherty D, Lile J, Bektesh S, Collins F (1993) GDNF: a glial cell line-derived neurotrophic factor for midbrain dopaminergic neurons. Science 260:1130–1132.

Lin Y, Chen S, Lai L, Chen J, Lai L-C, Chen J-H, Yang S-Y, Huang Y-L, Chen T-F, Sun Y, Wen L-L, Yip P-K, Chu Y-M, Chen WJ, Chen Y-C (2012) Genetic Polymorphisms of Clusterin gene are associated with a decreased risk of Alzheimer's disease. European Journal of Epidemiology 27:73–75.

Lindholm P, Peränen J, Andressoo J-O, Kalkkinen N, Kokaia Z, Lindvall O, Timmusk T, Saarma M (2008) MANF is widely expressed in mammalian tissues and differently regulated after ischemic and epileptic insults in rodent brain. Mol Cell Neurosci 39:356–371.

Lindholm P, Voutilainen MH, Laurén J, Peränen J, Leppänen V-M, Andressoo J-O, Lindahl M, Janhunen S, Kalkkinen N, Timmusk T, Tuominen RK, Saarma M (2007) Novel neurotrophic factor CDNF protects and rescues midbrain dopamine neurons in vivo. Nature 448:73–77.

Liu A, Niswander LA (2005) Bone morphogenetic protein signalling and vertebrate nervous system development. Nat Rev Neurosci 6:945–954.

Lledo P-M, Alonso M, Grubb MS (2006) Adult neurogenesis and functional plasticity in neuronal circuits. Nat Rev Neurosci 7:179–193.

Lois C, Alvarez-Buylla A (1994) Long-distance neuronal migration in the adult mammalian brain. Science 264:1145–1148.

Lois C, Garc a-Verdugo JM, Alvarez-Buylla A (1996) Chain Migration of Neuronal Precursors. Science 271:978–981.

Louridas M, Letourneau S, Lautatzis M-E, Vrontakis M (2009) Galanin is highly expressed in bone marrow mesenchymal stem cells and facilitates migration of cells both in vitro and in vivo. Biochem Biophys Res Commun 390:867–871.

López FJ, Merchenthaler I, Ching M, Wisniewski MG, Negro-Vilar A (1991) Galanin: a hypothalamic-hypophysiotropic hormone modulating reproductive functions. PNAS 88:4508–4512.

Lu CC, Brennan J, Robertson EJ (2001) From fertilization to gastrulation: axis formation in the mouse embryo. Current Opinion in Genetics & Development 11:384–392.

Lubetzki C, Demeres C, Anglade P, Villarroya H, Frankfurter A, Lee MY, Zalc B (1993) Even in culture, oligodendrocytes myelinate solely axons. PNAS 90:6820–6824

Lucas BK, Ormandy CJ, Binart N, Bridges RS, Kelly PA (1998) Null Mutation of the Prolactin Receptor Gene Produces a Defect in Maternal Behavior. Endocrinology 139:4102–4107.

Lucin K, Wyss-Coray T (2009) Immune Activation in Brain Aging and Neurodegeneration: Too Much or Too Little? Neuron 64:110–122.

Ludwin SK, Kosek JC, Eng LF (1976) The topographical distribution of S-100 and GFA proteins in the adult rat brain: an immunohistochemical study using horseradish peroxidase-labelled antibodies. J Comp Neurol 165:197-207.

Lumsden A, Krumlauf R (1996) Patterning the Vertebrate Neuraxis. Science 274:1109–1115.

Lundberg C, Björklund T, Jakobson J, Hantraye P, Déglon N, Kirik D (2008) Applications of Lentiviral Vectors for Biology and Gene Therapy of Neurological Disorders. Current Gene Therapy 8:461–473.

Ma J-F, Liu L, Zhang Y, Wang Y, Deng Y-L, Huang Y, Wang G, Xu W, Cui P-J, Fei Q-Z, Ding J-Q, Tang H-D, Chen S-D (2011) Association Study of Clusterin Polymorphism rs11136000 With Late Onset Alzheimer's Disease in Chinese Han Population. American Journal of Alzheimer's Disease and other Dementias 26:627–630.

Maetzler W, Liepelt I, Berg D (2009) Progression of Parkinson's disease in the clinical phase: potential markers. The Lancet Neurology 8:1158–1171.

Mahoney S-A, Hosking R, Farrant S, Holmes FE, Jacoby AS, Shine J, Iismaa TP, Scott MK, Schmidt R, Wynick D (2003) The second galanin receptor GalR2 plays a key role in neurite outgrowth from adult sensory neurons. J Neurosci 23:416–421.

Maisonpierre PC, Belluscio L, Friedman B, Alderson RF, Wiegand SJ, Furth ME, Lindsay RM, Yancopoulos GD (1990) NT-3, BDNF, and NGF in the developing rat nervous system: Parallel as well as reciprocal patterns of expression. Neuron 5:501–509.

Manzini MC, Walsh CA (2011) What disorders of cortical development tell us about the cortex: one plus one does not always make two. Current Opinion in Genetics & Development 21:333–339.

Marks WJ Jr, Bartus RT, Siffert J, Davis CS, Lozano A, Boulis N, Vitek J, Stacy M, Turner D, Verhagen L (2010) Gene delivery of AAV2-neurturin for Parkinson's disease: a double-blind, randomised, controlled trial. The Lancet Neurology 9:1164–1172.

Marks WJ Jr, Ostrem JL, Verhagen L, Starr PA, Larson PS, Bakay RA, Taylor R, Cahn-Weiner DA, Stoessl AJ, Olanow CW (2008) Safety and tolerability of intraputaminal delivery of CERE-120 (adeno-associated virus serotype 2–neurturin) to patients with idiopathic Parkinson's disease: an open-label, phase I trial. The Lancet Neurology 7:400–408.

Martel CL, Mackic JB, Matsubara E, Governale S, Miguel C, Miao W, McComb JG, Frangione B, Ghiso JJ, Zlokovic BV (2002) Isoform-Specific Effects of Apolipoproteins E2, E3, and E4 on Cerebral Capillary Sequestration and Blood-Brain Barrier Transport of Circulating Alzheimer's Amyloid β. J Neurochem 69:1995–2004.

Marti E, Takada R, Bumcrot DA, Sasaki H, McMahon AP (1995) Distribution of Sonic hedgehog peptides in the developing chick and mouse embryo. Development 121:2537–2547.

Masu Y, Wolf E, Holtmann B, Sendtner M, Brem G, Thoenen H (1993) Disruption of the CNTF gene results in motor neuron degeneration. Nat Cell Biol 365:27–32.

Matsubara E, Frangione B, Ghiso JJ (1995) Characterization of Apolipoprotein J-Alzheimer's Aβ Interaction. J Biol Chem 270:7563–7567.

Matsunaga E, Nakamura H (2000) Pax6 defines the di-mesencephalic boundary by repressing en1 and pax2. Development 127:2357–2365.

Matsuzaki H, Tamatani M, Yamaguchi A, Namikawa K, Kiyama H, Vitek MP, Mitsuda N, Tohyama M (2001) Vascular endothelial growth factor rescues hippocampal neurons from glutamate-induced toxicity: signal transduction cascades. FASEB Journal 15:1218–1220.

Mazarakis ND, Azzouz M, Rohll JB, Ellard FM, Wilkes FJ, Olsen AL, Carter EE, Barber RD, Baban DF, Kingsman SM, Kingsman AJ, O'Malley K, Mitrophanous KA (2001) Rabies virus glycoprotein pseudotyping of lentiviral vectors enables retrograde axonal transport and access to the nervous system after peripheral delivery. Human Molecular Genetics 10:2109–2121.

Mazarati A, Lu X, Kilk K, Langel Ü, Wasterlain C, Bartfai T (2004a) Galanin type 2 receptors regulate neuronal survival, susceptibility to seizures and seizure-induced neurogenesis in the dentate gyrus. Eur J Neurosci 19:3235–3244.

Mazarati A, Lu X, Shinmei S, Badie-Mahdavi H, Bartfai T (2004b) Patterns of seizures, hippocampal injury and neurogenesis in three models of status epilepticus in galanin receptor type 1 (GalR1) knockout mice. Neuroscience 128:431–441.

McCarthy KD, De Vellis J (1980) Preparation of separate astroglial and oligodendroglial cell cultures from rat cerebral tissue. J Cell Biol 85:890–902.

McLaughlin L, Zhu G, Mistry M, Ley-Ebert C, Stuart WD, Florio CJ, Groen PA, Witt SA, Kimball TR, Witte DP, Harmony JAK, Aronow BJ (2000) Apolipoprotein J/clusterin limits the severity of murine autoimmune myocarditis. J Clin Invest 106:1105–1113.

McMahon AP, Joyner AL, Bradley A, McMahon JA (1992) The midbrain-hindbrain phenotype of Wnt-1−Wnt-1− mice results from stepwise deletion of engrailed-expressing cells by 9.5 days postcoitum. Trends in Neurosciences 69:581–595.

Melander T, Hökfelt T, Rökaeus A, Cuello AC, Oertel WH, Verhofstad A, Goldstein M (1986) Coexistence of galanin-like immunoreactivity with catecholamines, 5- hydroxytryptamine, GABA and neuropeptides in the rat CNS. J Neurosci 6:3640–3654.

Melander T, Staines WA, Hökfelt T, Rökaeus A, Eckenstein F, Salvaterra PM, Wainer BH (1985) Galanin-like immunoreactivity in cholinergic neurons of the septum-basal forebrain complex projecting to the hippocampus of the rat. Brain Research 360:130–138.

Mengel-From J, Christensen K, McGue M, Christiansen L (2011) Genetic variations in the CLU and PICALM genes are associated with cognitive function in the oldest old. Neurobiology of Aging 32:554.e7–554.e11.

Mennicken F, Hoffert C, Pelletier M, Ahmad S, O'Donnell D (2002) Restricted distribution of galanin receptor 3 (GalR3) mRNA in the adult rat central nervous system. J Chem Neuroanat 24:257–268.

Meyers EN, Lewandoski1 M, Martin GR (1998) An Fgf8 mutant allelic series generated by Cre- and Flp-mediated recombination. Nat Genet 18:136–141.

Mi W, Pawlik M, Sastre M, Jung SS, Radvinsky DS, Klein AM, Sommer J, Schmidt SD, Nixon RA, Mathews PM, Levy E (2007) Cystatin C inhibits amyloid-β deposition in Alzheimer's disease mouse models. Nat Genet 39:1440–1442.

Michel D, Chatelain G, North S, Brun G (1997) Stress-induced transcription of the clusterin/apoJ gene. Biochemical Journal 328:45.

Milbrandt J et al. (1998) Persephin, a Novel Neurotrophic Factor Related to GDNF and Neurturin. Neuron 20:245–253.

Miller FD, Gauthier AS (2007) Timing Is Everything: Making Neurons versus Glia in the Developing Cortex. Neuron 54:357–369.

Miller MA, Kolb PE, Leverenz JB, Peskind E, Raskind MA (2002) Preservation of Noradrenergic Neurons in the Locus Ceruleus that Coexpress Galanin mRNA in Alzheimer's Disease. J Neurochem 73:2028–2036.

Mittermeyer G, Christine CW, Rosenbluth KH, Baker SL, Starr P, Larson P, Kaplan PL, Forsayeth J, Aminoff MJ, Bankiewicz KS (2012) Long-term evaluation of a phase 1 study of AADC gene therapy for Parkinson's disease. Human Gene Therapy 23:377–381.

Miyata T, Kawaguchi A, Saito K, Kawano M, Muto T, Ogawa M (2004) Asymmetric production of surface-dividing and non-surface-dividing cortical progenitor cells. Development 131:3133–3145.

Mizobuchi N, Hoseki J, Kubota H, Toyokuni S, Nozaki J-I, Naitoh M, Koizumi A, Nagata K (2007) ARMET is a soluble ER protein induced by the unfolded protein response via ERSE-II element. Cell Struct Funct 32:41–50.

Mogi M, Togari A, Kondo T, Mizuno Y, Komure O, Kuno S, Ichinose H, Nagatsu T (1999) Brain-derived growth factor and nerve growth factor concentrations are decreased in the substantia nigra in Parkinson's disease. Neuroscience Letters 270:45–48.

Molyneaux BJ, Arlotta P, Menezes JRL, Macklis JD (2007) Neuronal subtype specification in the cerebral cortex. Nat Rev Neurosci 8:427–437.

Montpied P, Bock F de, Baldy-Moulinier M, Rondouin G (1998) Alterations of metallothionein II and apolipoprotein J mRNA levels in kainate-treated rats. Neuroreport 9:79.

Moore MW, Klein RD, Fariñas I, Sauer H, Armanini M (1996) Renal and neuronal abnormalities in mice lacking GDNF. Nature 382:76–79.

Morgan T, Laping N, Rozovsky I, Oda T, Hogan TH, Finch CE, Pasinetti GM (1995) Clusterin expression by astrocytes is influenced by transforming growth factor β1 and heterotypic cell interactions. Journal of Neurimmunology 58:101–110.

Mowla SJ, Pareek S, Farhadi HF, Petrecca K, Fawcett JP, Seidah NG, Morris SJ, Sossin WS, Murphy RA (1999) Differential Sorting of Nerve Growth Factor and Brain-Derived Neurotrophic Factor in Hippocampal Neurons. J Neurosci 19:2069–2080.

Muramatsu S-I, Fujimoto K-I, Ikeguchi K, Shizuma N, Kawasaki K, Ono F, Shen Y, Wang L, Mizukami H, Kume A, Matsumura M, Nagatsu I, Urano F, Ichinose H, Nagatsu T, Terao K, Nakano I, Ozawa K (2002) Behavioral Recovery in a Primate Model of Parkinson's Disease by Triple Transduction of Striatal Cells with Adeno-Associated Viral Vectors Expressing Dopamine-Synthesizing Enzymes. Human Gene Therapy 13:345–354.

Muramatsu S-I, Fujimoto K-I, Kato S, Mizukami H, Asari S, Ikeguchi K, Kawakami T, Urabe M, Kume A, Sato T, Watanabe E, Ozawa K, Nakano I (2010) A Phase I Study of Aromatic L-Amino Acid Decarboxylase Gene Therapy for Parkinson's Disease. Nat Genet 18:1731–1735.

Nagahara AH, Merrill DA, Coppola G, Tsukada S, Schroeder BE, Shaked GM, Wang L, Blesch A, Kim A, Conner JM, Rockenstein E, Chao MV, Koo EH, Geschwind D, Masliah E, Chiba AA, Tuszynski MH (2009) Neuroprotective effects of brain-derived neurotrophic factor in rodent and primate models of Alzheimer's disease. Nat Med 15:331–337.

Nakayama T, Nakayama T, Inoue N (2003) Astrocyte-derived factors instruct differentiation of embryonic stem cells into neurons. Neuroscience research 46:241–249.

Namihira M, Kohyama J, Semi K, Sanosaka T, Deneen B, Taga T, Nakashima K (2009) Committed Neuronal Precursors Confer Astrocytic Potential on Residual Neural Precursor Cells. Developmental Cell 16:245–255.

Narayan P, Orte A, Clarke RW, Bolognesi B, Hook S, Ganzinger KA, Meehan S, Wilson MR, Dobson CM, Klenerman D (2012) The extracellular chaperone clusterin sequesters oligomeric forms of the amyloid-β1−40 peptide. Nat Struct Mol Biol 19:79–83.

Navab M, Anantharamaiah G, Reddy SR, Van Lenten BJ, Wagner AC, Hama S, Hough G, Bachini E, Garber DW, Mishra VK, Palgunachari MN, Fogelman A (2005) An Oral ApoJ Peptide Renders HDL Antiinflammatory in Mice and Monkeys and Dramatically Reduces Atherosclerosis in Apolipoprotein

E–Null Mice. Arteriosclerosis, Thrombosis and Vascular Biology 25:1932.1937.

Nayoung Kim WSC (2011) Proapoptotic role of nuclear clusterin in brain. Anatomy & Cell Biology 44:169.

Nguyen VH, Trout J, Connors SA, Andermann P, Weinberg E, Mullins MC (2000) Dorsal and intermediate neuronal cell types of the spinal cord are established by a BMP signaling pathway. Development 127:1209–1220.

Nichols J, Zevnik B, Anastassiadis K, Niwa H, Klewe-Nebenius D, Chambers I, Schöler H, Smith A (1998) Formation of Pluripotent Stem Cells in the Mammalian Embryo Depends on the POU Transcription Factor Oct4. Trends in Neurosciences 95:379–391.

Nishida E, Gotoh Y (1993) The MAP kinase cascade is essential for diverse signal transduction pathways. Trends in Biochemical Sciences 18:128–131.

Noctor SC, Flint AC, Weissman TA, Dammerman RS, Kriegstein AR (2001) Neurons derived from radial glial cells establish radial units in neocortex. Nat Cell Biol 409:714–720.

Noctor SC, Martínez-Cerdeño V, Ivic L, Kriegstein AR (2004) Cortical neurons arise in symmetric and asymmetric division zones and migrate through specific phases. Nat Neurosci 7:136–144.

Nottebohm F (2004) The road we travelled: discovery, choreography, and significance of brain replaceable neurons. Annals NY Acad Sci 1016:628-658.

Nutt JG, Burchiel KJ, Comella CL, Jankovic J, Lang AE, Laws ER, Lozano AM, Penn RD, Simpson RK, Stacy M, Wooten GF (2003) Randomized, double-blind trial of glial cell line-derived neurotrophic factor (GDNF) in PD. Neurology 60:69–73.

Nuutinen T, Huuskonen J, Suuronen T, Ojala J, Miettinen R, Salminen A (2007) Amyloid-β 1–42 induced endocytosis and clusterin/apoJ protein accumulation in cultured human astrocytes. Neurochemistry International 50:540–547.

O'Donnell D, Ahmad S, Wahlestedt C, Walker P (1999) Expression of the novel galanin receptor subtype GALR2 in the adult rat CNS: distinct distribution from GALR1. J Comp Neurol 409:469–481.

O'Meara G, Coumis U, Ma SY, Kehr J, Mahoney S, Bacon A, Allen SJ, Holmes F, Kahl U, Wang FH, Kearns IR, Ove-Ogren S, Dawbarn D, Mufson EJ, Davies C, Dawson G, Wynick D (2000) Galanin regulates the postnatal survival of a subset of basal forebrain cholinergic neurons. PNAS 97:11569–11574.

Oda T, Wals P, Osterburg HH, Johnson SA, Pasinetti GM, Morgan TE, Rozovsky I, Blaine Stine W, Snyder SW, Holzman TF, Krafft GA, Finch CE (1995) Clusterin (apoJ) Alters the Aggregation of Amyloid β-Peptide (Aβ1-42) and Forms Slowly Sedimenting Aβ Complexes That Cause Oxidative Stress. Experimental Neurology 136:22–31.

Oh I-H, Reddy EP (1999) The myb gene family in cell growth, differentiation and apoptosis. Oncogene 18:3017–3033.

Olalla JS, Covarrubias L (1999) Basic fibroblast growth factor promotes epidermal growth factor responsiveness and survival of mesencephalic neural precursor cells. Journal of neurobiology 40:14–27.

Olsson T, Nygren J, Hakansson K, Lundblad C, Grubb A, Smith M-L, Wieloch T (2004) Gene deletion of cystatin C aggravates brain damage following focal ischemia but mitigates the neuronal injury after global ischemia in the mouse. Neuroscience 128:65–71.

Oosthuyse B et al. (2001) Deletion of the hypoxia-response element in the vascular endothelial growth factor promoter causes motor neuron degeneration - Nature Genetics. Nat Genet 28:131–138.

Ostenfeld T, Joly E, Tai Y, Peters A, Caldwell MA, Jauniaux E, Svendsen CN (2002) Regional specification of rodent and human neurospheres. Developmental Brain Research 134:43–55.

Palfi S, Leventhal L, Chu Y, Ma SY, Emborg M, Bakay R, Déglon N, Hantraye P, Aebischer P, Kordower JH (2002) Lentivirally Delivered Glial Cell Line-Derived Neurotrophic Factor Increases the Number of Striatal Dopaminergic Neurons in Primate Models of Nigrostriatal Degeneration. The Journal of Neuroscience 22:4942–4954.

Palgi M, Lindström R, Peränen J, Piepponen TP, Saarma M, Heino TI (2009) Evidence that DmMANF is an invertebrate neurotrophic factor supporting dopaminergic neurons. PNAS 106:2429–2434.

Palmieri SL, Peter W, Hess H, Schöler HR (1994) Oct-4 Transcription Factor Is Differentially Expressed in the Mouse Embryo during Establishment of the First Two Extraembryonic Cell Lineages Involved in Implantation. Developmental Biology 166:259–267.

Pan-Montojo F, Anichtchik O, Dening Y, Knels L, Pursche S, Jung R, Jackson S, Gille G, Spillantini MG, Reichmann H, Funk RHW (2010) Progression of Parkinson's Disease Pathology Is Reproduced by Intragastric Administration of Rotenone in Mice. PLoS ONE 5:e8762.

Parkash V, Lindholm P, Peränen J, Kalkkinen N, Oksanen E, Saarma M, Leppänen V-M, Goldman A (2009) The structure of the conserved neurotrophic factors MANF and CDNF explains why they are bifunctional. Protein Eng Des Sel 22:233–241.

Pasinetti GM, Johnson S, Oda T, Rozovsky I, Finch CE (1994) Clusterin (SGP-2): A multifunctional glycoprotein with regional expression in astrocytes and neurons of the adult rat brain. J Comp Neurol 339:387–400.

Petreanu L, Alvarez-Buylla A (2002) Maturation and Death of Adult-Born Olfactory Bulb Granule Neurons: Role of Olfaction. The Journal of Neuroscience 22:6106–6113.

Petrova PS, Raibekas A, Pevsner J, Vigo N, Anafi M, Moore MK, Peaire AE, Shridhar V, Smith DI, Kelly J, Durocher Y, Commissiong JW (2003) MANF: A New Mesencephalic, Astrocyte-Derived Neurotrophic Factor

with Selectivity for Dopaminergic Neurons. Journal of Molecular Neuroscience 20:173–188.

Pérez SE, Wynick D, Steiner RA, Mufson EJ (2001) Distribution of galaninergic immunoreactivity in the brain of the mouse. J Comp Neurol 434:158–185.

Pfrieger FW, Barres B (1997) Synaptic Efficacy Enhanced by Glial Cells in Vitro. Science 277:1684–1687.

Pihlaja R, Koistinaho J, Kauppinen R, Sandholm J, Tanila H, Koistinaho M (2011) Multiple cellular and molecular mechanisms Are involved in human Aβ clearance by transplanted adult astrocytes. Glia 59:1643–1657.

Pirondi S, Giuliani A, Del Vecchio G, Giardino L, Hökfelt T, Calzà L (2009) The galanin receptor 2/3 agonist Gal2-11 protects the SN56 cells against β-amyloid 25-35 toxicity. J Neurosci Res 88:1064–1073.

Planas B, Kolb PE, Raskind MA, Miller MA (1997) Nerve growth factor induces galanin gene expression in the rat basal forebrain: implications for the treatment of cholinergic dysfunction. J Comp Neurol 379:563–570.

Polymeropoulos MH et al. (1997) Mutation in the α-Synuclein Gene Identified in Families with Parkinson's Disease. Science 276:2045–2047.

Poon S, Easterbrook-Smith SB, Rybchyn MS, Carver JA, Wilson MR (2000) Clusterin Is an ATP−Independent Chaperone with Very Broad Substrate Specificity that Stabilizes Stressed Proteins in a Folding-Competent State †. Biochemistry 39:15953–15960.

Qian X, Shen Q, Goderie SK, He W, Capela A, Davis AA, Temple S (2000) Timing of CNS Cell Generation: A Programmed Sequence of Neuron and Glial Cell Production from Isolated Murine Cortical Stem Cells. Neuron 28:69–80.

Qiu Z, Strickland DK, Hyman BT, Rebeck GW (2002) α2-Macroglobulin Enhances the Clearance of Endogenous Soluble β-Amyloid Peptide via Low-Density Lipoprotein Receptor-Related Protein in Cortical Neuron. J Neurochem 73:1393–1398.

Rakic P (1972) Mode of cell migration to the superficial layers of fetal monkey neocortex. J Comp Neurol 145:61–83.

Reddy KB, Jin G, Karode MC, Harmony JAK, Howe PH (1996) Transforming Growth Factor β (TGFβ)-Induced Nuclear Localization of Apolipoprotein J/Clusterin in Epithelial Cells †. Biochemistry 35:6157–6163.

Reichardt LF (2006) Neurotrophin-regulated signalling pathways. Philosophical Transactions of the Royal Society B: Biological Sciences 361:1545–1564.

Ren J, Koenig JI, Hooi SC (1999) Stimulation of anterior pituitary galanin and prolactin gene expression in sucking rats. Endocrine 11:251–256.

Reynolds BA, Tetzlaff W, Weiss S (1992) A multipotent EGF-responsive striatal embryonic progenitor cell produces neurons and astrocytes. The Journal of Neuroscience 12:4565–4574.

Reynolds BA, Weiss S (1996) Clonal and population analyses demonstrate that an EGF-responsive mammalian embryonic CNS precursor is a stem cell. Developmental Biology 175:1–13.

Ridet JL, Privat A, Malhotra SK, Gage FH (1997) Reactive astrocytes: cellular and molecular cues to biological function. Trends in Neurosciences 20:570-577.

Rios I, Alvarez-Rodríguez R, Martí E, Pons S (2004) Bmp2 antagonizes sonic hedgehog-mediated proliferation of cerebellar granule neurones through Smad5 signalling. Development 131:3159–3168.

Roky R, Paut-Pagano L, Goffiri V, Kitahama K, Valatx J-L, Kelly PA, Jouvet M (1996) Distribution of Prolactin Receptors in the Rat Forebrain. Neuroendocrinology 63:422–429.

Rosenberg M, Girton R, Finkel D, Chmielewski D, Barrie A, Witte DP, Zhu G, Bissler JJ, Harmony JAK, Aronow BJ (2002) Apolipoprotein J/Clusterin Prevents a Progressive Glomerulopathy of Aging. Molecular and Cellular Biology 22:1893–1902.

Rosenblad C, Martinez-Serrano A, Björklund A (1996) Glial cell line-derived neurotrophic factor increases survival, growth and function of intrastriatal fetal nigral dopaminergic grafts. Neuroscience 75:979–985.

Rosenblad C, Martinez-Serrano A, Björklund A (1997) Intrastriatal glial cell line-derived neurotrophic factor promotes sprouting of spared nigrostriatal dopaminergic afferents and induces recovery of function in a rat model of Parkinson's disease. Neuroscience 82:129–137.

Rossi C, Angelucci A, Costantin L, Braschi C, Mazzantini M, Babbini F, Fabbri ME, Tessarollo L, Maffei L, Berardi N, Caleo M (2006) Brain-derived neurotrophic factor (BDNF) is required for the enhancement of hippocampal neurogenesis following environmental enrichment. Eur J Neurosci 24:1850–1856.

Rowitch DH, McMahon AP (1995) Pax-2 expression in the murine neural plate precedes and encompasses the expression domains of Wnt-1 and En-1. Mechanisms of Development 52:3–8.

Ruberti F, Capsoni S, Comparini A, Di Daniel E, Franzot J, Gonfloni S, Rossi G, Berardi N, Cattaneo A (2000) Phenotypic Knockout of Nerve Growth Factor in Adult Transgenic Mice Reveals Severe Deficits in Basal Forebrain Cholinergic Neurons, Cell Death in the Spleen, and Skeletal Muscle Dystrophy. The Journal of Neuroscience 20:2589–2601.

Sachs HH, Wynick D, Zigmond RE (2007) Galanin plays a role in the conditioning lesion effect in sensory neurons. Neuroreport 18:1729–1733.

Sagare AP, Bell RD, Zlokovic BV (2012) Neurovascular Dysfunction and Faulty Amyloid Peptide Clearance in Alzheimer Disease. Cold Harbor Perspectives in Medicine:1–17

Sakamoto M, Imayoshi I, Ohtsuka T, Yamaguchi M, Mori K, Kageyama R (2011) Continuous neurogenesis in the adult forebrain is required for innate olfactory responses. PNAS 108:8479–8484.

Samii A, Nutt JG, Ransom BR (2004) Parkinson's disease. Neuron 363:1783–1793.

Santa-Olalla J, Baizabal J-M, Fregoso M, del Carmen Cardenas M, Covarrubias L (2003) The in vivo positional identity gene expression code is not preserved in neural stem cells grown in culture. Eur J Neurosci 18:1073–1084.

Sariola H, Saarma M (2003) Novel functions and signalling pathways for GDNF. Journal of Cell Science 116:3855–3862.

Sasai Y (2001) Roles of Sox factors in neural determination: conserved signaling in evolution? International Journal of Developmental Biology 45:321–326.

Sasaki K, Doh-ura K, Ironside JW, Iwaki T (2002) Increased clusterin (apolipoprotein J) expression in human and mouse brains infected with transmissible spongiform encephalopathies. Acta neuropathologica 103:199–208.

Sastre M, Calero M, Pawlik M, Mathews P, Kumar A, Danilov V, Schmidt SD, Nixon RA, Frangione B, Levy E (2004) Binding of cystatin C to Alzheimer's amyloid β inhibits in vitro amyloid fibril formation. Neurobiology of Aging 25:1033–1043.

Sauka-Spengler T, Bronner-Fraser M (2008) A gene regulatory network orchestrates neural crest formation. Nat Rev Mol Cell Biol 9:557–568.

Saura J, Petegnief V, Wu X, Liang Y, Paul SM (2003) Microglial apolipoprotein E and astroglial apolipoprotein J expression in vitro: opposite effects of lipopolysaccharide. J Neurochem 85:1455–1467.

Sawada H, Ibi M, Kihara T, Urushitani M, Nakanishi M, Akaike A, Shimohama S (2003) Neuroprotective Mechanism of Glial Cell Line-Derived Neurotrophic Factor in Mesencephalic Neurons. J Neurochem 74:1175-1184.

Scharfman H, Goodman J, Macleod A, Phani S, Antonelli C, Croll S (2005) Increased neurogenesis and the ectopic granule cells after intrahippocampal BDNF infusion in adult rats. Experimental Neurology 192:348–356.

Scharfman HE (2004) Functional Implications of Seizure-Induced Neurogenesis. Advances in experimental medicine and biology 548:192.

Schauwecker PE (2010) Galanin Receptor 1 Deletion Exacerbates Hippocampal Neuronal Loss after Systemic Kainate Administration in Mice. PLoS ONE 5:e15657.

Schmidt WE, Kratzin H, Eckart K, Drevs D, Mundkowski G, Clemens A, Katsoulis S, Schäfer H, Gallwitz B, Creutzfeldt W (1991) Isolation and primary structure of pituitary human galanin, a 30-residue nonamidated neuropeptide. PNAS 15:11435–11439.

Seri B, García-Verdugo JM, McEwen BS, Alvarez-Buylla A (2001) Astrocytes Give Rise to New Neurons in the Adult Mammalian Hippocampus. The Journal of Neuroscience 21:7153–7160.

Shayo M, McLay RN, Kastin AJ, Banks WA (1997) The putative blood-brain barrier transporter for the β-amyloid binding protein apolipoprotein j is saturated at physiological concentrations. Life Sciences 60:PL115–PL118.

Shen P-J, Larm JA, Gundlach A (2003) Expression and plasticity of galanin systems in cortical neurons, oligodendrocyte progenitors and proliferative

zones in normal brain and after spreading depression. Eur J Neurosci 18:1362–1376.

Shen PJ, Yuan CG, Ma J, Cheng S, Yao M, Turnley AM, Gundlach A (2005) Galanin in neuro(glio)genesis: expression of galanin and receptors by progenitor cells in vivo and in vitro and effects of galanin on neurosphere proliferation. Neuropeptides 39:201–205.

Shen Q, Goderie SK, Jin L, Karanth N, Sun Y, Abramova N, Vincent P, Pumiglia K, Temple S (2004) Endothelial Cells Stimulate Self-Renewal and Expand Neurogenesis of Neural Stem Cells. Science 304:1338–1340.

Shen Q, Wang Y, Dimos JT, Fasano CA, Phoenix TN, Lemischka IR, Ivanova NB, Stifani S, Morrisey EE, Temple S (2006) The timing of cortical neurogenesis is encoded within lineages of individual progenitor cells. Nat Neurosci 9:743–751.

Sherwood CC, Stimpson CD, Raghanti MA, Wildman DE, Uddin M, Grossman LI, Goodman M, Redmond JC, Bonar CJ, Erwin JM, Hof PR (2006) Evolution of increased glia–neuron ratios in the human frontal cortex. PNAS 103º37.

Shimazu K, Zhao M, Sakata K, Akbarian S, Bates B, Jaenisch R, Lu B (2006) NT-3 facilitates hippocampal plasticity and learning and memory by regulating neurogenesis. Learning & Memory 13:307–315.

Shimizu N, Kitada T, Asakawa S, Hattori N, Matsumine H, Yamamura Y, Minoshima S, Yokochi M, Mizuno Y (1998) Mutations in the : parkin: gene cause autosomal recessive juvenile parkinsonism. Nature 392:605–608.

Shingo T, Gregg C, Enwere E, Fujikawa H, Hassam R, Geary C, Cross JC, Weiss S (2003) Pregnancy-Stimulated Neurogenesis in the Adult Female Forebrain Mediated by Prolactin. Science 299:177–120.

Shults CW, Kimber T, Martin D (1996) Intrastriatal injection of GDNF attenuates the effects of 6-hydroxydopamine. Neuroreport 7:627–631.

Siemers E, Skinner M, Dean RA, Gonzales C, Satterwhite J, Farlow M, Ness D, May PC (2005) Safety, Tolerability, and Changes in Amyloid [beta] Concentrations After Administration of a [gamma]-Secretase Inhibitor in Volunteers. Clinical Neuropharmacology 28:126.

Simeone A, Acampora D, Gulisano M, Stornaiuolo A, Boncinelli E (1992) Nested expression domains of four homeobox genes in developing rostral brain. Nat Cell Biol 358:687–690.

Singleton AB et al. (2003) α-Synuclein Locus Triplication Causes Parkinson's Disease. Science 302:841–841.

Slevin JT, Gash DM, Smith CD, Gerhardt GA (2007) Unilateral intraputamenal glial cell line–derived neurotrophic factor in patients with Parkinson disease: response to 1 year of treatment and 1 year of withdrawal. The Journal of Neuroscience 106:614–620.

Smeyne RJ, Klein R, Schnapp A, Long LK, Bryant S, Lewin A, Lira SA, Barbacid M (1994) Severe sensory and sympathetic neuropathies in mice carrying a disrupted Trk/NGF receptor gene. Nat Cell Biol 368:246–249.

Smith DE, Roberts J, Gage FH, Tuszynski MH (1999) Age-associated neuronal atrophy occurs in the primate brain and is reversible by growth factor gene therapy. PNAS 96:10893–10898.

Smith K (2010) Neuroscience: Settling the great glia debate. Nature 468:160–162.

Sondell M, Sundler F, Kanje M (2008) Vascular endothelial growth factor is a neurotrophic factor which stimulates axonal outgrowth through the flk-1 receptor. European Journal of Neuroscience 12:4243–4254.

Song H, Stevens CF, Gage FH (2002) Astroglia induce neurogenesis from adult neural stem cells. Nature 417:39–44.

Soppet D, Escandon E, Maragos J, Middlemas DS, Raid SW, Blair J, Burton LE, Stanton BR, Kaplan DR, Hunter T, Nikolics K, Parade LF (1991) The neurotrophic factors brain-derived neurotrophic factor and neurotrophin-3 are ligands for the trkB tyrosine kinase receptor. Trends in Neurosciences 65:895–903.

Spillantini MG, Schmidt ML, Lee VM-Y, Trojanowski JQ, Jakes R, Goedert M (1997) |[alpha]|-Synuclein in Lewy bodies. Nature 388:839–840.

Stanic D, Kuteeva E, Nylander I, Hökfelt T (2010) Characterization of CGRP protein expression in “satellite-like” cells and dendritic arbours of the mouse olfactory bulb. J Comp Neurol 518:770–784.

Stanic D, Paratcha G, Ledda F, Herzog H, Kopin AS, Hökfelt T (2008) Peptidergic influences on proliferation, migration, and placement of neural progenitors in the adult mouse forebrain. PNAS 105:3610–3615.

Stankoff B, Aigrot M-S, Noël F, Wattilliaux A, Zalc B, Lubetzki C (2002) Ciliary neurotrophic factor (CNTF) enhances myelin formation: a novel role for CNTF and CNTF-related molecules. J Neurosci 22:9221–9227.

Steiner RA, Hohmann JG, Holmes A, Wrenn CC, Cadd G, Jureus A, Clifton DK, Luo M, Gutshall M, Ma SY, Mufson EJ, Crawley JN (2001) Galanin transgenic mice display cognitive and neurochemical deficits characteristic of Alzheimer's disease. PNAS 98:4184–4189.

Stöckli KA, Lillien LE, Näher-Noé M, Breitfeld G, Hughes RA, Raff MC, Thoenen H, Sendtner M (1991) Regional distribution, developmental changes, and cellular localization of CNTF-mRNA and protein in the rat brain. J Cell Biol 115:447–459.

Suh Y-H, Checler F (2002) Amyloid Precursor Protein, Presenilins, and α-Synuclein: Molecular Pathogenesis and Pharmacological Applications in Alzheimer's Disease. Pharmacological Reviews 54:470–512.

Sun Z-P, Gong L, Huang S-H, Geng Z, Cheng L, Chen Z-Y (2011) Intracellular trafficking and secretion of cerebral dopamine neurotrophic factor in neurosecretory cells. J Neurochem 117:121–132.

Svendsen CN, Borg ter MG, Armstrong RJ, Rosser AE, Chandran S, Ostenfeld T, Caldwell MA (1998) A new method for the rapid and long term growth of human neural precursor cells. J Neurosci Methods 85:141–152.

Takahashi T, Nowakowski RS, Caviness VS (1993) Cell cycle parameters and patterns of nuclear movement in the neocortical proliferative zone of the fetal mouse. The Journal of Neuroscience 13:820–833.

Takizawa T, Nakashima K, Namihira M, Ochiai W, Uemura A, Yanagisawa M, Fujita N, Nakao M, Taga T (2001) DNA Methylation Is a Critical Cell-Intrinsic Determinant of Astrocyte Differentiation in the Fetal Brain. Developmental Cell 1:749–758.

Tanaka JI, Horiike Y, Matsuzaki M, Miyazaki T, Ellis-Davies GCR, Kasai H (2008) Protein Synthesis and Neurotrophin-Dependent Structural Plasticity of Single Dendritic Spines. Science 319:1683–1687.

Tarasov KV, Tarasova YS, Crider DG, Anisimov SV, Wobus AM, Boheler KR (2002) Galanin and galanin receptors in embryonic stem cells: accidental or essential? Neuropeptides 36:239–245.

Tatemoto K, Rökaeus A, Jörnvall H, McDonald TJ, Mutt V (1983) Galanin — a novel biologically active peptide from porcine intestine. FEBS Lett 164:124–128.

Tatemoto K, Siimesmaa S, Jörnvall H, Allen JM, Polak JM, Bloom SR, Mutt V (1985) Isolation and characterization of neuropeptide Y from porcine intestine. FEBS Lett 179:181–184.

Taupin P, Ray J, Fischer WH, Suhr ST, Hakansson K, Grubb A, Gage FH (2000) FGF-2-Responsive Neural Stem Cell Proliferation Requires CCg, a Novel Autocrine/Paracrine Cofactor. Neuron 28:385–397.

Tebar F, Bohlander SK, Sorkin A (1999) Clathrin Assembly Lymphoid Myeloid Leukemia (CALM) Protein: Localization in Endocytic-coated Pits, Interactions with Clathrin, and the Impact of Overexpression on Clathrin-mediated Traffic. Molecular Biology of the Cell 10:2687.

Theofilopoulos S, Goggi J, Riaz SS, Jauniaux E, Stern GM, Bradford HF (2001) Parallel induction of the formation of dopamine and its metabolites with induction of tyrosine hydroxylase expression in foetal rat and human cerebral cortical cells by brain-derived neurotrophic factor and glial-cell derived neurotrophic factor. Developmental Brain Research 127:111–122.

Thiriet N, Agasse F, Nicoleau C, Guégan C, Vallette F, Cadet J-L, Jaber M, Malva JO, Coronas V (2011) NPY promotes chemokinesis and neurogenesis in the rat subventricular zone. J Neurochem 116:1018–1027.

Thomas P, Beddington R (1996) Anterior primitive endoderm may be responsible for patterning the anterior neural plate in the mouse embryo. Current Biology 6:1487–1496.

Thomas T, Thomas G, McLendon C, Sutton T, Mullan M (1996) β-Amyloid-mediated vasoactivity and vascular endothelial damage. Nature 380:168–171.

Tropepe V, Sibilia M, Ciruna BG, Rossant J, Wagner EF, van der Kooy D (1999) Distinct neural stem cells proliferate in response to EGF and FGF in the developing mouse telencephalon. Developmental Biology 208:166–188.

Tsai H-H, Li HL, Fuentealba LC, Molofsky AV, Taveira-Marques R, Zuang H, Tenney A, Murnen AT, Fancy SPJ, Merkle F, Kessaris N, Alvarez-Buylla A, Richardson WD, Rowitch DH (2012) Regional Astrocyte Allocation Regulates CNS Synaptogenesis and Repair. Science 337:358–361

Turner DL, Cepko CL (1987) A common progenitor for neurons and glia persists in rat retina late in development. Nat Cell Biol 328:131–136.

Tuszynski MH, Thal L, Pay M, Salmon DP (2005) A phase 1 clinical trial of nerve growth factor gene therapy for Alzheimer disease. Nat Med 11:551-555.

Uchikawa M, Yoshida M, Iwafuchi-Doi M, Matsuda K, Ishida Y, Takemoto T, Kondoh H (2011) B1 and B2 Sox gene expression during neural plate development in chicken and mouse embryos: Universal versus species-dependent features. Development, Growth & Differentiation 53:761–771.

Ullian EM, Sapperstein SK, Christopherson KS, Barres B (2001) Control of Synapse Number by Glia. Science 291:657–661.

Valente EM et al. (2004) Hereditary Early-Onset Parkinson's Disease Caused by Mutations in PINK1. Science 304:1158–1160.

Van Praag H, Kempermann G, Gage FH (1999) Running increases cell proliferation and neurogenesis in the adult mouse dentate gyrus. Nat Neurosci 2:266–270.

Vargas T, Bullido MJ, Martínez García A, Antequera D, Clarimon J, Rosich-Estrago M, Martin-Requero A, Maeto I, Rodriguez-Rodriguez E, Cuadrada EV, Frank A, Lleo A, Molina-Porcel L, Blesa R, Combarros O, Gomez-Isla T, Bermejo-Pareja F, Valdivieso F, Carro E (2010) A Megalin Polymorphism Associated With Promoter Activity and Alzheimer's Disease Risk. American Journal of Medical Genetics 153:895–902.

Voutilainen MH, Bäck S, Peränen J, Lindholm P, Raasmaja A, Männistö PT, Saarma M, Tuominen RK (2011) Chronic infusion of CDNF prevents 6-OHDA-induced deficits in a rat model of Parkinson's disease. Experimental Neurology 228:99–108.

Voutilainen MH, Bäck S, Pörsti E, Toppinen L, Lindgren L, Lindholm P, Peränen J, Saarma M, Tuominen RK (2009) Mesencephalic astrocyte-derived neurotrophic factor is neurorestorative in rat model of Parkinson's disease. The Journal of Neuroscience 29:9651–9659.

Wagner B, Natarajan A, Grünaug S, Kroismayr R, Wagner EF, Sibilia M (2006) Neuronal survival depends on EGFR signaling in cortical but not midbrain astrocytes. EMBO J 25:752–762.

Walz W (2000) Role of astrocytes in the clearance of excess extracellular potassium. Neurochemistry International 36:291–300.

Wang HY, Wild KD, Shank RP, Lee DH (1999) Galanin inhibits acetylcholine release from rat cerebral cortex via a pertussis toxin-sensitive G(i)protein. Neuropeptides 33:197–205.

Wang X, Lou N, Xu Q, Tian G-F, Peng WG, Han X, Kang J, Takano T, Nedergaard M (2006) Astrocytic Ca2+ signaling evoked by sensory stimulation in vivo. Nat Neurosci 9:816–823.

Wang Y, Ou Mao X, Xie L, Banwait S, Marti HH, Greenberg DA, Jin K (2007) Vascular Endothelial Growth Factor Overexpression Delays Neurodegeneration and Prolongs Survival in Amyotrophic Lateral Sclerosis Mice. The Journal of Neuroscience 27:304–307.

Wassarman KM, Lewandoski M, Campbell K, Joyner AL, Rubenstein JL, Martinez S, Martin GR (1997) Specification of the anterior hindbrain and establishment of a normal mid/hindbrain organizer is dependent on Gbx2 gene function. Development 124:2923–2934.

Wilson PA, Hemmati-Brivanlou A (1995) Induction of epidermis and inhibition of neural fate by Bmp-4. Nat Cell Biol 376:331–333.

Wraith DC, Pope R, Butzkueven H, Holder H, Vanderplank P, Lowrey P, Day MJ, Gundlach A, Kilpatrick TJ, Scolding N, Wynick D (2009) A role for galanin in human and experimental inflammatory demyelination. PNAS 106:15466–15471.

Wrenn CC, Harris AP, Saavedra MC, Crawley JN (2003) Social transmission of food preference in mice: Methodology and application to galanin-overexpressing transgenic mice. Behavioral Neuroscience 117:21–31.

Wrenn CC, Marriott LK, Kinney JW, Holmes A, Wenk GL, Crawley JN (2002) Galanin peptide levels in hippocampus and cortex of galanin-overexpressing transgenic mice evaluated for cognitive performance. Neuropeptides 36:413–426.

Wu X, Yu Y, Guo H, Shen Y, Zhou C, Paraoan L, Zhou J (2005) Cystatin C prevents degeneration of rat nigral dopaminergic neurons: in vitro and in vivo studies. Neurobiol Dis 18:152–165.

Wurst W, Bally-Cuif L (2001) Neural plate patterning: upstream and downstream of the isthmic organizer. Nat Rev Neurosci 2:99–108.

Wyatt AR, Yerbury JJ, Berghofer P, Greguric I, Katsifis A, Dobson CM, Wilson MR (2011) Clusterin facilitates in vivo clearance of extracellular misfolded proteins. Cell Mol Life Sci 68:3919–3931.

Wynick D, Hammond PJ, Akinsanya KO, Bloom SR (1993) Galanin regulates basal and oestrogen-stimulated lactotroph function. Nature 364:529–532.

Wynick D, Small CJ, Bacon A, Holmes FE, Norman M, Ormandy CJ, Kilic E, Kerr NCH, Ghatei M, Talamantes F, Bloom SR, Pachnis V (1998) Galanin regulates prolactin release and lactotroph proliferation. PNAS 95:12671-12676.

Wyss-Coray T, Loike JD, Brionne TC, Lu E, Anankov R, Yan F, Silverstein SC, Husemann J (2003) Adult mouse astrocytes degrade amyloid-β in vitro and in situ. Nat Med 9:453–457.

Xing B, Xin T, Zhao L, Hunter RL, Chen Y, Bing G (2010) Glial cell line-derived neurotrophic factor protects midbrain dopaminergic neurons against lipopolysaccharide neurotoxicity. Journal of Neuroimmunology 225:43–51.

Xu Q, Bernardo A, Walker D, Kanegawa T, Mahley RW, Huang Y (2006) Profile and regulation of apolipoprotein E (ApoE) expression in the CNS in mice with targeting of green fluorescent protein gene to the ApoE locus. The Journal of Neuroscience 26:4985–4994.

Yagita Y, Kitagawa K, Ohtsuki T, Takasawa K-I, Miyata T, Okano H, Hori M, Matsumoto M (2001) Neurogenesis by Progenitor Cells in the Ischemic Adult Rat Hippocampus. Stroke 32:1890–1896.

Yamada K, Mizuno M, Nabeshima T (2002) Role for brain-derived neurotrophic factor in learning and memory. Life Sciences 70:735–744.

Yasuhara O, Hanai K, Ohkubo I, Sasaki M, McGeer PL, Kimura H (1993) Expression of cystatin C in rat, monkey and human brains. Brain Research 628:85–92.

Yeh T-H, Lee DY, Gianino SM, Gutmann DH (2009) Microarray analyses reveal regional astrocyte heterogeneity with implications for neurofibromatosis type 1 (NF1)-regulated glial proliferation. Glia 57:1239–1249.

Yoshitake T, Wang F-H, Kuteeva E, Holmberg K, Yamaguchi M, Crawley JN, Steiner R, Bartfai T, Ogren SO, Hökfelt T, Kehr J (2004) Enhanced hippocampal noradrenaline and serotonin release in galanin-overexpressing mice after repeated forced swimming test. PNAS 101:354–359.

Yu Y-Q, Liu L-C, Wang F-C, Liang Y, Cha D-Q, Zhang J-J, Shen Y-J, Wang H-P, Fang S, Shen Y-X (2010) Induction profile of MANF/ARMET by cerebral ischemia and its implication for neuron protection. J Cereb Blood Flow Metab 30:79–91.

Zappone MV, Galli R, Catena R, Meani N, De Biasi S, Mattei E, Tiveron C, Vescovi AL, Lovell-Badge R, Ottonlenghi S, Nicolis SK (2000) Sox2 regulatory sequences direct expression of a β-geo transgene to telencephalic neural stem cells and precursors of the mouse embryo, revealing regionalization of gene expression in CNS stem cells. Development 127:2367–2382.

Zhang H, Kim JK, Edwards CA, Xu Z, Taichman R, Wang C-Y (2005) Clusterin inhibits apoptosis by interacting with activated Bax. Nat Cell Biol 7:909–915.

Zhang L, Yu W, Schroedter I, Kong J, Vrontakis M (2012) Galanin Transgenic Mice with Elevated Circulating Galanin Levels Alleviate Demyelination in a Cuprizone-Induced MS Mouse Model. PLoS ONE 7.

Zhang R, Zhang Z, Zhang C, Zhang L, Robin A, Wang Y, Lu M, Chopp M (2004) Stroke Transiently Increases Subventricular Zone Cell Division from Asymmetric to Symmetric and Increases Neuronal Differentiation in the Adult Rat. J Neurosci 24:5810–5815.

Zhao C, Deng W, Gage FH (2008) Mechanisms and Functional Implications of Adult Neurogenesis. Cell 132:645.660.

Zhou C, Xiao C, Commissiong JW, Krnjević K, Ye JH (2006) Mesencephalic astrocyte-derived neurotrophic factor enhances nigral gamma-aminobutyric acid release. Neuroreport 17:293–297.

Zimprich A et al. (2004) Mutations in LRRK2 Cause Autosomal-Dominant Parkinsonism with Pleomorphic Pathology. Neuron 44:601–607.

Zlokovic BV, Martel CL, Matsubara E, McComb JG, Zheng G, McCluskey RT, Frangione B, Ghiso JJ (1996) Glycoprotein 330/megalin: probable role in receptor-mediated transport of apolipoprotein J alone and in a complex with Alzheimer disease amyloid beta at the blood-brain and blood-cerebrospinal fluid barriers. PNAS 93:4229–4234.

Zufferey R, Donello JE, Trono D, Hope TJ (1999) Woodchuck Hepatitis Virus Posttranscriptional Regulatory Element Enhances Expression of Transgenes Delivered by Retroviral Vectors. Journal of Virology 73:2886–2892.

Apendix

APENDIX A List of Buffers

RIPA buffer

	CONCENTRATION	SUPPLIER
Igepal CA-630	**1%**	**Sigma**
Sodium Deoxycholate	**0.5%**	**Sigma**
SDS	**0.1%**	**Sigma**
Complete MINI (EDTA-free)	**1 tablet / 10ml**	**Roche**
PBS	**Final volume**	**Gibco**

Western Blot 5x Loading Dye

	CONCENTRATION	SUPPLIER
1M Tris pH6.8	**300mM**	**Melford**
Glycerol	**50%**	**Sigma**
SDS	**10%**	**Sigma**
Bromophenol Blue	**0.5%**	**Sigma**
ddH_20	**Up to 25ml**	

Western Blot 10x Running Buffer pH8.3

	CONCENTRATION	SUPPLIER
Tris Base	**250mM**	**Melford**
Glycine	**1.9M**	**Melford**
SDS	**0.5%**	**Sigma**
ddH_20	**Final volume**	

Western Blot 10x Wet Transfer Buffer pH8.3 (no methanol)

	CONCENTRATION	SUPPLIER
Tris Base	48mM	Melford
Glycine	39mM	Melford
SDS	0.037%	Sigma
ddH20	Final volume	

Western Blot 10x Tris Buffer Saline pH7.5 (10x TBS)

	CONCENTRATION		SUPPLIER
Tris Base	**200mM**	**4.72g**	**Melford**
Tris HCl		**25.4g**	**Melford**
NaCl	**1.5M**		**Melford**
ddH_20	**Up to 1l**		

Western Blot 1x TBS-T 0.1%

	CONCENTRATION	SUPPLIER
10x TBS	**200ml**	
Tween 20	**2ml**	**Sigma**
ddH_20	**Up to 2l**	

TUNEL assay 1x Permeabilisation Buffer

	CONCENTRATION	SUPPLIER
0.1M Sodium Citrate pH6.0	**0.1%**	**Sigma**
Triton X-100	**0.1%**	**Sigma**
ddH_20	**Final volume**	

HBS (Hepes buffered saline) pH7.05

	CONCENTRATION	SUPPLIER
HEPES	**50mM**	**Sigma**
NaCl	**280mM**	**Melford**
Na_2HPO_4	**1.5mM**	**Sigma**
ddH_20	**Final volume**	

TSSM buffer

	CONCENTRATION	SUPPLIER
Tromethamine	**20mM**	**Sigma**
NaCl	**100mM**	**Melford**
Sucrose	**1%**	**Melford**
D-Mannitol	**1%**	**Melford**
ddH_20	**final volume**	

Maxiprep: Solution I

	CONCENTRATION	SUPPLIER
Glucose	**50mM**	**Melford**
1M Tris pH8.0	**25mM**	**Melford**
0.5M EDTA pH8.0	**10mM**	**Sigma**
ddH_20	**Final volume**	

Maxiprep: Solution II

	CONCENTRATION	SUPPLIER
NaOH	**200mM**	**Melford**
SDS	**1%**	**Melford**
ddH_20	**Final volume**	

Maxiprep: Solution III

	CONCENTRATION	SUPPLIER
CH_3CO_2K	**3M**	**Melford**
CH_3CO_2H	**2M**	**Fisher**
ddH_20	**Final volume**	

Maxiprep: Tris-EDTA buffer

	CONCENTRATION	SUPPLIER
1M Tris pH8.0	**10mM**	**Melford**
0.5M EDTA pH8.0	**0.1mM**	**Sigma**
ddH_20	**Final volume**	

Antifreeze solution

	CONCENTRATION	SUPPLIER
Ethylene glycol	**30%**	**Sigma**
Glycerol	**30%**	**Sigma**
Na_2HPO_4	**3.8mM**	**Sigma**
NaH_2PO_4	**1.3mM**	**Sigma**
NaN_3	**0.01%**	**Sigma**
ddH_20	**Final volume**	

6X DNA Loading dye

	CONCENTRATION	SUPPLIER
Glycerol	**30%**	**Sigma**
Orange G	**0.09%**	**Sigma**
Xylene Cyanol / Bromophenol Blue / Cresol red	**0.09%**	**Sigma**

APENDIX B Culture Media

E. coli: LB-broth

	CONCENTRATION	SUPPLIER
LB-mixture	**25g·l^{-1}**	**Difco**
NaOH	**1mM**	**Melford**
ddH_20	**Up to 1l**	

E. coli: Solid LB

	CONCENTRATION	SUPPLIER
LB-mixture	**25g·l^{-1}**	**Difco**
Agar	**15g·l^{-1}**	**Difco**
NaOH	**1mM**	**Sigma**

E. coli: SOCs medium pH 7.0

	CONCENTRATION	SUPPLIER
Bacto-tryptone	**20 g/l**	**Difco**
Yeast extract	**5 g/l**	**Difco**
NaCl	**2.5mM**	**Melford**
$MgCl_2$	**10mM**	**Sigma**
D-Glucose	**20mM**	**Melford**

HEK293T: DMEM*

	CONCENTRATION	SUPPLIER
DMEM high glucose	**Final volume**	**Sigma**
Fetal calf serum	**10%**	**Gibco**
Glutamax	**1%**	**Gibco**
Penicillin-Streptomycin	**1%**	**Sigma**
MEM-Non essential aminoacids	**1%**	**Gibco**

Rat embryonic cortical neurons: Platting medium

	CONCENTRATION	SUPPLIER
DMEM high glucose	**Final volume**	**Sigma**
Fetal calf serum	**10%**	**Gibco**
Glutamax	**1%**	**Gibco**
Penicillin-Streptomycin	**1%**	**Sigma**
MEM-Non essential aminoacids	**1%**	**Gibco**

Rat embryonic cortical neurons: Feeding medium

	CONCENTRATION	SUPPLIER
DMEM high glucose	**Final volume**	**Sigma**
Fetal calf serum	**10%**	**Gibco**
Glutamax	**1%**	**Gibco**
Penicillin-Streptomycin	**1%**	**Sigma**
MEM-Non essential aminoacids	**1%**	**Gibco**

Mouse fetal NPCS: Expansion medium

	CONCENTRATION	SUPPLIER
DMEM high glucose	**73%**	**Sigma**
F12 nutrient mixture	**24%**	**Gibco**
B27 supplement	**2%**	**Gibco**
Penicillin-Streptomycin	**1%**	**Sigma**
Basic fibroblast growth factor	**20µg·l^{-1}**	**Peprotech**
Heparin	**5mg·l^{-1}**	**Sigma**

Mouse fetal and adult NPCS: Differentiation medium

	CONCENTRATION	SUPPLIER
DMEM high glucose	**72%**	**Sigma**
F12 nutrient mixture	**24%**	**Gibco**
B27 supplement	**2%**	**Gibco**
Penicillin-Streptomycin	**1%**	**Sigma**
Fetal calf serum	**1%**	**Gibco**

Mouse adult NPCS: Expansion medium

	CONCENTRATION	SUPPLIER
DMEM high glucose	**73%**	**Sigma**
F12 nutrient mixture	**24%**	**Gibco**
B27 supplement	**2%**	**Gibco**
Penicillin-Streptomycin	**1%**	**Sigma**
Basic fibroblast growth factor	**20µg·l^{-1}**	**Peprotech**
Heparin	**5 mg·l^{-1}**	**Sigma**
Epidermal growth factor	**20µg·l^{-1}**	**Sigma**

Human fetal NPCs: Primary Expansion medium

	CONCENTRATION	SUPPLIER
DMEM high glucose	**73%**	**Sigma**
F12 nutrient mixture	**24%**	**Gibco**
B27 supplement	**2%**	**Gibco**
Penicillin-Streptomycin	**1%**	**Sigma**
Basic fibroblast growth factor	**20µg·l^{-1}**	**Peprotech**
Heparin	**5 mg·l^{-1}**	**Sigma**
Epidermal growth factor	**20µg·l^{-1}**	**Sigma**

Human fetal NPCs: Long-term Expansion medium

	CONCENTRATION	SUPPLIER
DMEM high glucose	**74%**	**Sigma**
F12 nutrient mixture	**24%**	**Gibco**
N2 supplement	**1%**	**Gibco**
Penicillin-Streptomycin	**1%**	**Sigma**
Basic fibroblast growth factor	**20μg·l^{-1}**	**Peprotech**
Heparin	**5mg·l^{-1}**	**Sigma**

Human fetal NPCs: Differentiation medium

	CONCENTRATION	SUPPLIER
DMEM high glucose	**74%**	**Sigma**
F12 nutrient mixture	**24%**	**Gibco**
N2 supplement	**1%**	**Gibco**
Penicillin-Streptomycin	**1%**	**Sigma**
Forskolin	**5nM**	**Sigma**
N-acetyl-cysteine	**0.6 mg·l^{-1}**	**Sigma**
Bovine serum albumin	**1mg·l^{-1}**	

APENDIX C DNA Inserts

XhoI-hsCDNF-SpeI ***(582bp)***

5’ → 3’

CTCGAG *GCCACC* **ATG**TGGTGCGCGAGCCCAGTTGCTGTGGTGGCCTTT
XhoI *kozak* *start*

TGCGCCGGGCTTTTGGTCTCTCACCCGGTGCTGACGCAGGGCCAGGAG

GCCGGGGGGCGGCCAGGGGCCGACTGTGAAGTATGTAAAGAATTCTT

GAACCGATTCTACAAGTCACTGATAGACAGAGGAGTTAACTTTTCGCT

GGACACTATAGAGAAAGAATTGATCAGTTTTTGCTTGGACACCAAAGG

AAAAGAAAACCGCCTGTGCTATTATCTAGGAGCCACAAAAGACGCAG

CCACAAAGATCCTAAGTGAAGTCACTCGCCCAATGAGTGTGCATATGC

CTGCAATGAAGATTTGTGAGAAGCTGAAGAAGTTGGATAGCCAGATCT

GTGAGCTGAAATATGAAAAAACACTGGACTTGGCATCAGTTGACCTGC

GGAAGATGAGAGTGGCAGAGCTGAAGCAGATCCTGCATAGCTGGGGG

GAGGAGTGCAGGGCCTGTGCAGAAAAAACTGACTATGTGAATCTCATT

CAAGAGCTGGCCCCCAAGTATGCAGCGACACACCCCAAAACAGAGCT

C**TGA** ***ACTAGT***
stop *SpeI*

XhoI-hsGDNF-SpeI ***(654bp)***

5’ → 3’

CTCGAG *GCCACC* **ATG**AAGTTATGGGATGTCGTGGCTGTCTGCCTGGT
XhoI ***kozak*** ***start***
GCTGCTCCACACCGCGTCCGCCTTCCCGCTGCCCGCCGGTAAGAGGCC

TCCCGAGGCGCCCGCCGAAGACCGCTCCCTCGGCCGCCGCCGCGCGCC

CTTCGCGCTGAGCAGTGACTCAAATATGCCAGAGGATTATCCTGATCA

GTTCGATGATGTCATGGATTTTATTCAAGCCACCATTAAAAGACTGAA

AAGGTCACCAGATAAACAAATGGCAGTGCTTCCTAGAAGAGAGCGGA

ATCGGCAGGCTGCAGCTGCCAACCCAGAGAATTCCAGAGGAAAAGGT

CGGAGAGGCCAGAGGGGCAAAAACCGGGGTTGTGTCTTAACTGCAAT

ACATTTAAATGTCACTGACTTGGGTCTGGGCTATGAAACCAAGGAGGA

ACTGATTTTTAGGTACTGCAGCGGCTCTTGCGATGCAGCTGAGACAAC

GTACGACAAAATATTGAAAAACTTATCCAGAAATAGAAGGCTGGTGA

GTGACAAAGTAGGGCAGGCATGTTGCAGACCCATCGCCTTTGATGATG

ACCTGTCGTTTTTAGATGATAACCTGGTTTACCATATTCTAAGAAAGCA

TTCCGCTAAAAGGTGTGGATGTATC**TGA** ***ACTAGT***
stop ***SpeI***

XhoI-hsMANF-SpeI ***(552bp)***

5’ → 3’

CTCGAG ***GCCACC*** **ATG**TGGGCCACGCAGGGGCTGGCGGTGGCGCTGGCTCTG
XhoI ***kozak*** ***start***
AGCGTGCTGCCGGGCAGCCGGGCGCTGCGGCCGGGCGACTGCGAAGTTTGTA

TTTCTTATCTGGGAAGATTTTACCAGGACCTCAAAGACAGAGATGTCACATTC

TCACCAGCCACTATTGAAAACGAACTTATAAAGTTCTGCCGGGAAGCAAGAG

GCAAAGAGAATCGGTTGTGCTACTATATCGGGGCCACAGATGATGCAGCCAC

CAAAATCATCAATGAGGTATCAAAGCCTCTGGCCCACCACATCCCTGTGGAG

AAGATCTGTGAGAAGCTTAAGAAGAAGGACAGCCAGATATGTGAGCTTAAGT

ATGACAAGCAGATCGACCTGAGCACAGTGGACCTGAAGAAGCTCCGAGTTAA

AGAGCTGAAGAAGATTCTGGATGACTGGGGGGAGACATGCAAAGGCTGTGC

AGAAAAGTCTGACTACATCCGGAAGATAAATGAACTGATGCCTAAATATGCC

CCCAAGGCAGCCAGTGCACGGACCGATTTG**TAG** ***ACTAGT***
stop ***SpeI***

XhoI-hsCDNF-t2a-MANF-SpeI (1,197bp)

5’ → 3’

CTCGAG ***GCCACC*** **ATG**TGGTGCGCGAGCCCAGTTGCTGTGGTGGCCTTTTGCG
XhoI *kozak* *start*

CCGGGCTTTTGGTCTCTCACCCGGTGCTGACGCAGGGCCAGGAGGCCGGGGG

GCGGCCAGGGGCCGACTGTGAAGTATGTAAAGAATTCTTGAACCGATTCTAC

AAGTCACTGATAGACAGAGGAGTTAACTTTTCGCTGGACACTATAGAGAAAG

AATTGATCAGTTTTTGCTTGGACACCAAAGGAAAAGAAAACCGCCTGTGCTA

TTATCTAGGAGCCACAAAAGACGCAGCCACAAAGATCCTAAGTGAAGTCACT

CGCCCAATGAGTGTGCATATGCCTGCAATGAAGATTTGTGAGAAGCTGAAGA

AGTTGGATAGCCAGATCTGTGAGCTGAAATATGAAAAAACACTGGACTTGGC

ATCAGTTGACCTGCGGAAGATGAGAGTGGCAGAGCTGAAGCAGATCCTGCAT

AGCTGGGGGGAGGAGTGCAGGGCCTGTGCAGAAAAAACTGACTATGTGAAT

CTCATTCAAGAGCTGGCCCCCAAGTATGCAGCGACACACCCCAAAACAGAGC

TC ***GGAGGAGGAGGA***GAGGGCCGCGGCAGCCTGCTGACCTGCGGCGACGTGG
Glynk

AGGAGAACCCCGGCCCC***GGAGGAGGAGGA*** ATGTGGGCCACGCAGGGGCTGG
Glynk

CGGTGGCGCTGGCTCTGAGCGTGCTGCCGGGCAGCCGGGCGCTGCGGCCGGG

CGACTGCGAAGTTTGTATTTCTTATCTGGGAAGATTTTACCAGGACCTCAAAG

ACAGAGATGTCACATTCTCACCAGCCACTATTGAAAACGAACTTATAAAGTT

CTGCCGGGAAGCAAGAGGCAAAGAGAATCGGTTGTGCTACTATATCGGGGCC

ACAGATGATGCAGCCACCAAAATCATCAATGAGGTATCAAAGCCTCTGGCCC

ACCACATCCCTGTGGAGAAGATCTGTGAGAAGCTTAAGAAGAAGGACAGCC

AGATATGTGAGCTTAAGTATGACAAGCAGATCGACCTGAGCACAGTGGACCT

GAAGAAGCTCCGAGTTAAAGAGCTGAAGAAGATTCTGGATGACTGGGGGGA

GACATGCAAAGGCTGTGCAGAAAAGTCTGACTACATCCGGAAGATAAATGA

ACTGATGCCTAAATATGCCCCCAAGGCAGCCAGTGCACGGACCGATTTGTAG
stop

ACTAGT
SpeI

APENDIX D Publications